Implication of Death Receptor Antagonists in Neuroblastoma:

Role of Lifeguard

PhD THESIS

Laura Planells Ferrer

September, 2014

PhD Thesis

Implication of Death Receptor Antagonists in Neuroblastoma

Role of Lifeguard

Laura Planells Ferrer

Directors:

Joan X Comella Carnicé **Rana S Moubarak** **Miguel F Segura Ginard**

Doctorat en Neurociències
Institut de Neurociències
Universitat Autònoma de Barcelona
2014

Als meus pares i sa meua germana

ABSTRACT

ABSTRACT

Neuroblastoma (NBL) is the most common solid tumor in infants and accounts for 10% of all pediatric cancer deaths. Several risk factors predict NBL outcome, such as age at time of diagnosis, stage, chromosome alterations, and amplification of the oncogene *MYCN*, which characterizes the subset of the most aggressive neuroblastomas with an overall survival below 30%. *MYCN*-amplified tumors develop resistance against all treatment modalities and show a high metastatic capacity. These properties have been linked to alterations in the apoptotic machinery, either by silencing components of the extrinsic apoptotic pathway (e.g. caspase-8) or by overexpression of anti-apoptotic regulators (e.g. BCL-2, MCL-1 or c-FLIP). Very little is known on the implication of death receptors and their antagonists in NBL. In this thesis, the expression levels of several death receptor antagonists were analyzed in multiple human NBL data sets. We report that Lifeguard (LFG/FAIM2/NMP35) is downregulated in the most aggressive tumors and that low LFG levels correlate with poor patient survival. Intriguingly, although LFG has been initially characterized as an anti-apoptotic protein, we have found a new association with NBL differentiation. Moreover, LFG repression resulted in reduced cell adhesion, increased sphere growth and enhanced migration, thus conferring a higher metastatic capacity to NBL cells that was confirmed *in vivo*. Furthermore, LFG expression was found to be directly repressed by MYCN at the transcriptional level. Our data, which support a new functional role for a hitherto undiscovered MYCN target, provide a new link between MYCN overexpression and increased NBL metastatic properties.

RESUMEN

El neuroblastoma (NBL) es el tumor sólido más común en la infancia y representa un 10% de todas las muertes pediátricas por cáncer. Existen varios factores de riesgo que predicen el alcance de la enfermedad, tales como la edad en el momento del diagnóstico, el estadio, alteraciones cromosómicas y la amplificación del oncogén *MYCN*, que caracteriza el grupo de NBLs más agresivos con una probabilidad de supervivencia inferior al 30%. En general, los tumores *MYCN* amplificados desarrollan resistencia a todas las modalidades de tratamiento y muestran una alta capacidad metastática. Estas propiedades han sido atribuidas a alteraciones en la maquinaria apoptótica, ya sea por silenciamiento de componentes de la vía extrínseca (como caspasa-8) o por sobreexpresión de reguladores anti-apoptóticos (como BCL-2, MCL-1 o c-FLIP). Hasta hoy se sabe muy poco de la implicación de los receptores de muerte y sus antagonistas en NBL. En esta tesis se analizaron los niveles de expresión de varios antagonistas de receptores de muerte en múltiples bases de datos de NBL humano. Nuestro trabajo muestra que la expresión de Lifeguard (LFG/FAIM2/NMP35) se ve disminuida en los tumores más agresivos y que bajos niveles de LFG correlacionan con una peor supervivencia del paciente. Curiosamente, aunque LFG fue inicialmente caracterizada como una proteína anti-apoptótica, nosotros describimos una nueva asociación de esta proteína con la diferenciación del NBL. Asimismo, la represión de LFG resultó en una reducción de la adhesión celular, una mayor habilidad de formar de esferas y un aumento en la capacidad de migración de las células, confiriéndoles una mayor capacidad metastática que pudo ser confirmada en experimentos *in vivo*. Además, descubrimos que la expresión de LFG estaba directamente reprimida por MYCN a nivel transcripcional. Por tanto, nuestros datos respaldan una nueva función para una diana de MYCN antes desconocida y proporcionan una nueva conexión entre la sobreexpresión de MYCN y la mayor capacidad metastática del NBL.

CONTENTS

CONTENTS

ABBREVIATIONS

Abbreviations

Abs	Absorbance
ALK	Anaplastic lymphoma kinase
ANOVA	Analysis of variance
APAF-1	Apoptotic protease activating factor-1
ATCC	American Type Culture Collection
BAR	Bifunctional Apoptosis Regulator
BCL-2	B-cell lymphoma 2
bHLH	basic Helix-Loop-Helix
BI-1	BAX Inhibitor-1
BIR	Baculovirus IAP Repeat
BLI	Bioluminiscence
BMP	Bone Morphogenetic Protein
BSA	Bovine serum albumin
CaMKII	Calmodulin kinase II
CARD	Caspase Recruitment Domain
CCHS	Congenital Central Hypoventilation Syndrome
ChIP	Chromatin Immunoprecipitation
DD	Death Domain
DED	Death Effector Domain
DIABLO	Direct IAP binding protein with low pI
DISC	Death-Inducing Signaling Complex
DMEM	Dulbecco's Modified Eagle's Medium
DMSO	Dimethyl sulfoxide
DNA	Deoxyribonucleic acid
Dox	Doxycycline
DR	Death Receptor
DRG	Dorsal Root Ganglion
DTT	dithiothreitol
dNTPs	deoxynucleotides triphosphates
ECM	Extracellular matrix
EDTA	Ethylenediaminetetraacetic acid
EGF	Epidermal growth factor
EFGR	Epidermal growth factor receptor

EFS	Event-free survival
EMT	Epithelial to mesenchymal transition
ER	Endoplasmic Reticulum
ERK	Extracellular signal-regulated kinase
FADD	Fas Associated Death Domain
FAIM	Fas Apoptosis Inhibitory Molecule
FAP-1	Fas-associated phosphatase-1
FBS	Fetal bovine serum
FGF2	Fibroblast growth factor 2
FISH	Fluorescence in situ hybridisation
c-FLIP	cellular FLICE inhibitory protein
FLuc	Firefly Luciferase
Foxn1	Forkhead box N1
G-CSF	Granulocyte colony stimulating factor
GD2	Glycolipid disialoganglioside
GFP	Green fluorescent protein
GSK3	Glycogen synthase kinase-3
HAT	Histone acetyl transferase
HDAC	Histone deacetylase
H&E	Hematoxylin & Eosin
HRP	Horseradish peroxidase
IAP	Inhibitor of Apoptosis Protein
IDRF	Image-defined risk factors
IHC	Immunohistochemistry
IL-2	Interleukin-2
IMDM	Iscove's Modified Dulbecco's Media
INPC	International Neuroblastoma Pathology Classification
INRG	International Neuroblastoma Risk Group
INRGSS	International Neuroblastoma Risk Group Staging System
INSS	International Neuroblastoma Staging System
JAK	Janus kinase
kb	kilobase
KEGG	Kyoto Encyclopedia of Genes and Genomes
LFG	Lifeguard
LPS	Lipopolysaccharides

mAb	monoclonal antibody
MAPK	Mitogen-activated protein kinase
MDR	Multidrug resistance
MIBG	I-metaiodobenzylguanidine
MKC	mitosis-karyorrhexis index
MLR	Membrane Lipid Raft
MOMP	Mitochondrial Outer Membrane Permeabilization
MRI	Magnetic Resonance Imaging
MYCN	V-myc avian myelocytomatosis viral oncogene NBL derived homolog
mRNA	messenger Ribonucleic acid
NF-κB	Nuclear Factor kappaB
NB	Naphtol Blue
NBL	Neuroblastoma
NCC	Neural Crest Cell
NMP35	Neural Membrane Protein 35
OMA	Opsoclonus-Myoclonus Ataxia
OR	Odds ratio
PAGE	Polyacrylamide gel electrophoresis
PBS	Phosphate buffered saline
PC	Purkinje cell
PCA	Principal component analysis
PCR	Polymerase chain reaction
PEA-15	Phosphoprotein Enriched in Astrocytes-1
PHOX2B	Paired-like homeobox 2B
PI3K	Phosphatidylinositol 3-kinase
PKB	Protein kinase B
PKC	Protein kinase C
PLC	Phospholipase C
PVDF	Polyvinyl difluoride
qPCR	Quantitative real-time polymerase chain reaction
RA	Retinoic acid
RAS	Rat sarcoma
RING	Really Interesting New Gene
RNA	Ribonucleic acid
ROI	Region of interest

RPM	Revolutions per minute
Scr	Scrambled
SDS	Sodium dodecyl sulfate
S.E.M.	Standard error of the mean
sh	short hairpin
SMAC	Second mitochondria-derived activator of caspases
SODD	Silencer of Death Domains
STAT	Signal transducer and activator of transcription
SUMO-1	Small ubiquitin-related modifier 1
TJ	Tight junctions
TMBIM	Transmembrane BAX Inhibitor-1 Motif-containing
TNF	Tumor necrosis factor
TNFR	Tumor Necrosis Factor Receptor
TRAIL	TNF-related apoptosis-inducing ligand
Ub	Ubiquitin
XIAP	X-linked Inhibitor of Apoptosis Protein

MEDICAL TERMS

Medical terms

Anhidrosis	Absence of sweating.
Ataxia	Loss of coordination of voluntary muscular movements.
Contralateral	Located on or affecting the opposite side of the body.
Ecchymosis	A hemorrhagic spot in the skin or a mucous membrane caused by a diffuse extravasation of blood.
Hematogenous	Disseminated through the blood stream.
Hepatomegaly	Enlargement of the liver.
Ipsilateral	Located on or affecting the same side of the body.
Locoregional	Limited to a localized area, as contrasted with systemic or metastatic.
Miosis	Contraction of the pupil.
MKC index	Mitosis-karyorrhexis index, which indicates the percentage of cells that are undergoing division or apoptosis.
Proptosis	A bulging, protrusion or forward displacement of an organ, especially an eyeball.
Ptosis	Abnormal lowering or drooping of the upper eyelid caused by muscle weakness or paralysis.

INTRODUCTION

1. Introduction

1.1. Neuroblastoma

Neuroblastoma (NBL) is the most common solid tumor of infancy. It is the most frequently diagnosed neoplasm during early infancy, since a 90% of these tumors are diagnosed during the first 5 years of life, with a median age at presentation of 18.8 months (Figure 1) (Owens and Irwin 2012). NBL is by far the most prevalent cancer during the first year of life, with an incidence rate almost double than leukemia, the next most prevalent malignancy (Fisher and Tweddle 2012). In western countries, the annual incidence of NBL is 10.5 cases per million children below 15 years of age, and it occurs in 1 of 7000 live births (Ora and Eggert 2011, Park, Bagatell et al. 2013). NBL accounts for 8% of all childhood malignancies, while it causes around 10% of pediatric cancer deaths (Johnsen, Kogner et al. 2009) (SEER Cancer Statistics; http://seer.cancer.gov/).

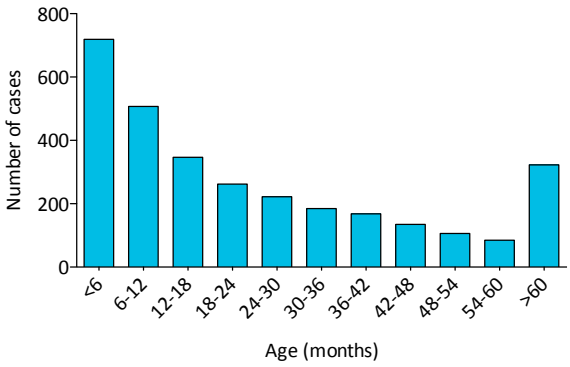

Figure 1. Age range for patients diagnosed with NBL. The age distribution is characterized by a peak incidence in the first year of life, followed by a rapid decline in subsequent years. Adapted from (Friedman and Castleberry 2007). Data from Children's Oncology Group.

NBL is an extremely heterogeneous malignancy, with prognosis ranging from spontaneous regression to fatal demise (Maris, Hogarty et al. 2007). Therefore, these tumors have disoriented, fascinated and frustrated oncologists and laboratory investigators due to their incredibly variable behavior. The following points will gradually explain the current understanding about the biological features of NBLs that make them so heterogeneous and that need to be clarified in order to correctly diagnose and assign the best therapeutic approach for each patient.

1.1.1. Neuroblastoma: cell of origin

In 1910, James Homer Wright pointed for the first time that NBL tumors were derived from neural cells ((Wright 1910), reviewed in (Owens and Irwin 2012)). In particular, NBL arises from cells derived from the neural crest during embryonic development. In fact, these tumors mimic the behavior of cells of the sympathetic lineage in terms of growth, migration and differentiation (Takahashi, Sipp et al. 2013).

Neural crest cells (NCCs) appear in the human embryo between the third and fifth week of pregnancy inside the neural folds of the newly formed neural tube (Figure 2). During the fusion of the neural folds, which ultimately yields a tube that will become the central nervous system, NCCs detach and undergo an epithelial-to-mesenchymal transition (EMT). This EMT transition provides cells with enhanced migratory abilities and decreased requirements for intercellular contact, which allows the NCCs to leave the dorsal neural tube and migrate throughout the body, integrating nearly every organ (Saint-Jeannet 2006).

The induction of NCCs is a complex process involving interactions between the neural plate, the non-neuronal ectoderm and the underlying mesoderm (Figure 2A). These interactions are thought to switch on the EMT program and induce cell detachment from the neural epithelium in order to become pluripotent migratory mesenchymal cells in a process known as delamination (Figure 2B). The EMT process includes a loss of apico-basal polarity, a modification of cell-cell and cell-matrix properties, a local degradation of extracellular matrix (ECM) or membrane receptors and acquisition of motility (Strobl-Mazzulla and Bronner 2012, Theveneau and Mayor 2012). EMT is controlled by an array of transcription factors downstream WNT and Bone Morphogenetic Protein (BMP) signaling. The main regulators of NCC EMT include SNAI1/2 (Nieto, Sargent et al. 1994), FOXD3 (Dottori, Gross et al. 2001), SOX9/10 (Cheung and Briscoe 2003), TWIST1 and ZEB1 (Cheung, Chaboissier et al. 2005, Sauka-Spengler and Bronner-Fraser 2008). WNT pathway plays a role in inducing MYCN expression, a proto-oncogene required for migration, differentiation and survival of the migrating cells (Grimmer and Weiss 2006). Together, these factors control various aspects of EMT required for delamination and in particular, they control changes in cell adhesion. Cells must switch to a different repertoire of adhesion molecules, and thus, these transcription factors directly repress the transcription of E-Cadherin, Cadherin6B and N-Cadherin, leading to loss of adherent junctions and cell polarity (Kerosuo and Bronner-Fraser 2012, Gheldof and Berx 2013). In addition, they induce the expression of multiple type-II cadherins, which mediate weaker adhesion forces (Taneyhill, Coles et al. 2007, Wheelock, Shintani et al. 2008,

Theveneau and Mayor 2012). This cadherin switch liberates NCCs and contributes to migration, supported by ECM rearrangements and integrin activation. A similar EMT may also play a role in NBL metastasis.

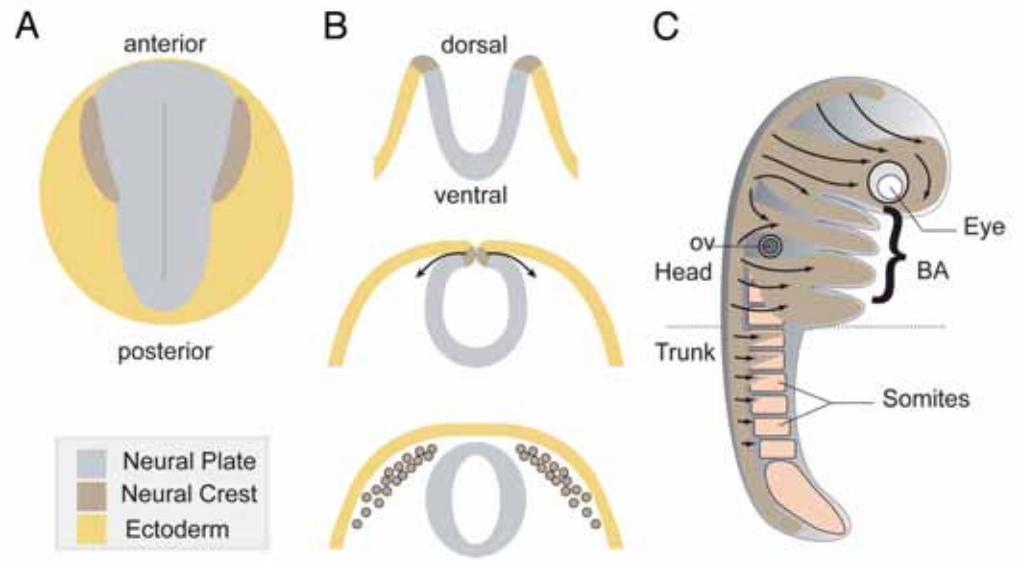

Figure 2. Neural crest development. **A,** Dorsal view of a vertebrate embryo at early developmental stages. **B,** Neural tube formation and neural crest delamination. **C,** Main NCCs migration routes through the embryo. (Fort and Theveneau 2014).

Therefore, NCCs are a transient population of progenitor cells that have the ability to migrate and give rise to a variety of differentiated cell types, including the entire peripheral nervous system (sensory, autonomic and enteric ganglia), pigment cells, the adrenal medulla and cells of the craniofacial skeleton (Figure 2C) (Nicole M. Le Douarin 1999, Saint-Jeannet 2006, Jiang, Stanke et al. 2011, Takahashi, Sipp et al. 2013).

There is a fine balance between cell death, proliferation, cell renewal, migration and differentiation that is crucial for neural development. However, genetic factors or exposure to environmental cues sometimes result in inappropriate NCC differentiation, leading to uncontrolled cell cycle and causing many pediatric pathologies, including NBL (Saint-Jeannet 2006). Several evidences set embryonic tumors apart from adult solid tumors. Since embryonic tumors develop from progenitor cells that are already proliferating as a normal part of the developmental process, these tumors show an extremely short latency period. Moreover, childhood solid tumors develop with fewer genetic aberrations (activation of oncogenes or loss of tumor suppressor genes) than adult cancers (Scotting, Walker et al. 2005). Instead, most genes expressed in embryonic tumors are critical regulators of the normal neural crest

development, such as *MYCN* in NBL (Grimmer and Weiss 2006). These defects in embryonic genes controlling neural crest development are likely to cause unbalances during proliferation and differentiation of neural precursors. But, are all NBLs derived from a common precursor? Instead of having a common precursor, their clinical behavior may reflect different stages of neuronal differentiation, where the most aggressive tumors probably originate from the less differentiated progenitor cells.

1.1.2. Neuroblastoma Oncogenes

Certain genes have been strongly associated to NBL development. In the early 1980's, the amplification of the oncogene *MYCN* was identified in NBL tumors (Brodeur, Seeger et al. 1984) and it was associated to neoplasic transformation and high-risk NBL in subsequent studies (Weiss, Aldape et al. 1997). A few years later, mutations of genes such as *PHOX2B* (Mosse, Laudenslager et al. 2004) and *ALK* (Mosse, Laudenslager et al. 2008) were associated to familial NBLs, which account for 1-2% of cases. These oncogenes and their implication in NBL development are discussed below.

1.1.2.1. MYCN

Amplification of *MYCN* (v-Myc avian myelocytomatosis viral oncogene neuroblastoma derived homolog), mapping to 2p24.1, is present in 20% of NBL cases and remains one of the most important genetic abnormalities associated with malignant progression of the disease (Domingo-Fernandez, Watters et al. 2013).

MYCN is a transcription factor that belongs to the MYC proto-oncogene family, together with c-MYC and MYCL. MYCN controls the expression of many target genes that are involved in a myriad of fundamental cellular processes related with proliferation, cell growth, protein synthesis, metabolism, apoptosis and differentiation (Eilers and Eisenman 2008) (Figure 3).

MYCN protein consists of an N-terminal transcription activator domain and a C-terminal DNA binding and protein interaction domain. MYCN recognizes and binds E-Box sequences (CACGTG) in a heterodimeric complex with its partner MAX and this complex recruits transcription co-factors and histone acetyl transferases (HATs) to induce transcription. Likewise, MYCN can also repress the expression of genes involved in adhesion and differentiation by binding to other transcription factors such as MIZ1 and SP1 (Gartel and Shchors 2003, Eilers and Eisenman 2008) (Figure 3).

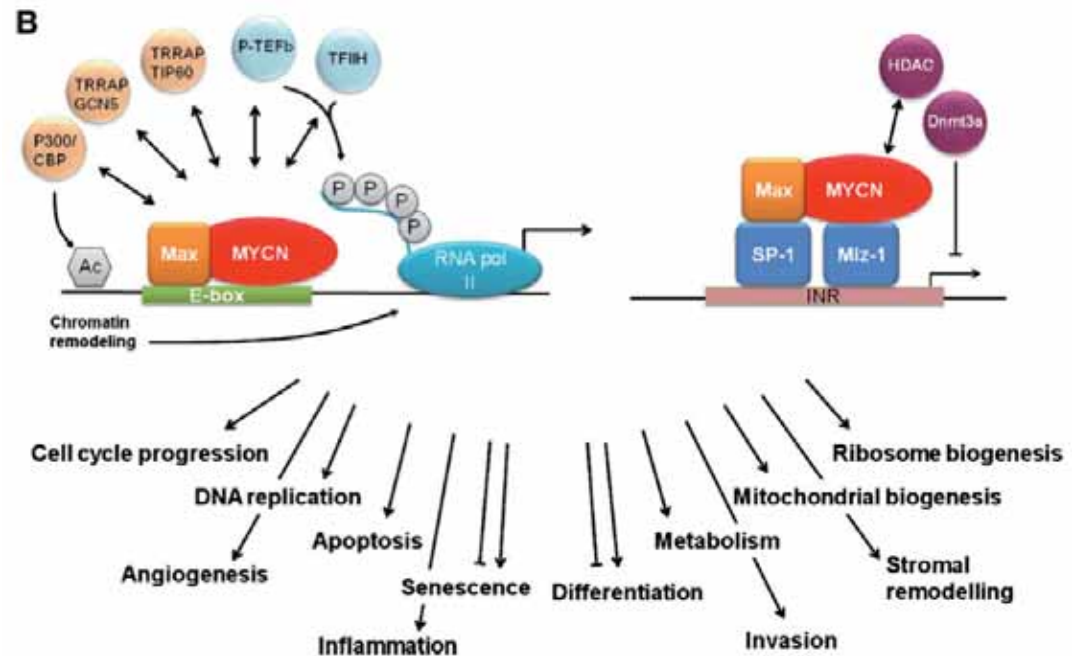

Figure 3. Cellular processes influenced by MYCN regulation of transcription. Left panel depicts transcription activation by MYCN/MAX dimer after binding to an E-Box sequence. They recruit HATs, leading to an open chromatin state and phosphorylate RNA polymerase II, resulting in stimulated transcriptional elongation. Right panel represents MYCN mediated repression of transcription. MYCN/MAX dimer recruits histone deacetylases (HDACs) and DNA methylase 3a (Dnmt3a) that mediate a repressed chromatin state. Adapted from (Westermark, Wilhelm et al. 2011).

In mice and human tissues, MYCN expression is restricted to certain tissues of the developing embryo, while its expression is very low or absent in adult tissues (Zimmerman, Yancopoulos et al. 1986, Grady, Schwab et al. 1987, Mugrauer, Alt et al. 1988). A number of *in vitro* and *in vivo* evidences demonstrate the profound role of MYCN in embryonic development. On the one hand, mutations of the *MYCN* gene cause birth defects. Mice knockout for *MYCN* die at embryonic day 11.5 and show hypoplasia in several organs and tissues, including central and peripheral nervous system (Charron, Malynn et al. 1992, Stanton, Perkins et al. 1992, Sawai, Shimono et al. 1993). On the other hand, Cotterman and colleagues demonstrated that MYCN induces the expression of pluripotency markers in NBL and neural cells (Cotterman and Knoepfler 2009). Moreover, exogenous MYCN expression, as well as c-MYC, promotes reprogramming of somatic cells to induced pluripotent stem cells (Nakagawa, Koyanagi et al. 2008). MYCN has an essential role in the expansion of neural progenitor cells, maintaining embryonic stem cell pluripotency, and controls early differentiation steps in the nervous system (Grady, Schwab et al. 1987, Hirning, Schmid et al. 1991, Knoepfler, Cheng et al. 2002,

Alam, Cui et al. 2009, Varlakhanova, Cotterman et al. 2010). Other studies show that the expression of MYCN needs to be downregulated to achieve terminal neuronal differentiation (Wakamatsu, Watanabe et al. 1997, Alam, Cui et al. 2009, Smith, Singh et al. 2010).

In 1997, Weiss and collaborators demonstrated that targeted overexpression of MYCN in neuroectodermal cells caused NBL in transgenic mice and that tumor formation was dosage-dependent (Weiss, Aldape et al. 1997). The obtained tumors mimicked histological characteristics of human NBLs, expressed human NBL markers such as synaptophysin and neuron-specific enolase and developed chromosome gains and losses in regions syntenic with those observed in human NBL.

1.1.2.2. PHOX2B

PHOX2B (paired-like homeobox 2B) is a homeodomain-containing transcription factor that plays an essential role during the development of the autonomic nervous system. PHOX2B binds to the promoter of noradrenergic marker genes such as tyrosine hydroxylase and dopamine-β-hydroxylase and activates their transcription (Lo, Morin et al. 1999). PHOX2B induces the differentiation of NCCs to noradrenergic neurons (Stanke, Stubbusch et al. 2004) and is an essential determinant of the noradrenergic phenotype, since homozygous *PHOX2B*-deficient mice die during gestation and the cause of death is the complete absence of noradrenergic neurons (Pattyn, Morin et al. 1999).

PHOX2B was the first identified gene predisposing to neuroblastic tumors (Bourdeaut, Trochet et al. 2005). Inherited frame-shift and missense mutations that result in a truncated protein have been reported in familial NBL. These mutations are often associated to other disorders derived from NCCs, such as Hirschprung's disease (a congenital cause of constipation) or congenital central hypoventilation syndrome (CCHS), characterized by an impaired autonomous breathing. Mutations in *PHOX2B* gene are only found in a 2-6% of familial cases and are rarely detected in sporadic NBLs (van Limpt, Schramm et al. 2004, Raabe, Laudenslager et al. 2008), indicating that it is not a major tumor-initiating event. Moreover, the mechanism by which these mutations exert their effect is still not clear (van Limpt, Chan et al. 2005, Fisher and Tweddle 2012).

1.1.2.3. ALK

Anaplastic lymphoma receptor Tyrosine kinase (*ALK*) gene maps to 2p and plays a role in normal development of the nervous system. Two heparin-binding growth factors (pleiotrophin and midkine) have been identified as candidate ALK ligands (Stoica, Kuo et al. 2001, Stoica, Kuo

et al. 2002). After the stimulation by its ligand, ALK receptor mediates its signaling through several pathways, including JAK/STAT (Janus kinase/signal transducer and activator of transcription), RAS/MAPK (rat sarcoma/mitogen-activated protein kinase), PI3K (phosphatidylinositol 3-kinase) and PLCγ (phospholipase C gamma), leading to proliferation and differentiation and impairing apoptosis (Sridhar, Al-Moallem et al. 2013).

Several chromosomal rearrangements and mutations that over-activate ALK have been reported in human cancers since it was described for the first time in anaplastic large cell lymphomas in 1994 (Murga-Zamalloa and Lim 2014). Recently, somatic and hereditary mutations and amplifications in the ALK gene have been identified as drivers of NBL progression (Figure 4) (De Brouwer, De Preter et al. 2010). These mutations often lead to constitutive phosphorylation of ALK or higher ALK activity, thus promoting downstream signaling events involved in proliferation and survival, conferring cells an increased oncogenic potential. In fact, newly published reports demonstrate that ALK is a transcriptional target of MYCN and that it mediates MYCN effects on proliferation, migration and invasion (Hasan, Nafady et al. 2013).

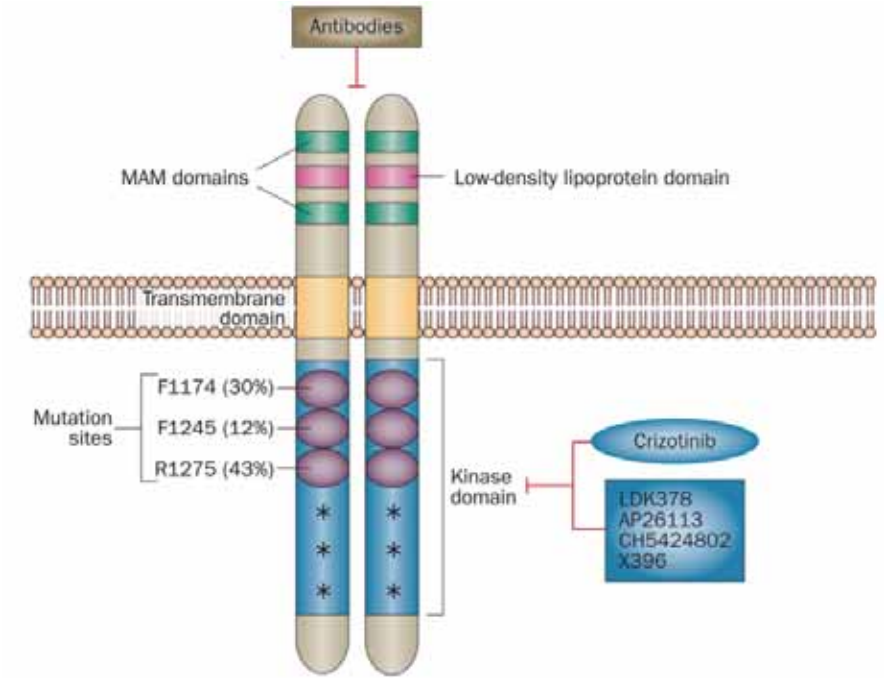

Figure 4. ALK protein structure and mutations found in NBL. The most frequent mutations in NBL are F1174, F1245 and R1275; the frequency of these mutations is provided in brackets. Other low frequency mutations are indicated with an asterisk. Some ALK inhibitors against its kinase domain such as crizotinib are undergoing clinical trials. Antibodies against the extracellular domains are also under development. Adapted from (Carpenter and Mosse 2012).

Although ALK mutations do not correlate with NBL stage, they occur in approximately 50% of familial NBL cases (Azarova, Gautam et al. 2011). Knockdown of mutant ALK in NBL cell lines significantly reduced cell proliferation and led to apoptosis, highlighting its oncogenic effect (George, Sanda et al. 2008). Recently, two mouse models for ALK-driven NBL have been established and both works demonstrate that the overexpression of ALK^{F1174L} mutant, capable of autophosphorylation, causes *in vivo* NBL (Berry, Luther et al. 2012, Heukamp, Thor et al. 2012).

1.1.3. Clinical presentation of neuroblastomas

Clinical presentation of NBL is dependent upon site of tumor origin, disease extent and the presence of paraneoplastic syndromes. Thus, clinical presentations range from tumors that undergo spontaneous regression to metastatic disease resistant to all treatments.

NBL tumors arise along the developing sympathetic chain, but the majority of cases arise in the abdomen (65%), frequently in the adrenal medulla, where the sympathoadrenal lineage is specified. Other cases are found in the paraspinal sympathetic ganglia in places such as the neck (5%), chest (20%), and pelvis (5%) (Figure 5). A small percentage of patients have no detectable primary tumor (Maris, Hogarty et al. 2007, Park, Eggert et al. 2008).

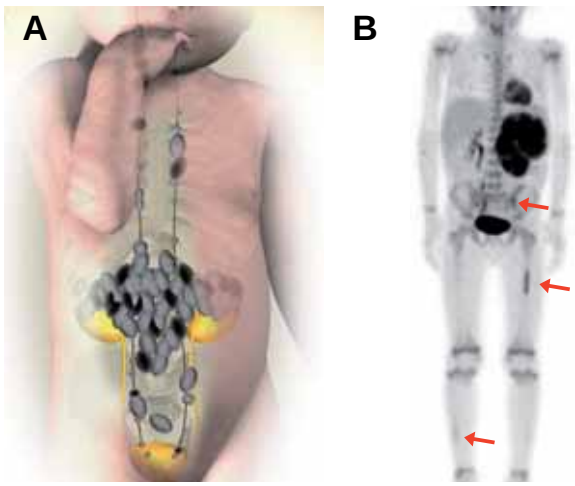

Figure 5. Localization of NBL tumors. A, NBL primary tumours arise in the sympathetic nervous system, including the adrenal medulla, sympathetic ganglia and paraganglia. Adapted from (Johnsen, Kogner et al. 2009). **B**, Primary NBL mass in the left abdomen with metastatic disease in the skeleton (red arrows) detected by bone scan and ^{123}I-MIBG. Adapted from (Howman-Giles, Shaw et al. 2007).

Symptoms are extremely variable depending on the localization of the primary tumor and the presence or absence of metastasis. Generally, locoregional tumors show biologically favorable characteristics and most of them are successfully treated with surgery alone. In fact, patients with localized tumors often lack symptomatology and some of them are detected by chance during routine analyses.

Nevertheless, around 50% of patients present widely metastatic tumors at the moment of diagnosis. The most common metastatic sites are bone, bone marrow, liver, lymph nodes and skin. Less frequent metastatic sites are lungs and central nervous system. In this case, patients present multiple systemic symptoms derived from NBL (Owens and Irwin 2012). Anemia often appears as a result of the infiltration of the bone marrow, while pain is caused by bone metastases (Berthold 2005). NBL has also propensity to metastasize to the eye orbits, causing ecchymosis and proptosis. These are the so called “racoon eyes”, which are sometimes accompanied by visual loss or even blindness (Lau, Trobe et al. 2004). Infiltration of the liver can cause hepatomegaly, which was already described by Pepper in 1901 (Pepper 1901). Cervical or upper thoracic tumors that compress the sympathetic chain result in Horner’s syndrome, characterized by ptosis, miosis and anhydrosis (Mahoney, Liu et al. 2006). Paraspinal tumors may present with acute spinal cord compression, causing weakness and decreased lower limb movements, requiring immediate chemo or radiotherapy (Katzenstein, Kent et al. 2001). Finally, a small percentage of NBLs are presented as a paraneoplasic syndrome known as Opsoclonus-Myoclonus Ataxia (OMA) that combines rapid eye movements, jerking limb movements and ataxia. It is hypothesized that OMA results from cross-reaction of antibodies raised against the tumor mass by the immune system that recognize host neural cells, particularly in the cerebellum. These children often survive with long-term motor and cognitive impairments (Hayward, Jeremy et al. 2001).

Diagnosis of NBL is based on an increase in catecholamines and catecholamine metabolites in the urine and/or serum of the patient and in histological diagnosis of a tumor specimen and/or a bone marrow aspirate (Brodeur, Pritchard et al. 1993). A small percentage of tumors do not produce catecholamines. In these cases, other markers such as neuron specific enolase are used. Moreover, imaging technologies allow clinicians to detect potential metastases (Figure 5) (Ora and Eggert 2011).

1.1.4. Biological behavior of neuroblastomas

Besides the clinical heterogeneity of NBLs, they have also a wide range of biological behaviors. Instead of following a common pattern of disease progression, NBLs have the unique characteristic of displaying extremely different, or even opposite behaviors.

NBL tumors, even with metastatic disease, can often undergo spontaneous regression, which is especially common for stage 4S tumors. It is characterized by a massive death of immature neuroblasts. First studies documenting spontaneous regression of NBLs were already published during the 1940's-1960's (Genest, Lapointe et al. 1964, Di Cagno and Ravetto 1967, Bill 1968, Carlsen 1990). There are several hypotheses that explain this phenomenon, based on mechanisms involving the immunologic system (Redlinger, Mailliard et al. 2004), the lack of neurotrophic factors in the tumor environment (Nakagawara 1998), and alterations of differentiation mechanisms (Bolande 1985,) or programmed cell death (Li and Nakagawara 2013). A murine model of liver metastasis showed the involvement of the immune system in tumor regression, since IL-2 infusion induced liver infiltration with natural killer cells, prompted tumor regression and cured animals. Histological analysis of livers dissected from those animals showed the same regression as seen in stage 4S human tumors (Ishizu, Bove et al. 1994). The involvement of neurotrophin receptors has been widely described in the normal development of the nervous system. Absent expression or abnormal function of these receptors or their ligands may render cells unable to undergo differentiation, so they would continue growing when they should differentiate, and surviving when they should die. The delayed activation of these normal developmental pathways could explain the spontaneous regression of the tumor (Brodeur, Minturn et al. 2009). Finally, many studies report that programmed cell death occurs in the spontaneous regression of NBLs, involving the activation of caspases and classical morphological markers of apoptosis such as DNA fragmentation. Nevertheless, other processes have been involved in this regression, such as autophagy or lysosomal-mediated cell death (Oue, Fukuzawa et al. 1996, Kitanaka, Kato et al. 2002, Inoue, Misawa et al. 2009). This suggests that NBL regression is a complex process that involves many cellular mechanisms.

In some cases, NBLs undergo maturation and spontaneously differentiate towards a benign neuroma or maturing NBL. Neuroblastic tumors mainly consist of two cellular populations: neuroblastic cells and Schwann cells (Ciccarone, Spengler et al. 1989, Walton, Kattan et al. 2004, Ross and Spengler 2007). In normal tissues, there is an interaction between normal neuroblasts and Schwann cells (Reynolds and Woolf 1993) and the same situation could

happen within the tumor. Some authors suggest that neoplasic neuroblasts produce mitogen agents and chemotactic factors that recruit Schwann cells. These cells, once in the transformed tissue, produce and release factors that inhibit proliferation and induce neuroblasts differentiation (Ambros, Zellner et al. 1996). Maturation ability is frequently related to neurotrophins and neurotrophin receptors (Park, Eggert et al. 2008).

Around 50% of NBLs, instead of having favorable biological behavior, present aggressive patterns. These tumors have the ability to metastasize and become refractory to all therapeutic strategies (Maris, Hogarty et al. 2007).

1.1.5. Neuroblastoma stratification and staging

Given the wide spectrum of clinical presentations and natural behaviors of NBLs, translational research has focused on defining and refining risk groups for these tumors. Over the last decades, these changing risk groups have been a guide to minimize or eliminate therapy for patients with lower risk tumors, to improve therapy for intermediate-risk tumors, and to identify new therapeutic strategies for high-risk disease.

Several classification attempts have been made since Dr. Audrey Evans developed the first NBL staging system (Evans, D'Angio et al. 1971), some of them detailed below. However, it is crucial to go further and unravel new factors implicated in the biology of NBL that will improve the management of patients and treatment effectiveness.

1.1.5.1. Histological classification

In 1984, Shimada and collaborators established a classification scheme that relates the histopathological features of the tumor to its clinical behavior. This way, tumors are classified as favorable or unfavorable depending on the degree of neuroblast differentiation, the content of Schwannian stroma, the mitosis-karyorrhexis index (MKC, which indicates the percentage of cells that are undergoing division or apoptosis) and age at diagnosis (Shimada, Chatten et al. 1984). Subsequent studies drove to a modification of the Shimada system. Thus, since 1999, tumors were classified using the International Neuroblastoma Pathology Classification System (INPC) (Shimada, Umehara et al. 2001). According to the INPC, tumors are assigned to one of four morphologic categories: neuroblastoma, ganglioneuroblastoma intermixed, ganglioneuroblastoma nodular and ganglioneuroma, as specified in the following scheme (Figure 6).

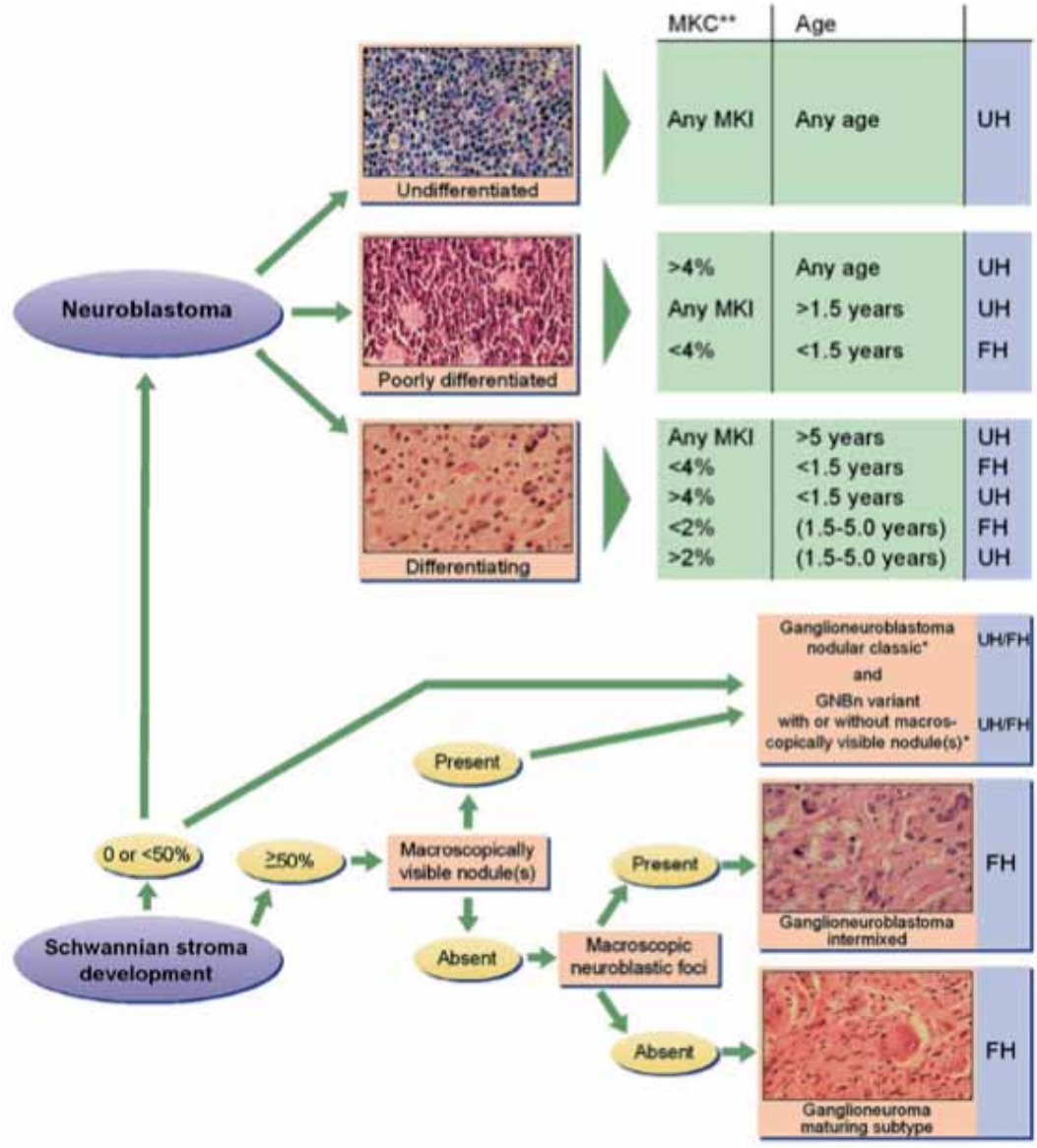

Figure 6. International Neuroblastoma Pathology Classification. Neuroblastoma tumors (Schwannian stroma-poor) consist of small, round cells called neuroblasts, which often do not show evidence of neural differentiation. This category comprises three subtypes: undifferentiated, poorly differentiated and differentiating. Other tumors show partial histological differentiation and are called ganglioneuroblastoma intermixed (Schwannian stroma-rich) and ganglioneuroblastoma nodular (composite, Schwannian stroma-rich, stroma-dominant and stroma-poor). The most differentiated tumors are ganglioneuromas (Schwannian stroma-dominant), consisting of clusters of mature neurons surrounded by a dense stroma of Schwann cells (Brodeur 2003, Park, Eggert et al. 2008).

1.1.5.2. INSS Classificatiton

The International Neuroblastoma Staging System (INSS) criteria were initially formulated in 1988 (Brodeur, Seeger et al. 1988), and revised in 1993 (Brodeur, Pritchard et al. 1993). The aim of this classification was to embody and standardize the most important elements of the already existing classification criteria. The proposed staging system was based on clinical, radiographic and surgical evaluation of children, as an approach to facilitate comparisons between different institutions.

The INSS definitions for NBL stages are listed in Table 1 and illustrated in Figure 7. Basically, completely resected tumors are classified as stage 1, while partially resected regional tumors with or without regional nodal involvement are classified as stages 2 and 3, dependent upon the amount of tumor resection, local invasion and regional lymph node involvement. Stage 4 is defined by the presence of distant nodal or hematogenous spread of the disease. There is a special case, stage 4S, with a unique pattern of dissemination limited to liver, skin and minimal bone marrow involvement. Stage 4S tumors have a high potential for spontaneous regression, in contrast to the disseminated aggressive disease seen in stage 4 tumors.

Table 1. International Neuroblastoma Staging System. (Adapted from (Maris, Hogarty et al. 2007))

Stage 1	Localized tumor with complete gross excision, with or without microscopic residual disease; representative ipsilateral lymph nodes negative for tumor microscopically (nodes attached and removed with the primary tumor may be positive).
Stage 2A	Localized tumor with incomplete gross excision; representative ipsilateral nonadherent lymph nodes negative for tumor microscopically.
Stage 2B	Localized tumor with or without complete gross excision, with ipsilateral nonadherent lymph nodes positive for tumor. Enlarged contralateral lymph nodes must be negative microscopically.
Stage 3	Unresectable unilateral tumor infiltrating across the midline[a], with or without regional lymph node involvement; or localized unilateral tumor with contralateral regional lymph node involvement; or midline tumor with bilateral extension by infiltration (unresectable) or by lymph node involvement.
Stage 4	Any primary tumor with dissemination to distant lymph nodes, bone, bone marrow, liver, skin and/or other organs (except as defined for stage 4S).
Stage 4S	Localized primary tumor (as defined for stage 1, 2A or 2B), with dissemination limited to skin, liver and/or bone marrow[b] (in infants <1 year of age).

[a] The midline is defined as the vertebral column. Tumors originating on one side that "cross the midline" must infiltrate to the opposite side of the vertebral column.

[b] In stage 4S, marrow involvement should be minimal. If >10% of total nucleated cells are identified as malignant, it will be considered as stage 4.

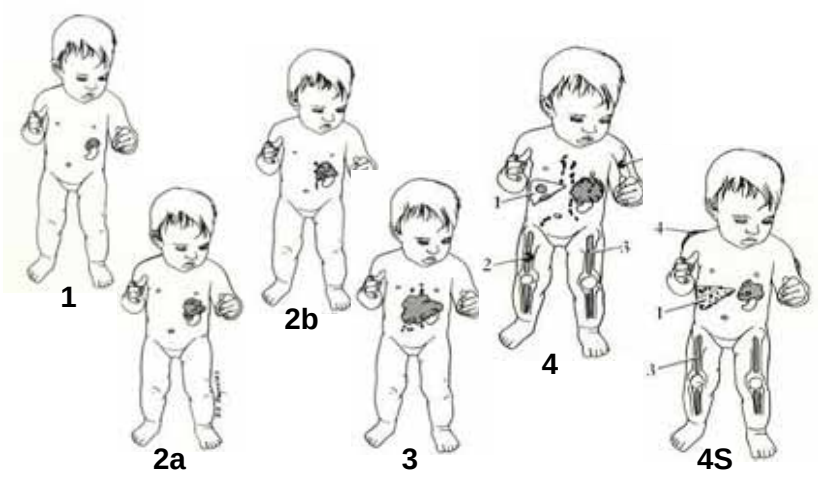

Figure 7. International Neuroblastoma Staging System

1.1.5.3. INRG Classification

Since INSS classification included surgical criteria, and surgical approaches differ from one institution to another, INSS stage for patients with locoregional disease can vary substantially. So many efforts were made to develop a consensus approach to permit the comparison of outcomes for patients with NBL around the world. In 2005, representatives from pediatric cooperative NBL groups worldwide met to devise a new International Neuroblastoma Risk Group (INRG) stratification. They reviewed data obtained from patients around the world between 1990 and 2002 to define a pre-surgical staging system that allows defining extent of disease at diagnosis in a uniform manner (Cohn, Pearson et al. 2009, Monclair, Brodeur et al. 2009).

The prognosis significance of 13 factors was tested in order to find the best ones to define homogeneous patient cohorts. Stage, age, histologic category, grade of tumor differentiation, amplification status of the *MYCN* oncogene, presence/absence of chromosome 11q aberrations and DNA ploidy were found to be the most relevant markers for patient stratification.

Stage

The International Neuroblastoma Risk Group designed a new clinical staging system (INRGSS) with the premise that a staging system based on preoperative diagnostic image will be more robust and reproducible that one based on operative approaches. So this system is based on clinical criteria and the so called image-defined risk factors (IDRFs). IDRFs consist of features

detected by imaging technologies that will make impracticable a safe tumor excision, such as compression or invasion of other tissues and organs (Monclair, Brodeur et al. 2009).

Patients are subdivided in stages as indicated in Table 2.

Table 2. International Neuroblastoma Risk Group staging. Adapted from (Monclair, Brodeur et al. 2009)

Stage	Description
L1	Localized tumor confined to one body compartment and not involving vital structures
L2	Locoregional tumor with presence of one or more image-defined risk factors
M	Distant metastatic disease, except those included in stage MS
MS	Metastatic disease in children younger than 18 months. Metastases confined to skin, liver and/or bone marrow

Age at diagnosis

Age is an important clinical prognostic factor. The predictive ability of age has shown to be continuous, because outcome gradually worsens with increasing age (Figure 8A). However, using two age groups was considered more feasible for patient classification and the optimal "cutoff" was set at 18 months (Figure 8B) (London, Castleberry et al. 2005, Cohn, Pearson et al. 2009). In fact, other authors also report that younger children mainly show localized tumors while metastases are more frequent in older children (Sano, Bonadio et al. 2006).

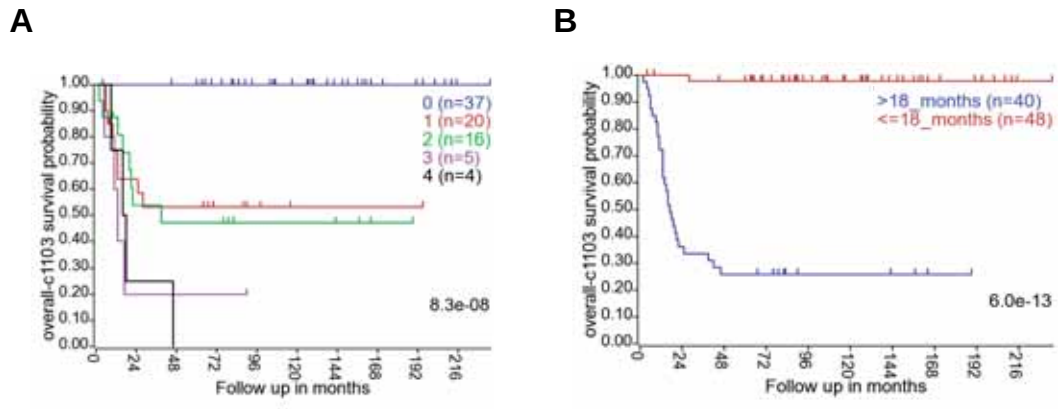

Figure 8. Overall survival curves correlating age at diagnosis with patient survival. A, Overall survival decreases dramatically with the increase of age. **B**, Patients can be divided in two age groups (<18 or ≥18 months), maintaining the prognostic precision. Data obtained from GSE16476.

Histology and grade of differentiation

NBLs are also known as "small blue round cell tumors", since the typical NBL is composed of small, uniformly sized cells containing dense hyperchromatic nuclei and scant cytoplasm. The differentiation state of the tumor, as explained before, has prognostic significance by itself and

has been previously used for patient stratification (Shimada, Chatten et al. 1984, Shimada, Umehara et al. 2001).

MYCN amplification

Amplification of the *MYCN* oncogene at 2p24 was first described by Schwab and collaborators in 1983 (Schwab, Alitalo et al. 1983) and is one of the few prediction markers for poor outcome (Westermark, Wilhelm et al. 2011). It occurs in about 20% of all NBLs, mainly associated to the most aggressive tumors, advanced stages and poor prognosis (Figure 9) (Reviewed in (Fisher and Tweddle 2012)). *MYCN* amplification status is routinely used in clinical practice to assign therapeutic intensity and predict prognosis.

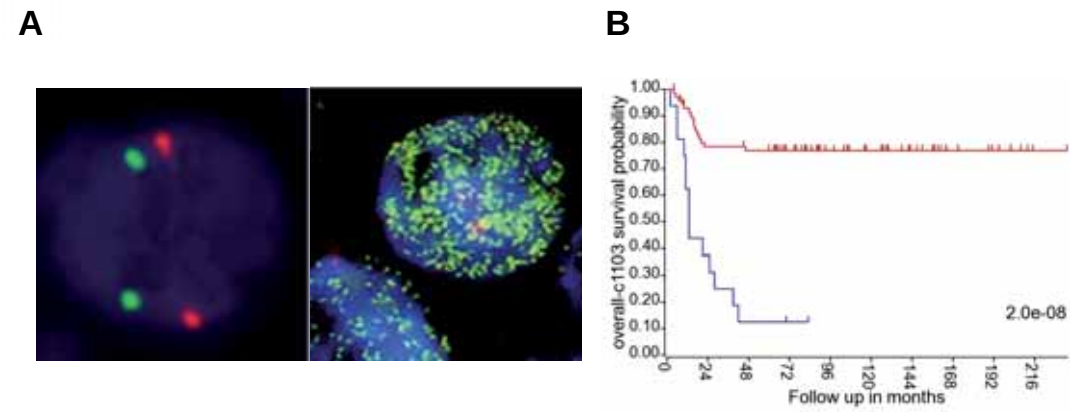

Figure 9. *MYCN* amplification in high-risk NBL. A, *MYCN* amplification (green) demonstrated by fluorescence in situ hybridisation (FISH). *CEP2* probes (red) hybridize with centromeric regions. Left image shows non-altered cells, while right image displays *MYCN*-amplified NBL cells. Image adapted from (Wang, Zhou et al. 2013). **B**, Kaplan-Meier curve based on *MYCN* amplification. Data obtained from GSE16476.

Chromosome 11q

Allelic loss or imbalance of chromosome 11q occurs in 35-40% of NBLs. Although loss of 11q is associated with unfavorable NBL, it inversely correlates with *MYCN* amplification. Thus, 11q deletions and *MYCN* amplification appear to represent two distinct subgroups of aggressive NBLs at the molecular level (Ora and Eggert 2011).

In a study of 1000 patients performed by the Children's Oncology Group, unbalanced deletion of 11q showed to be an independent prognostic factor for outcome in a multivariate analysis (Attiyeh, London et al. 2005).

DNA ploidy

DNA index is also a prognostic marker, especially for patients younger than 2 years who have disseminated disease. NBLs can be divided into those with a near-diploid nuclear DNA content and those near-triploid tumors. Near-triploid tumors are characterized by whole chromosome gains and losses, importantly without structural genetic aberrations. For this reason, near-triploid tumors are more often localized and show a favorable outcome. Near-diploid NBLs are characterized by the presence of genetic aberrations and chromosomal reorganizations that often enhance tumor aggressiveness. It seems that less aggressive tumors have a defect in mitosis, associated with whole chromosome gains and losses, while malignant NBLs show genomic instability, resulting in chromosomal rearrangements and unbalanced translocations (Brodeur 2003) (Maris, Hogarty et al. 2007).

Taking into account these criteria, an INRG classification system was developed. Patients were divided into 16 pre-treatment groups (Table 3). However, based on 5-year event-free survival, these 16 groups could be arranged into four risk categories: very low risk (EFS more than 85%), low risk (EFS between 75% and 85%), intermediate risk (EFS between 50% and 75%) or high risk (EFS less than 50%).

Table 3. International Neuroblastoma Risk Group Consensus Pre-treatment Classification Schema. Adapted from (Cohn, Pearson et al. 2009).

INRG stage	Age (months)	Histologic category	Grade of differentiation	*MYCN*	11q Aberration	Ploidy	Pretreatment risk group
L1/L2		GN maturing; GNB intermixed					Very low
L1		Any, except GN maturing or GNB intermixed		NA			Very low
				Amp			High
L2	<18	Any, except GN maturing or GNB intermixed		NA	No		Low
					Yes		Intermediate
	≥18	GNB nodular; neuroblastoma	Differentiating	NA	No		Low
					Yes		Intermediate
			Poorly diff or undifferentiated	NA			Intermediate
				Amp			High
M	<18			NA		Hyperdiploid	Low
	<12			NA		Diploid	Intermediate
	12 to <18			NA		Diploid	Intermediate
	<18			Amp			High
	≥18						High
MS	<18			NA	No		Very low
					Yes		High
				Amp			High

GN, ganglioneuroma; GNB, ganglioneuroblastoma; Amp, amplified; NA, non-amplified; Diff, differentiated.

1.2. Therapy

1.2.1. Treatment overview

The therapeutic approach used to treat NBL is based upon a patient's risk stratification. After assigning a patient to a risk group, clinicians assess the requirement for surgical resection, chemotherapy or radiotherapy, following the general principles that are outlined here:

Low-risk tumors show excellent survival rates with surgical resection as the unique treatment. This therapy is chosen for localized and resectable tumors, including those of stage 1, 2A, 2B (L1) and stage 4S *MYCN* non-amplified with favorable characteristics. In some cases of recurrence, progressive disease, or organ dysfunction due to the tumor mass, chemotherapy is used as a complementary treatment (Maris, Hogarty et al. 2007).

Intermediate-risk group includes a wide spectrum of the disease that generally is treated with surgical resection and moderate-dose multi-agent chemotherapy. With this strategy, survival rates for tumors of stage 3 and 4 with favorable behavior are higher than 95% (Maris, Hogarty et al. 2007). In fact, international groups have successfully reduced chemotherapy doses to minimize acute and long-term toxicity of the treatment, maintaining excellent survival rates (Baker 2007).

High-risk tumors, which account for 50% of NBL cases, remain the main challenge for pediatric oncologists. This group consists of *MYCN*-amplified tumors of all stages and metastatic stage 4 over the age of 18 months (INRG group M). Standard therapy for high-risk tumors includes at least 4 phases: induction therapy, local control, consolidation therapy, and biological agents to treat minimal residual disease (Owens and Irwin 2012). This protocol has evolved during the last 20 years, based on international cooperative groups, and is detailed here:

Induction therapy

The main goal of induction therapy is to reduce the entire tumor burden – both at the primary site and metastases – in order to ease the later surgical resection. Induction therapy consists of a combination of chemotherapeutic agents including anthracyclines, alkylators, platinum compounds and topoisomerase II inhibitors. This combination is known as COJEC: cisplatin, vincristine, carboplatin, etoposide, and cyclophosphamide (Owens and Irwin 2012). At Vall d'Hebron Hospital, COJEC is administered during three months at 10-day intervals (Figure 10).

Local control

An efficient surgical resection of the primary tumor, combined with radiotherapy at the primary site, strongly associates with complete remission of the tumor (Modak and Cheung 2010).

Consolidation therapy

The role of consolidation therapy is to remove any residual tumor cells after surgery. This phase has been one of the most recent improvements in overall survival (Adkins, Sawin et al. 2004). It is based on myeloablative chemotherapy cycles followed by autologous stem cell transplantation to re-populate the bone marrow. There are ongoing clinical trials to determine the best myeloablative chemotherapeutic approach: most current protocols use either carboplatinum/etoposide/melphalan or busulfan/melphalan (BuMel) as conditioning for autologous stem cell transplantation, often as randomized strategies (Owens and Irwin 2012). Patients at Vall d'Hebron Hospital are nowadays treated with the BuMel approach (Figure 10).

Biological therapy

Since relapse occurs frequently after autologous bone marrow transplantation, biological therapy has been included to eliminate persistent minimal residual disease. Differentiation is thought to play a major role in the spontaneous regression and/or maturation sometimes observed in these tumors, hence differentiating agents have been added to the therapeutic approach. The use of retinoids is widely extended, since they have shown to induce terminal differentiation and reduce proliferation of NBL cell lines (Encinas, Iglesias et al. 2000). Some reports show the benefits of the addition of immunotherapy to retinoids, which improves event-free survival. This has been achieved by the use of the anti-GD2 antibody ch14.18, interleukin 2 and GM-CSF (Yu, Gilman et al. 2010). The standard non-cytotoxic therapy consists of immunotherapy with monoclonal antibodies against GD2 and the differentiating agent 13-*cis*-retinoic acid, plus or minus IL-2.

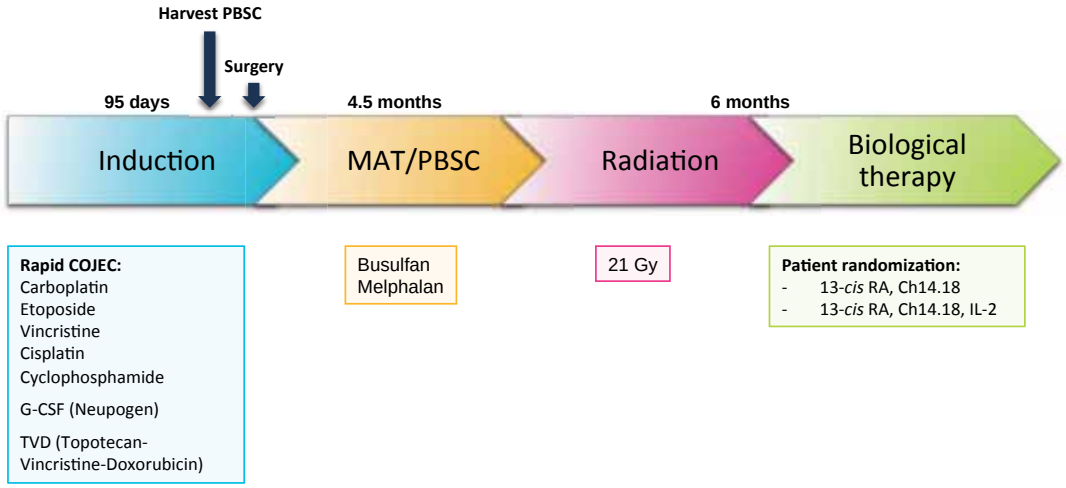

Figure 10. Treatment sequence for high-risk NBL at Vall d'Hebron Hospital. Induction therapy is accompanied by the growth factor G-CSF that stimulates the bone marrow to produce stem cells, granulocytes and neutrophils. When no response to COJEC is achieved, two doses of TVD are administered at the end of this phase. Induction is followed by a BuMel myeloablative therapy (MAT) and autotransplantation of peripheral blood stem cells (PBSC). After radiation, patients are randomized into two biological therapy strategies, including retinoids, the anti-GD2 antibody Ch14.18 and IL-2 (Aldesleukin).

Despite these improvements in NBL treatment, the prognosis for patients assigned to the high-risk group remains very poor: only 50% of patients with newly diagnosed aggressive tumors and less than 10% of patients with recurrent disease will survive (Park, Bagatell et al. 2013).

Many patients experience tumor recurrence soon after the treatment, especially those with *MYCN* amplification, and more than half of the long term survivors suffer from late sequelae, like high frequency hearing loss and endocrine defects (Hobbie, Moshang et al. 2008). For this reason, more effective therapies with less long-term sequelae are urgently needed, opening the door to novel targeted therapies.

1.2.2. Targeted therapies

In order to improve high-risk NBL outcome, there is extensive laboratory research and some early clinical trials investigating antibodies and small molecule inhibitors directly targeting relevant pathways implicated in NBL proliferation or antigens frequently expressed in NBL tumors. Below are summarized some of these approaches.

1.2.2.1. Targeting the human norepinephrine transporter with MIBG

^{131}I-metaiodobenzylguanidine (MIBG) is an aralkylguanidine norepinephrine analogue originally developed to visualize tissue of sympathetic neural origin (Matthay, Shulkin et al. 2010). It has recently been introduced for targeted radiopharmaceutical treatment for high-risk tumors. This molecule targets the norepinephrine transporter, which is present in 90% of NBLs, for cell specific uptake. Then, it destroys cells by directed radiation (Carlin, Mairs et al. 2003).

Early clinical trials in relapsed NBLs showed that this molecule produced significant response rates and that the principal acute toxicity was myelosuppression, which could be abrogated by hematopoietic stem cell transplant (Hutchinson, Sisson et al. 1992, Matthay, DeSantes et al. 1998). It has also been tested in combination with chemotherapy or other radiosensitizers (DuBois and Matthay 2008, DuBois, Chesler et al. 2012).

^{131}I-MIBG is a promising strategy and its practicability is rapidly increasing, with several pediatric centers in North America and in Europe that regularly administer this therapy (Matthay, George et al. 2012).

1.2.2.2. Anti-GD2 Immunotherapy

The surface glycolipid disialoganglioside (GD2) is expressed on more than 98% of NBLs, and other tumors as melanoma, glioma and sarcomas. In normal tissues, GD2 expression is weak and exclusively restricted to neurons, melanocytes and peripheral pain fibers (Hara 2012). Thus, GD2 becomes a great antigen for immunotherapy of these tumors.

Many monoclonal GD2-directed antibodies – murine, chimeric and humanized – have been developed and investigated in phase I and II studies. They have been combined with IL-2 and tested on high-risk NBL patients, with pain as the main toxic effect. Since GD2 antibody treatment only achieves partial responses, the treatment is nowadays used to eliminate minimal residual disease (Cheung, Lazarus et al. 1987, Cheung, Kushner et al. 1998, Matthay, George et al. 2012). Even more, given the documented synergism in other cancer types between chemotherapy and anti-cancer monoclonal antibodies (mAbs), such as trastuzumab (Slamon, Leyland-Jones et al. 2001), it will be interesting to assess the effectiveness of combining anti-GD2 mAbs with chemotherapy.

1.2.2.3. ALK inhibitors

The newly developed targeted therapy for NBL is the use of inhibitors against the ALK tyrosine kinase receptor. ALK-targeted therapies are a new but promising strategy, firstly because ALK

is expressed on the surface of most NBL cells, acting as a tumor-associated antigen (Lamant, Pulford et al. 2000). And most importantly, ALK inhibition (either wildtype or mutated) in these cells leads to cell death (Carpenter and Mosse 2012).

In this line, ALK inhibitors have been previously developed for adult tumors with *ALK* translocations, such as anaplastic large cell lymphoma, non-small cell lung cancer and inflammatory myofibroblastic tumors. The first drug approved by the FDA for the treatment of ALK-rearranged cancers was crizotinib (PF2341066; Pfizer), which binds to the inactive conformation of ALK and has shown remarkable effects in adult tumors (Christensen, Zou et al. 2007, Butrynski, D'Adamo et al. 2010, Gambacorti-Passerini, Messa et al. 2011). Currently, crizotinib is being tested in phase I and II trials for NBLs and other pediatric malignancies bearing ALK mutations and rearrangements (Clinical trial identifier NCT00939770, ClinicalTrials.gov). However, inhibition of mutated ALK is complex when compared with translocated ALK and remains a therapeutic challenge.

1.3. Resistance to therapy

Cancer cells may either exhibit a significant primary resistance to chemotherapeutic drugs (intrinsic resistance), or acquire characteristics of multidrug resistance (MDR) during chemotherapy (acquired resistance). The presence of a MDR phenotype of cancer cells severely limits the success of anti-cancer therapy. Three major mechanisms have been proposed to explain MDR in cancer (Figure 11) (Nooter and Stoter 1996, Szakacs, Paterson et al. 2006, Chai, To et al. 2010):

- Decreased uptake of water-soluble drugs, such as cisplatin, which requires transporters to enter cells.
- Changes in cancer cells that affect their susceptibility to cytotoxic drugs, including alteration of fundamental cellular processes, such as cell cycle control, apoptosis, DNA repair and metabolism of drugs.
- Increased energy-dependent efflux of hydrophobic cytotoxic drugs that enter cells by diffusion through the plasma membrane keeping intracellular concentrations below the cell-killing threshold. The efflux of cellular cytotoxic drugs is attributed to the overexpression or enhanced activity of a family of energy-dependent multi-drug transporters known as ATP-binding cassette (ABC) transporter proteins. These trans-

membrane proteins use the energy from the hydrolysis of ATP to actively export drugs from the cell, thus avoiding the drug-related toxic effects.

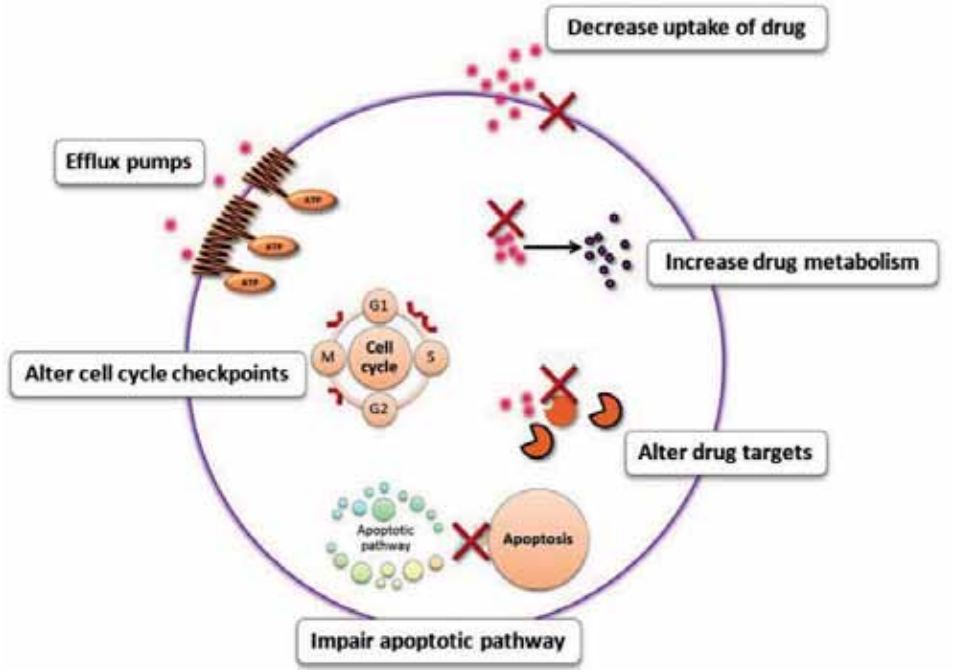

Figure 11. Mechanisms of multi-drug resistance of cancer cells. Transformed cells develop drug resistance by various mechanisms: reduced drug uptake, increased drug metabolism, altered or mutated drug targets, defects in the apoptotic machinery, alterations in cell cycle checkpoints or reducing intracellular drug concentration by exporting the chemotherapeutic agent. Adapted from (Chai, To et al. 2010).

Most current treatment approaches primarily exert their antitumor activity by triggering programmed cell death. However, evasion of apoptosis is a hallmark of basically all human cancers, conferring resistance to treatment (Hanahan and Weinberg 2000). As it will be explained later, many alterations in apoptotic mechanisms have been described for NBL tumors.

1.3.1. Apoptosis

Apoptosis is a physiological mechanism of programmed cell death that is crucial to control the number of cells during the development as well as during the entire life of an organism. De-regulation of apoptosis signaling may break the homeostasis of an organism and cause a wide range of pathologies.

This process was first described by Kerr, Wyllie and Currie in 1972 (Kerr, Wyllie et al. 1972) in order to define the morphological characteristics of the dying cell. The main morphological features characterizing apoptosis are loss of adhesion and rounding of adherent cells, cell shrinkage, chromatin condensation, nuclear fragmentation, formation of irregular bulges in the plasma membrane known as *blebbing*, and the formation of the apoptotic bodies, without structural alterations in the organelles (Saraste and Pulkki 2000) (Figure 12). These apoptotic bodies are later engulfed by macrophages through a process called phagocytosis without releasing intracellular contents and causing inflammation in the surroundings of the dying cell (Arends and Wyllie 1991, Cohen, Duke et al. 1992, Cohen 1994).

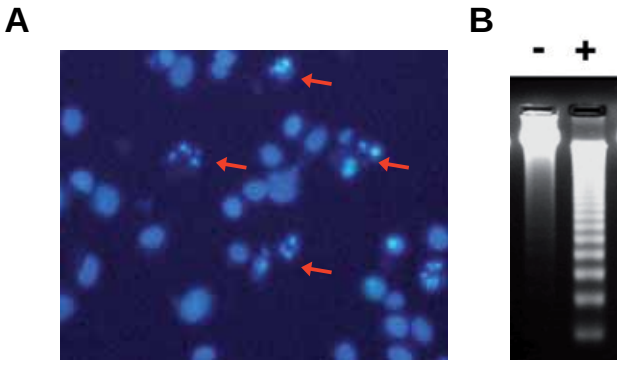

Figure 12. Hallmarks of apoptosis. A, Hoechst 22258 staining of apoptotic cells shows condensed chromatin and fragmented nucei (red arrows). **B,** Ladder resulting from oligonucleosomal DNA degradation after an apoptotic stimulus (+). Adapted from (Iglesias-Guimarais, Gil-Guinon et al. 2013).

All morphological changes are consequence of biochemical events that lead to disassemble and remove the cell. The main biochemical processes that take place during apoptosis are internucleosomal DNA degradation that can be visualized as DNA "ladders" when the nucleic acid is run on an agarose gel (Figure 12B) (Cohen, Sun et al. 1994), externalization of the phospholipid phosphatidylserine in order to allow macrophage recognition of the apoptotic cell (Martin, Reutelingsperger et al. 1995) and a complex cascade of proteolytic signaling (Martin and Green 1995).

1.3.1.1. Classical apoptotic pathways

There are two main apoptotic pathways that differ in the initial apoptotic stimuli and the mediators that are involved (Hengartner 2000). Initiation of apoptosis occurs through either intrinsic or extrinsic pathway (Figure 13), as detailed here:

The **intrinsic pathway**, also known as the mitochondrial pathway is activated in response to extracellular cues and internal insults such as DNA damage (Mignotte and Vayssiere 1998). This pathway proceeds through the mitochondria and involves the permeabilization of the outer mitochondrial membrane (MOMP) and the release of cytochrome *c*, a component of the respiratory chain, from the intermembrane space of the mitochondria into the cytoplasm. Cytoplasmatic cytochrome *c* then associates with APAF-1 (apoptotic protease activating factor-1) and caspase-9 to form the apoptosome. This structure will activate caspase-9 through dimerization and caspase-9, in turn, will cleave and activate downstream effector caspases, such as caspase-3 (Cai, Yang et al. 1998, Slee, Harte et al. 1999).

The **extrinsic pathway** originates at the plasma membrane when a specific extracellular ligand binds a cell surface transmembrane death receptor (DR), inducing its trimerization (Ashkenazi and Dixit 1999). Receptor clustering induces in turn the recruitment of adaptor proteins to the intracellular domain of the receptor in order to form a complex known as death-inducing signaling complex (DISC). These proteins bind the pro-domain of initiator caspases (i.e. caspase-8), promoting their dimerization and activation through "induced proximity" (Kischkel, Hellbardt et al. 1995). Caspase-8 activation can be blocked by recruitment of DR-antagonists such as the caspase homologue c-FLIP (Scaffidi, Schmitz et al. 1999), $FAIM_L$ (Segura, Sole et al. 2007) or Lifeguard (Fernandez, Segura et al. 2007). When caspase-8 becomes active, it can directly cleave and activate effector caspases, like caspase-3, that will cleave multiple substrates to induce cell death.

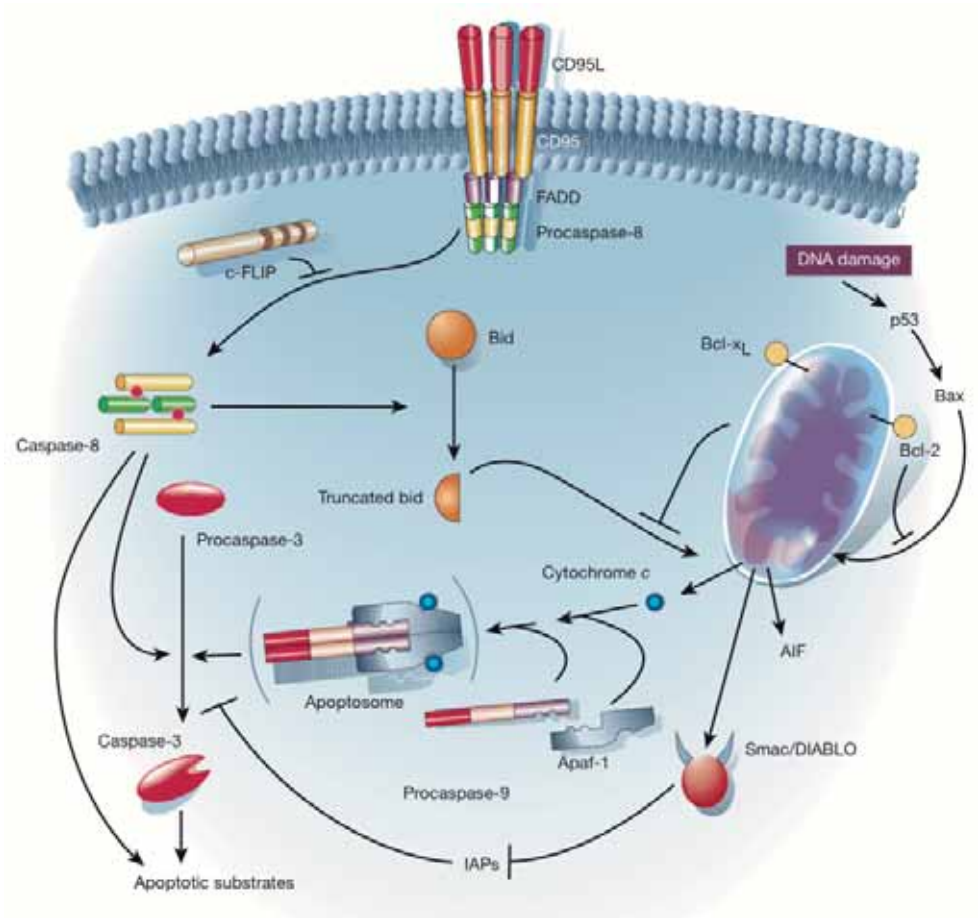

Figure 13. Intrinsic and extrinsic apoptotic pathways. The DR pathway (left) is triggered by members of the DR superfamily, such as Fas/CD95. The intrinsic pathway initiates at the mitochondria (right) in response to stimuli such as DNA damage. Both pathways trigger a proteolytic cascade and subsequent cell death. Adapted from (Hengartner 2000).

Both pathways converge at the level of caspase-3 activation, yet there is a crosstalk between them upstream caspase-3 activation. Integration between the DR and mitochondrial pathways is provided by BID. BID is a pro-apoptotic BCL-2 family member that can be cleaved by caspase-8 into tBID. The resulting resulting truncated form can be then translocated to the mitochondria, where it promotes its permeabilization and cytochrome *c* exit (Gross, Yin et al. 1999).

1.3.1.2. Mediators of apoptosis

1.3.1.2.1. Caspases

Caspases are the central mediators of apoptosis and the major responsible of all the previously stated morphological changes. They are a group of proteases specifically activated in apoptotic cells that are highly conserved between organisms. As their name indicates, Caspases are cysteine proteases that preferentially break bonds at aspartate residues (Cysteine-Aspartate Proteases). Given the critical role they play during apoptosis, and that they provoke irreversible changes within the dying cell, their activity must be highly specific and regulated. Caspases are synthesized as inactive zymogens without significant enzymatic activity and become active after being cleaved by another protease or by auto-activation. The basic structure of the pro-enzyme consists of an amino-terminal pro-domain and a carboxy-terminal protease domain, which contains the catalytic cystein residue (Figure 14) (Zimmermann, Bonzon et al. 2001, Shi 2002).

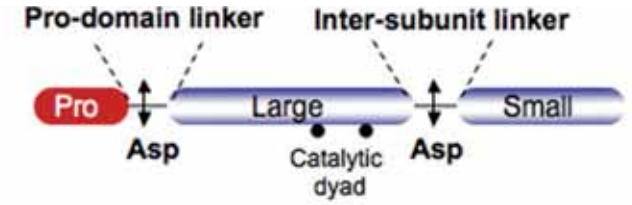

Figure 14. Pro-caspase organization. A prodomain precedes the catalytic domain, composed of two covalently linked subunits. Sites for (auto)proteolysis at Asp residues are indicated. Adapted from (Pop and Salvesen 2009).

During the last decades, 14 distinct caspases have been identified in mammals, 11 of them found in humans, and not all of them are involved in the apoptotic process (Riedl and Shi 2004). Caspases involved in apoptosis are divided into two classes, based on the position they occupy in the signaling cascade:

- Initiator caspases in mammals include caspase-2, -8, -9, and -10. This group acts apically in the apoptotic pathway and shares a common structure that consists of long pro-domains that include sequence motifs that promote their interaction with initiator molecules (a caspase-recruitment domain, named CARD, or a death effector domain, known as DED). These caspases are activated through “induced proximity” when their pro-domains interact with adaptor proteins that induce caspase dimerization (Bouchier-Hayes and Martin 2002, Valmiki and Ramos 2009).

- Effector caspases, which in mammals are caspase-3, and -7. These caspases are downstream the initiator enzymes and generally have shorter pro-domains. These enzymes exist in the cell as preformed homodimers that become active after cleavage mediated by an initiator caspase. When activated, they act on multiple and specific cellular substrates to dismantle the cell (Thornberry and Lazebnik 1998).

1.3.1.2.2. Inhibitor of Apoptosis Proteins

Inhibitor of apoptosis proteins (IAPs) are a conserved family of proteins that block cell death induced by a wide spectrum of apoptotic stimuli, including DRs, viral infection, growth factor withdrawal, radiation or chemotherapeutic agents (LaCasse, Baird et al. 1998, Deveraux and Reed 1999). IAPs were first identified in baculovirus as a mechanism to inhibit the apoptotic response of the host cell and allow viral propagation (Crook, Clem et al. 1993), but subsequently they were found in a range of species from *Drosophila* to vertebrates. This group of proteins is defined by the presence of at least one Baculovirus IAP Repeat (BIR) domain within the protein. BIR is a conserved zinc-binding fold of 70 amino acids that mediates protein-protein interaction and is essential for caspase inhibition (Silke and Vaux 2001). There are eight human IAPs described so far: X-linked Inhibitor of Apoptosis Protein (XIAP), cellular IAP1 (cIAP1), cellular IAP2 (cIAP2), IAP-Like Protein 2 (ILP2), Melanoma Inhibitor of Apoptosis Protein (ML-IAP), Neuronal IAP (NIAP), Survivin and BIR-containing Ubiquitin Conjugating Enzyme (BRUCE) (Figure 15).

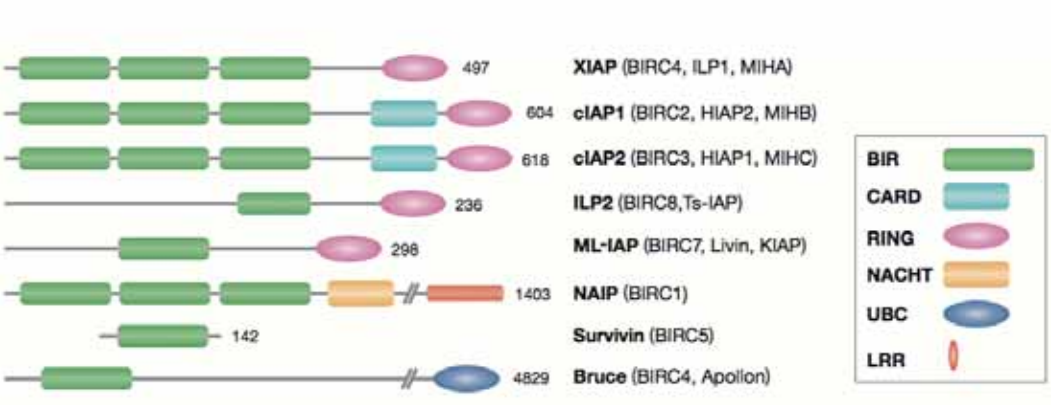

Figure 15. Human inhibitor of apoptosis protein family. IAPs contain between one and three BIR domains that allow them to interact with proteins such as TRAF2, caspases, and IAP antagonists. In addition, they include other functional domains. The RING domain confers IAPs E3 ligase activity that induces ubiquitin-proteasome degradation of its targets. CARDs are Caspase-Recruitment Domains that mediate protein-protein interactions and also prevent E3 ligase activity by blocking RING dimerization and blocking E2 binding and activation (Blankenship, Varfolomeev et al. 2009, Lopez, John et al. 2011), reviewed in (Darding and Meier 2012). The Ubiquitin-conjugation (UBC) domain binds to ubiquitin chains. Adapted from (Eckelman, Salvesen et al. 2006).

Among these proteins, cIAP1, cIAP2 and XIAP are the ones with the most remarkable role on DR-induced apoptosis. They all contain three BIR domains and one RING domain (Figure 15) and are able to bind caspases (Eckelman, Salvesen et al. 2006). XIAP can directly bind and inhibit the effector caspases -3 and -7 through its second BIR domain and the initiator caspase-9 through its third BIR domain (Deveraux, Leo et al. 1999, Silke, Ekert et al. 2001). XIAP overexpression efficiently inhibits caspase activation and cell death induced both by the mitochondrial or the extrinsic pathways (Deveraux, Takahashi et al. 1997, Wilkinson, Cepero et al. 2004). Moreover, the single BIR2 domain of XIAP has been reported to be sufficient to inhibit caspases -3 and -7 and partially block FasL-induced apoptosis (Takahashi, Deveraux et al. 1998). This inhibitory action of XIAP can be antagonized by mitochondrial proteins such as SMAC/DIABLO, which are released during an apoptotic stimulus (Du, Fang et al. 2000). cIAP1 and cIAP2 were initially thought to directly bind and inhibit caspases in the same way as XIAP (Roy, Deveraux et al. 1997). However, even though they are the closest paralogues of XIAP, they can bind caspases but are not able to directly inhibit them due to critical substitutions in the regions that target caspase inhibition found in XIAP (Eckelman and Salvesen 2006). The mechanism by which cIAPs have been reported to inhibit caspases is by ubiquitination, targeting them for proteasomal degradation (Choi, Butterworth et al. 2009).

IAPs have an important role in cell survival and tumorigenesis, since they positively regulate NF-κB signaling through non-degradative ubiquitination of components within the pathway. cIAP1 plays a role in TNFα-induced NF-κB activation by ubiquitylating several components of TNF-R1 complex I, including RIP1 and cIAP1 itself, and promoting a Ub-dependent stabilization of the complex. Thus, loss of cIAP1 completely abrogates ubiquitylation of RIP1 and NF-κB activation (Bianchi and Meier 2009). Interestingly, NF-κB induces expression of cIAP1, cIAP2, and XIAP, thereby promoting its activation in a positive feedback loop (Jin, Lee et al. 2009).

Survivin has a special interest in oncology, as its overexpression has been widely demonstrated to occur in various types of cancer, including NBLs (Azuhata, Scott et al. 2001, Cheung, Huang et al. 2013, Coumar, Tsai et al. 2013). Indeed, high survivin levels often correlate with tumor progression, aggressiveness and resistance to therapy (Azuhata, Scott et al. 2001, Waligorska-Stachura, Jankowska et al. 2012, Cheung, Huang et al. 2013). Unlike other IAPs, survivin is not expressed in differentiated normal tissues, but only during embryonic and fetal developmental stages (Cheung, Huang et al. 2013). Besides apoptosis inhibition, many roles have been attributed to survivin, such as inhibition of autophagy (Roca, Varsos et al. 2008), an important implication in mitosis (Kelly, Ghenoiu et al. 2010) and a role in enhancing DNA repair capability in cancer cells (Jiang, Ren et al. 2009) [For review, see (Coumar, Tsai et al. 2013)].

1.3.1.2.3. BCL-2 family

BCL-2 (B-cell lymphoma 2) was first identified as a proto-oncogene in a chromosome translocation breakpoint in follicular B-cell lymphoma. This translocation caused a relocation of the immunoglobulin heavy chain gene, joining it to the gene *BCL2* (Bakhshi, Jensen et al. 1985, Cleary and Sklar 1985, Tsujimoto, Gorham et al. 1985). As a result, overexpression of BCL-2 was able to block apoptotic cell death (Vaux, Cory et al. 1988). Thus, *BCL2* was identified as the first oncogene that inhibited cell death, instead of promoting cell proliferation. Later, it was recognized as a mammalian homologue of the apoptosis repressor ced-9 in *C. elegans*, unraveling that cell death components are highly conserved throughout evolution (Vaux 1993, Hengartner and Horvitz 1994). Since then, at least 19 members of this family have been identified in mammalian cells. Their complex network of interactions regulates cytochrome *c* release, a key step in apoptosis, thus determining the cell fate (Garcia-Saez 2012). The dynamics of this regulation are still controversial, and different models have been developed to explain the interactions between different BCL-2 family members that lead to MOMP (Kuwana, Bouchier-Hayes et al. 2005, Willis, Fletcher et al. 2007, Edlich, Banerjee et al. 2011, Llambi, Moldoveanu et al. 2011).

Proteins of the BCL-2 family are classified into three groups, depending on their structure and function (Garcia-Saez 2012) (Figure 16).

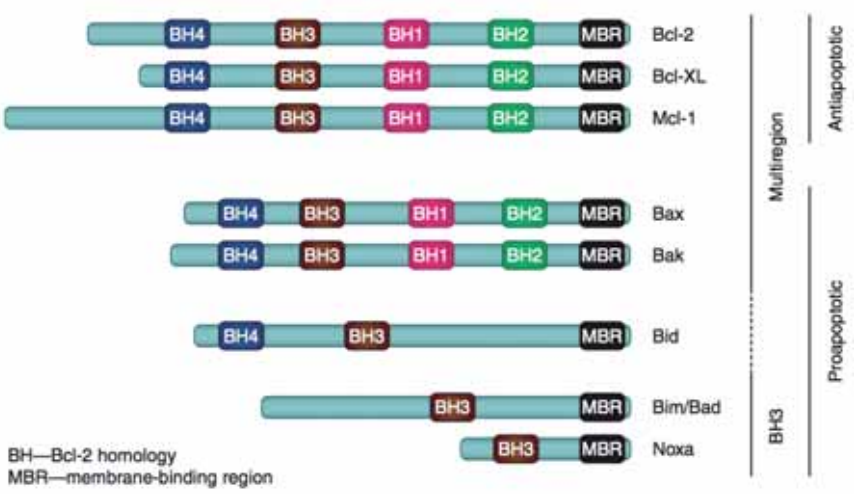

Figure 16. Members of the BCL-2 family. All members possess at least one of four conserved motifs known as BCL-2 Homology domains (BH1, BH2, BH3 and BH4). Anti-apoptotic proteins possess all four BH domains and inhibit apoptosis by interacting with the pro-apoptotic members of the family. Pro-apoptotic members are grouped into two subfamilies: the multi-domain members, which promote MOMP, and the BH3-only proteins. Adapted from (Shamas-Din, Kale et al. 2013).

After an apoptotic stimulus, the pro-apoptotic BCL-2 family members are activated and promote MOMP. It has been reported that the pro-apoptotic multi-domain members BAX and BAK are the final effectors of MOMP, since double knock-out for *bax* and *bak* cells (and no simple knockouts) become resistant to MOMP induction (Wei, Zong et al. 2001). Upon activation, BAX and BAK change their conformation, insert into the outer mitochondrial membrane and oligomerize to induce its permeabilization (reviewed in (Czabotar, Lessene et al. 2014)). Consequently, proteins contained within the mitochondrial inter-membrane space are released, including the key player cytochrome *c*.

1.3.1.2.4. Death receptors and ligands

DRs belong to the TNFR family (Tumor Necrosis Factor Receptor Family), which comprises around 27 members and encompasses a range of functions related to apoptosis, proliferation and differentiation (Locksley, Killeen et al. 2001, Bhardwaj and Aggarwal 2003). All members of this family are characterized by the presence of two to five copies of cysteine-rich extracellular repeats. DRs are type I transmembrane proteins, exposing their N-terminal domain to the extracellular part of the cell, while the C-terminal domain is intracellular (Tartaglia, Ayres et al. 1993, Curtin and Cotter 2003). The basic structure of DRs consists of cysteine-rich extracellular domains, one single transmembrane domain and an intracellular Death Domain (DD) of around

80 amino acids that interacts with adaptor proteins and recruits them to the signaling complex (Wilson, Dixit et al. 2009).

Eight human DRs are known to date (Figure 17). These are tumor necrosis factor receptor 1 (TNFR1; also known as DR1, CD120a, p55 and p60) (Fuchs, Strehl et al. 1992), CD95 (also known as DR2, APO-1 and Fas), DR3 (also known as APO-3, LARD, TRAMP and WSL1) (Chinnaiyan, O'Rourke et al. 1996, Marsters, Sheridan et al. 1996, Bodmer, Burns et al. 1997), TNF-related apoptosis-inducing ligand receptor 1 (TRAILR1; also known as DR4 and APO-2) (Pan, O'Rourke et al. 1997), TRAILR2 (also known as DR5, KILLER and TRICK2) (Schneider, Bodmer et al. 1997, Schneider, Bodmer et al. 1997), DR6 (Pan, Bauer et al. 1998), ectodysplasin A receptor (EDAR) (Mikkola, Pispa et al. 1999) and nerve growth factor receptor (NGFR or $p75^{NTR}$) [Reviewed in (French and Tschopp 2003, Wajant 2003)].

There is an additional group of related receptors known as decoy receptors, which lack the intracellular DD signaling motif and function as inhibitors of apoptosis by acting as dominant negatives (Ashkenazi and Dixit 1999). Therefore, decoy receptors operate as a system that modulates cell sensitivity to death ligands and death receptor signaling *in vivo*. Four decoy receptors have been identified so far: DcR1 (Sheridan, Marsters et al. 1997), DcR2 (Marsters, Sheridan et al. 1997), DcR3 (Pitti, Marsters et al. 1998,) and osteoprotegerin (OPG) (Simonet, Lacey et al. 1997) [Reviewed in (Lavrik, Golks et al. 2005)].

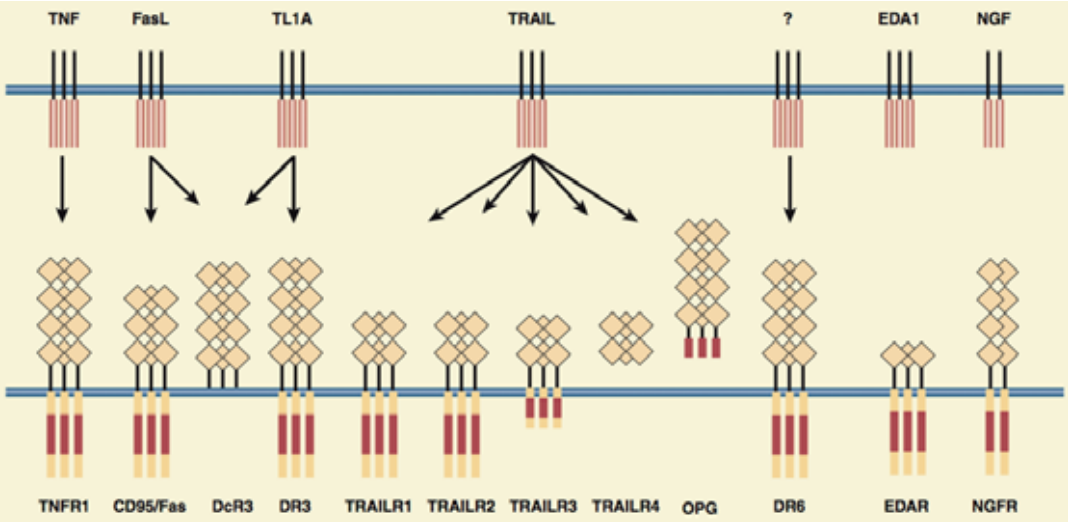

Figure 17. Death ligands and receptors. Ligands are represented on their membrane-bound form. Both functional receptors and decoy receptors are illustrated on this figure. Cysteine-rich motifs are represented as diamonds, transmembrane domains as black lines and cytoplasmic death domains are indicated in red. Adapted from (Lavrik, Golks et al. 2005).

Triggering DRs by their specific ligands causes the rapid recruitment of molecules to their cytoplasmic DD and the formation of the DISC. This domain is responsible for coupling the DR either to a cascade of caspases, leading to induction of apoptosis, or to the activation of kinase signaling pathways, resulting in pro-survival signals.

Differences found in the extracellular and intracellular domains of DRs determine both their affinity for different ligands and the recruitment of different adaptor proteins leading to the formation of signaling complexes with different fates. Thus, two types of DR signaling complexes can be distinguished. The first group comprises the DISCs that are formed at the CD95 receptor, TRAILR1 or TRAILR2. All three receptors recruit DISCs containing the adaptor protein FADD (Fas Associated Death Domain). In these cases, DISC formation results in the activation of caspase-8 and transduction of the apoptotic signal. The second group comprises the TNFR1, DR3, DR6 and EDAR. These recruit TRADD as an adaptor to form a protein complex that can transduce both apoptotic and survival signals (Chinnaiyan, O'Rourke et al. 1996, Marsters, Sheridan et al. 1996, Peter and Krammer 2003, Ermolaeva, Michallet et al. 2008, Pobezinskaya, Kim et al. 2008, Wilson, Dixit et al. 2009). It has been demonstrated that TRAIL receptors can also recruit TRADD in some situations, including pro-survival signaling (Varfolomeev, Maecker et al. 2005, Cao, Pobezinskaya et al. 2011).

1.3.1.2.5. Death receptor antagonists

DR signaling can be modulated at different levels by their post-translational modification or through the activity of several types of molecules, such as decoy receptors, IAPs and BCL-2 family members (Keppler, Peter et al. 1999, French and Tschopp 2003). In addition, there are other proteins capable of shutting down apoptotic signaling directly at the DR level. These proteins are known as death receptor antagonists. DR antagonists have a special interest in the nervous system, where DRs are involved in cell survival, differentiation and neuronal plasticity rather than cell death induction (Desbarats, Birge et al. 2003, Marchetti, Aucoin et al. 2004). Many evidences show that a variety of DR antagonists are expressed in the nervous system (Table 4):

Table 4. DR-antagonists expressed in the nervous system

Protein name	Alias
Zinc finger protein A20	A20
Bifunctional Apoptosis Regulator	BAR
Fas apoptosis inhibitory molecule	FAIM
Fas associated phosphatase-1	FAP-1
FLICE inhibitory protein	FLIP
Phosphoprotein Enriched in Astrocytes	PEA-15
Silencer of Death Domains	SODD
Small ubiquitin-related modifier 1	SUMO-1
Lifeguard	LFG

Zinc Finger protein A20

A20 was identified in endothelial cells as a primary response gene induced upon treatment with TNFα (Dixit, Green et al. 1990) and was initially characterized as an inhibitor of TNFα-induced apoptosis. It consists of a 80 kDa protein with seven Cys_2/Cys_2 zinc finger domains on C-terminal (Opipari, Boguski et al. 1990, Opipari, Hu et al. 1992). Stable overexpression of A20 in a panel of cell lines resulted in partial resistance to TNFα-induced apoptosis. This protection correlated with reduced collapse of mitochondrial membrane potential and decreased activation of caspase-3 (Beyaert, Heyninck et al. 2000). Apart from TNFα-induced apoptosis, A20 has also been shown to inhibit cell death by other stimuli as serum depletion (Varani, Dame et al. 1995), p53 overexpression (Fries, Miller et al. 1996), interleukin 1β (Jaattela, Mouritzen et al. 1996) or LPS (Hu, Yee et al. 1998).

Besides being an anti-apoptotic molecule, A20 is a ubiquitin-editing enzyme that potently suppresses NF-κB canonical pathway, while it functions as a positive regulator of the non-canonical pathway by promoting the stabilization of NIK (Yamaguchi, Oyama et al. 2013). As a NF-κB regulator, many studies highlight the role of this protein in inflammation and autoimmunity (Reviewed in (Catrysse, Vereecke et al. 2014)).

A recent study determined the regional distribution of A20 mRNA and protein levels in different brain regions, finding the highest levels in medulla and hippocampus (Pranski, Van Sanford et al. 2012). Some reports involve A20 in TRAIL and TNFα resistance of glioblastoma cells (Verbrugge and Johnstone 2012). More precisely, A20 seems to be overexpressed in glioblastoma stem cells, conferring them resistance to TNFα-mediated apoptosis. In this system, downregulation of A20 causes a decrease in cell proliferation and survival (Hjelmeland, Wu et al. 2010).

Bifunctional Apoptosis Regulator (BAR)

BAR was first discovered as an inhibitor of BAX-induced cell death by a yeast-two-hybrid approach (Zhang, Xu et al. 2000). This 450 kDa protein is mostly localized at the endoplasmic reticulum (ER) and antagonizes both intrinsic and extrinsic apoptotic stimuli. On the one hand, it interacts with BCL-2 and BCL-xL to supress BAX-induced cell death. On the other hand, BAR contains DED-like domains, which enable its interaction with DED-containing pro-caspases to suppress Fas-induced apoptosis. Furthermore, BAR is able to bridge procaspase-8 and BCL-2 into a protein complex capable of bridging the two major apoptosis pathways. This theory was supported by the fact that active caspase-8 subunits are sequestered to BCL-xL/BAR complexes, thus preventing further cleavage of caspase-8 substrates and apoptosis signaling (Stegh, Barnhart et al. 2002).

The role of BAR in the nervous system was later demonstrated by Roth and colleagues (Roth, Kermer et al. 2003). They provide evidence of BAR expression both in the central and peripheral nervous system and demonstrate that BAR overexpression/downregulation respectively protects or sensitizes neuronal cells from a broad range of cell death stimuli. These insults included treatment with the general kinase inhibitor staurosporine, serum starvation, TNFα and FasL stimulation and thapsigargin, a specific antagonist of the ER Ca^{2+}-ATPase that causes ER stress.

Fas Apoptosis Inhibitory Molecule (FAIM)

FAIM was initially isolated in B-lymphocytes as a protein that conferred resistance to Fas-induced cell death (Schneider, Fischer et al. 1999). Some years later, analysis of the genomic locus of FAIM identified two putative transcription initiation sites that generate two transcripts: the already isolated form, named $FAIM_S$, and a 22-aminoacids longer protein known as $FAIM_L$ (Figure 18) (Zhong, Schneider et al. 2001).

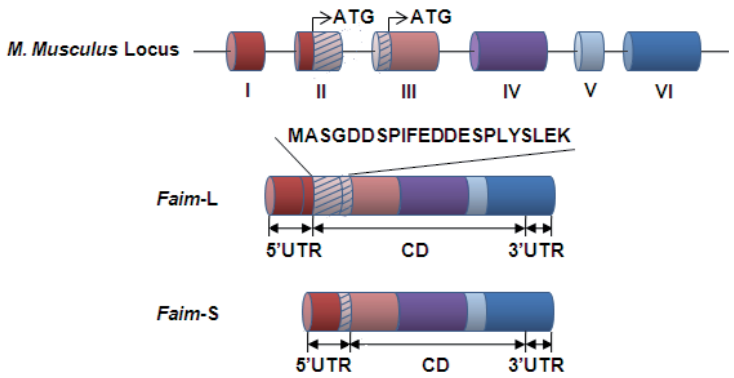

Figure 18. Genomic organization and splice variants of FAIM gene. The genomic structure of FAIM locus gives two alternative splicing results, $FAIM_S$ and $FAIM_L$, that share part of the 5'-UTR. The additional 22 amino acid sequence is indicated above the $FAIM_L$ scheme. Image from Atlas of Genetics and Cytogenetics in Oncology and Haematology, http://atlasgeneticsoncology.org (Segura, Sole et al. 2010).

Studies performed in our laboratory show that both isoforms are expressed in neurons, yet they have different physiological roles. On the one hand, $FAIM_S$ promotes neurite outgrowth in an ERK and NF-κB dependent manner in neuronal models such as the rat pheochromocytoma cell line PC12 and mouse primary neuronal cultures (Sole, Dolcet et al. 2004). However, it does not protect neurons from apoptotic stimuli such as FasL- or TNFα-induced cell death or trophic factor deprivation. On the other hand, $FAIM_L$ isoform is exclusively expressed in neurons and protects them from DR-induced cell death. Unlike $FAIM_S$, $FAIM_L$ is not required for neurite outgrowth. $FAIM_L$ can bind Fas receptor and prevent the activation of caspase-8, shutting down the apoptotic pathway at the level of the initiator caspases (Segura, Sole et al. 2007). Importantly, another mechanism of action has recently been described for $FAIM_L$ in our laboratory, downstream in the apoptotic pathway. We have demonstrated that $FAIM_L$ is an IAP-binding protein that interacts with XIAP, inhibiting its auto-ubiquitinylation and proteasomal degradation. Thus, $FAIM_L$ also protects neurons from apoptosis by stabilizing XIAP levels (Moubarak, Planells-Ferrer et al. 2013).

Fas-associated phosphatase-1 (FAP-1)

FAP-1 was also isolated by yeast-two-hybrid as a tyrosine phosphatase protein capable of interacting with the cytosolic domain of Fas. Upregulation of this protein partially abolished Fas-induced apoptosis in a T-lymphocyte derived cell line (Sato, Irie et al. 1995). Some years later, FAP-1 was shown to be expressed in several human cell types, including neurons, and also in the majority of cancers analyzed (Lee, Shin et al. 1999). FAP-1 might be promoting resistance to Fas-induced cell death by dephosphorylating tyrosine residues that could be necessary to recruit proteins such as FADD at the DISC (Foehr, Lorente et al. 2005). Other studies explain an alternative mechanism, where FAP-1 expression reduces the presence of Fas receptor at the plasma membrane (Ivanov, Lopez Bergami et al. 2003). Several authors relate FAP-1 expression to TRAIL, $p75^{NTR}$ and Fas resistance, and point it as a possible mechanism of tumor resistance to DR-induced apoptosis (Irie, Hachiya et al. 1999, Lee, Shin et al. 1999, Lee and Amoscato 2004, Yao, Song et al. 2004, Foehr, Lorente et al. 2005, Ivanov, Ronai et al. 2006,

Wieckowski, Atarashi et al. 2007). It has also been considered as a marker of chemo/radio sensitivity and prognosis for oral squamous cell carcinoma (Nariai, Mishima et al. 2011).

FLICE inhibitory protein (FLIP)

FLIP was first identified in 1997 as a viral protein (v-FLIP) in search for inhibitors of apoptosis induced by DRs (Thome, Schneider et al. 1997). Soon after characterization of v-FLIPs, human cellular homologues were identified (c-FLIPs). Three c-FLIP isoforms have been identified at the protein level: c-FLIP long (c-$FLIP_L$, 55kDa), c-FLIP short (c-$FLIP_S$, 27kDa) and c-FLIP Raji (c-$FLIP_R$, 25kDa) (Figure 19) (Irmler, Thome et al. 1997).

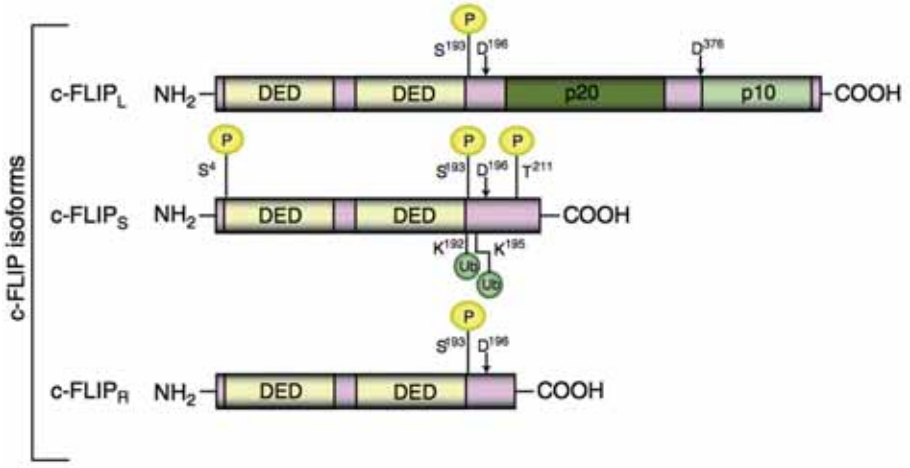

Figure 19. Human isoforms of c-FLIP. Three c-FLIP isoforms have been described, all of them containing two DEDs that are structurally similar to the N-terminal part of procaspase-8 and are required for the recruitment of c-FLIP at the DISC. The long form additionally carries two caspase-like subunits (p20 and p10), which are catalytically inactive due to critical amino acid substitutions. Moreover, it can be cleaved by caspase-8, generating the N-terminal fragments p22 and p43 of c-FLIP. Adapted from (Ozturk, Schleich et al. 2012).

c-FLIPs are well described inhibitors of DR-mediated apoptosis. It has been shown that c-FLIP blocks FasL, TRAIL and TNFα-induced apoptosis (Irmler, Thome et al. 1997, Scaffidi, Schmitz et al. 1999, Yeh, Itie et al. 2000, Krueger, Schmitz et al. 2001, Golks, Brenner et al. 2005). The short isoforms of c-FLIP block DR-induced apoptosis by binding to the DISC and inhibiting procaspase-8 processing and activation. However, the mechanism of action of the long isoform has been controversial. It has been shown that c-$FLIP_L$ can act similar to c-$FLIP_s$, and that c-$FLIP_L$ knockdown sensitizes cells towards DR-induced cell death (Sharp, Lawrence et al. 2005). Other reports suggest that c-$FLIP_L$ acts as a pro-apoptotic molecule by facilitating the activation of

caspase-8 at the DISC (Yeh, Itie et al. 2000, Chang, Xing et al. 2002, Micheau, Thome et al. 2002).

Besides their role as apoptosis modulators, c-FLIPs have an essential function in NF-κB activation (Hu, Johnson et al. 2000, Kataoka, Budd et al. 2000) and neuronal differentiation (Moubarak, Sole et al. 2010). Elevated c-FLIPs levels are found in many cancers, including NBL (Poulaki, Mitsiades et al. 2001, Fulda 2013). High levels of c-FLIP often correlate with more aggressive tumors that show resistance towards DR-induced cell death. This includes resistance to TRAIL, a promising cancer therapeutic since it is highly selective for malignant cells rather than normal cells. Downregulation of c-FLIP can overcome TRAIL resistance in several tumor cells (Safa, Day et al. 2008, Shirley and Micheau 2013). This renders c-FLIP as an important therapeutic target to restore apoptotic response in transformed cells.

Phosphoprotein Enriched in Astrocytes-15 (PEA-15)

PEA-15 is a 15 kDa cytosolic protein ubiquitously expressed in human tissues, but especially enriched in astrocytes (Araujo, Danziger et al. 1993). Many studies have revealed that PEA-15 serves as a multiprotein binding molecule that interacts and modulates the function of proteins involved in proliferation, apoptosis and glucose metabolism (Condorelli, Vigliotta et al. 1999, Renault, Formstecher et al. 2003, Vigliotta, Miele et al. 2004). It is highly expressed in the nervous system (Estelles, Yokoyama et al. 1996) and can be found in three different phosphorylation isoforms within the cell (Danziger, Yokoyama et al. 1995). In fact, two different serine phosphorylation sites have been identified: Ser_{104}, which is a protein kinase C (PKC) substrate and Ser_{116}, which is phosphorylated by Ca^{2+}/calmodulin kinase II (CaMKII) and by PKB (Kubes, Cordier et al. 1998). It contains an N-terminal DED domain that allows the interaction with different DED-containing proteins, such as Fas Receptor, TNFR1, caspase-8 or FADD (Renault, Formstecher et al. 2003). PEA-15 was reported to inhibit apoptotic responses to FasL and TNFα in different cell types by stably associating to both FADD and caspase-8 and interfering with the formation of the DISC (Condorelli, Vigliotta et al. 1999). It also protects from TRAIL-induced apoptosis in malignant glioma cells and silencing of PEA-15 renders glioma cells sensitive to apoptosis (Hao, Beguinot et al. 2001, Eramo, Pallini et al. 2005). Besides antagonizing the extrinsic pathway, PEA-15 also protects from intrinsic stimuli such as oxidative agents or serum deprivation (Condorelli, Trencia et al. 2002).

In addition, PEA-15 has been shown to restrain cellular proliferation by controlling the ERK pathway (Formstecher, Ramos et al. 2001). Nevertheless, PEA-15 phosphorylation by PKC, CaMKII or PKB facilitates the release of ERK and switches its binding specificity to FADD,

indicating that this protein has enormously versatile roles that must be tightly controlled (Renganathan, Vaidyanathan et al. 2005). Accordingly, the role of PEA-15 in cancer is controversial: some reports suggest that PEA-15 exerts tumor suppressor activity by inhibiting ERK (Gaumont-Leclerc, Mukhopadhyay et al. 2004, Glading, Koziol et al. 2007), while other authors suggest its contribution to development of malignancy in several tumors such as human gliomas or mammary carcinomas (Hwang, Kuo et al. 1997, Hao, Beguinot et al. 2001, Stassi, Garofalo et al. 2005).

Silencer of Death Domains (SODD)

Abundance of DRs in the plasma membrane can induce their spontaneous oligomerization and activation of the apoptotic cascade without the interaction with their ligand. However, DRs are constitutively expressed and present in the plasma membrane, often forming such oligomers but without inducing cell death (Chan, Chun et al. 2000). This suggests the presence of other molecules that keep them inactive. Concretely, SODD was found by Jiang and collaborators in a yeast-two-hybrid approach, while searching partners of DR3. They found that SODD was a 60 kDa protein capable of binding DR3 and TNFR1, but not Fas, DR4 or DR5. Overexpression of SODD suppressed TNFα-induced cell death and NF-κB activation (Jiang, Woronicz et al. 1999, Harrington 2000). Later studies involved SODD in Fas resistance as well (Eichholtz-Wirth, Fritz et al. 2003). *In vivo* approaches with *SODD* knockout mice are controversial: SODD does not seem essential for development, but its silencing increases the response to TNFα and enhances TNFα-induced activation of NF-κB. However, the apoptotic arm of TNFα signaling is not hyper-responsive in SODD-deficient cells, indicating that there might exist some functional redundancy (Takada, Chen et al. 2003).

Several reports demonstrate the significance of SODD expression in childhood and adult cancers. SODD mRNA levels are increased in pancreatic cancer in comparison to normal control tissues (Ozawa, Friess et al. 2000). Moreover, SODD expression seems to correlate with clinical classification, response to therapy and prognosis of acute lymphoblastic leukemia (Tao, Liu et al. 2014). In melanoma, SODD has an important role in protecting aggressive melanoma cells from apoptosis (Reuland, Smith et al. 2013).

Small ubiquitin-related modifier 1 (SUMO-1)

SUMO-1 was another protein found by yeast-two-hybrid approach using the cytoplasmic death domain shared by Fas and TNFR1 as bait. In this case, Okura *et al.* isolated a cDNA that coded for a 101-amino acid protein that interacts both with Fas and TNFR1, but not with FADD or

CD40. When overexpressed, it provides protection against both Fas- and TNFα-induced cell death (Okura, Gong et al. 1996). SUMO-1 has 18% sequence identity and 48% similarity to ubiquitin and both proteins share the same tertiary structure (Welchman, Gordon et al. 2005). Through post-translational modification of cellular proteins, SUMO-1 is involved in an innumerable amount of biological events related with cell cycle progression, the maintenance of genome integrity, nuclear transport and apoptosis (Seufert, Futcher et al. 1995, Pichler and Melchior 2002, Steffan, Agrawal et al. 2004, Hay 2005). SUMO-1 modifies several proteins involved in apoptosis, such as caspase-2, caspase-7, caspase-8, ASK-1 or the NEMO/IKKγ complex, thus affecting NF-κB activity (Huang, Wuerzberger-Davis et al. 2003, Besnault-Mascard, Leprince et al. 2005, Lee, Jang et al. 2005, Hayashi, Shirakura et al. 2006).

Lifeguard (LFG)

LFG (also known as FAIM2, NMP35) was originally isolated by Somia and colleagues in 1999 as an anti-apoptotic protein that protected cells from FasL-induced cell death, but not from TNFα-induced apoptosis. They found LFG while searching for molecules that inhibited Fas signaling in the Fas-resistant human lung fibroblast cell line MRC-5. LFG was expressed in most human tissues, predominantly in brain. Immunofluorescence and immunoprecipitation experiments demonstrated that LFG is associated to membranes and directly interacts with the Fas receptor, without displacing FADD binding. Moreover, overexpression of LFG in cell lines showed that exogenous LFG protected HeLa and Jurkat cells from FasL-induced apoptosis (Somia, Schmitt et al. 1999). Homology search revealed that this protein is the human homologue of a previously reported rat protein known as neural membrane protein 35 (NMP35). NMP35 was identified by differential display to find genes that were regulated during development of the rat sciatic nerve (Schweitzer, Taylor et al. 1998). The identified cDNA coded for a 35 kDa protein that is predominantly expressed in the adult central nervous system, with a neuronal expression pattern. NMP35 seemed to localize in somas, dendrites and postsynaptic membranes, suggesting a role in synapses of the adult central nervous system (Schweitzer, Suter et al. 2002).

The anti-apoptotic role of LFG in the nervous system was demonstrated by Beier *et al*. in 2005, when they reported LFG function in inhibiting Fas-induced neural cell death. In particular, they showed that LFG silencing by interfering RNAs leads to sensitization of rat cerebellar granular neurons to Fas-induced caspase-8 cleavage and cell death. They report that the expression of LFG that protected from cell death was dependent on the PI3K-AKT/PKB (phosphatidylinositol 3-kinase-Akt/protein kinase B) pathway, which is known to have a central pro-survival role in

many cellular systems (Beier, Wischhusen et al. 2005). The protective role of LFG has also been described in Purkinje cells (PCs), where loss of LFG increased caspase-8 and caspase-3 activity and sensitized organotypic cerebellar cultures to Fas-mediated apoptosis (Hurtado de Mendoza, Perez-Garcia et al. 2011). Fernandez *et al*. demonstrate that LFG antagonizes Fas-induced cell death in cortical neurons. Moreover, they report that LFG is localized in membrane microdomains known as lipid rafts, where it may interact with Fas receptor (Fernandez, Segura et al. 2007).

In silico analysis shows that LFG is evolutionarily conserved and has cytoprotective homologues in many species. Amino acid sequence analysis of LFG revealed a multi-transmembrane protein that shared structure with members of the TMBIM (Transmembrane BAX Inhibitor-1 Motif-containing) protein family (Figure 20) (Reimers, Choi et al. 2006). The TMBIM family is composed by 6 members in mammals: TMBIM1 or RECS1, TMBIM2 or LFG, TMBIM3 or GRINA, TMBIM4 or GAAP, TMBIM5 or GHITM, and TMBIM6 or BI-1. All these proteins have anti-apoptotic activity at different levels of the cascade, and are also involved in modulating calcium homeostasis at the ER, ER stress signaling and autophagy (Rojas-Rivera and Hetz 2014).

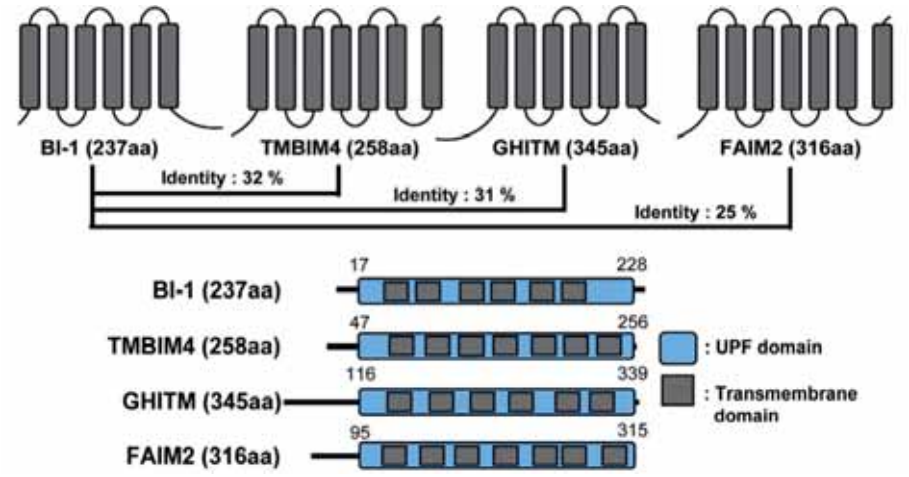

Figure 20. Protein domains and topology prediction of the TMBIM protein family. Comparison of the primary structure of BI-1 with other BI-1 family proteins revealed 32% identity with TMBIM4, 31% identity with GHITM, and 25% identity with Lifeguard (FAIM2). All members contain a conserved hydrophobic transmembrane domain, known as UPF0005 (uncharacterized protein family 0005), which mediates the localization of these proteins in membranes. Adapted from (Kim, Lee et al. 2012).

In the context of cancer, only four reports linking LFG and tumors have been published. All studies have been performed in breast cancer models and describe LFG as an anti-apoptotic protein that contributes to cancer progression (Bucan, Adili et al. 2010, Bucan, Reimers et al. 2010, Bucan, Choi et al. 2011, Dastagir, Lazaridis et al. 2014). Bucan and colleagues found that LFG was overexpressed in malignant breast cancer cell lines and that its expression levels correlated with a reduced sensitivity to Fas-induced cell death. High levels of LFG were found by immunohistochemistry in breast carcinoma when compared to control tissues in tissue microarrays. These data allowed them to hypothesize that LFG might have a role in protecting breast cancer cells from apoptosis, conferring them a more aggressive phenotype (Bucan, Reimers et al. 2010). One year later, the same authors reported that LFG downregulation enhanced sensitivity to an agonistic Fas antibody and to perifosine, an alkylphospholipid that induces apoptosis by inhibiting the AKT and PI3K pathway (Bucan, Choi et al. 2011). Recent studies describe a new LFG isoform known as LFGβ, which lacks one transmembrane domain. This isoform maintains its anti-apoptotic potential and has been found strongly expressed in breast tumor tissues (Dastagir, Lazaridis et al. 2014).

1.3.2. Targeting apoptosis pathways in neuroblastoma

Based on the concept that childhood malignancies show defective apoptosis, several approaches have been taken to directly induce cell death or, alternatively, lower the threshold for apoptotic induction by another stimulus.

On the one hand, there are strategies that directly target the extrinsic pathway. The death receptor ligand TRAIL has been reported to induce apoptosis in pediatric cancer cell lines (Petak, Douglas et al. 2000, Yang and Thiele 2003). Recombinant soluble TRAIL or monoclonal antibodies that specifically target TRAIL receptors (TRAIL-R1 and TRAIL-R2) are currently on clinical trials (Smith, Morton et al. 2010). However, it is frequent to find primary or acquired resistance towards TRAIL-induced apoptosis. This strongly limits the success of TRAIL as a therapeutic approach; however, several strategies have been developed to enhance sensitivity towards TRAIL-induced cell death (Gasparini, Vecchi Brumatti et al. 2013).

On the other hand, mitochondria plays a central role in regulating programmed cell death, so targeting this pathway remains as an alternative strategy to trigger apoptosis in cancer cells (Fulda, Galluzzi et al. 2010). In NBL, the expression of the anti-apoptotic molecules such as MCL-1 and/or BCL-2 have been linked to high-risk disease (Lestini, Goldsmith et al. 2009). Thus, BCL-2 inhibitors and antisense oligonucleotides have been evaluated in preclinical and clinical

trials in combination with chemotherapy, resulting in partial anti-tumor activity (Rheingold, Hogarty et al. 2007, Lock, Carol et al. 2008).

Finally, several approaches have been developed during the last years to counteract the anti-apoptotic functions of IAP proteins in childhood cancers. These approaches include the use of SMAC mimetics or antisense oligonucleotides against XIAP and survivin (Fulda 2013). In the case of survivin, YM155 is the most functionally evaluated small molecule inhibitor in both pre-clinical and clinical studies. Its anti-tumor activity relays on binding the promoter of survivin to inhibit its transcription and induce cell death (Nakahara, Kita et al. 2007).

1.3.3. Apoptotic deregulation in neuroblastoma

NBLs show several defects in their apoptotic machinery that could be the origin of their extended resistance to chemotherapy and radiotherapy. Indeed, these defects may impede the success of therapies that directly target the apoptotic pathways.

1.3.3.1. Silencing of caspase-8

Silencing of caspase-8 expression, an essential mediator of the extrinsic apoptotic pathway, is the most common and characterized apoptotic defect in NBL. Caspase-8 gene is frequently inactivated in unfavorable NBLs by hypermethylation of CpG islands (Lazcoz, Munoz et al. 2006, Kamimatsuse, Matsuura et al. 2009). Some authors correlate this epigenetic silencing to *MYCN* amplification, and show that caspase-8-null NBL cells become resistant to DR- and doxorubicin-induced apoptosis (Teitz, Wei et al. 2000, Kamimatsuse, Matsuura et al. 2009). Moreover, reintroduction of caspase-8 into NBL cell lines restored drug-induced apoptosis (Teitz, Lahti et al. 2001). Conversely, other authors did not find any correlation between caspase-8 silencing and *MYCN* amplification (Iolascon, Borriello et al. 2003, Lazcoz, Munoz et al. 2006). However, caspase-8 might be acting as a tumor suppressor gene in NBL, since its silencing provides resistance to treatment-induced apoptosis. Stupack and collaborators hypothesize that the loss of caspase-8 specifically potentiates NBL metastasis. They reported that caspase-8 induced apoptosis in NBL cells that lost attachment and invaded the collagenous stroma. This kind of cell death is known as integrin-mediated death. Loss of caspase-8 rendered cells immune to integrin-mediated death, allowing survival, migration and metastasis (Stupack, Teitz et al. 2006).

Some approaches have aimed to restore caspase-8 expression and, thus, re-sensitize NBL cells to programmed cell death. Pre-treatment of NBL cells with the DNA methyltransferase

inhibitor 5-aza-2'-deoxycytidine and interferon-*c* sensitized cells to TRAIL-induced apoptosis (Fulda and Debatin 2006), as well as exogenous expression of caspase-8 (Muhlethaler-Mottet, Balmas et al. 2003). Indeed, inhibition of caspase-8 enzymatic activity with the specific inhibitor z-IETD-FMK and the pan-caspase inhibitor z-VAD-FMK also inhibited apoptosis sensitization by caspase-8 re-expression (Fulda, Kufer et al. 2001). However, restoration of caspase-8 expression did not re-sensitize cells to TRAIL-induced cell death in all the studied models (Johnsen, Pettersen et al. 2004). Therefore, we assume that additional factors must be conferring resistance to DR-induced cell death.

1.3.3.2. Overexpression of anti-apoptotic proteins

Besides caspase-8 epigenetic silencing, overexpression of anti-apoptotic proteins such as MCL-1, BCL-xL, BCL-2, c-FLIP or survivin has been reported for high-risk NBL.

First, immunohistochemical analysis of primary NBL tissue microarrays showed that MCL-1 levels directly correlate with clinical prognostic factors and patient survival. At the functional level, MCL-1 knockdown induced apoptosis in various high-risk NBL cell lines and increased sensitivity to several chemotherapeutic agents, including etoposide, doxorubicin and small molecule inhibitors of the BCL-2 protein family (ABT-737 and AT-101). This suggests that MCL-1 has a pro-survival role in these tumors (Lestini, Goldsmith et al. 2009). Recently, a new variant of MCL-1 has been cloned from human NBL. This variant lacks 45 bp that encode for highly conserved amino acids and shows increased anti-apoptotic activity during DR-induced cell death. Thus, this new form of MCL-1 present in NBL could provide these cells a survival advantage (Hagenbuchner, Kiechl-Kohlendorfer et al. 2013).

Dole and colleagues show that BCL-xL is expressed in most NBL cell lines, conferring them resistance to apoptosis induced by the chemotherapeutic agents cisplatin and 4-hydroperoxy-cyclophosphamide (Dole, Jasty et al. 1995). Many evidences demonstrate that BCL-2 is implicated in NBL resistance to therapy: Castle *et al*. demonstrated that BCL-2 is widely expressed in NBL and correlates with poor prognosis markers such as unfavorable histology and *MYCN* amplification (Castle, Heidelberger et al. 1993). Furthermore, BCL-2 overexpression renders cells resistant to cisplatin and etoposide in a dose-dependent manner, enhancing the malignant phenotype of Shep-1 NBL cell line (Dole, Nunez et al. 1994). Fang *et al.* demonstrated that BCL-2 up-regulation leads to resistance to doxorubicin (Fang, Gu et al. 2008), while Fulda and colleagues reported that high levels of BCL-2 conferred resistance to TRAIL-induced apoptosis (Fulda, Meyer et al. 2002). Besides the fact that BCL-2 protects from cell death in NBL cell lines, the effect of BCL-2 has also been investigated in primary tumors.

Gallo *et al.* investigated BCL-2 and BAX expression in 15 cases of NBL. They detected that high levels of BCL-2 expression correlated with shorter survival of the patient than those with weak or moderate expression. In contrast, the expression of the pro-apoptotic protein BAX correlated with longer survival (Gallo, Giarnieri et al. 2003).

c-FLIP, as well as BCL-2 is frequently expressed in NBL tissues, preventing caspase-8 activation and FasL-induced cell death (Poulaki, Mitsiades et al. 2001) and also SMAC mimetics-induced cell death (Cheung, Mahoney et al. 2009). Other studies demonstrate that c-$FLIP_L$ expression is also involved in resistance to TRAIL induced apoptosis of NBL cells, and that $FLIP_L$ down-regulation restores DR-induced apoptosis in SH-EP NBL cell line (Flahaut, Muhlethaler-Mottet et al. 2006).

Finally, survivin is a member of the IAP family that is associated with tumors of high-risk and unfavorable prognosis. Moreover, its expression is associated with an increase of proliferation and a greater resistance to drug-induced and immune-mediated cell death (Azuhata, Scott et al. 2001).

HYPOTHESIS AND OBJECTIVES

2. Hypothesis and objectives

Our knowledge about deregulation of apoptotic pathways in NBL increases progressively, but is still not sufficient to overcome tumor chemoresistance and improve survival of high-risk patients. Hence, it is extremely necessary to further understand signal transduction pathways that regulate sensitivity to apoptosis in pediatric malignancies in order to open new treatment perspectives and find new molecular targets. Death receptor antagonists play a key role in cancer progression. Their implication in NBL has been poorly studied, since the extrinsic apoptotic pathway is often compromised due to caspase-8 silencing. Nevertheless, tumors that express caspase-8 still show resistance to therapy; therefore alternative resistance mechanisms must exist. We hypothesize that DR antagonists are involved in NBL behavior, either acting as anti-apoptotic proteins or by playing alternative roles. Thus, modulation of their expression can probably impact on tumor progression and aggressiveness.

Even though NBL outcome can be predicted by several risk factors, it is also crucial to find new biomarkers to improve the stratification of patients and we hypothesize that DR antagonists may be useful as prognostic markers.

The main purpose of this work is to unravel the possible implication of neuronal DR antagonists in NBL behavior, which will be addressed by the following objectives:

- **Objective 1**: Analyze the expression levels of DR-antagonists in primary NBL tumors data bases and correlate their expression with clinical variables such as patient survival.
- **Objective 2:** Study the functional role of the DR-antagonist that best correlates with clinical data to characterize its implication in NBL aggressiveness, both *in vivo* and *in vitro*.
- **Objective 3:** Test the prognostic value of DR-antagonists in NBL.

MATERIAL AND METHODS

3. Materials and Methods

3.1. Reagents

All reagents used for this work were dissolved to a stock solution following the manufacturer's recommendations. Afterwards, they were diluted in the appropriate culture media to reach the desired working concentrations. All biochemicals used for this study along with the working concentrations and their suppliers are listed in the following table:

Table 5. Reagents used for this study.

Product	Description	Dilution media	Working concentration	Provider
***All-trans* Retinoic Acid**	Inducer of neuronal differentiation	DMSO	10 µM	Sigma
Doxycycline hyclate	Tetracycline antibiotic	H_2O	100ng/mL	Sigma
Sodium Butyrate	HDAC inhibitor	PBS	1 mM	Sigma
5-aza-2'-deoxycytidine	DNA methyltransferase inhibitor	DMSO	1 µM	Calbiochem

3.2. Analysis of mRNA neuroblastoma data sets

Publicly available microarray expression data sets allow us to re-analyze these data and to establish preliminary correlations that give us clues for future hypothesis and help orientate our research. Moreover, these facilities give us the opportunity to extend our initial study to a wide range of candidates, and to a later stage, prioritize the most interesting ones for *in vitro* and *in vivo* studies.

In order to analyze the implication of death receptor antagonists expressed in the nervous system in NBL behavior, we used two public websites:

- R2: Genomics Analysis and Visualization Platform http://hgserver1.amc.nl/cgi-bin/r2/main.cgi
- Oncogenomics Section Data Center: http://pob.abcc.ncifcrf.gov/cgi-bin/JK

On the one hand, we used expression data from two different primary NBL datasets to find changes in mRNA levels (either up- or downregulation) between tumor stages. The expression of each individual DR-antagonist was analyzed comparing Stage 4 *MYCN*-amplified tumors versus the other stages present in the study (i.e. Stage 1, 3 and 4 without *MYCN* amplification). On the other hand, gene expression data of human samples from independent data sets were used to generate Kaplan-Meier survival curves. Kaplan-Meier analyses are used in medical

research to measure the fraction of patients that are alive for a certain amount of time. Therefore, Kaplan-Meier curves allow us to plot survival functions of patients. Patients were divided into two groups that expressed high or low levels (above or below median) of the gene of interest. Afterwards, survival curves were plotted in order to find differences in survival that correlated with the expression levels of a certain gene. The primary NBL data sets that were used for this thesis are listed in this table:

Table 6. NBL expression and prognosis data sets employed in this work.

Dataset	Number of cases	Used for…	Reference
GSE3960	101	mRNA levels	(Wang, Diskin et al. 2006)
GSE16237	51	mRNA levels	(Ohtaki, Otani et al. 2010)
GSE16476	88	Kaplan-Meier	(Molenaar, Koster et al. 2012)
GSE3446	102	Kaplan-Meier	(Asgharzadeh, Pique-Regi et al. 2006)
Oberthuer lab	251	Kaplan-Meier	(Oberthuer, Berthold et al. 2006)

3.3. Human samples

Primary tumor tissue samples from 38 NBL patients enrolled at the Vall d'Hebron Hospital (Barcelona, Spain) were obtained immediately after surgery and snap-frozen in liquid nitrogen and stored at -80°C until processing. Primary tumor samples were used for RNA and protein extraction and analysis, as explained later.

Tumors were examined by the pathologists in order to confirm NBL diagnosis. Pathologists also confirmed the presence of at least 80% of tumor tissue sample and carried out a histo-pathological classification of the sample. The 38-samples cohort included tumors from different stages, which were divided in four groups:

(A) Stage 1 tumors, n=10

(B) Stage 3 tumors, n=9

(C) Stage 4 tumors, n=10

(D) Stage 4 *MYCN* amplified tumors, n=9

Further patient characteristics are detailed in the following table:

Table 7. Clinical characteristics of the Vall d'Hebron Cohort of patients

Variables	n (%)
Age	
> 18 months	12 (31.6)
< 18 months	26 (68.4)
Sex	
Male	16 (42.1)
Female	22 (57.9)
Stage	
1	10 (26.3)
3	11 (28.9)
4	17 (44.8)
***MYCN* Status**	
Amplified	7 (7.0)
Non amplified	31 (93.0)
Anatomic Location	
Suprarenal	20 (52.6)
Abdominal	9 (23.7)
Thoracic	5 (13.1)
Other	3 (10.6)
Metastatic	
Yes	18 (47.3)
No	20 (52.7)

Parents of all patients gave written informed consent.

3.4. Gene expression analysis by qPCR

3.4.1. RNA extraction

Total RNA was extracted from NBL cell lines and tumor samples using the RNeasy Mini Kit (Qiagen) following the provider's instructions. Briefly, it consists on a guanidine-isothiocyanate sample lysis and homogenization. Then, ethanol is added to the lysate to provide ideal binding conditions of RNA to the silica membrane used for purification, allowing contaminants to be washed away. RNA is then efficiently eluted with RNase-free water.

3.4.2. Quantitative PCR

RNA was retro-transcribed using High Capacity RNA to cDNA kit (Applied Biosystems) following the manufacturer's protocol. Briefly, between 0.5 µg and 1 µg of total RNA was mixed with

retro-transcription buffer and enzymes and the reaction was loaded into a thermal cycler to undergo the following steps:

1. 37°C, 60 minutes, to retro-transcribe RNA.
2. 95°C, 5 minutes, to stop the reaction.
3. 4°C, ∞, to maintain samples in optimal conditions.

The obtained cDNA was stored at -20°C until the qPCR reaction was carried out. Gene expression analyses were performed using TaqMan® probes and, as a reaction buffer, we used TaqMan® Gene Expression Master Mix (Applied Biosystems). Briefly, cDNA samples were diluted 1:20 and the qPCR reaction was performed in a 384-well plate with the following mix:

- 5 µl 2x Reaction Buffer, that includes AmpliTaq Gold® DNA Polymerase and dNTPs
- 0.5 µl of the desired probe
- 4.5 µl of the diluted cDNA

All reactions were carried out in triplicates. In order to compare samples and to ensure that equal amounts of DNA were loaded on the plate, all expression analyses were normalized versus *18S* housekeeping gene. All probes used in this work are detailed in Table 8.

Alternatively, gene expression was also detected by qPCR using Power SYBR® Green PCR Master Mix (Applied Biosystems) as a reporter and normalized against *L27* with the primers shown in Table 9.

In all cases, analysis was performed using the 7900HT Sequence Detection Systems 2.3 Software (Applied Biosystems). There are two classical methods to analyze data from a real-time qPCR, which are absolute and relative quantifications. Absolute quantifications are employed to determine the input copy number using a standard curve, while relative quantifications give us relative changes in expression comparing the target group to a control reference. For this study, we used relative quantifications to assess expression differences after different treatments. The relative fold-change in expression was determined by the comparative $2^{(-\Delta\Delta CT)}$ method (Livak and Schmittgen 2001).

3.4.2.1. qPCR probes and primers

Table 8. TaqMan Probes used for this study.

Probe	Reporter	Reference
LFG	FAM	Hs00392342_m1
TRKB	FAM	Hs00178811_m1
FGF14	FAM	Hs00738588_m1
STK36	FAM	Hs00379662_m1
BCL2	FAM	Hs00608023_m1
RAP1A	FAM	Hs01092205_g1
TJP1	FAM	Hs01551861_m1
ITGA9	FAM	Hs00979865_m1
18S	FAM	Hs03928990_g1

Table 9. Primers used for this study

Gene	Primer Sequence	Reporter
ABCG2	Forward 5'-CGGGTGACTCATCCCAACAT-3'	SYBR green
	Reverse 5'-TCTGGAGAGTTTTTATCTTTTCAGC-3'	
CD133	Forward 5'-AAGCTGGACCCATTGGCATT-3'	SYBR green
	Reverse 5'-AGATTACAGTTTCTGGCTTGTCA-3'	
ERBB3	Forward 5'-CTGATCACCGGCCTCAAT-3'	SYBR green
	Reverse 5'-GGAAGACATTGAGCTTCTCTGG-3'	
GFP	Forward 5'-GGACGACGGCAACTACAAGA-3'	SYBR green
	Reverse 5'-TTGTACTCCAGCTTGTGCCC-3'	
KLF4	Forward 5'-TACCAAGAGCTCATGCCACC-3'	SYBR green
	Reverse 5'-CGCGTAATCACAAGTGTGGG-3'	
KRT19	Forward 5'-GCCACTACTACACGACCATCC-3'	SYBR green
	Reverse 5'-CAAACTTGGTTCGGAAGTCAT-3'	
L27	Forward 5'-AGCTGTCATCGTGAAGAA-3'	SYBR green
	Reverse 5'-CTTGGCGATCTTCTTCTTGCC-3'	
MYCN	Forward 5'-CCTGAGCGATTCAGATGATGA-3'	SYBR green
	Reverse 5'-GGTGAATGTGGTGACAGCCT-3'	
NANOG	Forward 5'-CAATGGTGTGACGCAGAAGG-3'	SYBR green
	Reverse 5'-GAAGGTTCCCAGTCGGGTTC-3'	
NESTIN	Forward 5'-CTCAGCTTTCAGGACCCCAA-3'	SYBR green
	Reverse 5'-GTCTCAAGGGTAGCAGGCAA-3'	
NOTCH	Forward 5'-GGGCCACTATGTGAGAACCC-3'	SYBR green

	Reverse 5’-TCAAACCCAGGAAGACAGGC-3’	
OCT4	Forward 5’-GCCCGAAAGAGAAAGCGAAC-3’	SYBR green
	Reverse 5’-CTCGGACCACATCCTTCTCG-3’	
SNAI1	Forward 5'-AGATGCACATCCGAAGCCAC-3'	SYBR green
	Reverse 5'-AGTGGGGACAGGAGAAGGG-3'	
SNAI2	Forward 5'-TGGTTGCTTCAAGGACACAT-3'	SYBR green
	Reverse 5'-GTTGCAGTGAGGGCAAGAA-3'	
SOX2	Forward 5’-GGGGAAAGTAGTTTGCTGCC-3’	SYBR green
	Reverse 5’-CGCCGCCGATGATTGTTATT-3’	
TCF3	Forward 5'-CTCGGTCATCCTGAACTTGG-3'	SYBR green
	Reverse 5'-TCTCCAACCACACCTGACAC-3'	
TWIST1	Forward 5'-AAGGCATCACTATGGACTTTCTCT-3'	SYBR green
	Reverse 5'-GCCAGTTTGATCCCAGTATTTT-3'	
ZEB1	Forward 5'-GGGAGGAGCAGTGAAAGAGA-3'	SYBR green
	Reverse 5'-TTTCTTGCCCTTCCTTTCTG-3'	

3.5. Protein extraction and detection

3.5.1. Protein extraction

Cells were rinsed once with ice-cold PBS pH 7.2 before lysis. Proteins must be extracted efficiently and without degradation to ensure an accurate representation of their physiological state in the living cell. With that purpose, different methods of protein extraction were used.

Cell homogenates were obtained in Triton lysis buffer (50mM Tris pH 7.4, 150mM NaCl, 1mM EDTA, 1% Triton™ X-100) and tissue homogenates were obtained in commercial RIPA buffer (Pierce/ThermoFisher Scientific), both supplemented with 1x EDTA-free complete protease inhibitor cocktail (Roche). Buffers were added keeping a proportion of 1:20 between cell pellet and lysis buffer. Cells were incubated in ice for 20 min prior centrifugation at 16,000 xg, 4°C for 5 min. Under these conditions, most nuclear and cytoskeleton proteins remain in the excluded pellet while the supernatant is enriched in cytosolic proteins. Supernatants were harvested and kept at -20°C.

Since LFG is a membrane protein, non-ionic detergents such as Triton may not release it completely and therefore, this could impair its detection by Western Blot. For this, reason, samples were lysed in SET lysis buffer (10 mM Tris-HCl pH 7.4, 150mM NaCl, 1mM EDTA and 1% sodium dodecyl sulfate (SDS)) when indicated. Denaturing cell lysis with SDS breaks

interactions between proteins and releases proteins from macromolecular structures, enhancing extraction efficiency. SET buffer was not supplemented with protease inhibitors because SDS completely denaturalizes and inactivates all enzymes in the sample, including proteases. SET buffer was added maintaining a relation of 1:50 (pellet:buffer). Samples were then heated at 95°C for 10 minutes in order to ensure fragmentation of genomic DNA and, consequently, reduce viscosity of the sample. Lysates were stored at -20°C.

3.5.2. Protein quantification

Protein concentration was quantified by a modified Lowry assay (DC protein assay, Bio-Rad). Once quantified, samples were prepared for further analysis in SDS-Polyacrylamide gel electrophoresis (SDS-PAGE) and Western Blot. 20–30µg of protein were mixed with Laemmli's loading buffer (60mM Tris-HCl pH 6.8, 4mM EDTA, 10% Glycerol, 2% SDS, 100mM dithiothreitol (DTT) and traces of Bromophenol blue) and denatured by incubating them at 95°C for 5 min. DTT reduces disulphide bonds and SDS is a powerful ionic detergent, which has an hydrophobic end and a negatively charged part. The hydrophobic dodecyl part interacts with hydrophobic amino acids in proteins, destroying 3D structures and transforming proteins into linear molecules coated with negatively charged SDS groups. More importantly, these charges give every protein the same charge-to-mass ratio and, therefore, they will only run depending on their molecular weigh when loaded on an SDS-PAGE.

3.5.3. SDS-PAGE

SDS-PAGE is a widely used method to separate proteins based on their electrophoretic mobility, formulated by Ulrich K. Laemmli in 1970 (Laemmli 1970).

Polyacrylamide gels are formed by the polymerization of acrylamide by the action of the cross-linking factor bis-acrylamide, an initiator and a catalyzer, all in the presence of 0.1% SDS. Acrylamide and bis-acrylamide are used in a final proportion of 37.5:1. The final percentage of acrylamide/bis-acrylamide determines the separation range of the gel. Chemical polymerization is initiated by ammonium persulfate (APS) 0.05% (w/v), which is a source of free radicals (persulfate ions, $S_2O_8^-$). TEMED (N, N, N', N'-tetramethylethylenediamine) 0.1% (v/v) is commonly used as a catalyzer, since it accelerates the rate of formation of free radicals from persulfate and improves polymerization.

The SDS-PAGE method is based on a discontinuous pH gel system, since gels are composed of two different parts that mainly differ in their pH and the acrylamide concentration: the *stacking* and the *resolving* gels. The *resolving* gel is buffered with Tris-HCl adjusted to pH 8.8, while the *stacking* is adjusted to pH 6.8. Running buffer is composed of Tris 25mM, Glycine 192mM and SDS 0.1%, pH 8.3. Glycine is a weak acid that at low pH is protonated and thus uncharged. At higher pH it is negatively charged. For this reason, in the *stacking* gel glycine ions lose a lot of their charge and slow down. Together with the chloride ions that move faster, glycine creates a tight band were all the proteins concentrate. This way, all the proteins reach the *resolving* gel at the same time, where protein migration is truly a function of their molecular size.

Electrophoresis was performed in a Mini-PROTEAN cuvette (Bio-Rad), at constant amperage (25 mA/gel).

3.5.4. Protein immunodetection by Western Blot

Immediately after migration, proteins were transferred to polyvinyl difluoride (PVDF) membranes (Millipore) that were previously activated with 100% methanol and washed with MilliQ water to hydrate them. Once proteins are transferred to the membrane, they become accessible for immunodetection with specific antibodies. Transference is done at 100 V for 90 min in ice-cold transfer buffer (25 mM Tris-HCl, 192 mM glycine, 20% methanol).

After transference, membranes were blocked in TBS-T (20 mM Tris–HCl, 150 mM NaCl pH 8 and 0.1% Tween 20) containing 5% nonfat dry milk, for 1 h at room temperature. Blocking of the membrane prevents unspecific binding of the antibodies that will be used at a later stage. Once blocked, membranes were washed three times for 5 min with TBS-T to eliminate excess blocking solution. Primary antibody was added at the required dilution (Table 10) and incubated overnight at 4°C or for 1 h at room temperature. Membranes were probed with the antibodies and dilutions detailed in 3.5.4.1.

Before incubating with the secondary antibody, membranes were washed again with TBS-T for 5 min three times to eliminate excess of primary antibody. Secondary antibody was diluted in blocking solution. The secondary antibody is coupled to the horseradish peroxidase enzyme (HRP), which allows detection. Incubation was done for 1 h at room temperature. After incubation, membranes were washed three times for 10 min with TBS-T to eliminate the secondary antibody excess.

Membranes were developed with SuperSignal Dura detection kit (Pierce/ThermoFisher Scientific) or EZ-ECL Chemiluminescence detection kit (Biological Industries). In the presence of peroxides, HRP that is bound to the secondary antibody catalyzes the oxidation reaction of luminol. This reaction produces light or chemoluminiscence, which can be detected using SuperRX Fuji Medical X-RAY Films (Fujifilm Corporation).

In some cases, after blotting membranes with the desired antibodies, Naphtol Blue Black stain (NB) was used as a loading control. NB is designed for rapid staining of protein bands on Western Blot membranes. It is useful to ensure equally loading when housekeeping protein levels (e.g. actin, α-tubulin…) are altered and do not correspond with the real amounts of total protein. This was the case of NBL primary tumors western blots, where NB was the best approach to control loading. Membranes were stained in a solution containing 10% methanol, 2% acetic acid and 0.1% naphtol blue black stain for 5 minutes. Then, membranes were washed twice in a decoloration solution (50% methanol, 7% acetic acid) and let dry.

3.5.4.1. Antibodies

The following primary and secondary antibodies were used:

Table 10. Antibodies used for this study and their respective dilutions.

Antibody	Antigen Mw	Type	Source	Working dilution	Dilution media	Supplier
anti-LFG	35 kDa	Polyclonal	Rabbit	1:1000	BSA	AnaSpec
anti-FAIM2 (H-21)	35 kDa	Polyclonal	Rabbit	1:1000	BSA	SCBT
anti-α-tubulin	50 kDa	Monoclonal	Mouse	1:10000	TBS-T	Sigma
anti-MYCN NCM-II-100	64 kDa	Monoclonal	Mouse	1:1000	BSA	Abcam
Secondary antibodies						
Ig Rabbit		Polyclonal	Goat	1:20000	5% milk	Sigma
Ig Mouse		Polyclonal	Goat	1:20000	5% milk	Sigma

SCBT, Santa Cruz Biotechnology

3.6. Immunohistochemistry

Immunohistochemistry (IHC) is a strategy used to detect protein antigens in tissue sections using specific antibodies. In order to detect the interaction between the primary antibody and the antigen, we use a secondary antibody conjugated to an enzyme such as peroxidase that catalyzes a reaction detectable by color. In this thesis, we performed IHC staining on NBL tissue slides in collaboration with the pathological anatomy service of Vall d'Hebron Hospital.

First, 3µm-sections were cut and deparaffinized in the EZ prep™ solution (Ventana Medical Systems). Epitope retrieval was performed with the Cell Conditioning solution at pH 8.0 for 20 min. Anti-LFG antibody (AnaSpec) was diluted 1:50 and incubated for 30 min at room temperature on Benchmark XT instrument (Ventana Medical Systems). Endogenous peroxidase activity was blocked with 3% hydrogen peroxide. Secondary streptavidin-HRP conjugate antibody was used to detect the primary antibody and the complex was visualized with 3,3-diaminobenzidene. Slides were counterstained with hematoxylin in order to visualize nuclei.

3.7. Cell culture

3.7.1. Cell Lines

A panel of human NBL cell lines with the following main characteristics has been used:

Table 11. Summary of NBL cell lines.

Cell line	Stage	Age (months)	*MYCN* status	Caspase-8
SH-SY5Y	4	48	Non amplified	-
CHLA-90	4	102	Non amplified	+
IMR-5	4	13	Amplified	-
IMR-32	4	13	Amplified	-
IMR-32 sh*MYCN*	4	13	Amplified[a]	-
SK-N-BE(2)	4	24	Amplified	+
LAI-5S	4	36	Amplified	+
Tet21N	4	48	Amplified[b]	+

[a] Doxycycline-Inducible sh*MYCN* to counteract *MYCN*-amplification.
[b] Ectopic MYCN is overexpressed under a tetracycline-regulated promoter.

SH-SY5Y, SK-N-BE(2), IMR-5 and IMR-32 were acquired from the American Type Culture Collection (ATCC). CHLA-90 cells were obtained from Children's Oncology Group Cell Line & Xenograft Repository (Lubbock, TX, USA). SK-N-BE(2) and LAI-5S cells were purchased from Public Health England Culture Collections (Salisbury, UK). IMR-32 cells stably transfected with an inducible shRNA against MYCN were kindly provided by Dr. Frank Westermann (DKFZ, Heidelberg, Germany). Tet21N were a generous gift from Prof. Manfred Schwab (DKFZ, Heidelberg, Germany). All cell lines obtained directly from the tissue banks were amplified and stored in liquid nitrogen. Upon resuscitation, cells were maintained in culture for no more than two months. SH-SY5Y were grown in Dulbecco's Modified Eagle Medium (DMEM) supplemented with 15% heat-inactivated FBS, 20U/mL penicillin, and 20µg/mL streptomycin.

IMR-5, IMR-32 and LAI-5S cells were maintained in DMEM plus with 10% heat-inactivated FBS, 20U/mL penicillin, and 20µg/mL streptomycin. IMR-32 stably transfected with an inducible sh*MYCN* were maintained with additional supplements: 5µg/mL blasticidin (Thermo Fisher Scientific) and 100µg/mL zeocin (Ibiantech). SK-N-BE(2) and CHLA-90 were maintained in Iscove's Modified Dulbecco's Medium (IMDM), supplemented with 20% heat-inactivated FBS, 1% of Insulin-Transferrin-Selenium, 100U/mL penicillin, and 100µg/mL streptomycin. To subculture cells, medium was removed and they were dissociated using a 1:5 dilution of 0.25% Trypsin-EDTA (Invitrogen). Cells were incubated at 37°C until detachment and trypsin was inhibited with fresh media. Cells were pelleted by centrifugation at 200 xg for 5 minutes and seeded in new culture dishes. Tet21N cells were grown in RPMI-1640 medium (Invitrogen) supplemented with 10% heat-inactivated FBS, 25mM Hepes (Invitrogen), 200µg/mL geneticin (G418), 0.5µg/mL amphotericin B, 10µg/mL hygromycin B, 100U/mL penicillin, and 100µg/mL streptomycin. Tet21N cells were dissociated using Versene (1x PBS plus 1mM EDTA, pH 7.0) and subcultured into new 100 mm dishes.

SH-SY5Y and CHLA-90 cells were chosen as models for functional knockdown experiments because they are both *MYCN* non-amplified cell lines and show high levels of LFG expression. SH-SY5Y is a thrice-cloned subline of the NBL cell line SK-N-SH (SK-N-SH → SH-SY → SH-SY5 → SH-SY5Y), which was established from a metastatic bone marrow from a 4-year female. CHLA-90 cells were established from a bone marrow of a stage 4 tumor. Concretely, tumor sample was obtained from an 8-year male post-chemotherapy (cisplatin, cyclophosphamide, doxorubicin, etoposide, melphalan, teniposide), total body irradiation and post-bone marrow transplant. Tet21N is a subclone of the NBL cell line SH-EP, which derives from the NBL cell line SK-N-SH. Tet21N cells harbor ectopic MYCN overexpression under a tetracycline-regulated promoter. In this cell line, MYCN expression is controlled by a Tet-OFF promoter and, therefore, treatment with tetracycline or its analogue doxycycline inhibits MYCN expression (Lutz, Stohr et al. 1996). During the last years, Tet21N have been extensively used in order to study genes or pathways regulated by MYCN and also to increase our knowledge about MYCN-driven transformation and drug resistance (Bell, Lunec et al. 2007, Cotterman and Knoepfler 2009, Murphy, Buckley et al. 2009).

HEK293T were obtained from ATCC. This cell line is a highly transfectable derivative of human embryonic kidney 293 cells and, therefore, it has been widely used for retroviral and lentiviral production, gene overexpression and protein production. This cell line contains the SV40 antigen, so it is competent to replicate vectors carrying the SV40 region of replication. In this

work, HEK293T cells were used for lentiviral production and maintained in DMEM medium supplemented with 10% FBS, 20U/mL penicillin and 20µg/mL streptomycin.

All cultures were maintained at 37°C in a saturated atmosphere of 95% air and 5%CO_2.

3.7.2. Thawing and cryopreservation

When thawing cells, it is crucial to ensure that they recover and to keep the highest viability as possible. For this reason, cells must be rapidly processed to place them in culture. Vials were thawed in a water bath at 37°C and 1mL of cell suspension was resuspended in 9 mL of PBS. Cells were then centrifuged at 200 xg for 5 min and the supernatant was removed to eliminate traces of DMSO from the freezing media, which can be toxic. Cells were resuspended in complete culture media and seeded into 100 mm culture dishes.

It is also extremely important to maintain a stock of cells without introducing selections or modifications that could alter the characteristics of the original population. For this reason, when cells were thawed they were kept in culture and new aliquots were immediately cryopreserved. To preserve cells, they were frozen in a mixture of FBS with 10% DMSO using a Mr. Frosty Freezing Container (Thermo Scientific) and stored at -80°C. Mr. Frosty containers are designed to achieve a rate of cooling close to -1°C/minute, which is the optimal rate for cell preservation. The next day, cells were transferred to a liquid nitrogen tank for long-term storage.

3.8. Retinoic acid differentiation

Retinoic acid (RA) is a metabolite of vitamin A that plays an important role in many biological processes such as cellular differentiation and embryogenesis. RA is a potent transcriptional activator that acts through its nuclear receptors to induce transcription of specific genes, including multitude of structural genes, transcription factors, cell surface molecules and also many cytokines. Due to its effects stopping cell proliferation and inducing differentiation, RA is now being used therapeutically in oncology. Concretely, in pediatric oncology, retinoids are administered for the treatment of acute promyelocytic leukemia and high-risk NBL.

Induction of differentiation of NBL cell lines was performed as described previously by our group (Encinas, Iglesias et al. 2000). Briefly, NBL cells were seeded at low density ($6x10^4$ cells/mL) on culture dishes previously coated with 65µg/mL type I collagen (BD Biosciences) and washed once with sterile water. *All-trans* retinoic acid was added the next day at a final

concentration of 10 µM in DMEM supplemented with 15% FBS and maintained during 1, 3 and 5 days. Then, cells were collected, pelleted at 200 xg for 5 min and rinsed once with PBS. Pellets were used for protein and RNA extraction as previously specified.

3.9. Sphere formation

Autonomous growth in serum-free media as non-adherent spheres is thought to be a surrogate marker of neural and malignant progenitors. Indeed, sphere cell populations have an increased tumor-initiating capacity and can undergo differentiation when exposed to the appropriate stimuli. This has been reported for NBL cell lines (Mahller, Williams et al. 2009), NBL cells derived from primary tumors (Hansford, McKee et al. 2007) and also for other tumors of the nervous system such as glioblastoma (Penuelas, Anido et al. 2009).

In this study, the *MYCN*-amplified cell lines SK-N-BE(2), IMR-5 and IMR-32 were seeded in neurosphere media in order to mimic an undifferentiated status of NBL cells. Cells were grown at low density ($5x10^4$ cells/mL) for sphere formation in serum-free Neurobasal Medium (Invitrogen), supplemented with B27 (Invitrogen), 2mM L-Glutamine (Invitrogen), 20ng/mL EGF (ProSpec-Tany Technogene Ltd.), 20ng/mL FGF2 (ProSpec-Tany Technogene Ltd.), 20U/mL penicillin and 20µg/mL streptomycin. Cells were maintained in standard culture conditions (37°C; 5%CO_2) for at least one week. Resulting spheres were pelleted as detailed above for RNA extraction.

3.10. Cell transfection

Cells were transfected using Lipofectamine 2000 Reagent (Invitrogen), a cationic liposoluble reagent. This method is based in the formation of liposomes in an aqueous environment that entrap DNA and are able to introduce it in the target cell (Dalby, Cates et al. 2004, Chu, Masoud et al. 2009). Because cell membranes have a negative net charge, anionic molecules, especially those with an elevated molecular weight, cannot be internalized. Since lipofectamine is a cationic reagent, it complexes with negatively charged nucleic acid molecules, neutralizing the negative charges and allowing them to overcome the electrostatic repulsion of the cell membrane. This way, liposomes that contain DNA and are positively charged can fuse with the negatively charged plasma membrane, allowing nucleic acid to enter the cell. Lipofectamine 2000 has been optimized to provide high transfection efficiencies en many eukaryotic cell types.

This reagent was used in this work to transfect HEK293T cells in order to produce high-titer lentiviral particles. The transfection protocol was adapted from the manufacturer's recommendations. According the manufacturer, one day before transfection, cells should be seeded at high density (90-95%) to achieve high transfection efficiency and avoid cytotoxicity. However, due to the high proliferation rate of HEK293T cells, and that lentiviral vectors must be harvested two days post transfection, we seeded cells at a lower density. In this case, to minimize transfection toxicity, culture plates were previously coated with Poly-D-Lysine and cells seeded in medium without antibiotics. On the day of transfection Lipofectamine 2000 and DNA were diluted separately in OptiMem I Reduced Serum Medium (Invitrogen). After 5 minutes of incubation, DNA and Lipofectamine 2000 were combined and incubated for 20 minutes to allow lipid complex formation. Then, complexes were added to the cell culture. Culture medium was changed 4-6 hours after transfection to avoid toxicity of the reagent.

3.11. Lentiviral production

Lentiviral vectors allow efficient internalization, integration and gene transfer in both dividing and quiescent cells, including terminally differentiated cells such as neurons (Naldini, Blomer et al. 1996, Naldini, Blomer et al. 1996, Zufferey, Nagy et al. 1997). Three generations of vectors have been developed for the production of lentiviruses. In each generation biosafety has been improved by dividing the necessary elements for the formation of the viruses in more plasmids.

Lentiviral particles are generated by coexpression of packaging elements and the transgene of interest in HEK293T cells. In this work, we used a second generation system designed by Professor Didier Trono (Laboratory of Virology and Genetics, École Polytechnique Fédérale de Lausanne, Lausanne, Switzerland, http://tronolab.epfl.ch/). This method consists of three plasmids that are transfected simultaneously:

1. A lentiviral vector, carrying the gene of interest or short hairpin (sh) RNAs. This vector only contains the genetic material to be transferred to the target cell. In our case, pLVTHM (for shScr and sh*LFG* constructs) and pGIPZ (for shScr2 and sh*LFG*2 constructs). The transgene is flanked by *cis* elements that are necessary for encapsidation, reverse transcription, and integration in the host genome. As in other retroviral vectors, we take advantage of the particularity of reverse transcription in order to obtain self-inactivating vectors derived from HIV-1, which lose the transcriptional capacity of the Long Terminal Repeats (LTR) once they have been

transferred to the cell. This minimizes the risk of the appearance recombinant particles competent for replication and promoter interferences.

2. psPAX2, a packaging plasmid for producing lentiviral particles. It contains a robust CAG promoter for efficient expression of packaging proteins, including TAT protein, DNA polymerase and reverse transcriptase.
3. pMD2.G, an envelope plasmid. To broaden the tropism of the vector, this plasmid encodes the G glycoprotein of vesicular stomatitis virus (VSV). It is an heterologous protein that enables pseudotyping of the viral particles and, at the same time, it confers enough stability to allow lentiviral concentration by ultracentrifugation (Naldini, Blomer et al. 1996).

The protocol used to produce lentiviral particles has been adapted from the one described by Naldini and collaborators (Naldini, Blomer et al. 1996, Naldini, Blomer et al. 1996).

The first day, culture dishes are coated with poly-D-Lysine 10µg/mL (Sigma) and 30 minutes later rinsed once with sterile water. Then, 4-5 million HEK293T cells are seeded per 100 mm dish. The next day, cells are transfected using Lipofectamine 2000 Reagent and the following proportions of plasmids:

- Vector: 12 µg
- psPAX2: 8 µg
- pMD2.G: 4 µg

48 hours post-transfection, the medium is removed and centrifuged at 2,500 rpm for 5 minutes to eliminate cells or particles in suspension. The supernatant is filtered through a 0.45 µm filter and can directly be used to infect cells. However, if components of the HEK293T medium may affect the future experiment, it is recommendable to concentrate the virus by ultracentrifugation using a TH-641 rotor (Thermo Scientific) at 25,000 rpm (107,000 xg) for 1.5 h. Once centrifuged, viruses are resuspended in a solution of PBS containing 2% BSA, a carrier protein that will ensure preservation of the virus. Viral particles can be stored at –80°C for long periods without apparent loss of efficiency.

In this work, lentiviral vectors were used for loss of function experiments. In order to knockdown LFG, two sets of shRNA lentiviral constructs were used: pLVTHM-shScr and pLVTHM-sh*LFG* were previously described by Fernandez and collaborators (Fernandez, Segura et al. 2007) and pGIPZ-shScr2 and pGIPZ-sh*LFG2* were purchased from Thermo Fisher Scientific (RHS4531-EG23017).

3.12. Cell proliferation and adhesion assays

For proliferation assays, infected NBL cells were seeded in 96-well plates at low density ($2x10^4$ cells/well) in order to leave them in standard culture conditions for several days and monitor their growth rates. At the indicated time points cells were fixed with 4% paraformaldehyde and left in PBS at 4˚C until further processing.

For adhesion assays, NBL cells were seeded in 96-well plates at high density ($2x10^5$ cells/well) and incubated for short periods of time at 37°C. Every 10-15 minutes culture medium was removed by aspiration, together with cells that were not still adhered. Adherent cells were rinsed once with PBS to remove the remaining non-adherent cells and new culture media was added to the well. Cells were incubated for 4-6 h to ensure they were properly adhered to culture plates and then fixed with 4% paraformaldehyde.

In both assays, quantification of cell number was performed by crystal violet staining (Sigma). Briefly, cells were rinsed once with PBS and stained with 0.5% crystal violet for 30 min. Plates were then washed thoroughly with distilled water to remove traces of dye and let dry. The next day, crystals were dissolved in 100 µl of 10% acetic acid and the absorbance was measured at 590nm.

3.13. Migration and invasion assays

Both migration and invasion assays are based on the formation of a serum gradient that prompts cells to move to the zone with higher concentration of nutrients. Taking advantage of this property, we were able to quantify migration and invasion abilities of NBL cell lines.

For migration assays, 300 µl of a suspension of $2.5x10^5$ SH-SY5Y NBL cells was added in serum-free media to 8µm-pore cell culture inserts (Falcon). 700 µl of complete media (DMEM supplemented with 15% FBS) were added to the lower part of the chamber in order to generate a FBS gradient that would function as a chemoattractant to induce cell migration to the lower well (Figure 21). Cells were incubated for 8h under standard culture conditions and viable cells that had migrated to the lower transwell chamber were quantified by WST-1 assay (Roche).

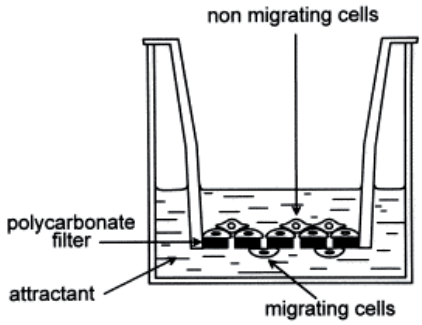

Figure 21. Representation of a migration assay.

To assess the invasion ability of SH-SY5Y cells, we took the same approach as for migration assays and introduced a new variable (Figure 22). In this case, polycarbonate filters were coated with 50 µl of a gelatinous protein mixture known as Matrigel (Corning) diluted 1:5 in DMEM (Matrigel:DMEM). Matrigel is secreted by Engelbreth-Holm-Swarm mouse sarcoma cells and resembles the extracellular matrix. Thus, cells with invasive properties should be able to cross this environment and migrate to the lower transwell chamber. Cells that crossed the matrigel coating and the polycarbonate filter were fixed with 4% paraformaldehyde, stained with 0.5% crystal violet for 30 min, thoroughly washed with distilled water and counted.

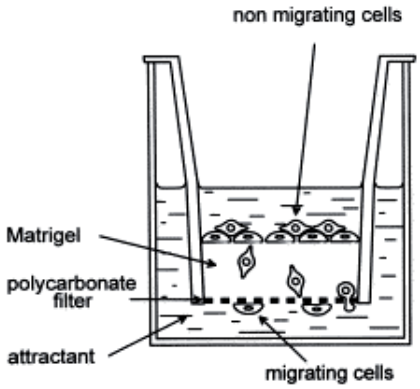

Figure 22. Representation of an invasion assay.

3.14. Cell viability WST-1 assay

The WST-1 assay (Roche) is a colorimetric approach that allows the quantification of cell proliferation and viability using a spectrophotometer. The WST-1 reagent (4-[3-(4-Iodophenyl)-2-(4-nitrophenyl)-2H-5-tetrazolio]-1,3-benzene disulfonate) is a tetrazolium salt, which can be cleaved to formazan by cellular mitochondrial dehydrogenases. Thus, an increase in the

number of metabolically active cells results in an augmented enzymatic activity and an increase in the amount of formazan dye formed. Quantification of the reaction product is performed by measuring Abs 450 nm – Abs 690nm (to remove background).
WST-1 assays were performed following the manufacturer's instructions.

3.15. *In vivo* experiments

3.15.1. Mice Xenografts

In order to assess the implication of LFG in tumor formation and metastasis, we performed a xenograft approach in immunodeficient mice using the human NBL cell line SH-SY5Y. Before injection, cells were transduced with shScr or sh*LFG* lentiviruses. In addition, they were stably infected with a lentiviral vector carrying the reporter gene firefly luciferase (pFLuc) to easily detect metastases by bioluminiscence (BLI) imaging. Then, $5x10^6$ cells were injected into the right flank of 6-week old NMRI-Foxn1^{nu}/Foxn1^{nu} female mice (Janvier) (n=10 for each condition) in a final volume of 300µl of PBS and Matrigel (1:1). NMRI-Foxn1^{nu}/Foxn1^{nu} mice bear a mutation in the *Foxn1* (forkhead box N1) gene that causes thymic aplasia, which results in a lack of T cells. This immunodeficient model has been widely used as a host for transplanted human tumors and xenografts (Geissler, Hambek et al. 2012, Henke, Meier et al. 2012, Lamers, Schild et al. 2012, Wolmer-Solberg, Baryawno et al. 2013).

Tumor growth was monitored using a digital caliper two or three times per week. Tumor volume was calculated using the sphere volume formula (width^2*length/2). When primary tumors reached the maximum allowed volume (~1600cm^3), mice were sacrificed by cervical dislocation. Then, the primary tumor mass was excised and weighed. Liver and lungs were collected from all the animals and the presence of micrometastases in these organs was analyzed BLI detection *ex vivo*. Immediately after imaging, tissues were rinsed once with PBS 1x and divided into 2 portions: one portion was fixed in 10% neutral buffered formalin while the other portion was frozen and stored at -80°C.

Animals were maintained under pathogen-free conditions. All procedures regarding animal care and experimentation were performed according to the guidelines of the Spanish Council for Animal Care and all protocols were approved by the Ethics Committee for Animal Experimentation of Vall d'Hebron Research Institute.

3.15.2. *In vitro* bioluminiscence imaging

For the *in vivo* experiments SH-SY5Y cells were stably infected with both pFLuc/mCherry and short hairpin (shScr or sh*LFG*) lentiviral vectors. In order to test BLI emission *in vitro*, we performed serial dilutions of the infected cells and seeded them into a black M96-well plate in a final volume of 50µl. Immediately after seeding, 50µl of D-luciferin substrate (Promega Biotech Ibérica) were added to reach a final concentration of 150 µg/mL and BLI was detected using IVIS® Spectrum (Figure 23).

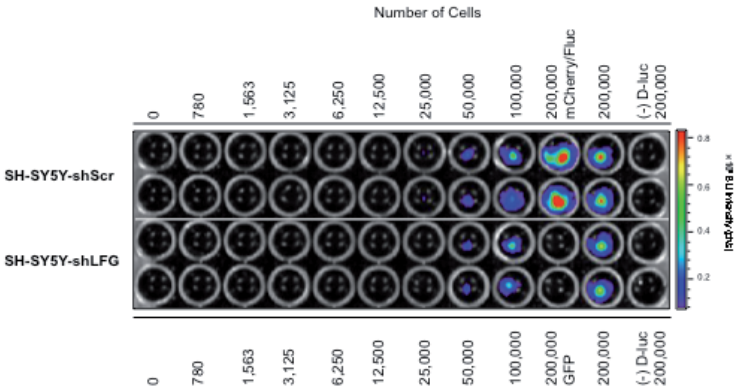

Figure 23. Serial dilutions of SH-SY5Y cells stably expressing firefly luciferase plus shScr/sh*LFG* constructs. The number of cells seeded in each well is indicated. Bioluminiscence of single lentiviral infections was also assessed: mCherry/Fluc cells were only infected with pFluc lentivirus that also carried the mCherry reporter gene; GFP indicates cells exclusively infected with shScr lentivirus. (-) D-luc was used as a negative control, since luciferase substrate was not added to the media.

BLI readouts were performed every 2 minutes after D-Luciferin addition. In order to ensure that both conditions – shScr and sh*LFG* cells – showed equivalent luciferase activity, total BLI was quantified using Living Image® 4.1 (Caliper Life Science, Inc.). For quantification, we used BLI readout at minute 13 post-D-Luciferin addition, since from then on, the signal was saturated (Figure 24).

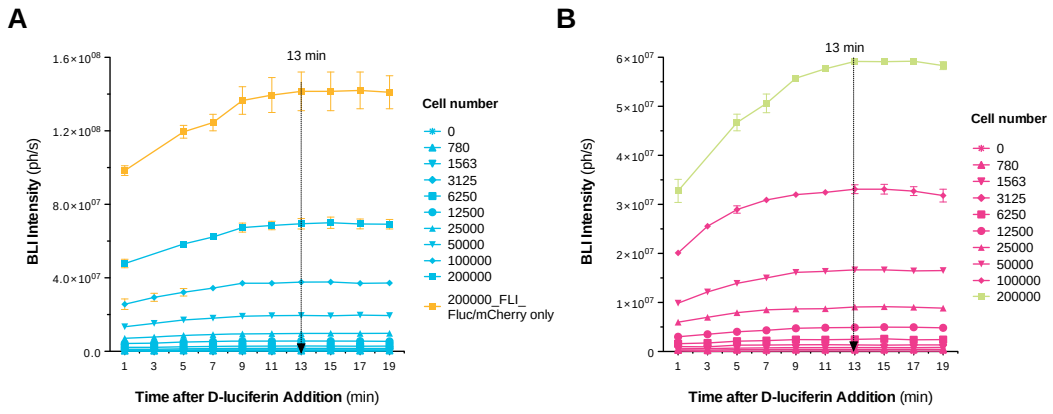

Figure 24. BLI kinetics after D-Luciferin addition to **A,** shScr and **B,** sh*LFG* pFLuc-SH-SY5Y cells. Kinetics were performed for every cell dilution represented in Figure 23.

3.15.3. *Ex vivo* bioluminiscence imaging

At the end of the *in vivo* experiment and five minutes before animal sacrifice, all mice were intraperitoneally injected with 150 mg/kg D-Luciferin substrate. During necropsy, a macroscopic evaluation of primary tumors and tissues was performed. Liver and lungs were collected and carefully separated into lobes. Livers where placed in M6 well plates, while lungs were disposed in black M24 plates. Tissues were immersed in a D-Luciferin 300µg/mL solution in PBS and maintained in ice-cold conditions and protected from light until *ex vivo* BLI imaging was performed.

BLI data was processed in two different ways using Living Image® 4.1:

- For total BLI flux quantification, non-saturated captures were used. For each tissue, we defined a region of interest (ROI) that covered the whole well and excluded external background (Figure 25). Total BLI intensity was measured in each ROI. In order to obtain a representative picture, the same scale was set for all conditions.

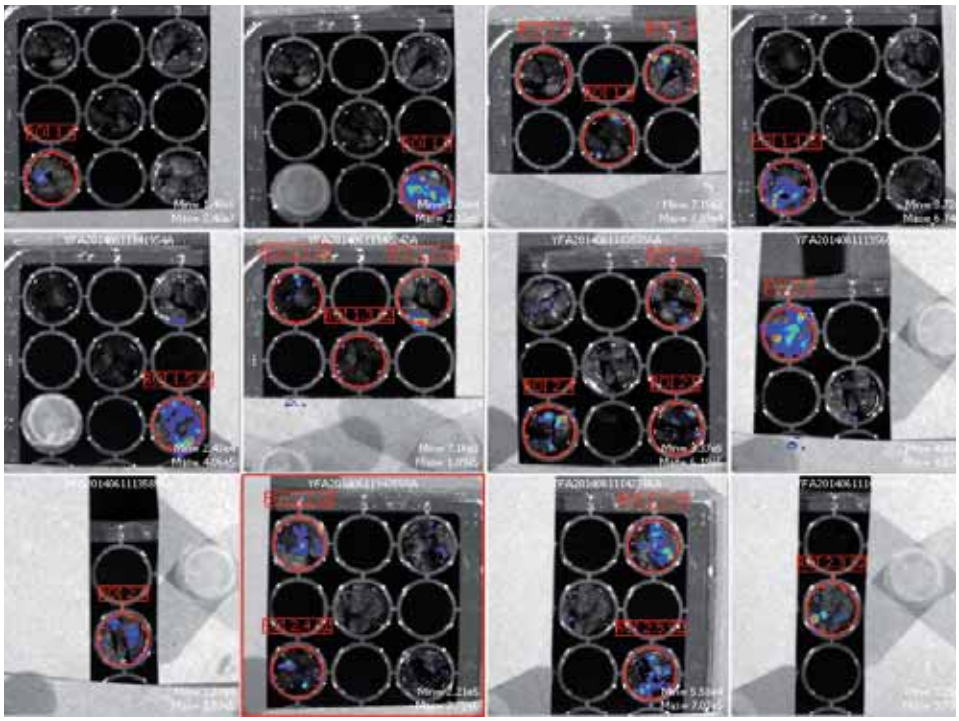

Figure 25. ROI selection in a lung *ex vivo* BLI capture.

- To assess the incidence of metastases, single bioluminiscent regions were counted. In this case, the intensity of BLI signal was not relevant and signal levels were increased and saturated in order to detect all bioluminiscent areas and count them.

3.16. mRNA microarray analysis

To analyze the differential gene expression signatures between SH-SY5Y cells infected with shScr and sh*LFG* lentiviruses, an expression profiling was performed using Affymetrix microarray platform and the Genechip Human Gene 1.0 ST Array.

RNA was extracted as previously specified and its quality was assessed using Agilent 2100 Bioanalyzer (Agilent Technologies). Samples that showed the best RNA quality were chosen for the array. In order to find reliable and statistically significant changes, this approach was performed on triplicate experimental sample groups (3xshScr versus 3xsh*LFG*).

Then, 200 ng of total RNA were hybridized to the arrays with the GeneChip WT Terminal Labeling and Hybridization Kit (Affymetrix). Chips were processed on an Affymetrix GeneChip Fluidics Station 450 and Scanner 3000.

Normalization of the raw data (.CEL files) was done with the Robust Multichip Average algorithm, a three-step process that integrates background correction, normalization and summarization of probe values (Irizarry, Hobbs et al. 2003). These normalized values were the basis for all analyses, and a Principal Component Analysis (PCA) verified their homogeneity. Previous to any analysis, normalized data were submitted to non-specific filtering in order to remove genes whose mean signal did not exceed a minimum threshold and genes with low variability.

The selection of differentially expressed genes between conditions was based on a linear model approach developed by Smyth (Smyth 2004). To perform differential expression analyses, a moderated *t*-test ($p<0.05$) and fold-change thresholding (>33% reproducible change) were considered. The results of this analysis consist on lists of up- or downregulated genes ranked from most to less differentially expressed.

Given that genes interact together in biological processes, it might be informative to understand these lists as a whole, what means finding the biological significance to the expression changes. This way, we should be able to detect whether genes appearing in the list have similar functionalities or are involved in the same processes. The functional annotations of resulting gene lists were performed using the Gene Ontology (Ashburner, Ball et al. 2000) and the Kyoto Encyclopedia of Genes and Genomes (KEGG) (Kanehisa and Goto 2000, Kanehisa, Goto et al. 2012) databases. These databases contain annotations describing

molecular functions, biological processes or cellular components associated with each gene, thereby allowing us to generate a list of enriched functional categories and the genes implied in each case, as well as the odd-ratios (OR) and *p*-values to assess the pathway's enrichment significance.

To build the heatmaps, array expression values were normalized to the median and $\log_2$ transformed. Values were converted to color scale using the Multiple Experiment Viewer software (TM4) (Saeed, Sharov et al. 2003).

3.17. Chromatin Immunoprecipitation array

Chromatin immunoprecipitation (ChIP) is a technique used to determine whether a specific protein is associated with a certain genomic region. With the aim to investigate the possible interaction between MYCN and *LFG* promoter, ChIP arrays were performed as described by Murphy *et al.* (Murphy, Buckley et al. 2009) and according to the standard NimbleGen ChIP protocol. Briefly, $1x10^9$ cells were fixed with 1% formaldehyde for 10 minutes on ice, to crosslink DNA and associated proteins. Lysates were then centrifuged and rinsed once with ice-cold PBS. Nuclei were isolated and sonicated to generate ~1 kb DNA fragments that still contained bound DNA-interacting proteins. The resulting fragmented chromatin was immunoprecipitated using 10 µg of NCMII-100 anti-MYCN antibody complexed to M-280 Sheep anti-Mouse Dynabeads (112-02D, Invitrogen). Afterwards, the formaldehyde crosslinks were removed from the immunoprecipitated DNA sample by heat denaturing, proteinase K and RNase A treatments. ChIP and input DNA were fluorescently labeled using Klenow fragment (M0212M, New England Biolabs) and Cy5/Cy3 random primers (N46-0001-50/N46-0002-50, TriLink BioTechnologies). Labeled DNA samples were co-hybridized to microarrays for 18 hours, washed and scanned using an Axon 4000B microarray scanner with GenePix 6.0 (Molecular Devices). This promoter array included an average coverage of 4.7 kb around gene promoters.

Image files generated during the scan were analyzed using NimbleScan Software Version 2.4. Sites of enrichment were identified using the normalized $\log_2$ ratios and the NimbleScan peak finding function.

3.18. Statistical analysis

Statistical significance was determined by unpaired *t*-test or One-way ANOVA when indicated (GraphPad Prism Software). * $P<0.05$, ** $P<0.01$ and *** $P<0.001$.

RESULTS

4. Results

4.1. Correlation of DR-antagonists expression with neuroblastoma prognosis.

Many studies have been performed to unravel the role of the extrinsic apoptotic pathway in high-risk NBL aggressiveness and chemoresistance. However, most of them have focused on the analysis of caspase-8 silencing and the restoration of its expression with the purpose of sensitizing cells to TRAIL-induced apoptosis (Teitz, Wei et al. 2000, Fulda, Kufer et al. 2001, Teitz, Lahti et al. 2001, Iolascon, Borriello et al. 2003, Johnsen, Pettersen et al. 2004, Fulda and Debatin 2006). Other approaches to understand and overcome NBL resistance have targeted inhibitor of apoptosis proteins such as XIAP or BCL-2 family members. However, the role of DR-antagonists remains poorly studied in NBL.

In order to check the expression levels of anti-apoptotic proteins in NBL and to establish correlations with tumor behavior, we took advantage of publicly available NBL microarray expression data sets. The mRNA levels of anti-apoptotic genes known to modulate the extrinsic pathway in the neural lineage were analyzed in different human expression NBL data sets. Table 12 shows the fold change variation between stage 4 *MYCN*-amplified tumors versus the rest of stages present in the respective study (i.e. stage 1, 2, 3 and 4 without *MYCN* amplification). As shown in the table, few DR-modulators were consistently altered in the two studied NBL data sets. Concretely, only *PEA15*, *FLIP* and *LFG* were downregulated in advanced stages of the disease and this downregulation was consistent in both data sets.

Table 12. Changes in expression of anti-apoptotic proteins between high-risk and low-risk NBLs.

Gene Symbol	Alias	GSE3960		GSE16237	
		Fold change	*P*-value	Fold change	*P*-value
FAIM	FAIM1	NA	NA	1.00	0.6430
FAIM2	LFG	-3.33	<0.0001	-3.22	0.0002
FAIM3	TOSO	-1.69	0.2831	1.00	0.8994
CFLAR	FLIP	-1.56	0.0154	-2.43	0.0235
XIAP	IAP3, BIRC4	1.57	0.3988	-1.20	0.0638
BIRC3	IAP2	-3,57	<0.0001	-1.28	0.2423
BIRC2	IAP1	-1.19	0.0011	-1.49	0.0954
TNFAIP3	A20	-2.27	<0.0001	1.05	0.2570
BFAR	BAR, RNF47	NA	NA	1.55	0.2570
PTPN13	FAP-1	1.36	0.1322	-1.19	0.7333
PEA15	HMAT1	-1.33	0.0154	-1.36	0.0247
SUMO1	UBL1, PIC1	1.25	0.0044	-2.27	0.3990
BTK	ATK, XLA	NA	NA	-1.20	0.9880

NA, not available. Statistically significant *P*-values are highlighted in grey.

PEA15, *FLIP* and *LFG* expression levels were further studied comparing different NBL stages. In particular, the highest differential expression for *FLIP* was found in stage 4 *MYCN*-non amplified NBLs, while *PEA15* and *LFG* were downregulated in stage 4 *MYCN*-amplified patients, which represents the group of NBLs with the worst prognosis (Figure 26).

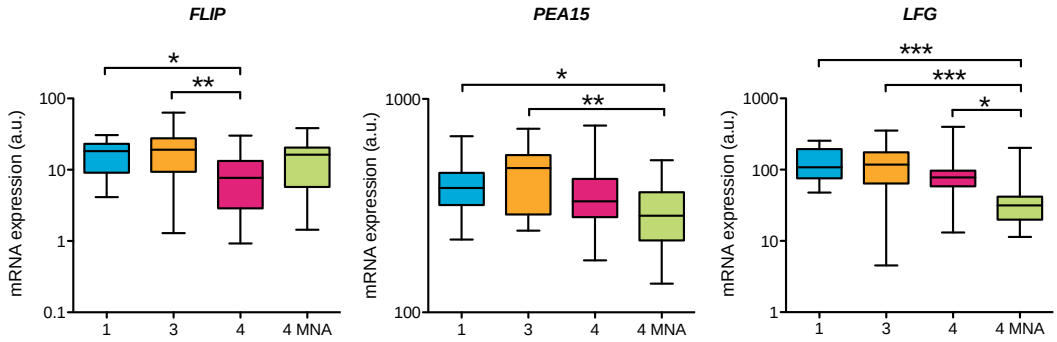

Figure 26. mRNA expression of the death receptor antagonists *FLIP* (1868_g_at), *PEA15* (32260_at) and *LFG* (33293_at) in different NBL stages obtained from GSE3960 data set. Data were analyzed by One-way ANOVA, **P*<0.05, ***P*<0.01, ****P*<0.001.

We also analyzed whether these differences in gene expression could be associated with patient outcome. In this case, the mRNA levels of the same genes were analyzed in two independent human prognosis NBL data sets (Table 13). These data sets allowed us to divide patients in two groups, either with high expression of the desired gene (expression levels above median) or with low expression of the same gene (mRNA expression below median). Then, we analyzed overall survival for each group of patients.

Table 13. Correlation between expression levels of anti-apoptotic proteins and patient overall survival in two independent NBL data sets.

Gene Symbol	Alias	GSE16476		Oberthuer Lab	
		Worse if…	*P*-value	Worse if…	*P*-value
FAIM	FAIM1	Low	0.419	NA	NA
FAIM2	LFG	Low	0.019	Low	$1.76e^{-9}$
FAIM3	TOSO	High	0.675	NA	NA
CFLAR	c-FLIP	Low	0.106	Low	0.978
XIAP	IAP3, BIRC4	Low	0.128	NA	NA
BIRC3	IAP2	Low	0.514	Low	0.026
BIRC2	IAP1	Low	$7.01e^{-9}$	Low	$5.6e^{-4}$
TNFAIP3	A20	Low	0.459	Low	0.141
BFAR	BAR, RNF47	High	0.001	High	0.024
PTPN13	FAP-1	High	$0.24e^{-3}$	NA	NA
PEA15	HMAT1	Low	0.367	NA	NA
SUMO1	UBL1, PIC1	High	0.547	High	0.031
BTK	ATK, XLA	High	0.373	Low	0.398

NA, not available. Statistically significant *P*-values are highlighted in grey.

Again, only *LFG*, *IAP1* and *BAR* consistently correlated with survival in both data sets (Figure 27).

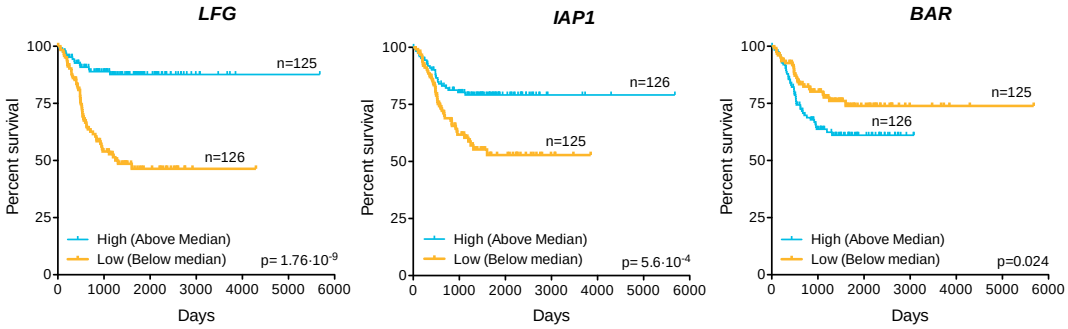

Figure 27. Kaplan-Meier overall survival curve in 251 tumors based on high or low *LFG* (A_23_P139891), *IAP1* (A_24_P115774) and *BAR* (A_24_P184931) expression. Data obtained from Oberthuer's Lab NBL data set.

Notably, only low expression levels of *LFG* were associated with both high-risk NBL and worse overall survival in all data sets (Tables 12, 13 and Figures 26, 27). These differences in *LFG* expression were then validated in an independent cohort of 38 primary tumor samples obtained at the Vall d'Hebron Hospital. mRNA was extracted from frozen tumor samples and analyzed by quantitative real-time PCR (qPCR). *LFG* levels were correlated with several available clinical variables. Low *LFG* expression correlated with *MYCN* amplification status and tumor histology. However, no association between *LFG* expression and other clinical variables such as age, patient status, presence of metastasis, tumor stage, tumor primary site or risk group was found (Table 14).

Table 14. Correlation between *LFG* levels and clinical data of the Vall d'Hebron Cohort.

Prognosis factor	Variables	Statistics [*P*-value]
MYCN	Amplified Non-amplified	Unpaired *t*-test [0.0121]
Histology	Favorable Unfavorable	Unpaired *t*-test [0.0041]
Age	<18 months >18 months	Unpaired *t*-test [0.9581]
Status	Dead Alive	Unpaired *t*-test [0.3609]
Metastasis	Yes No	Unpaired *t*-test [0.1176]
Stage	1 / 3 / 4	One-way ANOVA [0.4405]
Primary site	Suprarenal Thoracic Abdominal	One-way ANOVA [0.2488]
Risk	Low Intermediate High	One-way ANOVA [0.2560]

Statistically significant *P*-values are highlighted in grey.

In accordance with the expression of *LFG* in NBL data sets, tissue mRNA expression analysis revealed a significant reduction in *LFG* levels in stage 4 *MYCN*-amplified tumors, when compared to lower stages (Figure 28A). We were able to confirm by Western Blot analyses that the reported differences in mRNA expression were also evident at the protein level, where LFG was almost undetectable in *MYCN*-amplified tumors (Figure 28B).

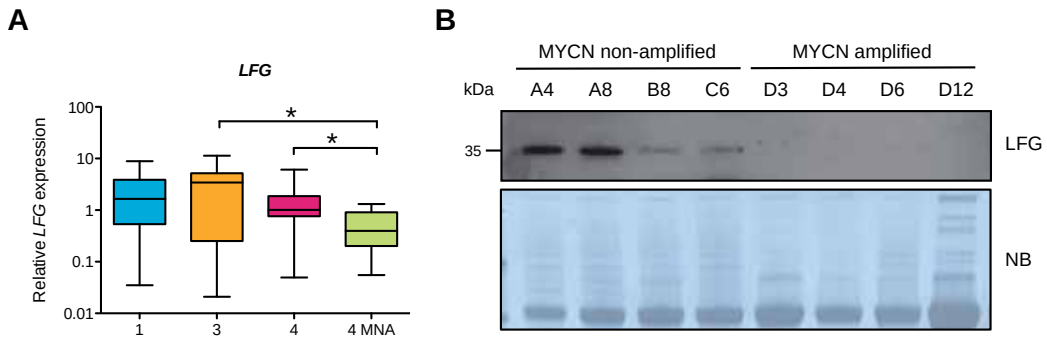

Figure 28. Lifeguard expression is reduced in *MYCN* amplified tumors. A, Relative *LFG* expression measured by qPCR in an independent cohort of NBL primary tumors collected at Vall d'Hebron Hospital. Data was analyzed by One-way ANOVA, **P*<0.05. MNA, *MYCN* amplified. **B,** Western blot showing LFG expression in four *MYCN* non-amplified versus four *MYCN* amplified primary NBL tumors. Legend: A, Stage 1; B, Stage 3; C, Stage 4 *MYCN* non-amplified; D, Stage 4 *MYCN* amplified tumors. Naphtol blue (NB) staining was used as a loading control.

LFG levels were decreased in *MYCN* amplified tumors, while *MYCN* non-amplified NBLs showed a wide variety in LFG expression. For this reason, we sought to analyze whether these variations in LFG expression within *MYCN* non-amplified tumors still maintained a correlation with prognosis. Thus, the association between *LFG* levels and patient survival was analyzed in three *MYCN* non-amplified tumor data sets. *LFG* expression correlated with patient survival in two out of three NBL data sets. The same tendency was observed in the third one, even though differences were not statistically significant (Figure 29), indicating that LFG could have a prognosis value independent of MYCN.

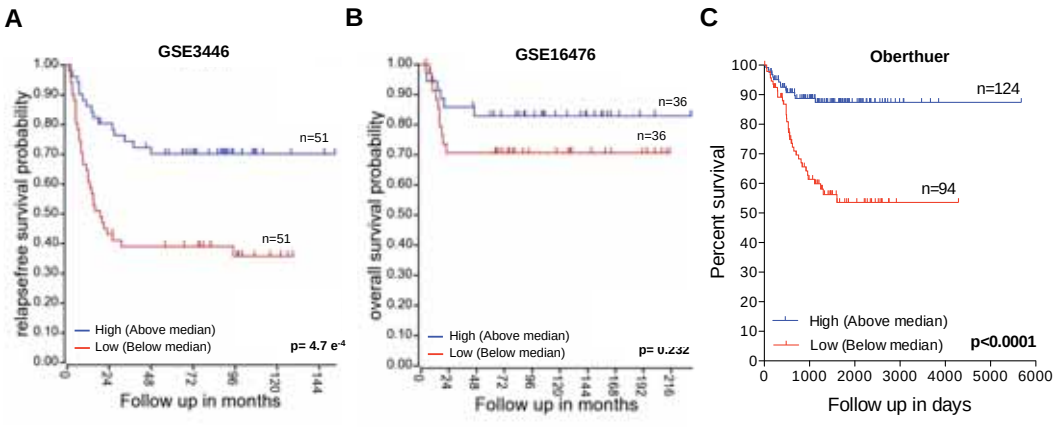

Figure 29. Kaplan-Meier curves in *MYCN* non-amplified NBL subsets. A, B, Curves were generated with R2 open source software with data from GSE3446 and GSE16476 studies (probe 203619_s_at). **C,** Survival curve was generated using data of *MYCN* non-amplified tumors from Oberthuer's NBL dataset.

In summary, LFG is the DR-antagonist with the highest differential expression and association with patient outcome in high-risk NBL. In particular, LFG levels are decreased in stage 4 *MYCN*-amplified tumors, the most aggressive and chemoresistant NBL subset. Moreover, the fact that LFG expression correlates with patient survival in *MYCN* non-amplified tumors points to LFG as a new prognosis marker in this NBL subset.

4.2. Lifeguard is associated with neuroblastoma histology and differentiation.

When *LFG* levels were correlated with a number of clinico-pathological variables (i.e. age at diagnosis, site of primary tumor, site of metastasis and histology), *LFG* expression was found to be closely associated with tumors presenting both *MYCN* amplification and unfavorable histology (Table 14). In particular, *LFG* was found downregulated in tumors diagnosed with unfavorable histology, which are often undifferentiated tumors (Westermark, Wilhelm et al. 2011) (Figure 30).

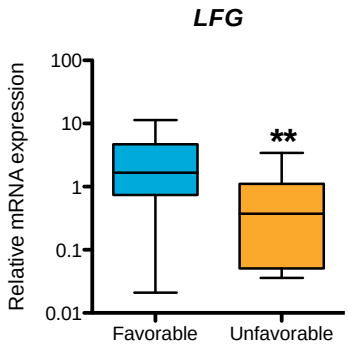

Figure 30. Relative *LFG* mRNA expression in histologically favorable (n=30) versus unfavorable (n=8) primary tumors. mRNA levels were measured by qPCR. Unpaired *t*-test, ***P*<0.01.

With the aim to confirm the results seen by qPCR, we next detected LFG by immunohistochemistry (IHC) in NBL tumor slices of patients with favorable and unfavorable histological diagnosis (Figure 31). *MYCN* non-amplified tumors presented a favorable histology with hints of differentiation, a higher stromal content and the formation of the classical Homer Wright rossettes. Rossettes consist of differentiated tumor cells surrounding the neuropil, a synaptically dense region with a low number of cell bodies and composed by citoplasmatic extensions, unmyelinated axons and dendrites. In these tumors, LFG showed a citoplasmatic staining that was strongly detected in the neuropil areas (black arrows) and in the citoplasms of cells that were undergoing ganglionar differentiation (red arrows). In contrast, *MYCN*-amplified tumors had an unfavorable histological diagnosis, and consisted on stroma poor, undifferentiated neuroblasts. LFG staining was weak and gained intensity in more mature regions of the tumors (see D12).

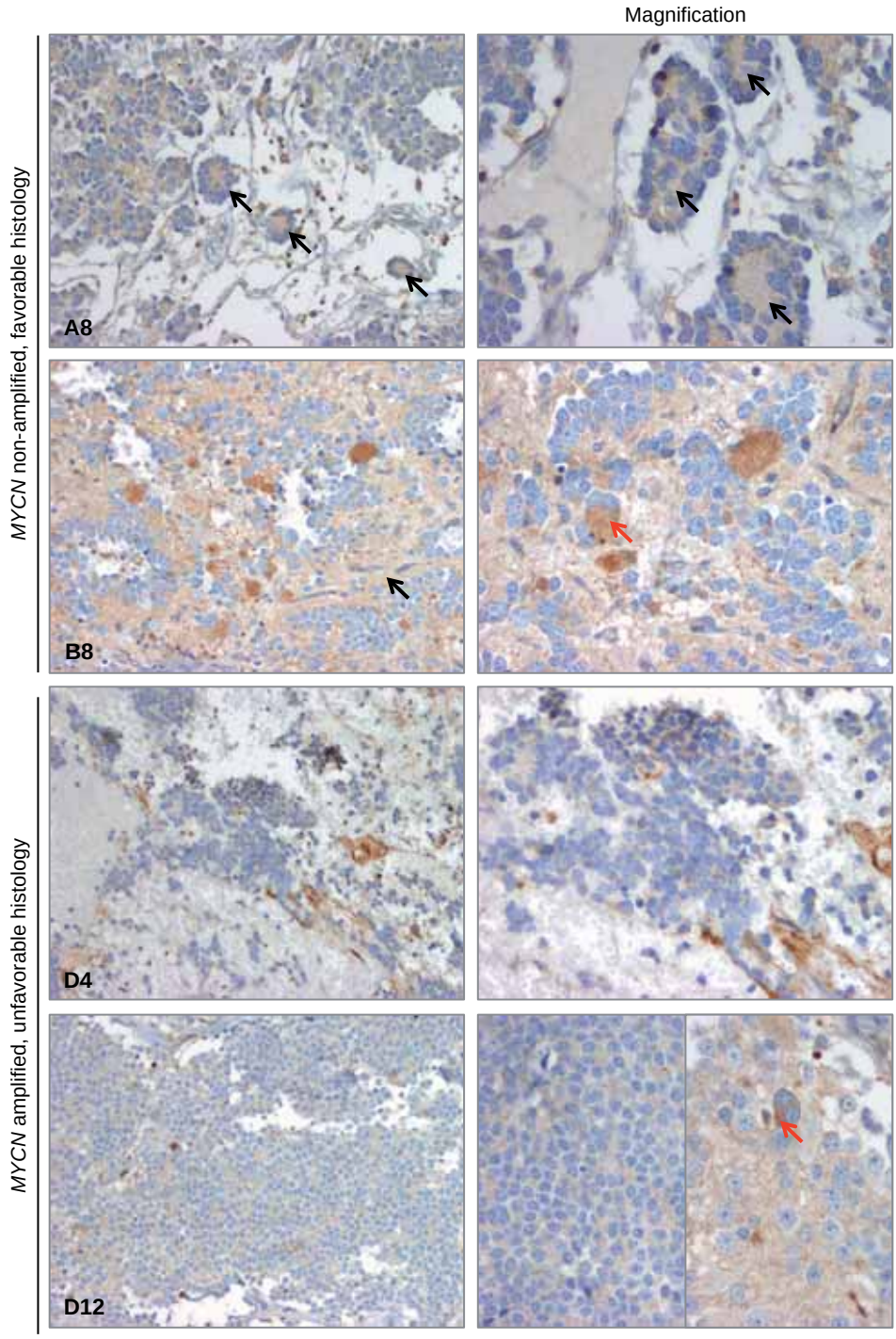

Figure 31. LFG Immunohistochemistry in primary NBL tissues. Images show four NBL tissue samples divided by histological diagnosis and *MYCN*-amplification status. Black arrows point Homer Wright rossettes, where differentiated tumor cells surround the neuropil, strongly stained by anti-LFG antibody. Red arrows point to cytoplasms of bigger cells that are undergoing ganglionar differentiation and show intense staining. Left image was obtained at 200x, while magnification images were obtained with 400x amplification. D12 tumor had regions with different maturation status, both represented in the magnification column: undifferentiated (left), differentiating (right).

Histological criteria for NBL classification include several factors such as age at time of diagnosis, the MKC index, the content of Schwannian stroma within the tumor mass and, importantly, the degree of differentiation of neuroblastic cells (Shimada, Chatten et al. 1984, Shimada, Umehara et al. 2001). With the view to validate the association between the differentiation status of NBL cells and *LFG* expression, we sought to characterize *LFG* levels in different cellular models of NBL differentiation. For this study, we induced the differentiation of NBL cells using retinoic acid (Encinas, Iglesias et al. 2000, Hammerle, Yanez et al. 2013). Alternatively, we maintained NBL cells in neurosphere-formation media to mimic a poorly differentiated NBL status (Hansford, McKee et al. 2007, Mahller, Williams et al. 2009).

On the one hand, we treated SH-SY5Y and SK-N-BE(2) cells with the differentiating agent *all-trans* retinoic acid for several days and *LFG* levels were analyzed by qPCR and western blot (Figure 32).

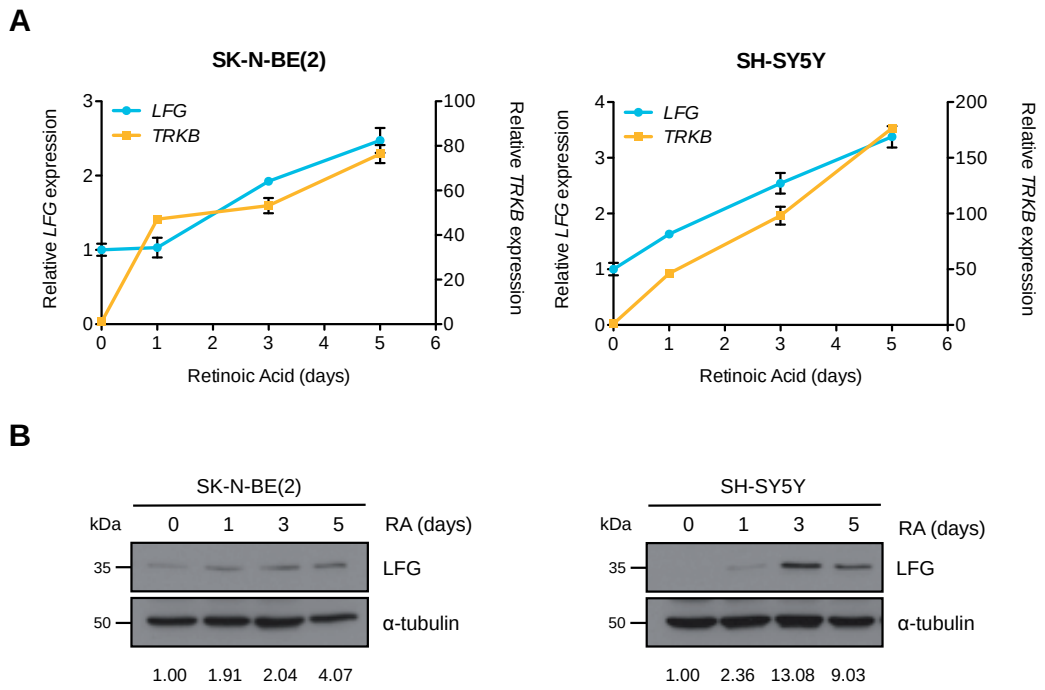

Figure 32. LFG levels increase during NBL cell lines differentiation. A, *All-trans* retinoic acid (10µM) induced differentiation in NBL cell lines SK-N-BE(2) and SH-SY5Y. *LFG* and *TRKB* expression were measured by qPCR at the indicated time points. Data presented as mean ± S.E.M of three independent experiments. **B,** Western Blot of LFG expression. α-tubulin was used as loading control. Bands were quantified using Image J software and normalized expression values are indicated.

All-trans retinoic acid-mediated differentiation of SK-N-BE(2) and SH-SY5Y cell lines increased *LFG* expression both at mRNA and protein levels. *TRKB* was used as a neuronal differentiation

marker to confirm the differentiation response of the NBL cell lines to the RA treatment (Encinas, Iglesias et al. 2000). As shown in Figure 32A, *LFG* mRNA levels increased concomitantly with *TRKB* in both cell lines. LFG upregulation was also confirmed by western blot (Figure 32B).

On the other hand, some NBL cell lines can be cultured in neurosphere formation medium, which consists of serum-free medium supplemented with the growth factors EGF and FGF2 to stimulate growth of cells with stem properties. In fact, many authors support the hypothesis that autonomous growth in serum-free media as non-adherent neurospheres is a representative model of neural and malignant progenitors (Bez, Corsini et al. 2003, Nagato, Heike et al. 2005, Hansford, McKee et al. 2007, Mahller, Williams et al. 2009). Mahller and colleagues demonstrated that the ability to grow as spheres directly correlates with the amplification of the oncogene *MYCN* (Mahller, Williams et al. 2009). Therefore, three *MYCN*-amplified NBL cell lines were seeded in neurosphere medium in order to mimic an undifferentiated status of NBL cells. Cells grown in neurosphere medium formed non-adherent spheres (Figure 33A). *LFG* expression levels were analyzed in SK-N-BE(2), IMR-5 and IMR-32 NBL spheres. *LFG* mRNA was found to be downregulated in sphere medium-cultured cells compared to cells cultured in standard conditions (P=0.0286 for SK-N-BE(2) and IMR-5; P=0.0294 for IMR-32) (Figure 33B).

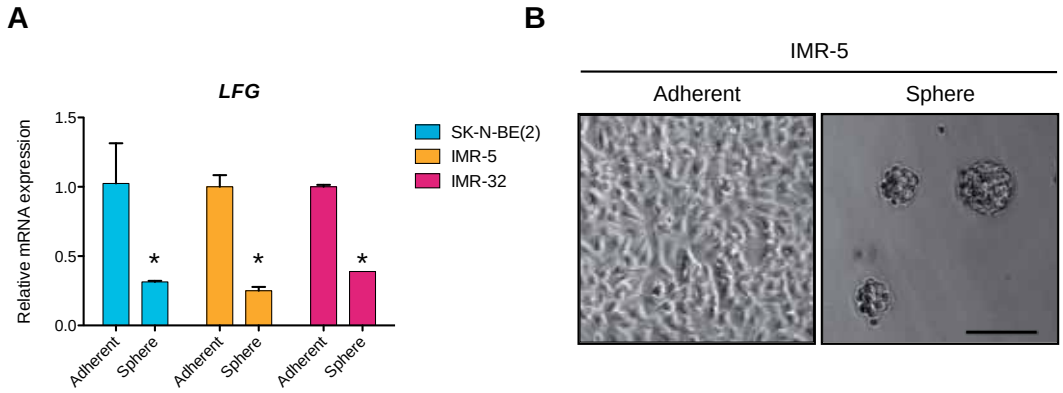

Figure 33. Neurosphere formation decreases *LFG* expression. A, Images show IMR-5 adherent and sphere-forming cultures. Scale bar, 100 µm. **B,** *LFG* expression detection by qPCR in the indicated NBL cell lines cultured with standard conditions (Adherent) or using neurosphere medium (Sphere). Unpaired *t*-test, **P*<0.05. Data represented as mean ± S.E.M, n=4.

These data allow us to conclude that *LFG* expression correlates with the histological classification of NBL tumors and, when analyzed in NBL cell lines, it associates with their differentiation status.

4.3. Lifeguard knockdown modulates proliferation, adhesion and migration of neuroblastoma cell lines.

Considering that LFG was found downregulated in *MYCN*-amplified and histologically unfavorable tumors, which often define the high-risk group of NBL tumors, we hypothesized that this protein could play a role in NBL behavior and aggressiveness. In order to assess the implication of LFG in NBL oncogenic properties, loss of function experiments were performed using two different shRNA targeting *LFG*. We chose as a model the NBL cell lines SH-SY5Y and CHLA-90 for three main reasons: first, because they show a neuronal phenotype; second, because none of them presents *MYCN* amplification; and third, because both express high levels of LFG.

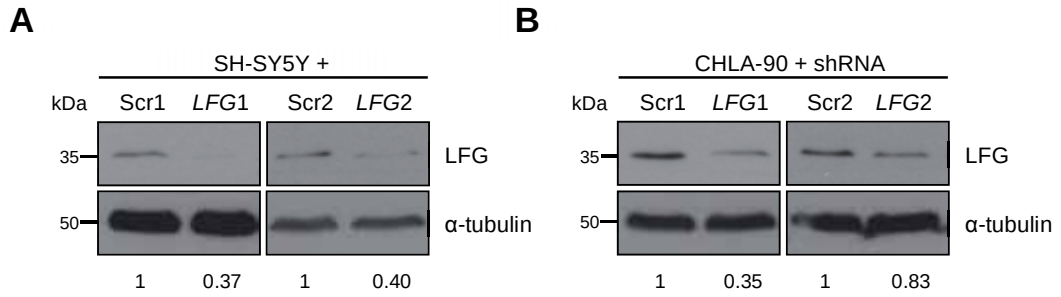

Figure 34. Western blot showing LFG downregulation in **A,** SH-SY5Y cells and **B,** CHLA-90 cell line. LFG knockdown was achieved by infection with two sets of shScr or sh*LFG* lentiviruses. LFG expression was detected using anti-FAIM2 (H-21) antibody (Santa Cruz Biotechnology, Inc). Bands were quantified using ImageJ and normalized versus α-tubulin.

Both sh*LFG* constructs notably knocked down LFG as seen by western blot (Figure 34) and LFG downregulation reduced proliferation of SH-SY5Y (*P*=0.0220 for sh*LFG* and *P*=0.0238 for sh*LFG*2) and CHLA-90 cells (*P*=0.0043 for sh*LFG* and *P*=0.0223 for sh*LFG*2) (Figure 35).

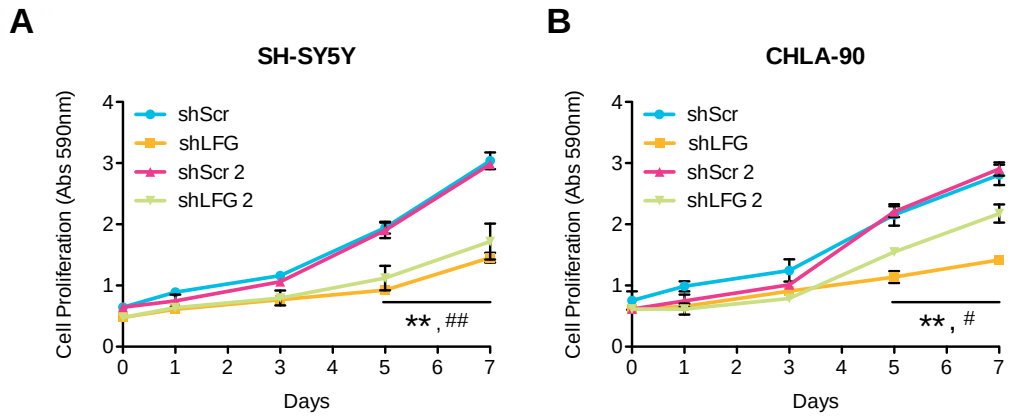

Figure 35. LFG knockdown decreases cell proliferation. Cell proliferation assay in **A,** SH-SY5Y and **B,** CHLA-90 cells after LFG downregulation with two shRNA sets (shScr/sh*LFG* and shScr2/sh*LFG*2). Cells were fixed with 4% paraformaldehyde at the indicated time points. Data presented as mean ± S.E.M of three independent experiments. Unpaired *t*-test, **P*<0.05 and ***P*<0.01; * accounts for shScr versus sh*LFG*, while # accounts for shScr2 versus sh*LFG*2.

Since the most efficient downregulation of LFG and its effects on cell proliferation was achieved by sh*LFG*, and to a lesser extent by sh*LFG2,* (Figures 34, 35) sh*LFG* was employed for the following experiments.

Next, we questioned whether LFG silencing could be affecting NBL cell adhesion. sh*LFG*-transduced cells exhibit a ~50% reduction in adhesion to adherent plates compared with scrambled-infected cells in both cell lines (*P*=0.0286 for SH-SY5Y and *P*=0.0043 for CHLA-90 cells) (Figure 36).

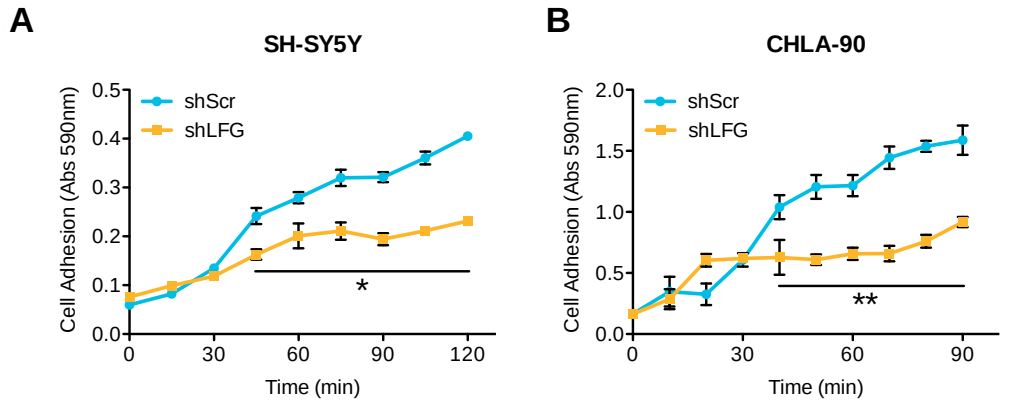

Figure 36. LFG downregulation decreases cell adhesion. Adhesion assay of **A,** SH-SY5Y and **B,** CHLA-90 cells transduced with either Scrambled or *LFG* shRNAs, measured at the indicated time points. Data represented as mean ± S.E.M, n=3. Unpaired *t*-test, **P*<0.05 and ***P*<0.01.

The effects of LFG knockdown on cell proliferation and adhesion were lost when they were studied in *MYCN*-amplified cell lines, which already showed lower LFG expression (Figure 37).

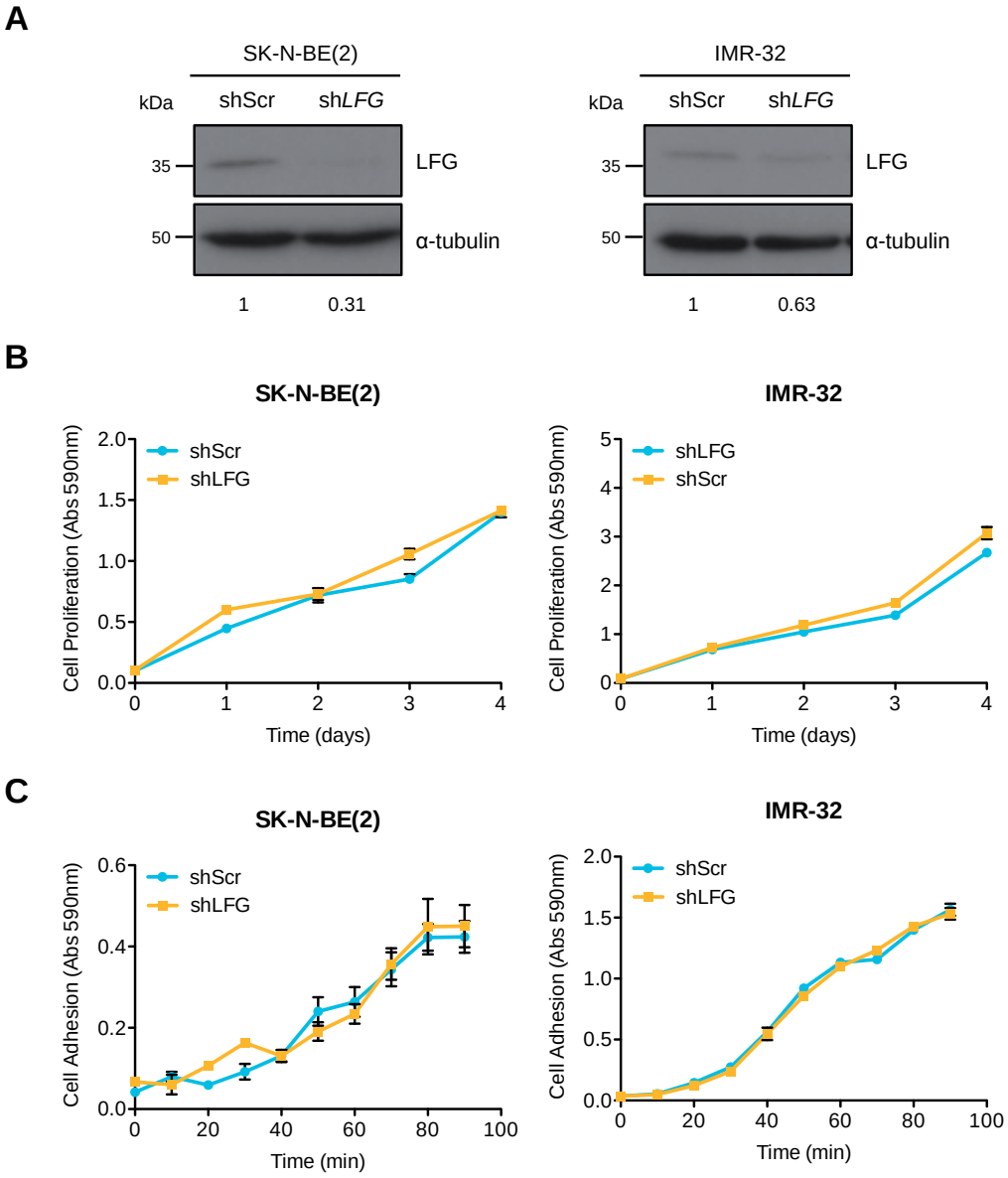

Figure 37. Effects of LFG knockdown in *MYCN*-amplified NBL cell lines. A, Western Blot confirming LFG downregulation in SK-N-BE(2) and IMR-32 cells transduced either with shScr or sh*LFG* lentiviruses. **B,** Cell proliferation experiments in infected SK-N-BE(2) and IMR-32 cells. **C,** Cell adhesion assays in the same cell lines, measured at the indicated time points after seeding.

The reduction in the adhesion capacity of sh*LFG*-transduced cells pointed to the possibility that LFG knockdown could be conferring cells the ability to grow autonomously in suspension. In fact, when NBL cells were seeded at low density in standard culture medium, loss of LFG

increased non-adherent growth compared to the scrambled shRNA (Figure 38A). Concretely, more than 10% of sh*LFG* cells were able to form viable spheres when they were seeded at low density in DMEM supplemented with 15% FBS, while less than 4% of control cells did so (*P*=0.0066) (Figure 38B).

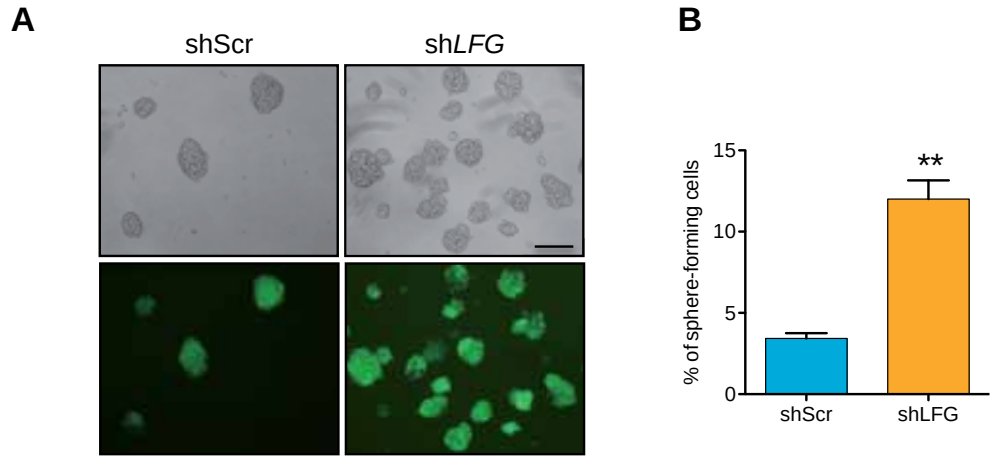

Figure 38. Silencing of LFG expression induces sphere formation in SH-SY5Y cells. A, Sphere formation assay of shScr and sh*LFG* SH-SY5Y cells seeded at low density in DMEM + 15% FBS and kept in standard culture conditions for four weeks. Infection efficiency was monitored by visualization of GFP. Scale bar, 100 µm. **B,** Graph represents the percentage of sphere formation. Data presented as mean ± S.E.M, n=9. Unpaired *t*-test, ***P*<0.01.

Sphere formation and non-adherent growth has been associated to an increase in stemness properties of cells derived from many tumor types, including NBL (Hansford, McKee et al. 2007, Mahller, Williams et al. 2009, Penuelas, Anido et al. 2009). For this reason, we proceeded to quantify the expression of several stem cell markers by qPCR, such as *ABCG2*, *CD133*, *KLF4*, *NANOG*, *NESTIN*, *NOTCH3*, *OCT4* and *SOX2* before and after *LFG* silencing. In our case, knockdown of LFG promoted non-adherent growth but did not induce the expression of any of the above-mentioned genes. Instead, *CD133* and *NESTIN* were significantly downregulated (*P*=0.0004 and *P*=0.0280) (Figure 39).

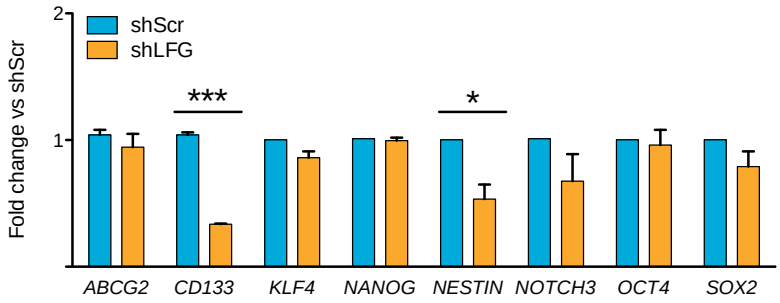

Figure 39. LFG knockdown does not increase stemness properties of NBL cell lines. qPCR for several stem cell marker genes in SH-SY5Y cells transduced with either shScr or sh*LFG* lentiviruses. Data presented as mean ± S.E.M, n=3. **P*<0.05, ****P*<0.001, unpaired *t*-test.

Instead of increasing stemness properties of NBL cells, downregulation of LFG could be driving a phenotypic shift towards an EMT-like phenotype. EMT is a process where cells acquire a motile and non-adherent phenotype that allows them to migrate to distant sites. EMT occurs during delamination of neural crest cells in the course of embryogenesis, but it is also related to metastasis in a pathologic context (Liu, Zhang et al. 2014). We assessed the expression of the main genes related to EMT (*SNAI1*, *TCF3*, *ZEB1*, *ERBB3*, *KRT19*, *SNAI2*, *TWIST1*) by qPCR in SH-SY5Y cells after LFG knockdown. The expression of *TWIST1*, a gene that is upregulated during the EMT process, was significantly increased in SH-SY5Y cells with reduced LFG expression (*P*=0.0388). In addition, *KRT19* and *ERBB3*, two genes that have shown to be downregulated during EMT, were also downregulated after LFG silencing in SH-SY5Y (*P*=0.0425 and *P*=0.0009). Contrary to what we would expect, the expression of *SNAI2*, another gene known to be upregulated during EMT, was strongly decreased in sh*LFG* cells (*P*=0.0002) (Figure 40).

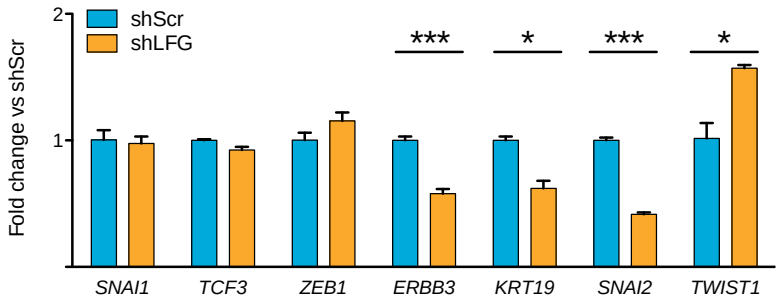

Figure 40. LFG knockdown alters the expression of EMT markers. qPCR of EMT-related genes in SH-SY5Y cells transduced with either shScr or sh*LFG* lentiviruses. Data presented as mean ± S.E.M, n=3. **P*<0.05, ****P*<0.001, unpaired *t*-test.

In the same line, we proceeded to analyze the expression of a pool of EMT-related genes (*CALD1, EGFR, DSP, SNAI2, SPARC, ZEB1, ZEB2, VIM, FN1, KRT19, ERRB3, RGS2, TCF3, TWIST1, ACTNB*) in LFG high-expressing and low-expressing NBL patients from the NBL data set GSE3960 (Wang, Diskin et al. 2006). Among those, several genes known to be increased during EMT showed higher expression levels in tumors with low LFG expression. Those upregulated genes were *CALD1*, *FN1*, *SPARC*, *TCF3* and *TWIST1*. *SNAI2* expression was also increased in low LFG tumors, although its expression levels were extremely low (Figure 41A). In addition, *KRT19* and *ERBB3* were downregulated in tumors with low LFG expression, again with very low levels of *ERBB3* mRNA expression (Figure 41B).

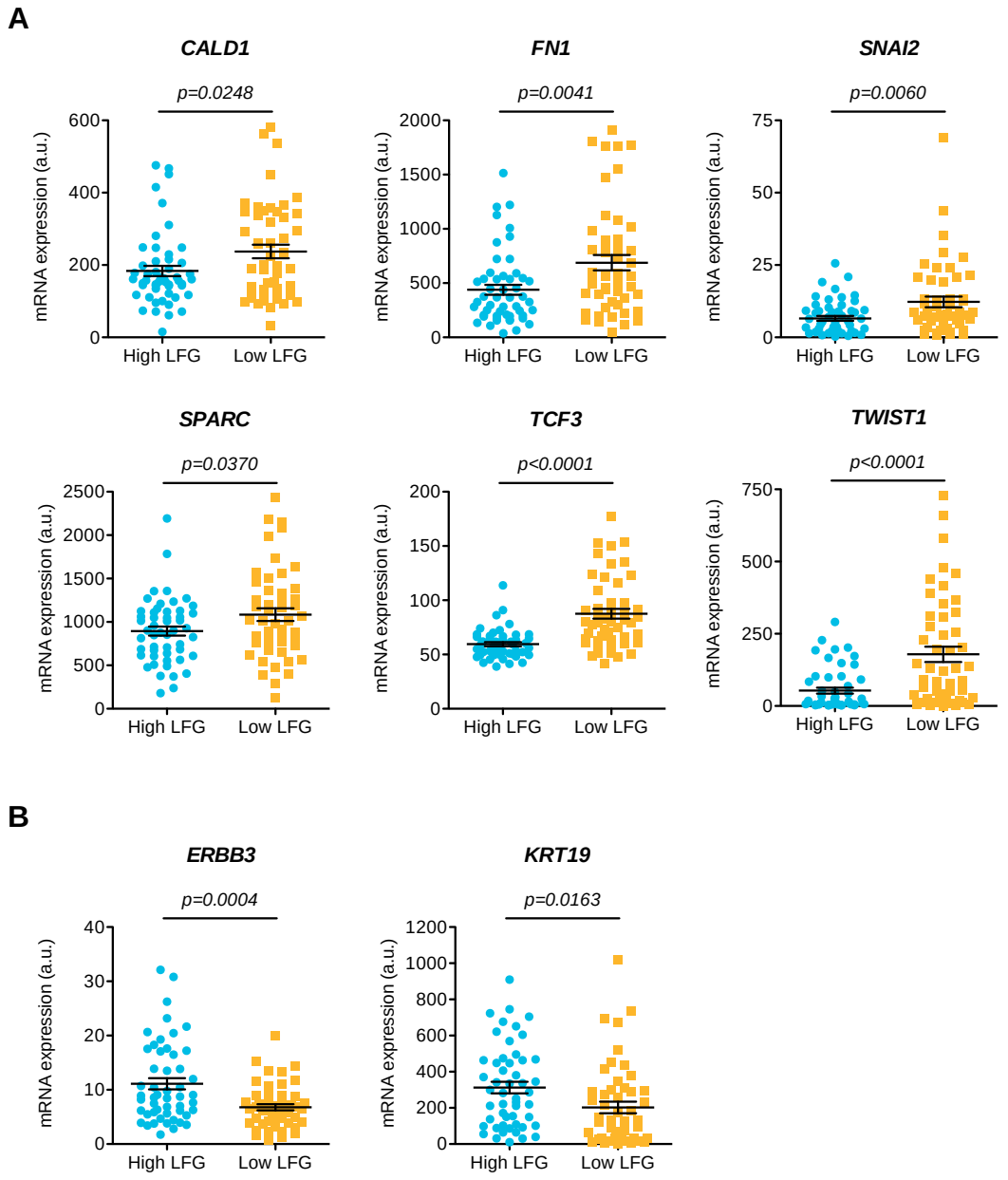

Figure 41. Expression levels of EMT genes in tumor samples grouped by LFG expression. Several genes involved in EMT were differentially regulated in tumors with high or low LFG levels. **A,** upregulated genes; **B,** downregulated genes. Data obtained from Wang's group data set (GSE3960).

Concurring with our *in vitro* results, *TWIST1* levels were higher in tumors with low LFG levels, while *KRT19* and *ERBB3* were downregulated. However, some differences were found between Wang's dataset data and our qPCR approach in SH-SY5Y cells. *TCF3* levels did not change after LFG knockdown in SH-SY5Y cells, while it was clearly upregulated in tumors with low LFG expression. *SNAI2* levels were downregulated in sh*LFG* SH-SY5Y cells but found to be upregulated in human samples with low levels of LFG.

EMT transitions and non-adherent growth are often related to increased migration and invasion abilities of tumor cells, a characteristic of aggressive and metastatic neoplasms (Hansford, McKee et al. 2007, Hanahan and Weinberg 2011, Nozato, Kaneko et al. 2013). In order to check if this was the case of sh*LFG*-transduced cells, we first performed migration assays in SH-SY5Y cells. Briefly, migration assays consisted in seeding cells into 8µm-transwell polycarbonate inserts and generating a FBS gradient that induced cells to cross the filter and migrate to the lower part of the well. Indeed, sh*LFG*-infected cells showed a 4-fold increased migration through the 8µm-transwell polycarbonate insert (*P*=0.0191) (Figure 42).

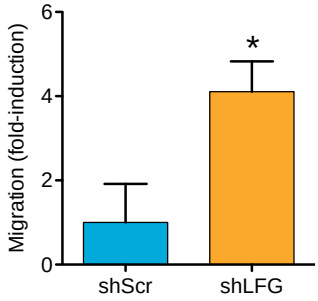

Figure 42. LFG silencing increases migration ability of SH-SY5Y neuroblastoma cell line. Transwell migration assay of shScr and sh*LFG*-transduced SH-SY5Y cells. Cells that migrated were quantified by WST-1 assay. Graph shows mean ± S.E.M, n=3. Unpaired *t*-test, **P*<0.05.

sh*LFG* cells show autonomous non-adherent growth and the ability to migrate. However, an increased migration potential does not necessarily mean that cells are able to invade other tissues. Invasion, on the other hand, implies that cancer cells actively cross the extracellular matrix to escape from the primary tumor and get into other tissues, often by secreting

enzymes such as proteases (Hanahan and Weinberg 2011). In order to assess the invasion potential of sh*LFG* NBL cells, we performed an invasion assay in infected SH-SY5Y cells. This assay was performed under the same conditions as the migration assay, with the difference that polycarbonate inserts were coated with matrigel, a mixture that resembles the extracellular environment, prior cell seeding. As shown in Figure 43, loss of LFG expression did not affect the invasion potential of SH-SY5Y cells.

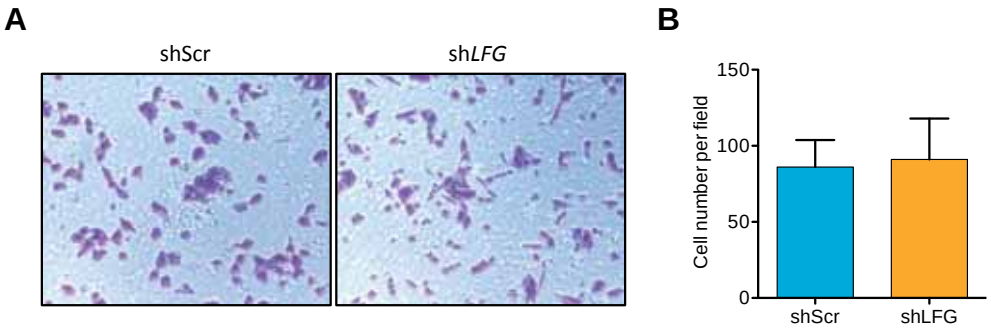

Figure 43. Invasion capacity of SH-SY5Y cells is not altered by loss of LFG expression. A, Representative image of a transwell invasion assay of shScr and sh*LFG*-transduced SH-SY5Y cells using matrigel-coated polycarbonate filters. **B,** Cells that crossed the matrigel matrix were fixed, stained with crystal violet and counted.

Taken together, these results indicate that the reduction on *LFG* levels switches the proliferation program to a mesenchymal migratory phenotype, altering the adhesion properties and thus potentially increasing the metastatic potential of NBL cells.

4.4. Lifeguard knockdown increases *in vivo* tumor formation and metastasis.

The impact of LFG knockdown on NBL cells behavior was further evaluated *in vivo* using NBL xenografts. To track the metastatic potential of shScr and sh*LFG,* SH-SY5Y cells were previously transduced with the reporter gene firefly luciferase vector (pFLuc), which allows its detection by bioluminescence (BLI) imaging.

Prior to NBL cell injection, BLI emission of shScr and sh*LFG* cells was evaluated *in vitro*. Quantification of BLI intensity demonstrated that both cellular variants showed a comparable luciferase activity and a linear correlation between the number of cells and the amount of light measured (Figure 44).

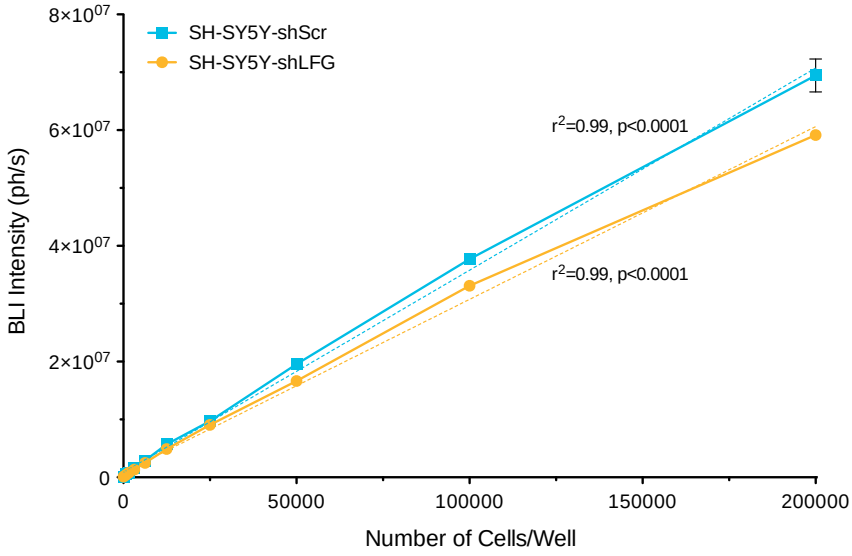

Figure 44. *In vitro* quantification of BLI intensity of shScr and sh*LFG* pFLuc-SH-SY5Y cells. BLI intensity was measured 13 minutes after the addition of D-luciferin substrate, just before saturation. Graph represents Mean ± S.E.M.

After this verification, sh*LFG* and shScr SH-SY5Y cells were injected into the flank of female NMRI-*Foxn1*^{nu}/*Foxn1*^{nu} mice (n=10 / group). Tumor formation was followed by palpation two or three times a week. Tumor-free survival was higher in the control group, as compared to sh*LFG* mice (Figure 45). This effect was more evident during the first two weeks post-injection. Later on, tumor incidence in the shScr group reached the same levels as sh*LFG* tumors.

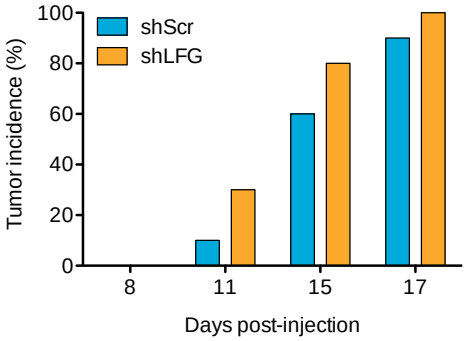

Figure 45. Tumor incidence in mice injected with SH-SY5Y cells transduced with shScr or sh*LFG* lenvitiruses.

No significant differences neither in tumor growth nor in tumor weight were found between the two groups (Figure 46), even though LFG knockdown reduced cell proliferation in NBL cell cultures (Figure 35).

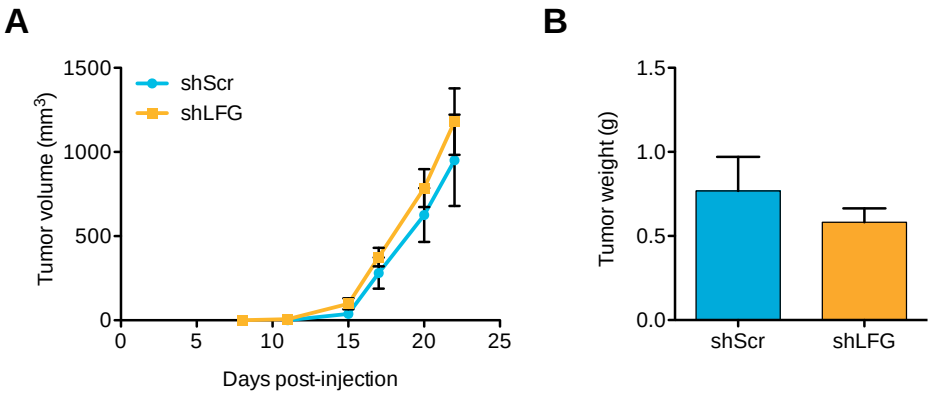

Figure 46. Tumor growth and tumor weight. A, Tumor growth was monitored using a digital caliper and tumor volume was calculated using the formula (width^2*length/2). Data represented as mean ± S.E.M. **B,** Tumor mass was weighted after necropsy. Graph shows mean ± S.E.M.

Since LFG knockdown conferred non-adherent growth abilities and an increased migration capacity of NBL cells *in vitro*, we hypothesized that sh*LFG* could enhance the metastatic potential of the NBL cells *in vivo*. Thus, we proceeded to evaluate the presence of spontaneous metastasis in distal organs by BLI detection. We evaluated total BLI flux in dissected lungs and livers of injected mice. A slight increase in total BLI flux was observed in livers and lungs from mice with sh*LFG* xenografts, but it did not reach statistically significant differences (Figure 47).

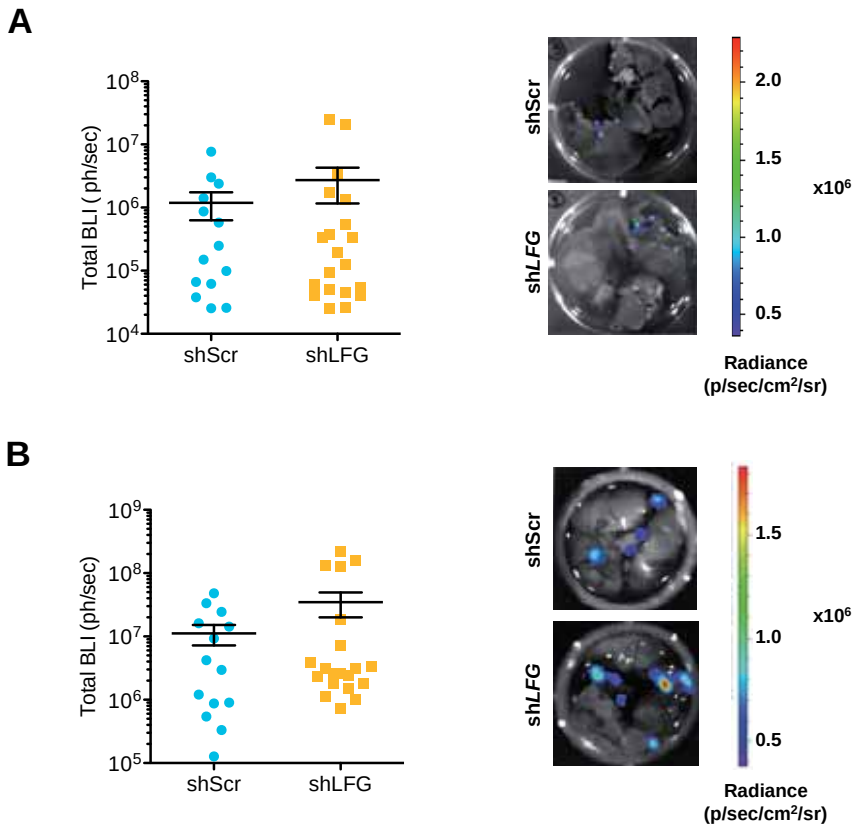

Figure 47. *Ex vivo* total BLI detected in livers and lungs from injected mice. Total BLI flux (photons/second) of **A,** liver and **B,** lung metastases from shScr and sh*LFG* SH-SY5Y injected mice. Representative images are shown. Pictures were set at the same scale to compare BLI between shScr and sh*LFG* conditions.

An increase of the metastatic potential could involve the formation of a higher number of micrometastases in the target tissue and this might not be detected by quantification of the total BLI flux. Thus, we decided to count the number of metastases in livers and lungs of injected mice. No significant differences were found in livers of both groups (Figure 48A), but a significant increase in the number of metastases was found in lungs from xenografts bearing sh*LFG* (P=0.0412) (Figure 48B).

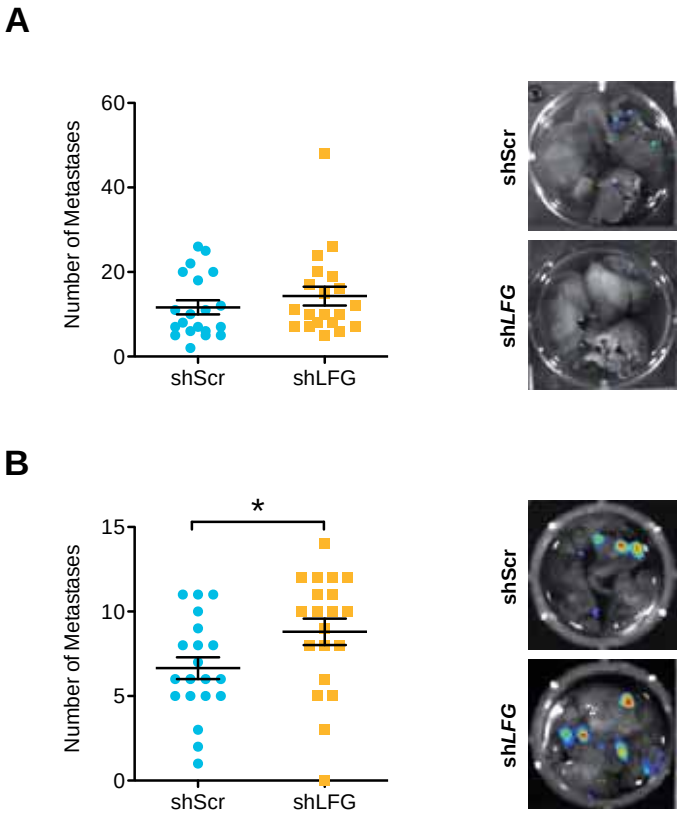

Figure 48. Scoring of metastases. Number of metastases detected by BLI in **A,** livers and **B,** lungs. Data is shown as mean ± S.E.M. Images are representative of *ex vivo* BLI showing metastases in organs dissected from shScr and sh*LFG* injected mice. Unpaired *t*-test, **P*<0.05.

In summary, LFG silencing does not affect primary tumor growth, but increases the non-adherent survival and migration of SH-SY5Y cells, thus increasing the number of metastases.

4.5. Lifeguard knockdown alters cell adhesion programs.

To further understand the mechanism through which LFG knockdown reduces cell adhesion, increases migration and potentiates metastasis of NBL cells, we performed a whole transcriptome analysis by Affymetrix expression arrays after LFG knockdown.

A Principal Component Analysis (PCA) was performed to assess sample homogeneity within the microarray data. PCA is a statistical procedure that reduces the dimensionality of the data obtained from the microarray, while retaining most of the variation in the data set. This mathematical algorithm identifies "principal components" along which the variation in the data is maximal. By using these components, each sample can be plotted, making it possible to visually assess similarities and differences between samples and to determine whether they can be grouped (Ringner 2008). Thus, we expect replicate samples to group together, indicating a general similarity in their overall expression patterns. As seen in Figure 49, PCA segregated the infected cells shScr versus sh*LFG* in two clearly defined groups, indicating a consistent transcriptional impact of *LFG* knockdown.

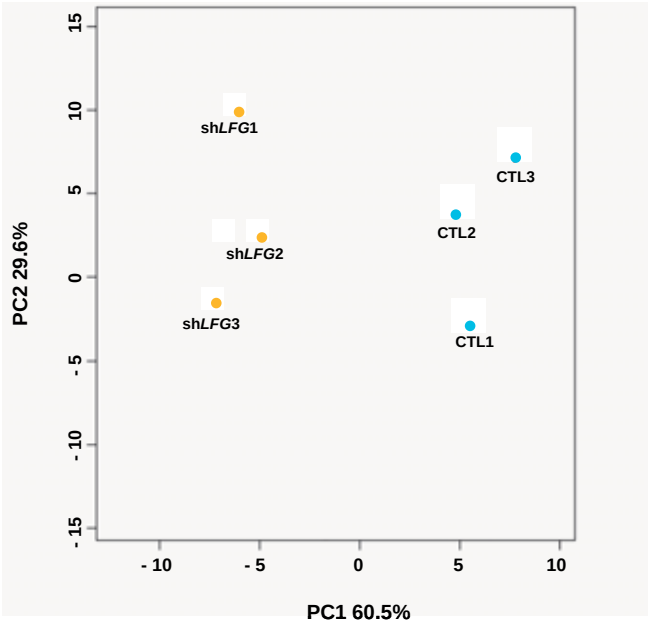

Figure 49. Principal component analysis 2D plot.

Once the homogeneity among replicates was confirmed, microarray data was analyzed to find networks of genes that were up- or downregulated when comparing shScr with sh*LFG* samples using the Kyoto Encyclopedia of Genes and Genomes (KEGG) pathway analysis (Kanehisa and Goto 2000, Kanehisa, Goto et al. 2012). KEGG is a data base resource useful to understand

biological systems and to interpret data from high-throughput techniques. This data base captures and organizes knowledge from the literature in order to integrate genes and proteins into networks that represent systemic functions of the cell and the organism. In our study, KEGG pathway analysis of genes differentially expressed in response to *LFG* knockdown revealed a reproducible modulation of genes mainly involved in cancer pathways and adhesion processes (Figure 50). The Odds ratio (OR) is a statistical measure that describes the strength of association between two variables, in this case *LFG* knockdown and changes in gene expression. An OR greater than 1 implies an association between the two variables, and the strength of the association increases with the OR.

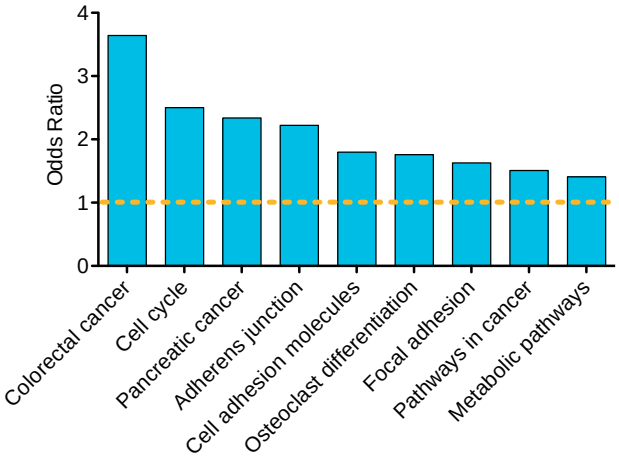

Figure 50. KEGG pathway enrichment analysis of differentially expressed genes between shScr and sh*LFG*-transduced SH-SY5Y cells.

When microarray data was analyzed in more detail, functional annotation analysis showed a remarkable modulation of genes implicated in focal adhesion, cell adhesion, adherent junctions, cancer pathways and cell cycle (Figure 51). The marked modulation of genes implicated in adhesion processes supported an active role of LFG in the tumorigenic properties of NBL cells.

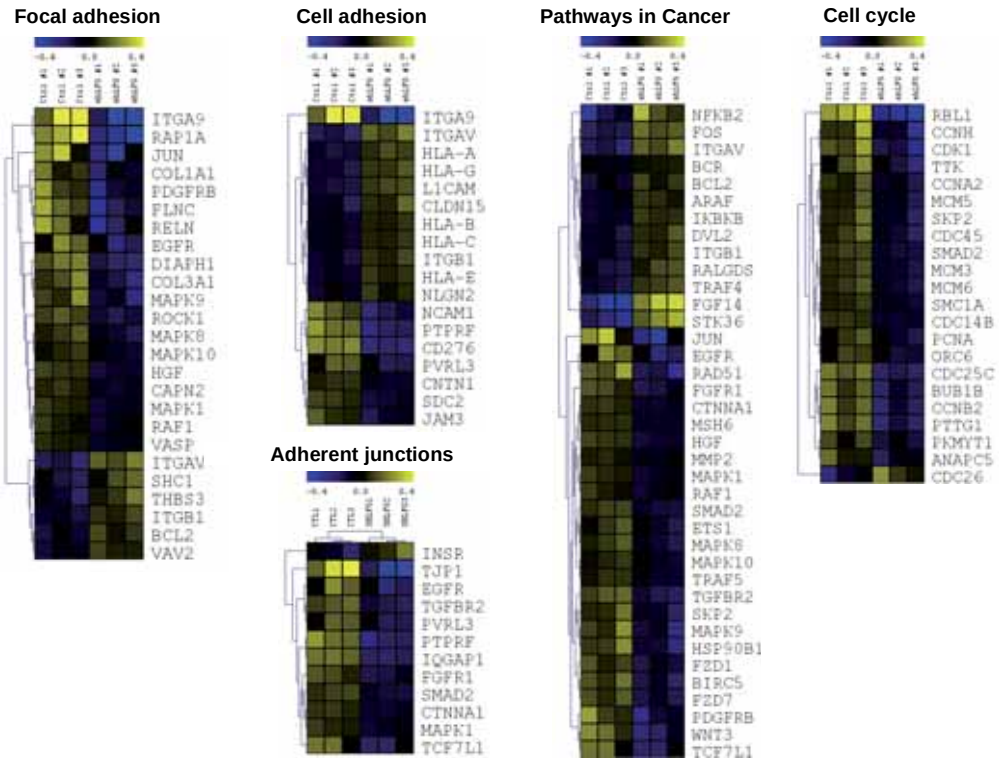

Figure 51. Gene set enrichment analysis performed on genes differentially expressed between shScr and sh*LFG* SH-SY5Y cells. Heatmaps show selected differentially expressed genes grouped in categories of functionally relevant pathways.

In order to validate microarray results, we performed a qPCR for some of the up- and downregulated genes after LFG knockdown, such as *FGF14*, *STK36*, *BCL2*, *RAP1A*, *TJP1, ITGA9* and *LFG* itself (Figure 52). All mRNA expression changes followed the same trend both in the array and qPCR analysis, thereby confirming the validity of the array results.

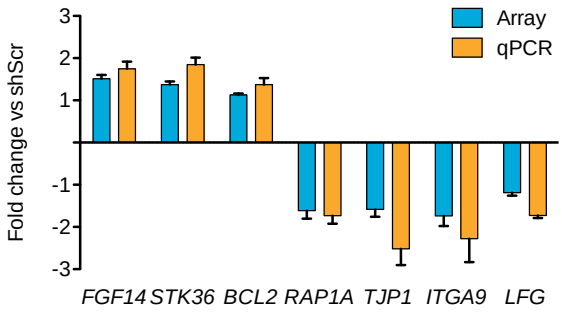

Figure 52. Array validation. qPCR using primers for three upregulated genes (*FGF14*, *STK36*, *BCL2*) and three downregulated genes (*RAP1A*, *TJP1*, *ITGA9*). *LFG* levels have been included as a control of the experiment. Values are represented as fold change versus shScr and are the mean ± S.E.M of three independent experiments.

4.6. MYCN directly represses Lifeguard expression.

Since *LFG* levels were significantly lower in *MYCN*-amplified tumors, we sought to determine whether MYCN participates in *LFG* repression. Our first approach consisted in using the SHEP MYCN-inducible Tet21N cell line, which constitutively overexpresses MYCN under the control of a tetracycline-responsive repressor element (Lutz, Stohr et al. 1996). Thus, doxycycline treatment of Tet21N cells turned off MYCN overexpression and allowed us to analyze LFG levels in response to MYCN silencing.

Doxycycline treatment resulted in a differentiated phenotype and a reduced proliferation rate of Tet21N cells, although it was not quantified (Figure 53).

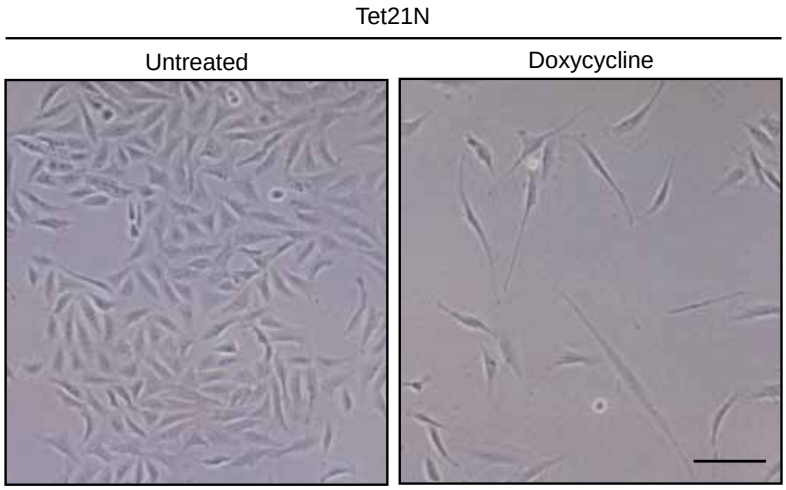

Figure 53. Conditional MYCN knockdown in Tet21N cells decreases proliferation and renders a more differentiated phenotype. Representative images of MYCN-Tet-off inducible Tet21N cells treated with or without doxycycline (100ng/mL) to silence MYCN expression during one week. Scale bar, 100 µm.

Tet21N differentiation was accompanied by a reduction in *MYCN* expression and a concomitant time-dependent upregulation of *LFG*. Both *MYCN* downregulation and the increase in *LFG* expression were detected at the mRNA level by qPCR and confirmed at the protein level by western blot (Figure 54).

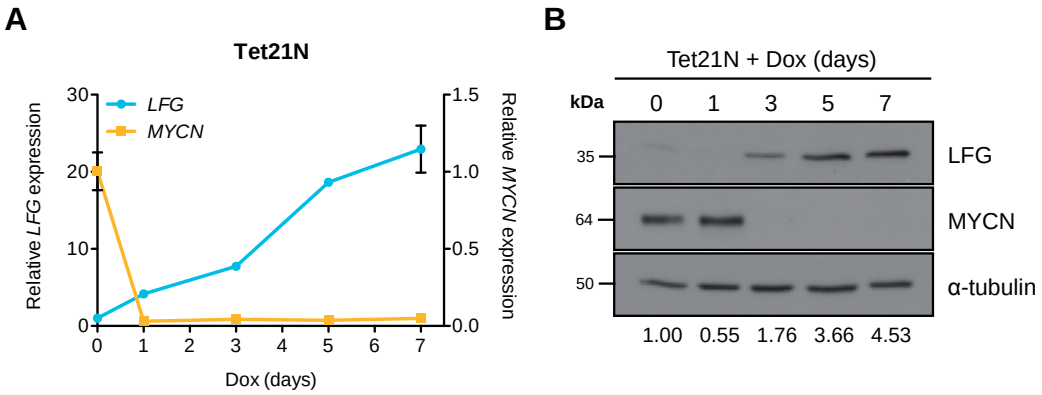

Figure 54. Conditional silencing of MYCN switches on *LFG* expression. A, Tet21N cell line treated with doxycycline (100ng/mL) for the indicated times. *LFG* and *MYCN* mRNA levels were detected by qPCR and normalized versus *L27*. Data on graph are presented as mean ± S.E.M, n=3. **B,** LFG and MYCN protein levels were also checked by Western Blot. α-tubulin was used as a loading control. Bands were quantified with ImageJ and normalized versus α-tubulin.

The regulation of LFG expression by MYCN was further confirmed in IMR-32, another *MYCN*-amplified NBL, stably transfected with an inducible shRNA against *MYCN*. When MYCN expression was silenced by doxycycline treatment, an increase in LFG mRNA was detected by qPCR (Figure 55). However, expression changes were smaller than in Tet21N cells, and two reasons might explain this effect. First, treatments were longer for Tet21N cells than for IMR-32. Second, the IMR-32 model consists of silencing endogenous MYCN expression, while doxycycline prevents MYCN overexpression in Tet21N cells.

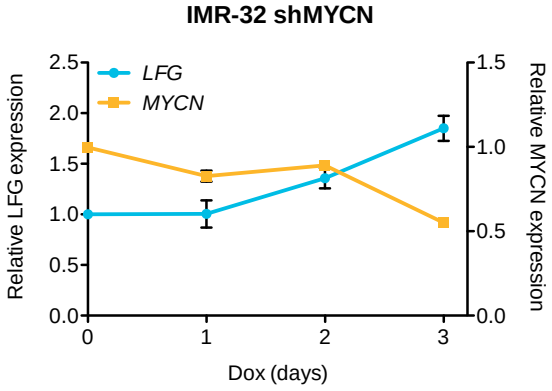

Figure 55. Conditional silencing of *MYCN* switches on *LFG* expression. IMR-32 cells stably expressing an inducible sh*MYCN* were treated with doxycycline (100ng/mL) for the indicated times. *LFG* and *MYCN* mRNA levels were detected by qPCR and normalized versus *L27*. Data on graph are presented as mean ± S.E.M, n=3.

Additionally, we analyzed LFG expression in the GSE39218 data set, where Valentijn *et al.* knocked down MYCN in IMR-32 cells also using a doxycycline-inducible shRNA against MYCN (Valentijn, Koster et al. 2012). Consistently with our results, *LFG* levels were increased upon doxycycline treatment at 48 and 72h post-treatment (Figure 56).

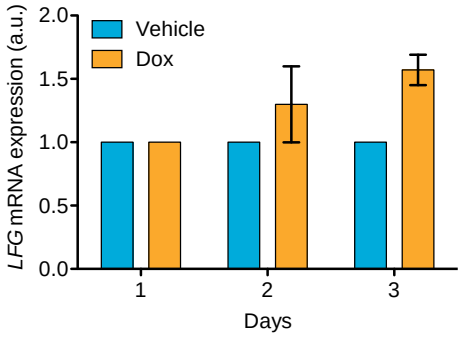

Figure 56. Conditional silencing of *MYCN* switches on *LFG* expression. IMR-32 cells stably transfected with an inducible sh*MYCN* were treated with doxycycline for the indicated times. *LFG* mRNA levels are represented. Data from GSE39218 (Valentijn, Koster et al. 2012).

The increase of LFG expression after MYCN downregulation in Tet21N and IMR-32 cells points to MYCN as a repressor of *LFG* transcription. Therefore, we performed a *LFG* promoter analysis to find putative MYCN binding sites (E-Boxes). In addition, we also looked for SP1 and MIZ1 binding sites, two transcription factors that are known to collaborate with MYCN in the repression of gene transcription (Westermark, Wilhelm et al. 2011). Indeed, *LFG* promoter analysis reported two MYCN putative binding sites, five consensus sites for SP1 and two predicted sequences for MIZ1 binding (Figure 57).

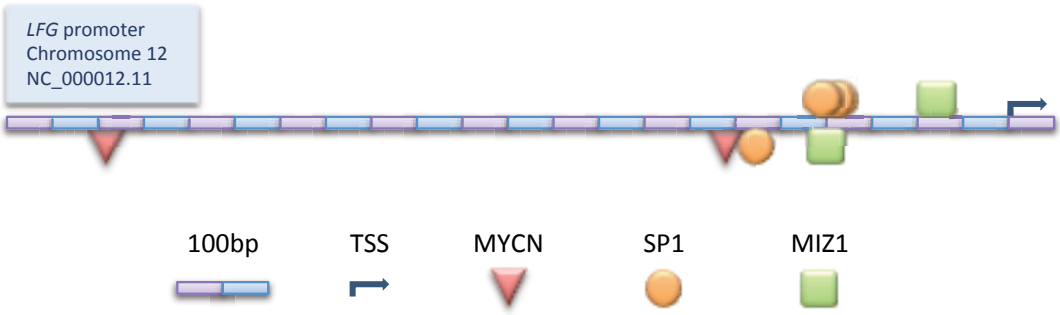

Figure 57. Representation of *LFG* promoter. Putative binding sites for MYCN, SP1 and MIZ1 upstream of the transcription start site (TSS) are indicated, either on the sense (above) or antisense (below) DNA strands. Promoter analysis was performed using the Matinspector Software from Genomatix Software Suite v2.7.

In order to address whether MYCN directly binds to *LFG* promoter, a chromatin immunoprecipitation data set in Tet21N cells with and without doxycycline treatment was examined for MYCN binding (Murphy, Buckley et al. 2009). A high confidence MYCN-binding peak was identified in the *LFG* proximal promoter of Tet21N cells. Furthermore, this binding peak was lost when MYCN expression was repressed by doxycycline treatment (Figure 58).

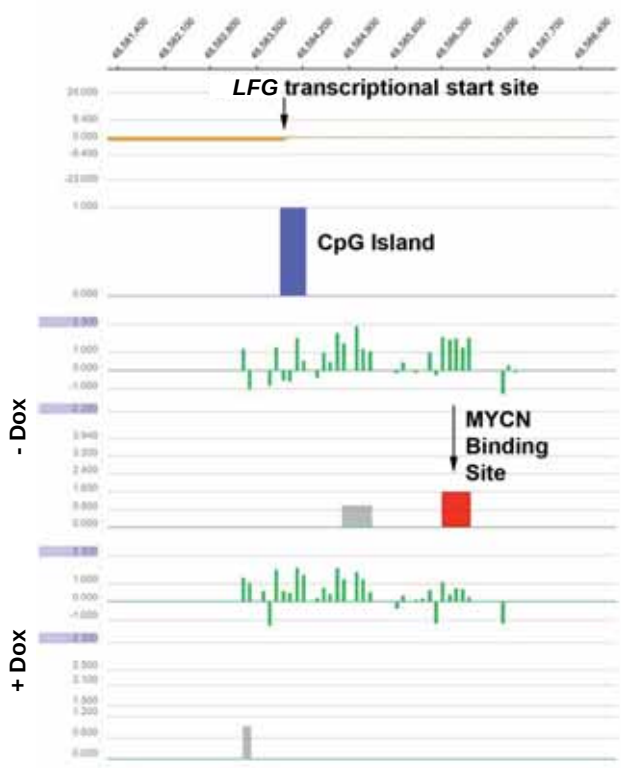

Figure 58. MYCN directly binds *LFG* promoter to repress its expression. Identification of MYCN binding site at *LFG* promoter (gene ID: *FAIM2*) by ChIP in Tet21N cells. The scale on the top of the panel indicates position on chromosome 12. Green bars represent fluorescent intensity of probes around the *LFG* promoter, expressed as $\log_2$ ratios. The red bar represents a high confidence MYCN peak, identified by the NimbleScan peak finding algorithm.

MYCN-mediated transcription repression is now considered to be at least as important as transcription activation (Gherardi, Valli et al. 2013). However, the repressing mechanisms remain unclear. It has been proposed that MYCN interacts with transcription factors or transcriptional complexes, inducing DNA and histone modifications (Westermark, Wilhelm et al. 2011). To further characterize how MYCN represses *LFG* transcription, *MYCN*-amplified NBL cell lines were treated with the DNA methyltransferase inhibitor 5-aza-2'-deoxycytidine and the HDAC inhibitor sodium butyrate (Figure 59).

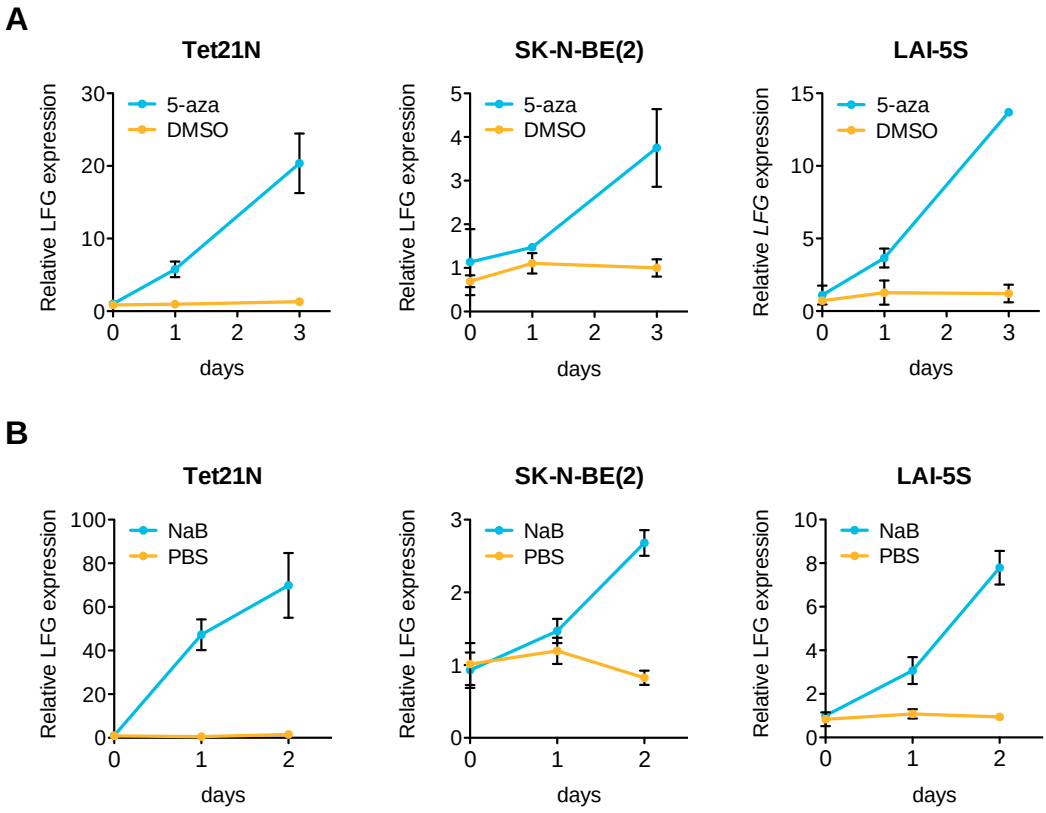

Figure 59. Inhibition of DNA methylation and histone deacetylation increases *LFG* expression. *LFG* levels measured by qPCR in the indicated cell lines treated with **A,** 1µM of the DNA methyltransferase inhibitor 5-aza-2'-deoxycytidine or **B,** 1mM of the HDAC inhibitor sodium butyrate or for the indicated times. Mean ± S.E.M, n=3.

Both treatments induced an increase in *LFG* mRNA levels in all cell lines tested, thereby suggesting that MYCN represses *LFG* expression by favoring histone deacetylation and *LFG* DNA promoter methylation.

DISCUSSION

5. Discussion

High-risk neuroblastoma, a challenge for clinicians

NBL is the most common solid tumor in children and accounts for ~10% of pediatric cancer deaths (Johnsen, Kogner et al. 2009, Owens and Irwin 2012). It is characterized by an enormous clinical and biological heterogeneity, with prognosis ranging from spontaneous regression to aggressive metastatic tumors (Maris, Hogarty et al. 2007).

High-risk NBL therapy combines chemotherapy, surgery, myeloablative therapy, autologous bone marrow transplantation, radiotherapy and biological therapy to eliminate minimal residual disease. However, despite all efforts, the prognosis for patients in this group remains very poor (Park, Bagatell et al. 2013). Thus, it is important to understand fundamental cellular processes that play a role in tumor formation and resistance to therapy.

Since the main goal of therapy is to ultimately induce the death of cancer cells, a number of approaches that target the apoptotic machinery have been tested for NBL treatment, such as BCL-2 inhibitors (Rheingold, Hogarty et al. 2007, Lock, Carol et al. 2008), Smac mimetics, antisense oligonucleotides against XIAP and survivin (Nakahara, Kita et al. 2007, Fulda 2013), recombinant soluble TRAIL and monoclonal antibodies against TRAIL receptors (Smith, Morton et al. 2010). Strategies targeting TRAIL seemed extremely promising, since tumor cells have an increased sensitivity to TRAIL when compared to normal cells (Daniels, Turley et al. 2005). However, it is frequent to find resistance to DR-induced apoptosis in NBL, which strongly limits the success of therapies targeting the extrinsic pathway (Gasparini, Vecchi Brumatti et al. 2013). This resistance is mainly due to defects in the DR pathway, which has not been completely characterized yet.

The extrinsic apoptotic machinery in neuroblastoma

Alterations of key elements of the apoptotic pathway have been shown to be determinant in the outcome of NBLs. While characterization of the mitochondrial or intrinsic pathway elements has been extensive, limited attention has been paid to the components of the extrinsic or DR pathway.

The most characterized element of the extrinsic pathway is caspase-8, which is lost in ~70% of NBLs (Fulda, Poremba et al. 2006, Grau, Martinez et al. 2011). Some authors correlate caspase-

8 silencing by hypermethylation with *MYCN* amplification, but this association has been widely controversial (Teitz, Wei et al. 2000, Iolascon, Borriello et al. 2003, Lazcoz, Munoz et al. 2006, Kamimatsuse, Matsuura et al. 2009). It has been extensively demonstrated that loss of caspase-8 prevents DR-induced apoptosis of NBL cells (Eggert, Grotzer et al. 2000, Hopkins-Donaldson, Bodmer et al. 2000, Fulda, Kufer et al. 2001) and renders them resistant to treatment with doxorubicin, a drug used in cancer chemotherapy (Teitz, Wei et al. 2000). Moreover, caspase-8 silencing has been shown to potentiate NBL metastasis (Stupack, Teitz et al. 2006, Teitz, Inoue et al. 2013). Caspase-8 also contributes to the expression of epithelial, endothelial and myeloid differentiation markers and attenuates NBL cell proliferation. These functions occur independently of caspase-8 catalytic activity, since the sole expression of its DED fragment in caspase-8 deficient NBL cells induces senescence and differentiation (Mielgo, Torres et al. 2009). All these reports point to caspase-8 as a tumor suppressor gene through different mechanisms of action. Alternatively, when other components of the apoptotic cascade are compromised, caspase-8 can also induce migration and metastasis (Barbero, Mielgo et al. 2009, Torres, Mielgo et al. 2010, Graf, Keller et al. 2014). In fact, the pro-metastatic role of caspase-8 is independent of its catalytic activity. Rather, caspase-8 interacts with a multi-protein complex involved in cell adhesion and its presence enhances cleavage of focal adhesion substrates and cell migration. *In vivo* knockdown of caspase-8 in apoptosis-resistant tumors disrupts metastasis (Barbero, Mielgo et al. 2009). How can these opposite roles of caspase-8 in tumor progression be understood? Steven M. Frisch hypothesizes that procaspase-8 acts as an adhesion/migration factor, while cleaved caspase-8 induces apoptosis and this provides a mechanism to switch these functions (Frisch 2008).

We hypotesized that DR antagonists could play a role in NBL behavior and our results show that LFG is strongly downregulated in high-risk NBL tumors, suggesting its role as a tumor suppressor gene. This newly described role for LFG is not exceptional, since there are other members of the apoptotic machinery that are associated to tumor aggressiveness. Indeed, the anti-apoptotic protein PEA-15 has been reported to be involved in tumor cell migration. PEA-$15^{-/-}$ astrocytes underwent an enhanced motility *in vitro* compared with their wild-type counterparts and re-expression of PEA-15 restored the wild-type behavior. PEA-15 effects on migration were studied in glioblastoma tumors, which originate from astrocytes. Yet, analysis of PEA-15 expression in glioblastoma organotypic cultures revealed lower levels of PEA-15 in cells that migrated away from the tumor explants, regardless of the expression levels in the originating samples (Renault-Mihara, Beuvon et al. 2006). PEA-15 has also been linked to NBL prognosis. High levels of this protein correlate with favorable clinical features. PEA-15 was

shown to block NBL migration through inhibition of ERK/RSK2 signaling, suggesting a metastatic limiting role in the progression of NBL (Gawecka, Geerts et al. 2012). Similarly to PEA-15, loss of LFG potentiates cell detachment, adherence-independent growth and migration.

The DR-antagonist c-FLIP is frequently expressed in NBL tissues, and it has been reported to be equally important as caspase-8 silencing in conferring Fas-resistance to NBL cells. *In vitro* studies performed by Poulaki and collaborators show that c-FLIP is recruited to the DISC, where it prevents caspase-8 activation and FasL-induced cell death (Poulaki, Mitsiades et al. 2001). c-FLIP was found to protect from Smac mimetics-induced cell death in a panel of tumor cell lines, including NBL (Cheung, Mahoney et al. 2009) and Flahaut *et al.* show that c-FLIP$_L$ down-regulation restores DR-induced apoptosis in SH-EP NBL cell line (Flahaut, Muhlethaler-Mottet et al. 2006).

Other DR-antagonists have been shown to play unexpected roles involved in tumor biology. For instance, Miyazaki and colleagues described that FAP-1 overexpression enhanced susceptibility to apoptosis induced by Fas in human colon cancer cells (Miyazaki, Atarashi et al. 2006). SODD expression has been related to aggressiveness of cancer, since high levels of this protein marked less aggressive ovarian tumors (Annunziata, Kleinberg et al. 2007). Disruption of SUMO-1 has been implicated in breast cancer, as it plays a role in DNA damage response. Concretely, SUMOylation of BRCA1 enhances its ubiquitin ligase activity and promotes the accumulation of proteins responsible of double-strand break repair. Thus, loss of SUMO-1 drives to a lack of ligase activity of BRCA1 and is associated with breast cancer development (Morris, Boutell et al. 2009).

The DR Fas, which is antagonized by LFG, has been related with tumor infiltration in glioblastoma multiforme. In this context, binding of FasL to Fas receptor activates the phosphatidylinositol 3-kinase (PI3K) pathway, which signals invasion via the glycogen synthase kinase 3-beta (GSK3β) and subsequent expression of matrix metalloproteinases. Moreover, in a murine model of intracranial glioblastoma, neutralization of Fas activity dramatically reduced the ability of invasion (Kleber, Sancho-Martinez et al. 2008). A clear role of FasL/Fas in NBL biology has not been described yet, but recent findings support the hypothesis that genetic polymorphisms in both genes may increase the risk of NBL development (Han, Zhou et al. 2013). Recently, Valiente *et al*. unraveled a new role of serpins and Fas signaling in brain metastasis from breast and lung primary tumors. They report that soluble FasL is released from astrocytes by the plasminogen/plasmin system and induces death of the invading cancer

cells, thus protecting from metastasis. However, cells that express determinate serpins that inhibit the plasminogen/plasmin system are able to overcome this protection mechanism and invade the brain (Valiente, Obenauf et al. 2014).

Lifeguard, an anti-apoptotic protein with alternative functions

LFG was first described in 1999 by Somia and collaborators as an anti-apoptotic protein that specifically protected cells from Fas-induced cell death, but not from the stimulation of TNFR1. Further characterization showed that LFG was expressed predominantly in the brain and, more abundantly, in hippocampus and cerebellum (Somia, Schmitt et al. 1999). The anti-apoptotic role of LFG in the nervous system was demonstrated by Beier and collaborators, who reported LFG function in inhibiting neural cell death induced by Fas (Beier, Wischhusen et al. 2005). The protective role of LFG has also been described in Purkinje cells (PCs) (Hurtado de Mendoza, Perez-Garcia et al. 2011) and cortical neurons (Fernandez, Segura et al. 2007).

Since LFG has been described as an anti-apoptotic protein, one would expect to find it overexpressed in the most aggressive tumors, with a potential role in protecting malignant cells from apoptosis induced by the immune system and other therapeutic approaches. So far, only four reports linking LFG and cancer have been published and all of them describe LFG as an anti-apoptotic protein that contributes to breast cancer malignancy and resistance to Fas and the alkylphospholipid perifosine-induced apoptosis (Bucan, Adili et al. 2010, Bucan, Reimers et al. 2010, Bucan, Choi et al. 2011, Dastagir, Lazaridis et al. 2014).

Nevertheless, we found LFG downregulated in the most aggressive NBLs. This made us suppose that, in our model, this protein might be playing alternative roles to the anti-apoptotic function. Interestingly, new studies involve LFG in other apoptotic-independent processes, such as differentiation, axonal growth and neuroplasticity (Hurtado de Mendoza, Perez-Garcia et al. 2011, Merianda, Vuppalanchi et al. 2013, Tauber, Harms et al. 2014). Hurtado de Mendoza *et al.* describe a role of LFG in cerebellar development. In early postnatal stages, loss of LFG reduced cerebellar volume and PC development, which presented an abnormal morphology and a reduced cellular density (Hurtado de Mendoza, Perez-Garcia et al. 2011). Another group identified LFG mRNA as an axonal mRNA in cultured adult dorsal root ganglion (DRG) neurons (Willis, van Niekerk et al. 2007, Gumy, Yeo et al. 2011). Recently, they have demonstrated that localized translation of LFG in axons provides a function in axonal growth, while the anti-apoptotic role is apparently restricted to the cell body. They report an increase of LFG mRNA in axons after axonal injury, accompanied by a decrease in LFG mRNA levels in

the cell body. Moreover, using siRNA strategies and axon-targeted versus cell-body-restricted mRNA constructs, they show that LFG promotes axonal growth (Merianda, Vuppalanchi et al. 2013).

These data are in accordance with our results, since LFG's role in NBL adhesion and differentiation seems to be more relevant than its anti-apoptotic function. Our work shows that LFG expression increases with the differentiation status of NBL cell lines and tumors with unfavorable histology present low LFG levels. But, is LFG expression a cause or a consequence of the differentiation status of NBL cells? Initially, we could think that changes on LFG expression are a consequence of cell differentiation, as seen by RA treatments or neurosphere formation in NBL cell lines. However, the sole downregulation of LFG induced non-adherent growth of SH-SY5Y cells, indicating that it could somehow induce their de-differentiation (even though the expression of stem cell markers was not altered). This question should be addressed in-depth by modulating LFG levels and checking cell responsiveness to differentiation stimuli.

Is there a reason to explain this shift in LFG function in NBL cells? NBL tumors often show alterations in the extrinsic pathway such as caspase-8 silencing, c-FLIP overexpression or the expression of decoy receptors that prevent the activation of the apoptotic cascade. Thus, the anti-apoptotic effect of LFG may have lost importance in a cellular model where the extrinsic apoptotic pathway is already compromised.

LFG is a member of the TMBIM family of anti-apoptotic proteins, which includes five other members – RECS1, GRINA, GAAP, GHITM, and BI-1 – that share the same transmembrane structure (Rojas-Rivera and Hetz 2014). We questioned if other TMBIM members could be also involved in NBL aggressiveness, since their role in these tumors has not been studied at all. Interestingly, the expression of all TMBIM members significantly correlates with NBL prognosis (Table 15). Low expression of all TMBIM members, except from GRINA, is associated to poor overall survival. Surprisingly, GRINA levels significantly correlate with patient survival in the opposite way, even though it shares its anti-apoptotic role with other family members and has no remarkable structural changes (Nielsen, Chambers et al. 2011).

Table 15. Correlation between TMBIM family members expression and NBL patient survival in GSE16476 data set.

TMBIM family member	Alias	Probe	Worse if… (P-value) [a]	Worse if… (P-value) [b]
TMBIM1	*RECS1*	217730_at	Low (0.029)	Low (0.148)
TMBIM2	*FAIM2*	203619_s_at	Low ($1.6e^{-4}$)	Low (0.019)
TMBIM3	*GRINA*	212090_at	High ($8.5e^{-4}$)	High (0.029)
TMBIM4	*GAAP*	222845_x_at	Low ($6.9e^{-5}$)	Low ($1.5e^{-5}$)
TMBIM5	*GHITM*	209248_at	Low ($2.1e^{-4}$)	Low (0.032)
TMBIM6	*BI1*	200804_at	Low ($3.0e^{-6}$)	Low (0.244)

[a] Correlation values using the high/low expression cutoff recommended by the R2 software.
[b] Correlation values dividing patients by the median.

These data open new questions about the mechanisms involved in NBL aggressiveness. Which is the relevance of TMBIM family members in NBL prognosis? Do all these proteins act coordinately to restrain NBL aggressiveness or, instead, they have redundant roles? Is the expression of all TMBIM members regulated by MYCN?

Lifeguard as a prognosis marker in neuroblastoma

We have analyzed the expression of several DR-antagonists in multiple NBL datasets and found that LFG was the most differentially expressed DR-antagonist in *MYCN*-amplified tumors. Low levels of LFG were also found to correlate with worse overall survival.

Could we consider LFG as a new prognostic marker? Initially, we found lower LFG expression in high-risk and *MYCN*-amplified NBL tumors and a correlation between low levels of LFG and shorter progression-free and poor overall survival. Moreover, we demonstrated that LFG expression can be directly regulated by MYCN. If LFG expression levels were directly related to *MYCN*-amplification status, LFG would not represent a useful and independent tool for NBL risk stratification. However, the correlation between LFG levels and patient outcome is maintained even in the subset of *MYCN*-non amplified tumors, indicating that in this group of patients LFG could certainly have a prognosis value independent from MYCN status. This concept is in agreement with the one proposed by Valentijn and collaborators, who demonstrate that a functional MYCN signature predicts NBL outcome in a more powerful way than *MYCN*-amplification itself (Valentijn, Koster et al. 2012). They identified a 157-gene signature composed by genes that are directly induced by MYCN and this signature correlated with poor prognosis. Interestingly, a sub-group of tumors displaying this signature and poor

outcome did not present *MYCN* amplification, but they showed high levels of nuclear MYCN protein. This can be explained because *MYCN*-amplification status does not always correlate with MYCN protein levels, since there are other cellular mechanisms that stabilize the protein (Otto, Horn et al. 2009, Suenaga, Islam et al. 2014). Thus, the strength of using MYCN targets such as LFG for NBL prognosis instead of the genomic information could lead to a more accurate patient stratification, specially for those cases that are considered high-risk but do not have genomic amplification of MYCN.

Lifeguard knockdown increases migration and metastatic potential of NBL cells

We show for the first time the implication of the DR-antagonist LFG in NBL aggressiveness and metastasis. LFG knockdown blocked cell proliferation and reduced cell adhesion of NBL cell lines. Autonomous non-adherent growth and increased migration properties are tightly related to aggressive tumors. In fact, some authors correlate the sphere-forming ability with the tumor-initiating potential of NBL cells and high-risk tumors (Hansford, McKee et al. 2007, Mahller, Williams et al. 2009). Non-adherent sh*LFG* cells show increased migration ability. However, their invasion potential is not enhanced, indicating that LFG modulation does not affect the function of proteins that remodel the extracellular matrix (ECM), such as matrix metalloproteinases.

As a result of an increased migration capacity *in vitro*, sh*LFG* cells have an enhanced metastatic potential *in vivo* when compared to control cells. However, while *in vitro* results are clear, LFG knockdown seems to have lesser effects in our *in vivo* approach. No significant differences in the metastatic potential of sh*LFG* and shScr cells are found by total bioluminescence flux measurements. Indeed, differences are found when scoring the number of metastatic sites, which is higher after LFG knockdown. This could be explained by the fact that despite sh*LFG* cells show an increased ability to metastasize, they present reduced proliferation rates and the metastatic foci are more, but probably smaller. The choice of the animal model does also influence the obtained results. SH-SY5Y cells were injected into the flank of nude mice in order to form tumors, so tumor cells had to leave the primary tumor and reach the blood stream in order to colonize distant organs. Taking into account that LFG knockdown does not enhance invasion, but only facilitates non-adherent growth and migration, a tail vein injection of cells might better reflect an increased metastatic potential of sh*LFG* cells.

LFG is localized in membrane lipid rafts (MLR) (Fernandez, Segura et al. 2007), which are membrane microdomains enriched in sphingolipids and cholesterol that organize several

proteins and receptors. MLRs coordinate a number of cellular signaling functions such as apoptosis, differentiation, trafficking, adhesion and migration (Head, Patel et al. 2014). The interplay between MLR-associated proteins and the cytoskeleton impacts on cellular organization, signal transduction and polarity. This may explain the morphological changes and the increased migration abilities observed after LFG knockdown. MLRs have recently been connected to cell invasiveness and metastasis and are now considered as a target to prevent and treat metastasis (Hryniewicz-Jankowska, Augoff et al. 2014). In fact, the purine/pyrimidine receptor $P2Y_2$ has been shown to couple with G proteins and integrins in the lipid rafts and mediate migration of several cell types, such as epidermal keratinocytes, lung epithelial carcinoma cells, astrocytoma cells and smooth muscle cells (Greig, Linge et al. 2003, Greig, Linge et al. 2003, Greig, Linge et al. 2003). In the NBL/glioma hybrid cell line NG 108-15, lipid rafts are critical for $P2Y_2$ receptor-mediated $G_{q/11}$-phospholipase C-Ca^{2+} signaling and this cascade mediates cell migration (Ando, Obara et al. 2010).

Lifeguard knockdown modulates the expression of cell adhesion molecules and EMT- related genes

Our work shows that LFG knockdown decreased cell adhesion and increased NBL cell migration and metastatic potential. Because the expression levels of this DR-antagonist are related to the differentiation status of NBL cell lines, our first hypothesis was that cells lacking LFG presented a more undifferentiated or stem-cell like phenotype. This hypothesis was discarded after assessing the expression of stemness markers such as *CD133, NESTIN, NANOG, NOTCH* or *OCT4,* which were not upregulated after LFG knockdown. Furthermore, *CD133* and *NESTIN,* two widely used neuronal stem cell markers (Mahller, Williams et al. 2009, Schiapparelli, Enguita-German et al. 2010), were significantly downregulated in sh*LFG* cells. Even though downregulation of *CD133* and *NESTIN* was unexpected, a direct correlation between *NESTIN* and *LFG* expression was also found in the NBL data set GSE16476.

NBL originates from neural crest cells and these progenitors undergo an EMT process that allows them to migrate and give rise to many tissues within the organism. We then hypothesized that LFG knockdown phenotype could be related to an EMT behavior. We checked the expression of several EMT markers in the NBL cell line SH-SY5Y after LFG knockdown and in NBL tumor datasets with high or low LFG expression. We found upregulation of *TWIST1* upon LFG knockdown and the same correlation was seen in human samples. TWIST1 belongs to the bHLH transcription factor family and is an important EMT and

metastasis-promoter gene (Karreth and Tuveson 2004). It facilitates EMT by repressing the expression of E-cadherin, leading to a disassembly of adherent junctions and allowing cell migration (Yang, Mani et al. 2004). It has been found overexpressed in *MYCN*-amplified NBLs and the cooperation between both genes is thought to cause the malignant transformation of the cell (Valsesia-Wittmann, Magdeleine et al. 2004, Nozato, Kaneko et al. 2013).

By contrast, *ERBB3* and *KRT19* genes were found to be reduced in NBL cells infected with sh*LFG* and downregulated in NBL human samples with low LFG levels. ERBB3 belongs to the epidermal growth factor receptor (EGFR) family and participates in the activation of proliferation (Richards, Zweidler-McKay et al. 2010) and differentiation pathways (Izycka-Swieszewska, Wozniak et al. 2011). KRT19 is a member of the keratin family and participates in the organization of the cytoskeleton (Zhou, Liao et al. 1999). Deregulation of members of the keratin family has long been recognized as a marker of tumor progression (Moll, Franke et al. 1982). The expression of *KRT19* or *ERBB3* was also found to be low in NBL patients with poor prognosis (Nozato, Kaneko et al. 2013).

While data from NBL data sets showed a differential expression of *TCF3* between low-LFG and high-LFG tumors, NBL cell lines infected with sh*LFG* did not show any variation in *TCF3* levels. TCF3 is a bHLH transcription factor that has been previously implicated as a repressor of E-cadherin and the acquisition of a mesenchymal phenotype (Perez-Moreno, Locascio et al. 2001). This difference between the NBL data set and our qPCR approach could be due to the transient nature of gene regulations, that is, LFG knockdown might orchestrate a series of changes related to EMT that are punctual and we did not detect them all. In this line, a time-course experiment after LFG knockdown might be more informative to check the regulation of EMT genes. Finally, SNAI2 was found downregulated in sh*LFG* cells, even if it is a transcription factor strongly implicated in apoptosis resistance and invasion of NBL cells (Vitali, Mancini et al. 2008, Tanno, Sesti et al. 2010).

The mechanism through which sh*LFG* cells lost adhesion and acquired migration abilities is still unknown, but results obtained by microarray approaches gave us some clues to understand the role of LFG in NBL behavior.

Microarray analyses showed that LFG knockdown indirectly impacted the modulation of cell adhesion genes. One example is *ITGA9*, which has been shown to be essential for the adhesion of rhabdomyosarcoma cells (Masia, Almazan-Moga et al. 2012). Other pro-metastatic integrins were found to be upregulated (eg. *ITGAV*, *ITGB1*). For example, overexpression of ITGAV has been found to correlate with metastasis of laryngeal (Lu, Li et al. 2011), hypopharyngeal

squamous cell carcinomas (Lu, Sun et al. 2009) and colorectal cancer (Viana Lde, Affonso et al. 2013). Moreover, ITGAV knockdown decreased proliferation and increased apoptosis in Hep-2 carcinoma cells (Lu, Sun et al. 2009). Several tight-junctions (TJ) genes were also downregulated (e.g *TJP1*) and loss of cohesion of the TJ structure can lead to invasion and ultimately to metastasis of cancer cells (Martin, Mason et al. 2011). Other genes such as *FGF14*, *STK36* or *BCL2* may contribute in a different manner to the metastatic process. STK36 is a serine/threonine kinase that plays an important role in the activation of the sonic hedgehog pathway, reported to be essential for NBL proliferation and tumor growth (Xu, Wang et al. 2012). The upregulation of *BCL2* may also contribute to inhibit apoptosis when cells grow in anchorage-independent conditions, while *FGF14* could act as a pro-angiogenic factor as previously demonstrated for murine and human fibrosarcomas (Ding, Liu et al. 2002).

Regulation of Lifeguard expression

So far, the regulation of LFG expression has been poorly studied. Only Beier and colleagues described it in cerebellar granule neurons (Beier, Wischhusen et al. 2005). They report that the expression of LFG is dependent on the phosphatidylinositol 3-kinase (PI3-kinase)-Akt/protein kinase B (PKB) pathway, which is known to have central pro-survival role in many cellular systems. Reporter gene experiments showed that inhibition of PI3K activity by specific inhibitors induced a massive reduction of LFG transcription and increased sensitivity to FasL-induced apoptosis. In the same line, overexpression of a dominant negative form of Akt/PKB resulted in a complete suppression of LFG promoter luciferase activity, while a constitutive active Akt/PKB overcame the suppression of LFG transcription by PI3K inhibitors. Akt/PKB activates many transcription factors such as NF-κB. Thus, inhibition of NF-κB by transient overexpression of its inhibitor IκB was followed by a reduction of LFG promoter luciferase activity. These results indicate that the PI3K-Akt/PKB/NF-κB signaling axis is involved in the expression of LFG in neurons. Actually, RA has been shown to induce neuronal differentiation of NBL cells through the PI3K-Akt/PKB pathway (Lopez-Carballo, Moreno et al. 2002, Nishida, Adati et al. 2008, Qiao, Paul et al. 2012), while we demonstrate that *all-trans* RA treatment increases LFG expression.

In the context of cancer, Bucan *et al.* found that LFG expression was regulated by the Akt/LEF-1 signaling pathway. It is known that Akt-mediated phosphorylation of the glycogen synthase kinase-3 (GSK3) results on GSK3 inhibition and the stabilization of its target protein β-catenin. Accumulated β-catenin can then translocate to the nucleus and bind transcription factors of the TCF/LEF family (T Cell Factor/Lymphoid Enhanced Factor) (Pap and Cooper 1998, Eastman

and Grosschedl 1999). Concretely, LEF-1 has been reported to function downstream of β-catenin and induce the expression of oncogenes and proteins that play important roles in development, such as c-myc or cyclin D1 (He, Sparks et al. 1998, Shtutman, Zhurinsky et al. 1999). Bucan and collaborators identified LFG as a new target of the Akt/LEF-1 pathway in a breast cancer cell line and demonstrated that LEF-1 binds directly to LFG promoter and induced its transcription. With these data, they speculate that LFG could be a newly identified mediator involved in breast cancer progression (Bucan, Adili et al. 2010).

All reports addressing LFG regulation point towards Akt-related pathways as responsible for LFG expression. Nonetheless, nothing has been described regarding its repression. We provide evidence that low expression of LFG is not a mere association with the differentiation status of the cell but it is directly repressed by the oncogene MYCN. *MYCN* encodes a protein with a bHLH domain known to be a transcriptional regulator of genes controlling cell cycle and proliferation, cell invasion, angiogenesis and cell survival and death pathways (reviewed in (Westermark, Wilhelm et al. 2011)). MYCN has been shown to participate in NBL metastasis by direct or indirect repression of integrin subunits altering cell-matrix or cell-cell interactions (Judware and Culp 1997, Judware and Culp 1997) or repressing Caveolin-1, whose downregulation elicits anchorage-independent growth and tumor formation (Galbiati, Volonte et al. 1998). We show that repression of LFG impacts on the expression of several molecules that participate in cell adhesion processes, recapitulating some of the MYCN reported effects.

It has been proved that MYCN-mediated transcription repression goes through the formation of the SP1/MIZ1/MYCN complex (Iraci, Diolaiti et al. 2011, Westermark, Wilhelm et al. 2011). Indeed, in our *in silico* promoter analysis we found several putative binding sites for SP1 and MIZ1, which could be possible mediators of LFG transcriptional repression. Thus, it might be worthwhile to perform ChIP assays against SP1, MIZ1 and MYCN on *LFG* promoter to further confirm which mechanism is involved in LFG repression.

Our study demonstrates that treatment with HDAC inhibitors and DNA methyl-transferase inhibitors such as sodium butyrate and 5-aza-2'-deoxycytidine (respectively) restores LFG expression in several *MYCN*-amplified cell lines, suggesting that MYCN represses LFG transcription through histone deacetylation and DNA methylation. It has been previously described in NBL models that MYCN represses gene transcription through epigenetic modifications. This is the case of *PTGER2* (Prostaglandin E Receptor 2 gene), which is repressed in *MYCN*-amplified cell lines and its expression is restored after 5-aza-2'-deoxycytidine or the HDAC inhibitor trichostatin A treatment. Particularly, methylation of CpG islands of *PTGER2*

promoter and consequent silencing of *PTGER2* expression was observed more frequently in high-risk NBL primary tumors (Sugino, Misawa et al. 2007). *In silico* analysis of the *LFG* promoter using MethPrimer (Li and Dahiya 2002) revealed one CpG island, located between -341 and -54 bps before the TSS, coinciding with the nuclei of predicted binding sites of the transcription factors SP1, MIZ1 and MYCN (Figure 60). The analysis of the methylation status of this CpG island could be performed using one of the inducible models employed in this work (Tet21N or IMR-32 sh*MYCN*) to further characterize the mechanism of LFG repression by MYCN.

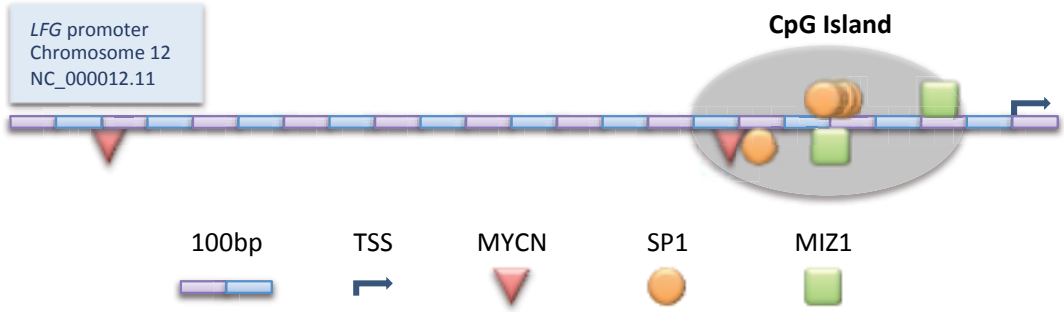

Figure 60. Representation of LFG promoter and the CpG Island predicted by MethPrimer (Li and Dahiya 2002).

LFG gene is located at chromosome 12q13, a region reported to be amplified in a few NBL cell lines and tumors. However, the main interest in this chromosomal region was raised because of the presence of *MDM2,* a well-known inhibitor of the tumor suppressor p53 (Corvi, Savelyeva et al. 1995, Corvi, Savelyeva et al. 1995, Su, Alaminos et al. 2004). In fact, amplification of 12q13-15 fragments has been found in other human cancers, such as gliomas and sarcomas, with several candidate oncogenes like *MDM2* or *CDK4* (Elkahloun, Bittner et al. 1996). *LFG* gene is located in the same region, but in this case, we would expect to find it amplified in low-risk NBLs. A recent study about 12q13 amplification in NBL divided patients in three groups: 1, NBLs with regional amplifications without *MYCN*-amplification; 2, *MYCN*-amplified tumors with amplifications at other loci; 3, tumors with only *MYCN*-amplification. They studied the genomic profile of the three groups in order to correlate their results with clinical data and patient survival. Notably, the amplified region 12q13-14 was recurrent in group 1, and not in the *MYCN*-amplified tumor subsets. They did not detect any correlation with clinical data, but in agreement with our results, patients of group 1 presented a significantly better overall survival probability than those patients harboring *MYCN*-amplification (groups 2 and 3 together) (Guimier, Ferrand et al. 2014).

Therapeutic implications

Our findings may have two direct consequences on NBL patient's diagnosis and therapy:

On the one hand, LFG is a direct target of MYCN, the most widely used prognosis marker in NBL. However, we have shown that in *MYCN*-non amplified tumor subsets, LFG levels also show a significant correlation with NBL outcome. The need to find new tools to classify patients within the already existing *MYCN*-amplified and *MYCN*-non amplified groups will lead to the use of novel prognosis markers. Here, we demonstrate that LFG is a promising candidate.

On the other hand, several compounds are used in NBL therapeutic approaches because they cause cell death or induce cell differentiation. This is the case of RA and HDAC inhibitors (Bell, Chen et al. 2010). Both of these compounds have been shown to downregulate MYCN expression and induce cell differentiation (Thiele, Reynolds et al. 1985, Peverali, Orioli et al. 1996, Cinatl, Kotchetkov et al. 2002), while we demonstrate that they increase LFG expression. Thus, the newly described role of LFG could be used to engineer new therapeutic approaches that directly upregulate its expression.

According to our data, LFG upregulation would not inhibit primary tumor growth, but its main effect would consist on avoiding NBL metastasis. Metastasis is the main cause of death from cancer, even if it is a rather inefficient process. Most tumor cells that leave the environment of the primary tumor die, and much of this death happens when tumor cells lose adherence and infiltrate target tissues (MacDonald, Groom et al. 2002). In this context, low LFG levels could be conferring an advantage to those cells that are able to migrate from the primary tumor and, by this mechanism, favoring metastasis.

In summary, this thesis provides a new link between *MYCN* amplification and early steps of NBL metastasis that is summarized in Figure 61. Our data uncover the role of LFG in preventing NBL aggressiveness by modulating cell adhesion, anchorage-independent growth and migration. The most immediate applicability of our findings to the clinics would be using LFG as a NBL prognosis marker, but we do not discard its value for future therapeutic approaches.

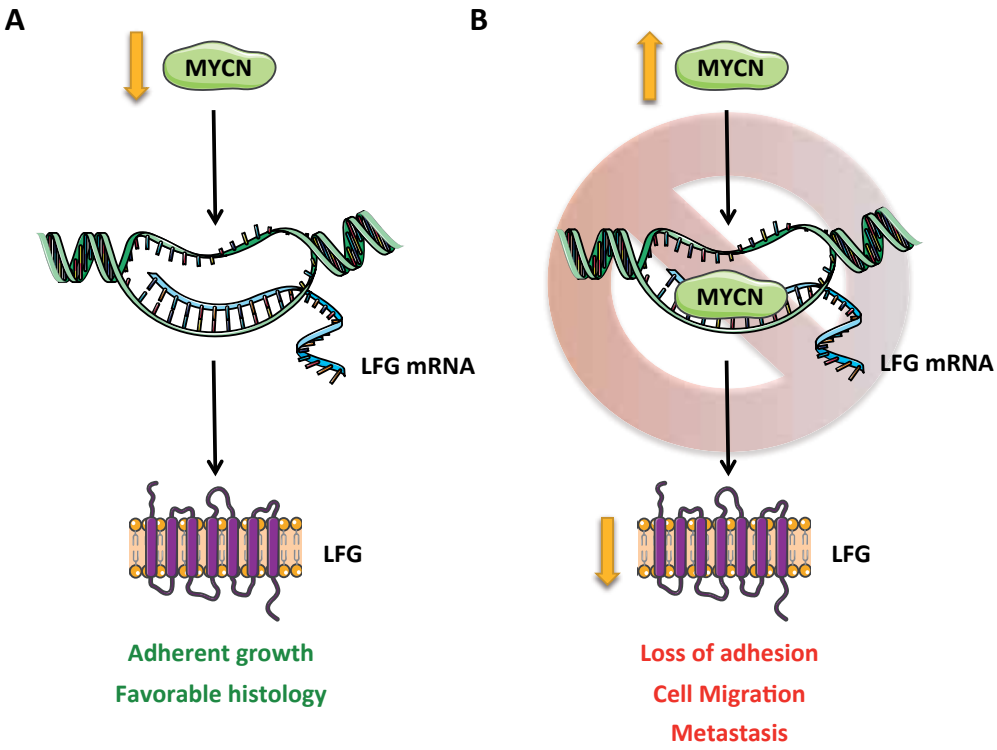

Figure 61. Proposed mechanism linking MYCN–mediated repression of LFG to NBL aggressiveness. A, Tumor cells with low levels of MYCN show LFG expression. In general, these tumors present histologically favorable diagnosis and NBL cell lines show adherent growth. **B,** MYCN contributes to the malignant behavior of NBL. When MYCN is present at high levels (either as a cause of genetic amplification or by its stabilization at the protein level in *MYCN* non-amplified tumors) it binds to *LFG* promoter and directly represses its transcription. LFG downregulation induces changes in the expression of cell adhesion molecules and EMT-related genes promoting non-adherent growth and cell migration, and thus, enhancing the metastatic potential of NBL cells.

CONCLUSIONS

6. Conclusions

First. LFG is the DR-antagonist with the highest differential expression between low-risk and high-risk NBL. High-risk, *MYCN*-amplified tumors show a reduced expression of LFG.

Second. LFG is the DR-antagonist with the strongest association with patient outcome in NBL. Low LFG levels correlate with worse overall survival of NBL patients.

Third. LFG is a new prognostic marker independent of *MYCN* amplification in NBL, and thus, its expression correlates with outcome in *MYCN* non-amplified NBL subsets.

Fourth. LFG levels are reduced in NBLs with unfavorable histology and correlate with the differentiation status of NBL cell lines.

Fifth. LFG knockdown reduces proliferation and adhesion of *MYCN*-non amplified SH-SY5Y and CHLA-90 NBL cells, but not of the *MYCN*-amplified cell lines SK-N-BE(2) and IMR-32.

Sixth. Reduction of LFG switches the proliferation program to a mesenchymal phenotype, increasing non-adherent growth and the migration properties of NBL cells.

Seventh. LFG silencing affects neither the stemness properties of NBL cell lines, nor its invasion ability.

Eighth. Reduction of LFG levels does not alter primary tumor growth but it increases the metastatic potential of SH-SY5Y cells *in vivo*.

Ninth. Changes in LFG expression modulate genes implicated in focal adhesion, cell adhesion, adherent junctions, cancer pathways and cell cycle, supporting an active role of LFG in the tumorigenic potential of NBLs.

Tenth. MYCN is a direct repressor of LFG by promoting histone deacetylation and DNA methylation.

Lifeguard, by name and by nature

REFERENCES

6. References

Adkins, E.S., Sawin, R., Gerbing, R.B., London, W.B., Matthay, K.K., and Haase, G.M. (2004). Efficacy of complete resection for high-risk neuroblastoma: a Children's Cancer Group study. Journal of pediatric surgery *39*, 931-936.

Alam, G., Cui, H., Shi, H., Yang, L., Ding, J., Mao, L., Maltese, W.A., and Ding, H.F. (2009). MYCN promotes the expansion of Phox2B-positive neuronal progenitors to drive neuroblastoma development. The American journal of pathology *175*, 856-866.

Ambros, I.M., Zellner, A., Roald, B., Amann, G., Ladenstein, R., Printz, D., Gadner, H., and Ambros, P.F. (1996). Role of ploidy, chromosome 1p, and Schwann cells in the maturation of neuroblastoma. The New England journal of medicine *334*, 1505-1511.

Ando, K., Obara, Y., Sugama, J., Kotani, A., Koike, N., Ohkubo, S., and Nakahata, N. (2010). P2Y2 receptor-Gq/11 signaling at lipid rafts is required for UTP-induced cell migration in NG 108-15 cells. The Journal of pharmacology and experimental therapeutics *334*, 809-819.

Annunziata, C.M., Kleinberg, L., Davidson, B., Berner, A., Gius, D., Tchabo, N., Steinberg, S.M., and Kohn, E.C. (2007). BAG-4/SODD and associated antiapoptotic proteins are linked to aggressiveness of epithelial ovarian cancer. Clinical cancer research : an official journal of the American Association for Cancer Research *13*, 6585-6592.

Araujo, H., Danziger, N., Cordier, J., Glowinski, J., and Chneiweiss, H. (1993). Characterization of PEA-15, a major substrate for protein kinase C in astrocytes. The Journal of biological chemistry *268*, 5911-5920.

Arends, M.J., and Wyllie, A.H. (1991). Apoptosis: mechanisms and roles in pathology. International review of experimental pathology *32*, 223-254.

Asgharzadeh, S., Pique-Regi, R., Sposto, R., Wang, H., Yang, Y., Shimada, H., Matthay, K., Buckley, J., Ortega, A., and Seeger, R.C. (2006). Prognostic significance of gene expression profiles of metastatic neuroblastomas lacking MYCN gene amplification. Journal of the National Cancer Institute *98*, 1193-1203.

Ashburner, M., Ball, C.A., Blake, J.A., Botstein, D., Butler, H., Cherry, J.M., Davis, A.P., Dolinski, K., Dwight, S.S., Eppig, J.T.*, et al.* (2000). Gene ontology: tool for the unification of biology. The Gene Ontology Consortium. Nature genetics *25*, 25-29.

Ashkenazi, A., and Dixit, V.M. (1999). Apoptosis control by death and decoy receptors. Current opinion in cell biology *11*, 255-260.

Attiyeh, E.F., London, W.B., Mosse, Y.P., Wang, Q., Winter, C., Khazi, D., McGrady, P.W., Seeger, R.C., Look, A.T., Shimada, H.*, et al.* (2005). Chromosome 1p and 11q deletions and outcome in neuroblastoma. The New England journal of medicine *353*, 2243-2253.

Azarova, A.M., Gautam, G., and George, R.E. (2011). Emerging importance of ALK in neuroblastoma. Seminars in cancer biology *21*, 267-275.

Azuhata, T., Scott, D., Takamizawa, S., Wen, J., Davidoff, A., Fukuzawa, M., and Sandler, A. (2001). The inhibitor of apoptosis protein survivin is associated with high-risk behavior of neuroblastoma. Journal of pediatric surgery *36*, 1785-1791.

Baker, D. (2007). In 43rd Annual meeting of the American Society of Clinical Oncology (Chicago).

Bakhshi, A., Jensen, J.P., Goldman, P., Wright, J.J., McBride, O.W., Epstein, A.L., and Korsmeyer, S.J. (1985). Cloning the chromosomal breakpoint of t(14;18) human lymphomas: clustering around JH on chromosome 14 and near a transcriptional unit on 18. Cell *41*, 899-906.

Barbero, S., Mielgo, A., Torres, V., Teitz, T., Shields, D.J., Mikolon, D., Bogyo, M., Barila, D., Lahti, J.M., Schlaepfer, D*., et al.* (2009). Caspase-8 association with the focal adhesion complex promotes tumor cell migration and metastasis. Cancer research *69*, 3755-3763.

Beier, C.P., Wischhusen, J., Gleichmann, M., Gerhardt, E., Pekanovic, A., Krueger, A., Taylor, V., Suter, U., Krammer, P.H., Endres, M*., et al.* (2005). FasL (CD95L/APO-1L) resistance of neurons mediated by phosphatidylinositol 3-kinase-Akt/protein kinase B-dependent expression of lifeguard/neuronal membrane protein 35. The Journal of neuroscience : the official journal of the Society for Neuroscience *25*, 6765-6774.

Bell, E., Chen, L., Liu, T., Marshall, G.M., Lunec, J., and Tweddle, D.A. (2010). MYCN oncoprotein targets and their therapeutic potential. Cancer letters *293*, 144-157.

Bell, E., Lunec, J., and Tweddle, D.A. (2007). Cell cycle regulation targets of MYCN identified by gene expression microarrays. Cell cycle *6*, 1249-1256.

Berry, T., Luther, W., Bhatnagar, N., Jamin, Y., Poon, E., Sanda, T., Pei, D., Sharma, B., Vetharoy, W.R., Hallsworth, A*., et al.* (2012). The ALK(F1174L) mutation potentiates the oncogenic activity of MYCN in neuroblastoma. Cancer cell *22*, 117-130.

Berthold, F.S., T. (2005). Neuroblastoma, S.L.C. Nai-Kong V. Cheung, ed. (Germany: Springer).

Besnault-Mascard, L., Leprince, C., Auffredou, M.T., Meunier, B., Bourgeade, M.F., Camonis, J., Lorenzo, H.K., and Vazquez, A. (2005). Caspase-8 sumoylation is associated with nuclear localization. Oncogene *24*, 3268-3273.

Beyaert, R., Heyninck, K., and Van Huffel, S. (2000). A20 and A20-binding proteins as cellular inhibitors of nuclear factor-kappa B-dependent gene expression and apoptosis. Biochemical pharmacology *60*, 1143-1151.

Bez, A., Corsini, E., Curti, D., Biggiogera, M., Colombo, A., Nicosia, R.F., Pagano, S.F., and Parati, E.A. (2003). Neurosphere and neurosphere-forming cells: morphological and ultrastructural characterization. Brain research *993*, 18-29.

Bhardwaj, A., and Aggarwal, B.B. (2003). Receptor-mediated choreography of life and death. Journal of clinical immunology *23*, 317-332.

Bianchi, K., and Meier, P. (2009). A tangled web of ubiquitin chains: breaking news in TNF-R1 signaling. Molecular cell *36*, 736-742.

Bill, A.H., Jr. (1968). The regression of neuroblastoma. Journal of pediatric surgery *3*, 103-106.

Blankenship, J.W., Varfolomeev, E., Goncharov, T., Fedorova, A.V., Kirkpatrick, D.S., Izrael-Tomasevic, A., Phu, L., Arnott, D., Aghajan, M., Zobel, K.*, et al.* (2009). Ubiquitin binding modulates IAP antagonist-stimulated proteasomal degradation of c-IAP1 and c-IAP2(1). The Biochemical journal *417*, 149-160.

Bouchier-Hayes, L., and Martin, S.J. (2002). CARD games in apoptosis and immunity. EMBO reports *3*, 616-621.

Bourdeaut, F., Trochet, D., Janoueix-Lerosey, I., Ribeiro, A., Deville, A., Coz, C., Michiels, J.F., Lyonnet, S., Amiel, J., and Delattre, O. (2005). Germline mutations of the paired-like homeobox 2B (PHOX2B) gene in neuroblastoma. Cancer letters *228*, 51-58.

Brodeur, G.M. (2003). Neuroblastoma: biological insights into a clinical enigma. Nature reviews Cancer *3*, 203-216.

Brodeur, G.M., Minturn, J.E., Ho, R., Simpson, A.M., Iyer, R., Varela, C.R., Light, J.E., Kolla, V., and Evans, A.E. (2009). Trk receptor expression and inhibition in neuroblastomas. Clinical cancer research : an official journal of the American Association for Cancer Research *15*, 3244-3250.

Brodeur, G.M., Pritchard, J., Berthold, F., Carlsen, N.L., Castel, V., Castelberry, R.P., De Bernardi, B., Evans, A.E., Favrot, M., Hedborg, F.*, et al.* (1993). Revisions of the international criteria for neuroblastoma diagnosis, staging, and response to treatment. Journal of clinical oncology : official journal of the American Society of Clinical Oncology *11*, 1466-1477.

Brodeur, G.M., Seeger, R.C., Schwab, M., Varmus, H.E., and Bishop, J.M. (1984). Amplification of N-myc in untreated human neuroblastomas correlates with advanced disease stage. Science *224*, 1121-1124.

Bucan, V., Adili, M.Y., Choi, C.Y., Eddy, M.T., Vogt, P.M., and Reimers, K. (2010a). Transactivation of lifeguard (LFG) by Akt-/LEF-1 pathway in MCF-7 and MDA-MB 231 human breast cancer cells. Apoptosis : an international journal on programmed cell death *15*, 814-821.

Bucan, V., Choi, C.Y., Lazaridis, A., Vogt, P.M., and Reimers, K. (2011). Silencing of anti-apoptotic transmembrane protein lifeguard sensitizes solid tumor cell lines MCF-7 and SW872 to perifosine-induced cell death activation. Oncology letters *2*, 419-422.

Bucan, V., Reimers, K., Choi, C.Y., Eddy, M.T., and Vogt, P.M. (2010b). The anti-apoptotic protein lifeguard is expressed in breast cancer cells and tissues. Cellular & molecular biology letters *15*, 296-310.

Butrynski, J.E., D'Adamo, D.R., Hornick, J.L., Dal Cin, P., Antonescu, C.R., Jhanwar, S.C., Ladanyi, M., Capelletti, M., Rodig, S.J., Ramaiya, N.*, et al.* (2010). Crizotinib in ALK-rearranged inflammatory myofibroblastic tumor. The New England journal of medicine *363*, 1727-1733.

Cai, J., Yang, J., and Jones, D.P. (1998). Mitochondrial control of apoptosis: the role of cytochrome c. Biochimica et biophysica acta *1366*, 139-149.

Cao, X., Pobezinskaya, Y.L., Morgan, M.J., and Liu, Z.G. (2011). The role of TRADD in TRAIL-induced apoptosis and signaling. FASEB journal : official publication of the Federation of American Societies for Experimental Biology *25*, 1353-1358.

Carlin, S., Mairs, R.J., McCluskey, A.G., Tweddle, D.A., Sprigg, A., Estlin, C., Board, J., George, R.E., Ellershaw, C., Pearson, A.D., *et al.* (2003). Development of a real-time polymerase chain reaction assay for prediction of the uptake of meta-[(131)I]iodobenzylguanidine by neuroblastoma tumors. Clinical cancer research : an official journal of the American Association for Cancer Research *9*, 3338-3344.

Carlsen, N.L. (1990). How frequent is spontaneous remission of neuroblastomas? Implications for screening. British journal of cancer *61*, 441-446.

Carpenter, E.L., and Mosse, Y.P. (2012). Targeting ALK in neuroblastoma--preclinical and clinical advancements. Nature reviews Clinical oncology *9*, 391-399.

Castle, V.P., Heidelberger, K.P., Bromberg, J., Ou, X., Dole, M., and Nunez, G. (1993). Expression of the apoptosis-suppressing protein bcl-2, in neuroblastoma is associated with unfavorable histology and N-myc amplification. The American journal of pathology *143*, 1543-1550.

Catrysse, L., Vereecke, L., Beyaert, R., and van Loo, G. (2014). A20 in inflammation and autoimmunity. Trends in immunology *35*, 22-31.

Chai, S., To, K.K., and Lin, G. (2010). Circumvention of multi-drug resistance of cancer cells by Chinese herbal medicines. Chinese medicine *5*, 26.

Chan, F.K., Chun, H.J., Zheng, L., Siegel, R.M., Bui, K.L., and Lenardo, M.J. (2000). A domain in TNF receptors that mediates ligand-independent receptor assembly and signaling. Science *288*, 2351-2354.

Chang, D.W., Xing, Z., Pan, Y., Algeciras-Schimnich, A., Barnhart, B.C., Yaish-Ohad, S., Peter, M.E., and Yang, X. (2002). c-FLIP(L) is a dual function regulator for caspase-8 activation and CD95-mediated apoptosis. The EMBO journal *21*, 3704-3714.

Charron, J., Malynn, B.A., Fisher, P., Stewart, V., Jeannotte, L., Goff, S.P., Robertson, E.J., and Alt, F.W. (1992). Embryonic lethality in mice homozygous for a targeted disruption of the N-myc gene. Genes & development *6*, 2248-2257.

Cheung, C.H., Huang, C.C., Tsai, F.Y., Lee, J.Y., Cheng, S.M., Chang, Y.C., Huang, Y.C., Chen, S.H., and Chang, J.Y. (2013). Survivin - biology and potential as a therapeutic target in oncology. OncoTargets and therapy *6*, 1453-1462.

Cheung, H.H., Mahoney, D.J., Lacasse, E.C., and Korneluk, R.G. (2009). Down-regulation of c-FLIP Enhances death of cancer cells by smac mimetic compound. Cancer research *69*, 7729-7738.

Cheung, N.K., Kushner, B.H., Cheung, I.Y., Kramer, K., Canete, A., Gerald, W., Bonilla, M.A., Finn, R., Yeh, S.J., and Larson, S.M. (1998). Anti-G(D2) antibody treatment of minimal residual stage 4 neuroblastoma diagnosed at more than 1 year of age. Journal of clinical oncology : official journal of the American Society of Clinical Oncology *16*, 3053-3060.

Cheung, N.K., Lazarus, H., Miraldi, F.D., Abramowsky, C.R., Kallick, S., Saarinen, U.M., Spitzer, T., Strandjord, S.E., Coccia, P.F., and Berger, N.A. (1987). Ganglioside GD2 specific monoclonal antibody 3F8: a phase I study in patients with neuroblastoma and malignant melanoma. Journal of clinical oncology : official journal of the American Society of Clinical Oncology *5*, 1430-1440.

Chinnaiyan, A.M., O'Rourke, K., Yu, G.L., Lyons, R.H., Garg, M., Duan, D.R., Xing, L., Gentz, R., Ni, J., and Dixit, V.M. (1996). Signal transduction by DR3, a death domain-containing receptor related to TNFR-1 and CD95. Science *274*, 990-992.

Choi, Y.E., Butterworth, M., Malladi, S., Duckett, C.S., Cohen, G.M., and Bratton, S.B. (2009). The E3 ubiquitin ligase cIAP1 binds and ubiquitinates caspase-3 and -7 via unique mechanisms at distinct steps in their processing. The Journal of biological chemistry *284*, 12772-12782.

Christensen, J.G., Zou, H.Y., Arango, M.E., Li, Q., Lee, J.H., McDonnell, S.R., Yamazaki, S., Alton, G.R., Mroczkowski, B., and Los, G. (2007). Cytoreductive antitumor activity of PF-2341066, a novel inhibitor of anaplastic lymphoma kinase and c-Met, in experimental models of anaplastic large-cell lymphoma. Molecular cancer therapeutics *6*, 3314-3322.

Chu, Y., Masoud, M., and Gebeyehu, G. (2009). Cationic lipids capable of facilitating transport of biologically active agents or substances into cells; lipid aggregate macromolecular complex interacts with cells making the polyanionic macromolecule available for absorption and uptake by the cell (Google Patents).

Ciccarone, V., Spengler, B.A., Meyers, M.B., Biedler, J.L., and Ross, R.A. (1989). Phenotypic diversification in human neuroblastoma cells: expression of distinct neural crest lineages. Cancer research *49*, 219-225.

Cinatl, J., Jr., Kotchetkov, R., Blaheta, R., Driever, P.H., Vogel, J.U., and Cinatl, J. (2002). Induction of differentiation and suppression of malignant phenotype of human neuroblastoma BE(2)-C cells by valproic acid: enhancement by combination with interferon-alpha. International journal of oncology *20*, 97-106.

Cleary, M.L., and Sklar, J. (1985). Nucleotide sequence of a t(14;18) chromosomal breakpoint in follicular lymphoma and demonstration of a breakpoint-cluster region near a transcriptionally active locus on chromosome 18. Proceedings of the National Academy of Sciences of the United States of America *82*, 7439-7443.

Cohen, G.M., Sun, X.M., Fearnhead, H., MacFarlane, M., Brown, D.G., Snowden, R.T., and Dinsdale, D. (1994). Formation of large molecular weight fragments of DNA is a key committed step of apoptosis in thymocytes. Journal of immunology *153*, 507-516.

Cohen, J.J. (1994). Apoptosis: physiologic cell death. The Journal of laboratory and clinical medicine *124*, 761-765.

Cohen, J.J., Duke, R.C., Fadok, V.A., and Sellins, K.S. (1992). Apoptosis and programmed cell death in immunity. Annual review of immunology *10*, 267-293.

Cohn, S.L., Pearson, A.D., London, W.B., Monclair, T., Ambros, P.F., Brodeur, G.M., Faldum, A., Hero, B., Iehara, T., Machin, D*., et al.* (2009). The International Neuroblastoma Risk Group (INRG) classification system: an INRG Task Force report. Journal of clinical oncology : official journal of the American Society of Clinical Oncology *27*, 289-297.

Condorelli, G., Trencia, A., Vigliotta, G., Perfetti, A., Goglia, U., Cassese, A., Musti, A.M., Miele, C., Santopietro, S., Formisano, P*., et al.* (2002). Multiple members of the mitogen-activated protein kinase family are necessary for PED/PEA-15 anti-apoptotic function. The Journal of biological chemistry *277*, 11013-11018.

Condorelli, G., Vigliotta, G., Cafieri, A., Trencia, A., Andalo, P., Oriente, F., Miele, C., Caruso, M., Formisano, P., and Beguinot, F. (1999). PED/PEA-15: an anti-apoptotic molecule that regulates FAS/TNFR1-induced apoptosis. Oncogene *18*, 4409-4415.

Corvi, R., Savelyeva, L., Amler, L., Handgretinger, R., and Schwab, M. (1995a). Cytogenetic evolution of MYCN and MDM2 amplification in the neuroblastoma LS tumour and its cell line. European journal of cancer *31A*, 520-523.

Corvi, R., Savelyeva, L., Breit, S., Wenzel, A., Handgretinger, R., Barak, J., Oren, M., Amler, L., and Schwab, M. (1995b). Non-syntenic amplification of MDM2 and MYCN in human neuroblastoma. Oncogene *10*, 1081-1086.

Cotterman, R., and Knoepfler, P.S. (2009). N-Myc regulates expression of pluripotency genes in neuroblastoma including lif, klf2, klf4, and lin28b. PloS one *4*, e5799.

Coumar, M.S., Tsai, F.Y., Kanwar, J.R., Sarvagalla, S., and Cheung, C.H. (2013). Treat cancers by targeting survivin: just a dream or future reality? Cancer treatment reviews *39*, 802-811.

Crook, N.E., Clem, R.J., and Miller, L.K. (1993). An apoptosis-inhibiting baculovirus gene with a zinc finger-like motif. Journal of virology *67*, 2168-2174.

Curtin, J.F., and Cotter, T.G. (2003). Live and let die: regulatory mechanisms in Fas-mediated apoptosis. Cellular signalling *15*, 983-992.

Czabotar, P.E., Lessene, G., Strasser, A., and Adams, J.M. (2014). Control of apoptosis by the BCL-2 protein family: implications for physiology and therapy. Nature reviews Molecular cell biology *15*, 49-63.

Dalby, B., Cates, S., Harris, A., Ohki, E.C., Tilkins, M.L., Price, P.J., and Ciccarone, V.C. (2004). Advanced transfection with Lipofectamine 2000 reagent: primary neurons, siRNA, and high-throughput applications. Methods *33*, 95-103.

Daniels, R.A., Turley, H., Kimberley, F.C., Liu, X.S., Mongkolsapaya, J., Ch'En, P., Xu, X.N., Jin, B.Q., Pezzella, F., and Screaton, G.R. (2005). Expression of TRAIL and TRAIL receptors in normal and malignant tissues. Cell research *15*, 430-438.

Danziger, N., Yokoyama, M., Jay, T., Cordier, J., Glowinski, J., and Chneiweiss, H. (1995). Cellular expression, developmental regulation, and phylogenic conservation of PEA-15, the astrocytic major phosphoprotein and protein kinase C substrate. Journal of neurochemistry *64*, 1016-1025.

Darding, M., and Meier, P. (2012). IAPs: guardians of RIPK1. Cell death and differentiation *19*, 58-66.

Dastagir, N., Lazaridis, A., Dastagir, K., Reimers, K., Vogt, P.M., and Bucan, V. (2014). Role of Lifeguard beta-isoform in the development of breast cancer. Oncology reports.

De Brouwer, S., De Preter, K., Kumps, C., Zabrocki, P., Porcu, M., Westerhout, E.M., Lakeman, A., Vandesompele, J., Hoebeeck, J., Van Maerken, T.*, et al.* (2010). Meta-analysis of neuroblastomas reveals a skewed ALK mutation spectrum in tumors with MYCN amplification. Clinical cancer research : an official journal of the American Association for Cancer Research *16*, 4353-4362.

Desbarats, J., Birge, R.B., Mimouni-Rongy, M., Weinstein, D.E., Palerme, J.S., and Newell, M.K. (2003). Fas engagement induces neurite growth through ERK activation and p35 upregulation. Nature cell biology *5*, 118-125.

Deveraux, Q.L., Leo, E., Stennicke, H.R., Welsh, K., Salvesen, G.S., and Reed, J.C. (1999). Cleavage of human inhibitor of apoptosis protein XIAP results in fragments with distinct specificities for caspases. The EMBO journal *18*, 5242-5251.

Deveraux, Q.L., and Reed, J.C. (1999). IAP family proteins--suppressors of apoptosis. Genes & development *13*, 239-252.

Deveraux, Q.L., Takahashi, R., Salvesen, G.S., and Reed, J.C. (1997). X-linked IAP is a direct inhibitor of cell-death proteases. Nature *388*, 300-304.

Di Cagno, L., and Ravetto, F. (1967). [On an unusual case of neuroblastoma with multiple osseous metastases with spontaneous regression]. Minerva pediatrica *19*, 275-283.

Ding, I., Liu, W., Sun, J., Fenton, B., and Okunieff, P. (2002). Comparison and modulation of angiogenic responses by FGFs, VEGF and SCF in murine and human fibrosarcomas. Comparative biochemistry and physiology Part A, Molecular & integrative physiology *132*, 17-25.

Dixit, V.M., Green, S., Sarma, V., Holzman, L.B., Wolf, F.W., O'Rourke, K., Ward, P.A., Prochownik, E.V., and Marks, R.M. (1990). Tumor necrosis factor-alpha induction of novel gene products in human endothelial cells including a macrophage-specific chemotaxin. The Journal of biological chemistry *265*, 2973-2978.

Dole, M., Nunez, G., Merchant, A.K., Maybaum, J., Rode, C.K., Bloch, C.A., and Castle, V.P. (1994). Bcl-2 inhibits chemotherapy-induced apoptosis in neuroblastoma. Cancer research *54*, 3253-3259.

Dole, M.G., Jasty, R., Cooper, M.J., Thompson, C.B., Nunez, G., and Castle, V.P. (1995). Bcl-xL is expressed in neuroblastoma cells and modulates chemotherapy-induced apoptosis. Cancer research *55*, 2576-2582.

Domingo-Fernandez, R., Watters, K., Piskareva, O., Stallings, R.L., and Bray, I. (2013). The role of genetic and epigenetic alterations in neuroblastoma disease pathogenesis. Pediatric surgery international *29*, 101-119.

Du, C., Fang, M., Li, Y., Li, L., and Wang, X. (2000). Smac, a mitochondrial protein that promotes cytochrome c-dependent caspase activation by eliminating IAP inhibition. Cell *102*, 33-42.

DuBois, S.G., Chesler, L., Groshen, S., Hawkins, R., Goodarzian, F., Shimada, H., Yanik, G., Tagen, M., Stewart, C., Mosse, Y.P*., et al.* (2012). Phase I study of vincristine, irinotecan, and (1)(3)(1)I-metaiodobenzylguanidine for patients with relapsed or refractory neuroblastoma: a new approaches to neuroblastoma therapy trial. Clinical cancer research : an official journal of the American Association for Cancer Research *18*, 2679-2686.

DuBois, S.G., and Matthay, K.K. (2008). Radiolabeled metaiodobenzylguanidine for the treatment of neuroblastoma. Nuclear medicine and biology *35 Suppl 1*, S35-48.

Eastman, Q., and Grosschedl, R. (1999). Regulation of LEF-1/TCF transcription factors by Wnt and other signals. Current opinion in cell biology *11*, 233-240.

Eckelman, B.P., and Salvesen, G.S. (2006). The human anti-apoptotic proteins cIAP1 and cIAP2 bind but do not inhibit caspases. The Journal of biological chemistry *281*, 3254-3260.

Eckelman, B.P., Salvesen, G.S., and Scott, F.L. (2006). Human inhibitor of apoptosis proteins: why XIAP is the black sheep of the family. EMBO reports *7*, 988-994.

Edlich, F., Banerjee, S., Suzuki, M., Cleland, M.M., Arnoult, D., Wang, C., Neutzner, A., Tjandra, N., and Youle, R.J. (2011). Bcl-x(L) retrotranslocates Bax from the mitochondria into the cytosol. Cell *145*, 104-116.

Eggert, A., Grotzer, M.A., Zuzak, T.J., Wiewrodt, B.R., Ikegaki, N., and Brodeur, G.M. (2000). Resistance to TRAIL-induced apoptosis in neuroblastoma cells correlates with a loss of caspase-8 expression. Medical and pediatric oncology *35*, 603-607.

Eichholtz-Wirth, H., Fritz, E., and Wolz, L. (2003). Overexpression of the 'silencer of death domain', SODD/BAG-4, modulates both TNFR1- and CD95-dependent cell death pathways. Cancer letters *194*, 81-89.

Eilers, M., and Eisenman, R.N. (2008). Myc's broad reach. Genes & development *22*, 2755-2766.

Elkahloun, A.G., Bittner, M., Hoskins, K., Gemmill, R., and Meltzer, P.S. (1996). Molecular cytogenetic characterization and physical mapping of 12q13-15 amplification in human cancers. Genes, chromosomes & cancer *17*, 205-214.

Encinas, M., Iglesias, M., Liu, Y., Wang, H., Muhaisen, A., Cena, V., Gallego, C., and Comella, J.X. (2000). Sequential treatment of SH-SY5Y cells with retinoic acid and brain-derived neurotrophic factor gives rise to fully differentiated, neurotrophic factor-dependent, human neuron-like cells. Journal of neurochemistry *75*, 991-1003.

Eramo, A., Pallini, R., Lotti, F., Sette, G., Patti, M., Bartucci, M., Ricci-Vitiani, L., Signore, M., Stassi, G., Larocca, L.M.*, et al.* (2005). Inhibition of DNA methylation sensitizes glioblastoma for tumor necrosis factor-related apoptosis-inducing ligand-mediated destruction. Cancer research *65*, 11469-11477.

Ermolaeva, M.A., Michallet, M.C., Papadopoulou, N., Utermohlen, O., Kranidioti, K., Kollias, G., Tschopp, J., and Pasparakis, M. (2008). Function of TRADD in tumor necrosis factor receptor 1 signaling and in TRIF-dependent inflammatory responses. Nature immunology *9*, 1037-1046.

Estelles, A., Yokoyama, M., Nothias, F., Vincent, J.D., Glowinski, J., Vernier, P., and Chneiweiss, H. (1996). The major astrocytic phosphoprotein PEA-15 is encoded by two mRNAs conserved on their full length in mouse and human. The Journal of biological chemistry *271*, 14800-14806.

Evans, A.E., D'Angio, G.J., and Randolph, J. (1971). A proposed staging for children with neuroblastoma. Children's cancer study group A. Cancer *27*, 374-378.

Fang, J., Gu, L., Zhu, N., Tang, H., Alvarado, C.S., and Zhou, M. (2008). Tissue factor/FVIIa activates Bcl-2 and prevents doxorubicin-induced apoptosis in neuroblastoma cells. BMC cancer *8*, 69.

Fernandez, M., Segura, M.F., Sole, C., Colino, A., Comella, J.X., and Cena, V. (2007). Lifeguard/neuronal membrane protein 35 regulates Fas ligand-mediated apoptosis in neurons via microdomain recruitment. Journal of neurochemistry *103*, 190-203.

Fisher, J.P., and Tweddle, D.A. (2012). Neonatal neuroblastoma. Seminars in fetal & neonatal medicine *17*, 207-215.

Flahaut, M., Muhlethaler-Mottet, A., Auderset, K., Bourloud, K.B., Meier, R., Popovic, M.B., Joseph, J.M., and Gross, N. (2006). Persistent inhibition of FLIP(L) expression by lentiviral small hairpin RNA delivery restores death-receptor-induced apoptosis in neuroblastoma cells. Apoptosis : an international journal on programmed cell death *11*, 255-263.

Foehr, E.D., Lorente, G., Vincent, V., Nikolich, K., and Urfer, R. (2005). FAS associated phosphatase (FAP-1) blocks apoptosis of astrocytomas through dephosphorylation of FAS. Journal of neuro-oncology *74*, 241-248.

Formstecher, E., Ramos, J.W., Fauquet, M., Calderwood, D.A., Hsieh, J.C., Canton, B., Nguyen, X.T., Barnier, J.V., Camonis, J., Ginsberg, M.H.*, et al.* (2001). PEA-15 mediates cytoplasmic sequestration of ERK MAP kinase. Developmental cell *1*, 239-250.

Fort, P., and Theveneau, E. (2014). PleiotRHOpic: Rho pathways are essential for all stages of Neural Crest development. Small GTPases *5*.

French, L.E., and Tschopp, J. (2003). Protein-based therapeutic approaches targeting death receptors. Cell death and differentiation *10*, 117-123.

Friedman, G.K., and Castleberry, R.P. (2007). Changing trends of research and treatment in infant neuroblastoma. Pediatric blood & cancer *49*, 1060-1065.

Fries, K.L., Miller, W.E., and Raab-Traub, N. (1996). Epstein-Barr virus latent membrane protein 1 blocks p53-mediated apoptosis through the induction of the A20 gene. Journal of virology *70*, 8653-8659.

Frisch, S.M. (2008). Caspase-8: fly or die. Cancer research *68*, 4491-4493.

Fuchs, P., Strehl, S., Dworzak, M., Himmler, A., and Ambros, P.F. (1992). Structure of the human TNF receptor 1 (p60) gene (TNFR1) and localization to chromosome 12p13 [corrected]. Genomics *13*, 219-224.

Fulda, S. (2013a). Targeting apoptosis pathways in childhood malignancies. Cancer letters *332*, 369-373.

Fulda, S. (2013b). Targeting c-FLICE-like inhibitory protein (CFLAR) in cancer. Expert opinion on therapeutic targets *17*, 195-201.

Fulda, S., and Debatin, K.M. (2006). 5-Aza-2'-deoxycytidine and IFN-gamma cooperate to sensitize for TRAIL-induced apoptosis by upregulating caspase-8. Oncogene *25*, 5125-5133.

Fulda, S., Galluzzi, L., and Kroemer, G. (2010). Targeting mitochondria for cancer therapy. Nature reviews Drug discovery *9*, 447-464.

Fulda, S., Kufer, M.U., Meyer, E., van Valen, F., Dockhorn-Dworniczak, B., and Debatin, K.M. (2001). Sensitization for death receptor- or drug-induced apoptosis by re-expression of caspase-8 through demethylation or gene transfer. Oncogene *20*, 5865-5877.

Fulda, S., Meyer, E., and Debatin, K.M. (2002). Inhibition of TRAIL-induced apoptosis by Bcl-2 overexpression. Oncogene *21*, 2283-2294.

Fulda, S., Poremba, C., Berwanger, B., Hacker, S., Eilers, M., Christiansen, H., Hero, B., and Debatin, K.M. (2006). Loss of caspase-8 expression does not correlate with MYCN amplification, aggressive disease, or prognosis in neuroblastoma. Cancer research *66*, 10016-10023.

Galbiati, F., Volonte, D., Engelman, J.A., Watanabe, G., Burk, R., Pestell, R.G., and Lisanti, M.P. (1998). Targeted downregulation of caveolin-1 is sufficient to drive cell transformation and hyperactivate the p42/44 MAP kinase cascade. The EMBO journal *17*, 6633-6648.

Gallo, G., Giarnieri, E., Bosco, S., Cappelli, C., Alderisio, M., Giovagnoli, M.R., Giordano, A., and Vecchione, A. (2003). Aberrant bcl-2 and bax protein expression related to chemotherapy response in neuroblastoma. Anticancer research *23*, 777-784.

Gambacorti-Passerini, C., Messa, C., and Pogliani, E.M. (2011). Crizotinib in anaplastic large-cell lymphoma. The New England journal of medicine *364*, 775-776.

Garcia-Saez, A.J. (2012). The secrets of the Bcl-2 family. Cell death and differentiation *19*, 1733-1740.

Gartel, A.L., and Shchors, K. (2003). Mechanisms of c-myc-mediated transcriptional repression of growth arrest genes. Experimental cell research *283*, 17-21.

Gasparini, C., Vecchi Brumatti, L., Monasta, L., and Zauli, G. (2013). TRAIL-based therapeutic approaches for the treatment of pediatric malignancies. Current medicinal chemistry *20*, 2254-2271.

Gaumont-Leclerc, M.F., Mukhopadhyay, U.K., Goumard, S., and Ferbeyre, G. (2004). PEA-15 is inhibited by adenovirus E1A and plays a role in ERK nuclear export and Ras-induced senescence. The Journal of biological chemistry *279*, 46802-46809.

Gawecka, J.E., Geerts, D., Koster, J., Caliva, M.J., Sulzmaier, F.J., Opoku-Ansah, J., Wada, R.K., Bachmann, A.S., and Ramos, J.W. (2012). PEA15 impairs cell migration and correlates with clinical features predicting good prognosis in neuroblastoma. International journal of cancer Journal international du cancer *131*, 1556-1568.

Geissler, C., Hambek, M., Eckardt, A., Arnoldner, C., Diensthuber, M., Stover, T., and Wagenblast, J. (2012). The role of recombinant epidermal growth factor and serotonin in the stimulation of tumor growth in a SCCHN xenograft model. Oncology reports *28*, 785-790.

Genest, L., Lapointe, V., and Lalancette, A.M. (1964). [the Natural History of Neuroblastomas]. Laval medical *35*, 1084-1090.

George, R.E., Sanda, T., Hanna, M., Frohling, S., Luther, W., 2nd, Zhang, J., Ahn, Y., Zhou, W., London, W.B., McGrady, P.*, et al.* (2008). Activating mutations in ALK provide a therapeutic target in neuroblastoma. Nature *455*, 975-978.

Gheldof, A., and Berx, G. (2013). Cadherins and epithelial-to-mesenchymal transition. Progress in molecular biology and translational science *116*, 317-336.

Gherardi, S., Valli, E., Erriquez, D., and Perini, G. (2013). MYCN-mediated transcriptional repression in neuroblastoma: the other side of the coin. Front Oncol *3*, 42.

Glading, A., Koziol, J.A., Krueger, J., and Ginsberg, M.H. (2007). PEA-15 inhibits tumor cell invasion by binding to extracellular signal-regulated kinase 1/2. Cancer research *67*, 1536-1544.

Golks, A., Brenner, D., Fritsch, C., Krammer, P.H., and Lavrik, I.N. (2005). c-FLIPR, a new regulator of death receptor-induced apoptosis. The Journal of biological chemistry *280*, 14507-14513.

Grady, E.F., Schwab, M., and Rosenau, W. (1987). Expression of N-myc and c-src during the development of fetal human brain. Cancer research *47*, 2931-2936.

Graf, R.P., Keller, N., Barbero, S., and Stupack, D. (2014). Caspase-8 as a regulator of tumor cell motility. Current molecular medicine *14*, 246-254.

Grau, E., Martinez, F., Orellana, C., Canete, A., Yanez, Y., Oltra, S., Noguera, R., Hernandez, M., Bermudez, J.D., and Castel, V. (2011). Hypermethylation of apoptotic genes as independent prognostic factor in neuroblastoma disease. Molecular carcinogenesis *50*, 153-162.

Greig, A.V., Linge, C., Cambrey, A., and Burnstock, G. (2003a). Purinergic receptors are part of a signaling system for keratinocyte proliferation, differentiation, and apoptosis in human fetal epidermis. The Journal of investigative dermatology *121*, 1145-1149.

Greig, A.V., Linge, C., Healy, V., Lim, P., Clayton, E., Rustin, M.H., McGrouther, D.A., and Burnstock, G. (2003b). Expression of purinergic receptors in non-melanoma skin cancers and their functional roles in A431 cells. The Journal of investigative dermatology *121*, 315-327.

Greig, A.V., Linge, C., Terenghi, G., McGrouther, D.A., and Burnstock, G. (2003c). Purinergic receptors are part of a functional signaling system for proliferation and differentiation of human epidermal keratinocytes. The Journal of investigative dermatology *120*, 1007-1015.

Grimmer, M.R., and Weiss, W.A. (2006). Childhood tumors of the nervous system as disorders of normal development. Current opinion in pediatrics *18*, 634-638.

Gross, A., Yin, X.M., Wang, K., Wei, M.C., Jockel, J., Milliman, C., Erdjument-Bromage, H., Tempst, P., and Korsmeyer, S.J. (1999). Caspase cleaved BID targets mitochondria and is required for cytochrome c release, while BCL-XL prevents this release but not tumor necrosis factor-R1/Fas death. The Journal of biological chemistry *274*, 1156-1163.

Guimier, A., Ferrand, S., Pierron, G., Couturier, J., Janoueix-Lerosey, I., Combaret, V., Mosseri, V., Thebaud, E., Gambart, M., Plantaz, D.*, et al.* (2014). Clinical Characteristics and Outcome of Patients with Neuroblastoma Presenting Genomic Amplification of Loci Other than MYCN. PloS one *9*, e101990.

Gumy, L.F., Yeo, G.S., Tung, Y.C., Zivraj, K.H., Willis, D., Coppola, G., Lam, B.Y., Twiss, J.L., Holt, C.E., and Fawcett, J.W. (2011). Transcriptome analysis of embryonic and adult sensory axons reveals changes in mRNA repertoire localization. Rna *17*, 85-98.

Hagenbuchner, J., Kiechl-Kohlendorfer, U., Obexer, P., and Ausserlechner, M.J. (2013). A novel Mcl1 variant inhibits apoptosis via increased Bim sequestration. Oncotarget *4*, 1241-1252.

Hammerle, B., Yanez, Y., Palanca, S., Canete, A., Burks, D.J., Castel, V., and Font de Mora, J. (2013). Targeting neuroblastoma stem cells with retinoic acid and proteasome inhibitor. PloS one *8*, e76761.

Han, W., Zhou, Y., Zhong, R., Wu, C., Song, R., Liu, L., Zou, L., Qiao, Y., Zhai, K., Chang, J.*, et al.* (2013). Functional polymorphisms in FAS/FASL system increase the risk of neuroblastoma in Chinese population. PloS one *8*, e71656.

Hanahan, D., and Weinberg, R.A. (2000). The hallmarks of cancer. Cell *100*, 57-70.

Hanahan, D., and Weinberg, R.A. (2011). Hallmarks of cancer: the next generation. Cell *144*, 646-674.

Hansford, L.M., McKee, A.E., Zhang, L., George, R.E., Gerstle, J.T., Thorner, P.S., Smith, K.M., Look, A.T., Yeger, H., Miller, F.D.*, et al.* (2007). Neuroblastoma cells isolated from bone marrow metastases contain a naturally enriched tumor-initiating cell. Cancer research *67*, 11234-11243.

Hao, C., Beguinot, F., Condorelli, G., Trencia, A., Van Meir, E.G., Yong, V.W., Parney, I.F., Roa, W.H., and Petruk, K.C. (2001). Induction and intracellular regulation of tumor necrosis factor-related apoptosis-inducing ligand (TRAIL) mediated apotosis in human malignant glioma cells. Cancer research *61*, 1162-1170.

Hara, J. (2012). Development of treatment strategies for advanced neuroblastoma. International journal of clinical oncology *17*, 196-203.

Harrington, J.R. (2000). SODD-silencer of death domains. Stem cells *18*, 388-389.

Hasan, M.K., Nafady, A., Takatori, A., Kishida, S., Ohira, M., Suenaga, Y., Hossain, S., Akter, J., Ogura, A., Nakamura, Y.*, et al.* (2013). ALK is a MYCN target gene and regulates cell migration and invasion in neuroblastoma. Scientific reports *3*, 3450.

Hay, R.T. (2005). SUMO: a history of modification. Molecular cell *18*, 1-12.

Hayashi, N., Shirakura, H., Uehara, T., and Nomura, Y. (2006). Relationship between SUMO-1 modification of caspase-7 and its nuclear localization in human neuronal cells. Neuroscience letters *397*, 5-9.

Hayward, K., Jeremy, R.J., Jenkins, S., Barkovich, A.J., Gultekin, S.H., Kramer, J., Crittenden, M., and Matthay, K.K. (2001). Long-term neurobehavioral outcomes in children with neuroblastoma and opsoclonus-myoclonus-ataxia syndrome: relationship to MRI findings and anti-neuronal antibodies. The Journal of pediatrics *139*, 552-559.

He, T.C., Sparks, A.B., Rago, C., Hermeking, H., Zawel, L., da Costa, L.T., Morin, P.J., Vogelstein, B., and Kinzler, K.W. (1998). Identification of c-MYC as a target of the APC pathway. Science *281*, 1509-1512.

Head, B.P., Patel, H.H., and Insel, P.A. (2014). Interaction of membrane/lipid rafts with the cytoskeleton: impact on signaling and function: membrane/lipid rafts, mediators of cytoskeletal arrangement and cell signaling. Biochimica et biophysica acta *1838*, 532-545.

Hengartner, M.O. (2000). The biochemistry of apoptosis. Nature *407*, 770-776.

Hengartner, M.O., and Horvitz, H.R. (1994). Activation of C. elegans cell death protein CED-9 by an amino-acid substitution in a domain conserved in Bcl-2. Nature *369*, 318-320.

Henke, G., Meier, V., Lindner, L.H., Eibl, H., Bamberg, M., Belka, C., Budach, W., and Jendrossek, V. (2012). Effects of ionizing radiation in combination with Erufosine on T98G glioblastoma xenograft tumours: a study in NMRI nu/nu mice. Radiation oncology *7*, 172.

Heukamp, L.C., Thor, T., Schramm, A., De Preter, K., Kumps, C., De Wilde, B., Odersky, A., Peifer, M., Lindner, S., Spruessel, A.*, et al.* (2012). Targeted expression of mutated ALK induces neuroblastoma in transgenic mice. Science translational medicine *4*, 141ra191.

Hirning, U., Schmid, P., Schulz, W.A., Rettenberger, G., and Hameister, H. (1991). A comparative analysis of N-myc and c-myc expression and cellular proliferation in mouse organogenesis. Mechanisms of development *33*, 119-125.

Hjelmeland, A.B., Wu, Q., Wickman, S., Eyler, C., Heddleston, J., Shi, Q., Lathia, J.D., Macswords, J., Lee, J., McLendon, R.E.*, et al.* (2010). Targeting A20 decreases glioma stem cell survival and tumor growth. PLoS biology *8*, e1000319.

Hobbie, W.L., Moshang, T., Carlson, C.A., Goldmuntz, E., Sacks, N., Goldfarb, S.B., Grupp, S.A., and Ginsberg, J.P. (2008). Late effects in survivors of tandem peripheral blood stem cell transplant for high-risk neuroblastoma. Pediatric blood & cancer *51*, 679-683.

Hopkins-Donaldson, S., Bodmer, J.L., Bourloud, K.B., Brognara, C.B., Tschopp, J., and Gross, N. (2000). Loss of caspase-8 expression in highly malignant human neuroblastoma cells correlates with resistance to tumor necrosis factor-related apoptosis-inducing ligand-induced apoptosis. Cancer research *60*, 4315-4319.

Howman-Giles, R., Shaw, P.J., Uren, R.F., and Chung, D.K. (2007). Neuroblastoma and other neuroendocrine tumors. Seminars in nuclear medicine *37*, 286-302.

Hryniewicz-Jankowska, A., Augoff, K., Biernatowska, A., Podkalicka, J., and Sikorski, A.F. (2014). Membrane rafts as a novel target in cancer therapy. Biochimica et biophysica acta *1845*, 155-165.

Hu, W.H., Johnson, H., and Shu, H.B. (2000). Activation of NF-kappaB by FADD, Casper, and caspase-8. The Journal of biological chemistry *275*, 10838-10844.

Hu, X., Yee, E., Harlan, J.M., Wong, F., and Karsan, A. (1998). Lipopolysaccharide induces the antiapoptotic molecules, A1 and A20, in microvascular endothelial cells. Blood *92*, 2759-2765.

Huang, T.T., Wuerzberger-Davis, S.M., Wu, Z.H., and Miyamoto, S. (2003). Sequential modification of NEMO/IKKgamma by SUMO-1 and ubiquitin mediates NF-kappaB activation by genotoxic stress. Cell *115*, 565-576.

Hurtado de Mendoza, T., Perez-Garcia, C.G., Kroll, T.T., Hoong, N.H., O'Leary, D.D., and Verma, I.M. (2011). Antiapoptotic protein Lifeguard is required for survival and maintenance of Purkinje and granular cells. Proceedings of the National Academy of Sciences of the United States of America *108*, 17189-17194.

Hutchinson, R.J., Sisson, J.C., Shapiro, B., Miser, J.S., Normole, D., Shulkin, B.L., Francis, I.R., Zasadny, K., Carey, J.E., Johnson, J.W*., et al.* (1992). 131-I-metaiodobenzylguanidine treatment in patients with refractory advanced neuroblastoma. American journal of clinical oncology *15*, 226-232.

Hwang, S., Kuo, W.L., Cochran, J.F., Guzman, R.C., Tsukamoto, T., Bandyopadhyay, G., Myambo, K., and Collins, C.C. (1997). Assignment of HMAT1, the human homolog of the murine mammary transforming gene (MAT1) associated with tumorigenesis, to 1q21.1, a region frequently gained in human breast cancers. Genomics *42*, 540-542.

Iglesias-Guimarais, V., Gil-Guinon, E., Sanchez-Osuna, M., Casanelles, E., Garcia-Belinchon, M., Comella, J.X., and Yuste, V.J. (2013). Chromatin collapse during caspase-dependent apoptotic cell death requires DNA fragmentation factor, 40-kDa subunit-/caspase-activated deoxyribonuclease-mediated 3'-OH single-strand DNA breaks. The Journal of biological chemistry *288*, 9200-9215.

Inoue, J., Misawa, A., Tanaka, Y., Ichinose, S., Sugino, Y., Hosoi, H., Sugimoto, T., Imoto, I., and Inazawa, J. (2009). Lysosomal-associated protein multispanning transmembrane 5 gene (LAPTM5) is associated with spontaneous regression of neuroblastomas. PloS one *4*, e7099.

Iolascon, A., Borriello, A., Giordani, L., Cucciolla, V., Moretti, A., Monno, F., Criniti, V., Marzullo, A., Criscuolo, M., and Ragione, F.D. (2003). Caspase 3 and 8 deficiency in human neuroblastoma. Cancer genetics and cytogenetics *146*, 41-47.

Iraci, N., Diolaiti, D., Papa, A., Porro, A., Valli, E., Gherardi, S., Herold, S., Eilers, M., Bernardoni, R., Della Valle, G*., et al.* (2011). A SP1/MIZ1/MYCN repression complex recruits HDAC1 at the TRKA and p75NTR promoters and affects neuroblastoma malignancy by inhibiting the cell response to NGF. Cancer research *71*, 404-412.

Irie, S., Hachiya, T., Rabizadeh, S., Maruyama, W., Mukai, J., Li, Y., Reed, J.C., Bredesen, D.E., and Sato, T.A. (1999). Functional interaction of Fas-associated phosphatase-1 (FAP-1) with p75(NTR) and their effect on NF-kappaB activation. FEBS letters *460*, 191-198.

Irizarry, R.A., Hobbs, B., Collin, F., Beazer-Barclay, Y.D., Antonellis, K.J., Scherf, U., and Speed, T.P. (2003). Exploration, normalization, and summaries of high density oligonucleotide array probe level data. Biostatistics *4*, 249-264.

Irmler, M., Thome, M., Hahne, M., Schneider, P., Hofmann, K., Steiner, V., Bodmer, J.L., Schroter, M., Burns, K., Mattmann, C*., et al.* (1997). Inhibition of death receptor signals by cellular FLIP. Nature *388*, 190-195.

Ishizu, H., Bove, K.E., Ziegler, M.M., and Arya, G. (1994). Immune-mediated regression of 'metastatic' neuroblastoma in the liver. Journal of pediatric surgery *29*, 155-159; discussion 159-160.

Ivanov, V.N., Lopez Bergami, P., Maulit, G., Sato, T.A., Sassoon, D., and Ronai, Z. (2003). FAP-1 association with Fas (Apo-1) inhibits Fas expression on the cell surface. Molecular and cellular biology *23*, 3623-3635.

Ivanov, V.N., Ronai, Z., and Hei, T.K. (2006). Opposite roles of FAP-1 and dynamin in the regulation of Fas (CD95) translocation to the cell surface and susceptibility to Fas ligand-mediated apoptosis. The Journal of biological chemistry *281*, 1840-1852.

Izycka-Swieszewska, E., Wozniak, A., Drozynska, E., Kot, J., Grajkowska, W., Klepacka, T., Perek, D., Koltan, S., Bien, E., and Limon, J. (2011). Expression and significance of HER family receptors in neuroblastic tumors. Clinical & experimental metastasis *28*, 271-282.

Jaattela, M., Mouritzen, H., Elling, F., and Bastholm, L. (1996). A20 zinc finger protein inhibits TNF and IL-1 signaling. Journal of immunology *156*, 1166-1173.

Jiang, G., Ren, B., Xu, L., Song, S., Zhu, C., and Ye, F. (2009). Survivin may enhance DNA double-strand break repair capability by up-regulating Ku70 in human KB cells. Anticancer research *29*, 223-228.

Jiang, M., Stanke, J., and Lahti, J.M. (2011). The connections between neural crest development and neuroblastoma. Current topics in developmental biology *94*, 77-127.

Jiang, Y., Woronicz, J.D., Liu, W., and Goeddel, D.V. (1999). Prevention of constitutive TNF receptor 1 signaling by silencer of death domains. Science *283*, 543-546.

Jin, H.S., Lee, D.H., Kim, D.H., Chung, J.H., Lee, S.J., and Lee, T.H. (2009). cIAP1, cIAP2, and XIAP act cooperatively via nonredundant pathways to regulate genotoxic stress-induced nuclear factor-kappaB activation. Cancer research *69*, 1782-1791.

Johnsen, J.I., Kogner, P., Albihn, A., and Henriksson, M.A. (2009). Embryonal neural tumours and cell death. Apoptosis : an international journal on programmed cell death *14*, 424-438.

Johnsen, J.I., Pettersen, I., Ponthan, F., Sveinbjornsson, B., Flaegstad, T., and Kogner, P. (2004). Synergistic induction of apoptosis in neuroblastoma cells using a combination of cytostatic drugs with interferon-gamma and TRAIL. International journal of oncology *25*, 1849-1857.

Judware, R., and Culp, L. (1997a). Persistent alpha 1 integrin subunit expression in human neuroblastoma cell lines which overexpress N-myc and downregulate other integrin subunits. Oncology reports *4*, 433-437.

Judware, R., and Culp, L.A. (1997b). Concomitant down-regulation of expression of integrin subunits by N-myc in human neuroblastoma cells: differential regulation of alpha2, alpha3 and beta1. Oncogene *14*, 1341-1350.

Kamimatsuse, A., Matsuura, K., Moriya, S., Fukuba, I., Yamaoka, H., Fukuda, E., Kamei, N., Hiyama, K., Sueda, T., and Hiyama, E. (2009). Detection of CpG island hypermethylation of caspase-8 in neuroblastoma using an oligonucleotide array. Pediatric blood & cancer *52*, 777-783.

Kanehisa, M., and Goto, S. (2000). KEGG: kyoto encyclopedia of genes and genomes. Nucleic acids research *28*, 27-30.

Kanehisa, M., Goto, S., Sato, Y., Furumichi, M., and Tanabe, M. (2012). KEGG for integration and interpretation of large-scale molecular data sets. Nucleic acids research *40*, D109-114.

Karreth, F., and Tuveson, D.A. (2004). Twist induces an epithelial-mesenchymal transition to facilitate tumor metastasis. Cancer biology & therapy *3*, 1058-1059.

Kataoka, T., Budd, R.C., Holler, N., Thome, M., Martinon, F., Irmler, M., Burns, K., Hahne, M., Kennedy, N., Kovacsovics, M.*, et al.* (2000). The caspase-8 inhibitor FLIP promotes activation of NF-kappaB and Erk signaling pathways. Current biology : CB *10*, 640-648.

Katzenstein, H.M., Kent, P.M., London, W.B., and Cohn, S.L. (2001). Treatment and outcome of 83 children with intraspinal neuroblastoma: the Pediatric Oncology Group experience. Journal of clinical oncology : official journal of the American Society of Clinical Oncology *19*, 1047-1055.

Kelly, A.E., Ghenoiu, C., Xue, J.Z., Zierhut, C., Kimura, H., and Funabiki, H. (2010). Survivin reads phosphorylated histone H3 threonine 3 to activate the mitotic kinase Aurora B. Science *330*, 235-239.

Keppler, O.T., Peter, M.E., Hinderlich, S., Moldenhauer, G., Stehling, P., Schmitz, I., Schwartz-Albiez, R., Reutter, W., and Pawlita, M. (1999). Differential sialylation of cell surface glycoconjugates in a human B lymphoma cell line regulates susceptibility for CD95 (APO-1/Fas)-mediated apoptosis and for infection by a lymphotropic virus. Glycobiology *9*, 557-569.

Kerosuo, L., and Bronner-Fraser, M. (2012). What is bad in cancer is good in the embryo: importance of EMT in neural crest development. Seminars in cell & developmental biology *23*, 320-332.

Kerr, J.F., Wyllie, A.H., and Currie, A.R. (1972). Apoptosis: a basic biological phenomenon with wide-ranging implications in tissue kinetics. British journal of cancer *26*, 239-257.

Kim, J.H., Lee, E.R., Jeon, K., Choi, H.Y., Lim, H., Kim, S.J., Chae, H.J., Park, S.H., Kim, S., Seo, Y.R.*, et al.* (2012). Role of BI-1 (TEGT)-mediated ERK1/2 activation in mitochondria-mediated apoptosis and splenomegaly in BI-1 transgenic mice. Biochimica et biophysica acta *1823*, 876-888.

Kischkel, F.C., Hellbardt, S., Behrmann, I., Germer, M., Pawlita, M., Krammer, P.H., and Peter, M.E. (1995). Cytotoxicity-dependent APO-1 (Fas/CD95)-associated proteins form a death-inducing signaling complex (DISC) with the receptor. The EMBO journal *14*, 5579-5588.

Kitanaka, C., Kato, K., Ijiri, R., Sakurada, K., Tomiyama, A., Noguchi, K., Nagashima, Y., Nakagawara, A., Momoi, T., Toyoda, Y.*, et al.* (2002). Increased Ras expression and caspase-independent neuroblastoma cell death: possible mechanism of spontaneous neuroblastoma regression. Journal of the National Cancer Institute *94*, 358-368.

Kleber, S., Sancho-Martinez, I., Wiestler, B., Beisel, A., Gieffers, C., Hill, O., Thiemann, M., Mueller, W., Sykora, J., Kuhn, A.*, et al.* (2008). Yes and PI3K bind CD95 to signal invasion of glioblastoma. Cancer cell *13*, 235-248.

Knoepfler, P.S., Cheng, P.F., and Eisenman, R.N. (2002). N-myc is essential during neurogenesis for the rapid expansion of progenitor cell populations and the inhibition of neuronal differentiation. Genes & development *16*, 2699-2712.

Krueger, A., Schmitz, I., Baumann, S., Krammer, P.H., and Kirchhoff, S. (2001). Cellular FLICE-inhibitory protein splice variants inhibit different steps of caspase-8 activation at the CD95 death-inducing signaling complex. The Journal of biological chemistry *276*, 20633-20640.

Kubes, M., Cordier, J., Glowinski, J., Girault, J.A., and Chneiweiss, H. (1998). Endothelin induces a calcium-dependent phosphorylation of PEA-15 in intact astrocytes: identification of Ser104 and Ser116 phosphorylated, respectively, by protein kinase C and calcium/calmodulin kinase II in vitro. Journal of neurochemistry *71*, 1307-1314.

Kuwana, T., Bouchier-Hayes, L., Chipuk, J.E., Bonzon, C., Sullivan, B.A., Green, D.R., and Newmeyer, D.D. (2005). BH3 domains of BH3-only proteins differentially regulate Bax-mediated mitochondrial membrane permeabilization both directly and indirectly. Molecular cell *17*, 525-535.

LaCasse, E.C., Baird, S., Korneluk, R.G., and MacKenzie, A.E. (1998). The inhibitors of apoptosis (IAPs) and their emerging role in cancer. Oncogene *17*, 3247-3259.

Laemmli, U.K. (1970). Cleavage of structural proteins during the assembly of the head of bacteriophage T4. Nature *227*, 680-685.

Lamant, L., Pulford, K., Bischof, D., Morris, S.W., Mason, D.Y., Delsol, G., and Mariame, B. (2000). Expression of the ALK tyrosine kinase gene in neuroblastoma. The American journal of pathology *156*, 1711-1721.

Lamers, F., Schild, L., den Hartog, I.J., Ebus, M.E., Westerhout, E.M., Ora, I., Koster, J., Versteeg, R., Caron, H.N., and Molenaar, J.J. (2012). Targeted BCL2 inhibition effectively inhibits neuroblastoma tumour growth. European journal of cancer *48*, 3093-3103.

Lau, J.J., Trobe, J.D., Ruiz, R.E., Cho, R.W., Wechsler, D.S., Shah, G.V., and Gebarski, S.S. (2004). Metastatic neuroblastoma presenting with binocular blindness from intracranial compression of the optic nerves. Journal of neuro-ophthalmology : the official journal of the North American Neuro-Ophthalmology Society *24*, 119-124.

Lavrik, I., Golks, A., and Krammer, P.H. (2005). Death receptor signaling. Journal of cell science *118*, 265-267.

Lazcoz, P., Munoz, J., Nistal, M., Pestana, A., Encio, I., and Castresana, J.S. (2006). Frequent promoter hypermethylation of RASSF1A and CASP8 in neuroblastoma. BMC cancer *6*, 254.

Lee, S.H., Shin, M.S., Lee, J.Y., Park, W.S., Kim, S.Y., Jang, J.J., Dong, S.M., Na, E.Y., Kim, C.S., Kim, S.H*., et al.* (1999a). In vivo expression of soluble Fas and FAP-1: possible mechanisms of Fas resistance in human hepatoblastomas. The Journal of pathology *188*, 207-212.

Lee, S.H., Shin, M.S., Park, W.S., Kim, S.Y., Kim, H.S., Lee, J.H., Han, S.Y., Lee, H.K., Park, J.Y., Oh, R.R*., et al.* (1999b). Immunohistochemical localization of FAP-1, an inhibitor of Fas-mediated apoptosis, in normal and neoplastic human tissues. APMIS : acta pathologica, microbiologica, et immunologica Scandinavica *107*, 1101-1108.

Lee, Y.J., and Amoscato, A.A. (2004). TRAIL and ceramide. Vitamins and hormones *67*, 229-255.
Lee, Y.S., Jang, M.S., Lee, J.S., Choi, E.J., and Kim, E. (2005). SUMO-1 represses apoptosis signal-regulating kinase 1 activation through physical interaction and not through covalent modification. EMBO reports *6*, 949-955.

Lestini, B.J., Goldsmith, K.C., Fluchel, M.N., Liu, X., Chen, N.L., Goyal, B., Pawel, B.R., and Hogarty, M.D. (2009). Mcl1 downregulation sensitizes neuroblastoma to cytotoxic chemotherapy and small molecule Bcl2-family antagonists. Cancer biology & therapy *8*, 1587-1595.

Li, L.C., and Dahiya, R. (2002). MethPrimer: designing primers for methylation PCRs. Bioinformatics *18*, 1427-1431.

Li, Y., and Nakagawara, A. (2013). Apoptotic cell death in neuroblastoma. Cells *2*, 432-459.

Liu, H., Zhang, X., Li, J., Sun, B., Qian, H., and Yin, Z. (2014). The biological and clinical importance of epithelial-mesenchymal transition in circulating tumor cells. Journal of cancer research and clinical oncology.

Livak, K.J., and Schmittgen, T.D. (2001). Analysis of relative gene expression data using real-time quantitative PCR and the 2(-Delta Delta C(T)) Method. Methods *25*, 402-408.

Llambi, F., Moldoveanu, T., Tait, S.W., Bouchier-Hayes, L., Temirov, J., McCormick, L.L., Dillon, C.P., and Green, D.R. (2011). A unified model of mammalian BCL-2 protein family interactions at the mitochondria. Molecular cell *44*, 517-531.

Lo, L., Morin, X., Brunet, J.F., and Anderson, D.J. (1999). Specification of neurotransmitter identity by Phox2 proteins in neural crest stem cells. Neuron *22*, 693-705.

Lock, R., Carol, H., Houghton, P.J., Morton, C.L., Kolb, E.A., Gorlick, R., Reynolds, C.P., Maris, J.M., Keir, S.T., Wu, J.*, et al.* (2008). Initial testing (stage 1) of the BH3 mimetic ABT-263 by the pediatric preclinical testing program. Pediatric blood & cancer *50*, 1181-1189.

Locksley, R.M., Killeen, N., and Lenardo, M.J. (2001). The TNF and TNF receptor superfamilies: integrating mammalian biology. Cell *104*, 487-501.

London, W.B., Castleberry, R.P., Matthay, K.K., Look, A.T., Seeger, R.C., Shimada, H., Thorner, P., Brodeur, G., Maris, J.M., Reynolds, C.P.*, et al.* (2005). Evidence for an age cutoff greater than 365 days for neuroblastoma risk group stratification in the Children's Oncology Group. Journal of clinical oncology : official journal of the American Society of Clinical Oncology *23*, 6459-6465.

Lopez, J., John, S.W., Tenev, T., Rautureau, G.J., Hinds, M.G., Francalanci, F., Wilson, R., Broemer, M., Santoro, M.M., Day, C.L.*, et al.* (2011). CARD-mediated autoinhibition of cIAP1's E3 ligase activity suppresses cell proliferation and migration. Molecular cell *42*, 569-583.

Lopez-Carballo, G., Moreno, L., Masia, S., Perez, P., and Barettino, D. (2002). Activation of the phosphatidylinositol 3-kinase/Akt signaling pathway by retinoic acid is required for neural differentiation of SH-SY5Y human neuroblastoma cells. The Journal of biological chemistry *277*, 25297-25304.

Lu, J.G., Li, Y., Li, L., and Kan, X. (2011). Overexpression of osteopontin and integrin alphav in laryngeal and hypopharyngeal carcinomas associated with differentiation and metastasis. Journal of cancer research and clinical oncology *137*, 1613-1618.

Lu, J.G., Sun, Y.N., Wang, C., Jin de, J., and Liu, M. (2009). Role of the alpha v-integrin subunit in cell proliferation, apoptosis and tumor metastasis of laryngeal and hypopharyngeal squamous cell carcinomas: a clinical and in vitro investigation. European archives of oto-rhino-laryngology : official journal of the European Federation of Oto-Rhino-Laryngological Societies *266*, 89-96.

Lutz, W., Stohr, M., Schurmann, J., Wenzel, A., Lohr, A., and Schwab, M. (1996). Conditional expression of N-myc in human neuroblastoma cells increases expression of alpha-prothymosin and ornithine decarboxylase and accelerates progression into S-phase early after mitogenic stimulation of quiescent cells. Oncogene *13*, 803-812.

MacDonald, I.C., Groom, A.C., and Chambers, A.F. (2002). Cancer spread and micrometastasis development: quantitative approaches for in vivo models. BioEssays : news and reviews in molecular, cellular and developmental biology *24*, 885-893.

Mahller, Y.Y., Williams, J.P., Baird, W.H., Mitton, B., Grossheim, J., Saeki, Y., Cancelas, J.A., Ratner, N., and Cripe, T.P. (2009). Neuroblastoma cell lines contain pluripotent tumor initiating cells that are susceptible to a targeted oncolytic virus. PloS one *4*, e4235.

Mahoney, N.R., Liu, G.T., Menacker, S.J., Wilson, M.C., Hogarty, M.D., and Maris, J.M. (2006). Pediatric horner syndrome: etiologies and roles of imaging and urine studies to detect neuroblastoma and other responsible mass lesions. American journal of ophthalmology *142*, 651-659.

Marchetti, D., Aucoin, R., Blust, J., Murry, B., and Greiter-Wilke, A. (2004). p75 neurotrophin receptor functions as a survival receptor in brain-metastatic melanoma cells. Journal of cellular biochemistry *91*, 206-215.

Maris, J.M., Hogarty, M.D., Bagatell, R., and Cohn, S.L. (2007). Neuroblastoma. Lancet *369*, 2106-2120.

Marsters, S.A., Sheridan, J.P., Donahue, C.J., Pitti, R.M., Gray, C.L., Goddard, A.D., Bauer, K.D., and Ashkenazi, A. (1996). Apo-3, a new member of the tumor necrosis factor receptor family, contains a death domain and activates apoptosis and NF-kappa B. Current biology : CB *6*, 1669-1676.

Martin, S.J., and Green, D.R. (1995). Protease activation during apoptosis: death by a thousand cuts? Cell *82*, 349-352.

Martin, S.J., Reutelingsperger, C.P., McGahon, A.J., Rader, J.A., van Schie, R.C., LaFace, D.M., and Green, D.R. (1995). Early redistribution of plasma membrane phosphatidylserine is a general feature of apoptosis regardless of the initiating stimulus: inhibition by overexpression of Bcl-2 and Abl. The Journal of experimental medicine *182*, 1545-1556.

Martin, T.A., Mason, M.D., and Jiang, W.G. (2011). Tight junctions in cancer metastasis. Frontiers in bioscience *16*, 898-936.

Masia, A., Almazan-Moga, A., Velasco, P., Reventos, J., Toran, N., Sanchez de Toledo, J., Roma, J., and Gallego, S. (2012). Notch-mediated induction of N-cadherin and alpha9-integrin confers higher invasive phenotype on rhabdomyosarcoma cells. British journal of cancer *107*, 1374-1383.

Matthay, K.K., DeSantes, K., Hasegawa, B., Huberty, J., Hattner, R.S., Ablin, A., Reynolds, C.P., Seeger, R.C., Weinberg, V.K., and Price, D. (1998). Phase I dose escalation of 131I-metaiodobenzylguanidine with autologous bone marrow support in refractory neuroblastoma. Journal of clinical oncology : official journal of the American Society of Clinical Oncology *16*, 229-236.

Matthay, K.K., George, R.E., and Yu, A.L. (2012). Promising therapeutic targets in neuroblastoma. Clinical cancer research : an official journal of the American Association for Cancer Research *18*, 2740-2753.

Matthay, K.K., Shulkin, B., Ladenstein, R., Michon, J., Giammarile, F., Lewington, V., Pearson, A.D., and Cohn, S.L. (2010). Criteria for evaluation of disease extent by (123)I-metaiodobenzylguanidine scans in neuroblastoma: a report for the International Neuroblastoma Risk Group (INRG) Task Force. British journal of cancer *102*, 1319-1326.

Merianda, T.T., Vuppalanchi, D., Yoo, S., Blesch, A., and Twiss, J.L. (2013). Axonal transport of neural membrane protein 35 mRNA increases axon growth. Journal of cell science *126*, 90-102.

Micheau, O., Thome, M., Schneider, P., Holler, N., Tschopp, J., Nicholson, D.W., Briand, C., and Grutter, M.G. (2002). The long form of FLIP is an activator of caspase-8 at the Fas death-inducing signaling complex. The Journal of biological chemistry *277*, 45162-45171.

Mielgo, A., Torres, V.A., Schmid, M.C., Graf, R., Zeitlin, S.G., Lee, P., Shields, D.J., Barbero, S., Jamora, C., and Stupack, D.G. (2009). The death effector domains of caspase-8 induce terminal differentiation. PloS one *4*, e7879.

Mignotte, B., and Vayssiere, J.L. (1998). Mitochondria and apoptosis. European journal of biochemistry / FEBS *252*, 1-15.

Mikkola, M.L., Pispa, J., Pekkanen, M., Paulin, L., Nieminen, P., Kere, J., and Thesleff, I. (1999). Ectodysplasin, a protein required for epithelial morphogenesis, is a novel TNF homologue and promotes cell-matrix adhesion. Mechanisms of development *88*, 133-146.

Miyazaki, T., Atarashi, Y., Yasumura, S., Minatoya, I., Ogawa, K., Iwamoto, M., Minemura, M., Shimizu, Y., Sato, T.A., Watanabe, A.*, et al.* (2006). Fas-associated phosphatase-1 promotes Fas-mediated apoptosis in human colon cancer cells: novel function of FAP-1. Journal of gastroenterology and hepatology *21*, 84-91.

Modak, S., and Cheung, N.K. (2010). Neuroblastoma: Therapeutic strategies for a clinical enigma. Cancer treatment reviews *36*, 307-317.

Molenaar, J.J., Koster, J., Zwijnenburg, D.A., van Sluis, P., Valentijn, L.J., van der Ploeg, I., Hamdi, M., van Nes, J., Westerman, B.A., van Arkel, J.*, et al.* (2012). Sequencing of neuroblastoma identifies chromothripsis and defects in neuritogenesis genes. Nature *483*, 589-593.

Moll, R., Franke, W.W., Schiller, D.L., Geiger, B., and Krepler, R. (1982). The catalog of human cytokeratins: patterns of expression in normal epithelia, tumors and cultured cells. Cell *31*, 11-24.

Monclair, T., Brodeur, G.M., Ambros, P.F., Brisse, H.J., Cecchetto, G., Holmes, K., Kaneko, M., London, W.B., Matthay, K.K., Nuchtern, J.G.*, et al.* (2009). The International Neuroblastoma Risk Group (INRG) staging system: an INRG Task Force report. Journal of clinical oncology : official journal of the American Society of Clinical Oncology *27*, 298-303.

Morris, J.R., Boutell, C., Keppler, M., Densham, R., Weekes, D., Alamshah, A., Butler, L., Galanty, Y., Pangon, L., Kiuchi, T.*, et al.* (2009). The SUMO modification pathway is involved in the BRCA1 response to genotoxic stress. Nature *462*, 886-890.

Moubarak, R.S., Planells-Ferrer, L., Urresti, J., Reix, S., Segura, M.F., Carriba, P., Marques-Fernandez, F., Sole, C., Llecha-Cano, N., Lopez-Soriano, J.*, et al.* (2013). FAIM-L is an IAP-binding protein that inhibits XIAP ubiquitinylation and protects from Fas-induced apoptosis. The Journal of neuroscience : the official journal of the Society for Neuroscience *33*, 19262-19275.

Moubarak, R.S., Sole, C., Pascual, M., Gutierrez, H., Llovera, M., Perez-Garcia, M.J., Gozzelino, R., Segura, M.F., Iglesias-Guimarais, V., Reix, S.*, et al.* (2010). The death receptor antagonist FLIP-L interacts with Trk and is necessary for neurite outgrowth induced by neurotrophins. The Journal of neuroscience : the official journal of the Society for Neuroscience *30*, 6094-6105.

Mugrauer, G., Alt, F.W., and Ekblom, P. (1988). N-myc proto-oncogene expression during organogenesis in the developing mouse as revealed by in situ hybridization. The Journal of cell biology *107*, 1325-1335.

Muhlethaler-Mottet, A., Balmas, K., Auderset, K., Joseph, J.M., and Gross, N. (2003). Restoration of TRAIL-induced apoptosis in a caspase-8-deficient neuroblastoma cell line by stable re-expression of caspase-8. Annals of the New York Academy of Sciences *1010*, 195-199.

Murga-Zamalloa, C., and Lim, M.S. (2014). ALK-driven tumors and targeted therapy: focus on crizotinib. Pharmacogenomics and personalized medicine *7*, 87-94.

Murphy, D.M., Buckley, P.G., Bryan, K., Das, S., Alcock, L., Foley, N.H., Prenter, S., Bray, I., Watters, K.M., Higgins, D.*, et al.* (2009). Global MYCN transcription factor binding analysis in neuroblastoma reveals association with distinct E-box motifs and regions of DNA hypermethylation. PloS one *4*, e8154.

Nagato, M., Heike, T., Kato, T., Yamanaka, Y., Yoshimoto, M., Shimazaki, T., Okano, H., and Nakahata, T. (2005). Prospective characterization of neural stem cells by flow cytometry analysis using a combination of surface markers. Journal of neuroscience research *80*, 456-466.

Nakagawa, M., Koyanagi, M., Tanabe, K., Takahashi, K., Ichisaka, T., Aoi, T., Okita, K., Mochiduki, Y., Takizawa, N., and Yamanaka, S. (2008). Generation of induced pluripotent stem cells without Myc from mouse and human fibroblasts. Nature biotechnology *26*, 101-106.

Nakahara, T., Kita, A., Yamanaka, K., Mori, M., Amino, N., Takeuchi, M., Tominaga, F., Hatakeyama, S., Kinoyama, I., Matsuhisa, A.*, et al.* (2007). YM155, a novel small-molecule survivin suppressant, induces regression of established human hormone-refractory prostate tumor xenografts. Cancer research *67*, 8014-8021.

Naldini, L., Blomer, U., Gage, F.H., Trono, D., and Verma, I.M. (1996a). Efficient transfer, integration, and sustained long-term expression of the transgene in adult rat brains injected with a lentiviral vector. Proceedings of the National Academy of Sciences of the United States of America *93*, 11382-11388.

Naldini, L., Blomer, U., Gallay, P., Ory, D., Mulligan, R., Gage, F.H., Verma, I.M., and Trono, D. (1996b). In vivo gene delivery and stable transduction of nondividing cells by a lentiviral vector. Science *272*, 263-267.

Nariai, Y., Mishima, K., Yoshimura, Y., and Sekine, J. (2011). FAP-1 and NF-kappaB expressions in oral squamous cell carcinoma as potential markers for chemo-radio sensitivity and prognosis. International journal of oral and maxillofacial surgery *40*, 419-426.

Nicole M. Le Douarin, C.K. (1999). The Neural Crest (Cambridge University Press).

Nielsen, J.A., Chambers, M.A., Romm, E., Lee, L.Y., Berndt, J.A., and Hudson, L.D. (2011). Mouse transmembrane BAX inhibitor motif 3 (Tmbim3) encodes a 38 kDa transmembrane protein expressed in the central nervous system. Molecular and cellular biochemistry *357*, 73-81.

Nishida, Y., Adati, N., Ozawa, R., Maeda, A., Sakaki, Y., and Takeda, T. (2008). Identification and classification of genes regulated by phosphatidylinositol 3-kinase- and TRKB-mediated signalling pathways during neuronal differentiation in two subtypes of the human neuroblastoma cell line SH-SY5Y. BMC research notes *1*, 95.

Nooter, K., and Stoter, G. (1996). Molecular mechanisms of multidrug resistance in cancer chemotherapy. Pathology, research and practice *192*, 768-780.

Nozato, M., Kaneko, S., Nakagawara, A., and Komuro, H. (2013). Epithelial-mesenchymal transition-related gene expression as a new prognostic marker for neuroblastoma. International journal of oncology *42*, 134-140.

Oberthuer, A., Berthold, F., Warnat, P., Hero, B., Kahlert, Y., Spitz, R., Ernestus, K., Konig, R., Haas, S., Eils, R.*, et al.* (2006). Customized oligonucleotide microarray gene expression-based classification of neuroblastoma patients outperforms current clinical risk stratification. Journal of clinical oncology : official journal of the American Society of Clinical Oncology *24*, 5070-5078.

Ohtaki, M., Otani, K., Hiyama, K., Kamei, N., Satoh, K., and Hiyama, E. (2010). A robust method for estimating gene expression states using Affymetrix microarray probe level data. BMC bioinformatics *11*, 183.

Okura, T., Gong, L., Kamitani, T., Wada, T., Okura, I., Wei, C.F., Chang, H.M., and Yeh, E.T. (1996). Protection against Fas/APO-1- and tumor necrosis factor-mediated cell death by a novel protein, sentrin. Journal of immunology *157*, 4277-4281.

Opipari, A.W., Jr., Boguski, M.S., and Dixit, V.M. (1990). The A20 cDNA induced by tumor necrosis factor alpha encodes a novel type of zinc finger protein. The Journal of biological chemistry *265*, 14705-14708.

Opipari, A.W., Jr., Hu, H.M., Yabkowitz, R., and Dixit, V.M. (1992). The A20 zinc finger protein protects cells from tumor necrosis factor cytotoxicity. The Journal of biological chemistry *267*, 12424-12427.

Ora, I., and Eggert, A. (2011). Progress in treatment and risk stratification of neuroblastoma: impact on future clinical and basic research. Seminars in cancer biology *21*, 217-228.

Otto, T., Horn, S., Brockmann, M., Eilers, U., Schuttrumpf, L., Popov, N., Kenney, A.M., Schulte, J.H., Beijersbergen, R., Christiansen, H*., et al.* (2009). Stabilization of N-Myc is a critical function of Aurora A in human neuroblastoma. Cancer cell *15*, 67-78.

Oue, T., Fukuzawa, M., Kusafuka, T., Kohmoto, Y., Imura, K., Nagahara, S., and Okada, A. (1996). In situ detection of DNA fragmentation and expression of bcl-2 in human neuroblastoma: relation to apoptosis and spontaneous regression. Journal of pediatric surgery *31*, 251-257.

Owens, C., and Irwin, M. (2012). Neuroblastoma: the impact of biology and cooperation leading to personalized treatments. Critical reviews in clinical laboratory sciences *49*, 85-115.

Ozawa, F., Friess, H., Zimmermann, A., Kleeff, J., and Buchler, M.W. (2000). Enhanced expression of Silencer of death domains (SODD/BAG-4) in pancreatic cancer. Biochemical and biophysical research communications *271*, 409-413.

Ozturk, S., Schleich, K., and Lavrik, I.N. (2012). Cellular FLICE-like inhibitory proteins (c-FLIPs): fine-tuners of life and death decisions. Experimental cell research *318*, 1324-1331.

Pap, M., and Cooper, G.M. (1998). Role of glycogen synthase kinase-3 in the phosphatidylinositol 3-Kinase/Akt cell survival pathway. The Journal of biological chemistry *273*, 19929-19932.

Park, J.R., Bagatell, R., London, W.B., Maris, J.M., Cohn, S.L., Mattay, K.M., Hogarty, M., and Committee, C.O.G.N. (2013). Children's Oncology Group's 2013 blueprint for research: neuroblastoma. Pediatric blood & cancer *60*, 985-993.

Park, J.R., Eggert, A., and Caron, H. (2008). Neuroblastoma: biology, prognosis, and treatment. Pediatric clinics of North America *55*, 97-120, x.

Pattyn, A., Morin, X., Cremer, H., Goridis, C., and Brunet, J.F. (1999). The homeobox gene Phox2b is essential for the development of autonomic neural crest derivatives. Nature *399*, 366-370.

Penuelas, S., Anido, J., Prieto-Sanchez, R.M., Folch, G., Barba, I., Cuartas, I., Garcia-Dorado, D., Poca, M.A., Sahuquillo, J., Baselga, J*., et al.* (2009). TGF-beta increases glioma-initiating cell self-renewal through the induction of LIF in human glioblastoma. Cancer cell *15*, 315-327.

Pepper, W. (1901). Congenital sarcoma of the liver and suprarenal. The American journal of the medical sciences *121*, 287-299.

Perez-Moreno, M.A., Locascio, A., Rodrigo, I., Dhondt, G., Portillo, F., Nieto, M.A., and Cano, A. (2001). A new role for E12/E47 in the repression of E-cadherin expression and epithelial-mesenchymal transitions. The Journal of biological chemistry *276*, 27424-27431.

Petak, I., Douglas, L., Tillman, D.M., Vernes, R., and Houghton, J.A. (2000). Pediatric rhabdomyosarcoma cell lines are resistant to Fas-induced apoptosis and highly sensitive to TRAIL-induced apoptosis. Clinical cancer research : an official journal of the American Association for Cancer Research *6*, 4119-4127.

Peter, M.E., and Krammer, P.H. (2003). The CD95(APO-1/Fas) DISC and beyond. Cell death and differentiation *10*, 26-35.

Peverali, F.A., Orioli, D., Tonon, L., Ciana, P., Bunone, G., Negri, M., and Della-Valle, G. (1996). Retinoic acid-induced growth arrest and differentiation of neuroblastoma cells are counteracted by N-myc and enhanced by max overexpressions. Oncogene *12*, 457-462.

Pichler, A., and Melchior, F. (2002). Ubiquitin-related modifier SUMO1 and nucleocytoplasmic transport. Traffic *3*, 381-387.

Pobezinskaya, Y.L., Kim, Y.S., Choksi, S., Morgan, M.J., Li, T., Liu, C., and Liu, Z. (2008). The function of TRADD in signaling through tumor necrosis factor receptor 1 and TRIF-dependent Toll-like receptors. Nature immunology *9*, 1047-1054.

Pop, C., and Salvesen, G.S. (2009). Human caspases: activation, specificity, and regulation. The Journal of biological chemistry *284*, 21777-21781.

Poulaki, V., Mitsiades, N., Romero, M.E., and Tsokos, M. (2001). Fas-mediated apoptosis in neuroblastoma requires mitochondrial activation and is inhibited by FLICE inhibitor protein and Bcl-2. Cancer research *61*, 4864-4872.

Pranski, E.L., Van Sanford, C.D., Dalal, N.V., Orr, A.L., Karmali, D., Cooper, D.S., Costa, N., Heilman, C.J., Gearing, M., Lah, J.J*., et al.* (2012). Comparative distribution of protein components of the A20 ubiquitin-editing complex in normal human brain. Neuroscience letters *520*, 104-109.

Qiao, J., Paul, P., Lee, S., Qiao, L., Josifi, E., Tiao, J.R., and Chung, D.H. (2012). PI3K/AKT and ERK regulate retinoic acid-induced neuroblastoma cellular differentiation. Biochemical and biophysical research communications *424*, 421-426.

Raabe, E.H., Laudenslager, M., Winter, C., Wasserman, N., Cole, K., LaQuaglia, M., Maris, D.J., Mosse, Y.P., and Maris, J.M. (2008). Prevalence and functional consequence of PHOX2B mutations in neuroblastoma. Oncogene *27*, 469-476.

Reimers, K., Choi, C.Y., Mau-Thek, E., and Vogt, P.M. (2006). Sequence analysis shows that Lifeguard belongs to a new evolutionarily conserved cytoprotective family. International journal of molecular medicine *18*, 729-734.

Renault, F., Formstecher, E., Callebaut, I., Junier, M.P., and Chneiweiss, H. (2003). The multifunctional protein PEA-15 is involved in the control of apoptosis and cell cycle in astrocytes. Biochemical pharmacology *66*, 1581-1588.

Renault-Mihara, F., Beuvon, F., Iturrioz, X., Canton, B., De Bouard, S., Leonard, N., Mouhamad, S., Sharif, A., Ramos, J.W., Junier, M.P*., et al.* (2006). Phosphoprotein enriched in astrocytes-15 kDa expression inhibits astrocyte migration by a protein kinase C delta-dependent mechanism. Molecular biology of the cell *17*, 5141-5152.

Renganathan, H., Vaidyanathan, H., Knapinska, A., and Ramos, J.W. (2005). Phosphorylation of PEA-15 switches its binding specificity from ERK/MAPK to FADD. The Biochemical journal *390*, 729-735.

Reuland, S.N., Smith, S.M., Bemis, L.T., Goldstein, N.B., Almeida, A.R., Partyka, K.A., Marquez, V.E., Zhang, Q., Norris, D.A., and Shellman, Y.G. (2013). MicroRNA-26a is strongly downregulated in melanoma and induces cell death through repression of silencer of death domains (SODD). The Journal of investigative dermatology *133*, 1286-1293.

Reynolds, M.L., and Woolf, C.J. (1993). Reciprocal Schwann cell-axon interactions. Current opinion in neurobiology *3*, 683-693.

Rheingold, S.R., Hogarty, M.D., Blaney, S.M., Zwiebel, J.A., Sauk-Schubert, C., Chandula, R., Krailo, M.D., Adamson, P.C., and Children's Oncology Group, S. (2007). Phase I Trial of G3139, a bcl-2 antisense oligonucleotide, combined with doxorubicin and cyclophosphamide in children with relapsed solid tumors: a Children's Oncology Group Study. Journal of clinical oncology : official journal of the American Society of Clinical Oncology *25*, 1512-1518.

Richards, K.N., Zweidler-McKay, P.A., Van Roy, N., Speleman, F., Trevino, J., Zage, P.E., and Hughes, D.P. (2010). Signaling of ERBB receptor tyrosine kinases promotes neuroblastoma growth in vitro and in vivo. Cancer *116*, 3233-3243.

Riedl, S.J., and Shi, Y. (2004). Molecular mechanisms of caspase regulation during apoptosis. Nature reviews Molecular cell biology *5*, 897-907.

Ringner, M. (2008). What is principal component analysis? Nature biotechnology *26*, 303-304.

Roca, H., Varsos, Z., and Pienta, K.J. (2008). CCL2 protects prostate cancer PC3 cells from autophagic death via phosphatidylinositol 3-kinase/AKT-dependent survivin up-regulation. The Journal of biological chemistry *283*, 25057-25073.

Rojas-Rivera, D., and Hetz, C. (2014). TMBIM protein family: ancestral regulators of cell death. Oncogene.

Ross, R.A., and Spengler, B.A. (2007). Human neuroblastoma stem cells. Seminars in cancer biology *17*, 241-247.

Roth, W., Kermer, P., Krajewska, M., Welsh, K., Davis, S., Krajewski, S., and Reed, J.C. (2003). Bifunctional apoptosis inhibitor (BAR) protects neurons from diverse cell death pathways. Cell death and differentiation *10*, 1178-1187.

Roy, N., Deveraux, Q.L., Takahashi, R., Salvesen, G.S., and Reed, J.C. (1997). The c-IAP-1 and c-IAP-2 proteins are direct inhibitors of specific caspases. The EMBO journal *16*, 6914-6925.

Saeed, A.I., Sharov, V., White, J., Li, J., Liang, W., Bhagabati, N., Braisted, J., Klapa, M., Currier, T., Thiagarajan, M.*, et al.* (2003). TM4: a free, open-source system for microarray data management and analysis. BioTechniques *34*, 374-378.

Safa, A.R., Day, T.W., and Wu, C.H. (2008). Cellular FLICE-like inhibitory protein (C-FLIP): a novel target for cancer therapy. Current cancer drug targets *8*, 37-46.

Saint-Jeannet, J.-P. (2006). Neural Crest Induction and Differentiation (Landes Bioscience).

Sano, H., Bonadio, J., Gerbing, R.B., London, W.B., Matthay, K.K., Lukens, J.N., and Shimada, H. (2006). International neuroblastoma pathology classification adds independent prognostic information beyond the prognostic contribution of age. European journal of cancer *42*, 1113-1119.

Saraste, A., and Pulkki, K. (2000). Morphologic and biochemical hallmarks of apoptosis. Cardiovascular research *45*, 528-537.

Sato, T., Irie, S., Kitada, S., and Reed, J.C. (1995). FAP-1: a protein tyrosine phosphatase that associates with Fas. Science *268*, 411-415.

Sawai, S., Shimono, A., Wakamatsu, Y., Palmes, C., Hanaoka, K., and Kondoh, H. (1993). Defects of embryonic organogenesis resulting from targeted disruption of the N-myc gene in the mouse. Development *117*, 1445-1455.

Scaffidi, C., Schmitz, I., Krammer, P.H., and Peter, M.E. (1999). The role of c-FLIP in modulation of CD95-induced apoptosis. The Journal of biological chemistry *274*, 1541-1548.

Schiapparelli, P., Enguita-German, M., Balbuena, J., Rey, J.A., Lazcoz, P., and Castresana, J.S. (2010). Analysis of stemness gene expression and CD133 abnormal methylation in neuroblastoma cell lines. Oncology reports *24*, 1355-1362.

Schneider, T.J., Fischer, G.M., Donohoe, T.J., Colarusso, T.P., and Rothstein, T.L. (1999). A novel gene coding for a Fas apoptosis inhibitory molecule (FAIM) isolated from inducibly Fas-resistant B lymphocytes. The Journal of experimental medicine *189*, 949-956.

Schwab, M., Alitalo, K., Klempnauer, K.H., Varmus, H.E., Bishop, J.M., Gilbert, F., Brodeur, G., Goldstein, M., and Trent, J. (1983). Amplified DNA with limited homology to myc cellular oncogene is shared by human neuroblastoma cell lines and a neuroblastoma tumour. Nature *305*, 245-248.

Schweitzer, B., Suter, U., and Taylor, V. (2002). Neural membrane protein 35/Lifeguard is localized at postsynaptic sites and in dendrites. Brain research Molecular brain research *107*, 47-56.

Schweitzer, B., Taylor, V., Welcher, A.A., McClelland, M., and Suter, U. (1998). Neural membrane protein 35 (NMP35): a novel member of a gene family which is highly expressed in the adult nervous system. Molecular and cellular neurosciences *11*, 260-273.

Scotting, P.J., Walker, D.A., and Perilongo, G. (2005). Childhood solid tumours: a developmental disorder. Nature reviews Cancer *5*, 481-488.

Segura, M.F., Sole, C., Moubarak, R.S., Yuste, V.J., and Comella, J.X. (2010). FAIM (Fas apoptotic inhibitory molecule). Atlas Genet Cytogenet Oncol Haematol *14*.

Segura, M.F., Sole, C., Pascual, M., Moubarak, R.S., Perez-Garcia, M.J., Gozzelino, R., Iglesias, V., Badiola, N., Bayascas, J.R., Llecha, N.*, et al.* (2007). The long form of Fas apoptotic inhibitory molecule is expressed specifically in neurons and protects them against death receptor-triggered apoptosis. The Journal of neuroscience : the official journal of the Society for Neuroscience *27*, 11228-11241.

Seufert, W., Futcher, B., and Jentsch, S. (1995). Role of a ubiquitin-conjugating enzyme in degradation of S- and M-phase cyclins. Nature *373*, 78-81.

Shamas-Din, A., Kale, J., Leber, B., and Andrews, D.W. (2013). Mechanisms of action of Bcl-2 family proteins. Cold Spring Harbor perspectives in biology *5*, a008714.

Sharp, D.A., Lawrence, D.A., and Ashkenazi, A. (2005). Selective knockdown of the long variant of cellular FLICE inhibitory protein augments death receptor-mediated caspase-8 activation and apoptosis. The Journal of biological chemistry *280*, 19401-19409.

Sheridan, J.P., Marsters, S.A., Pitti, R.M., Gurney, A., Skubatch, M., Baldwin, D., Ramakrishnan, L., Gray, C.L., Baker, K., Wood, W.I.*, et al.* (1997). Control of TRAIL-induced apoptosis by a family of signaling and decoy receptors. Science *277*, 818-821.

Shi, Y. (2002). Mechanisms of caspase activation and inhibition during apoptosis. Molecular cell *9*, 459-470.

Shimada, H., Chatten, J., Newton, W.A., Jr., Sachs, N., Hamoudi, A.B., Chiba, T., Marsden, H.B., and Misugi, K. (1984). Histopathologic prognostic factors in neuroblastic tumors: definition of subtypes of ganglioneuroblastoma and an age-linked classification of neuroblastomas. Journal of the National Cancer Institute *73*, 405-416.

Shimada, H., Umehara, S., Monobe, Y., Hachitanda, Y., Nakagawa, A., Goto, S., Gerbing, R.B., Stram, D.O., Lukens, J.N., and Matthay, K.K. (2001). International neuroblastoma pathology classification for prognostic evaluation of patients with peripheral neuroblastic tumors: a report from the Children's Cancer Group. Cancer *92*, 2451-2461.

Shirley, S., and Micheau, O. (2013). Targeting c-FLIP in cancer. Cancer letters *332*, 141-150.

Shtutman, M., Zhurinsky, J., Simcha, I., Albanese, C., D'Amico, M., Pestell, R., and Ben-Ze'ev, A. (1999). The cyclin D1 gene is a target of the beta-catenin/LEF-1 pathway. Proceedings of the National Academy of Sciences of the United States of America *96*, 5522-5527.

Silke, J., Ekert, P.G., Day, C.L., Hawkins, C.J., Baca, M., Chew, J., Pakusch, M., Verhagen, A.M., and Vaux, D.L. (2001). Direct inhibition of caspase 3 is dispensable for the anti-apoptotic activity of XIAP. The EMBO journal *20*, 3114-3123.

Silke, J., and Vaux, D.L. (2001). Two kinds of BIR-containing protein - inhibitors of apoptosis, or required for mitosis. Journal of cell science *114*, 1821-1827.

Simonet, W.S., Lacey, D.L., Dunstan, C.R., Kelley, M., Chang, M.S., Luthy, R., Nguyen, H.Q., Wooden, S., Bennett, L., Boone, T.*, et al.* (1997). Osteoprotegerin: a novel secreted protein involved in the regulation of bone density. Cell *89*, 309-319.

Slamon, D.J., Leyland-Jones, B., Shak, S., Fuchs, H., Paton, V., Bajamonde, A., Fleming, T., Eiermann, W., Wolter, J., Pegram, M.*, et al.* (2001). Use of chemotherapy plus a monoclonal antibody against HER2 for metastatic breast cancer that overexpresses HER2. The New England journal of medicine *344*, 783-792.

Slee, E.A., Harte, M.T., Kluck, R.M., Wolf, B.B., Casiano, C.A., Newmeyer, D.D., Wang, H.G., Reed, J.C., Nicholson, D.W., Alnemri, E.S.*, et al.* (1999). Ordering the cytochrome c-initiated

caspase cascade: hierarchical activation of caspases-2, -3, -6, -7, -8, and -10 in a caspase-9-dependent manner. The Journal of cell biology *144*, 281-292.

Smith, K.N., Singh, A.M., and Dalton, S. (2010a). Myc represses primitive endoderm differentiation in pluripotent stem cells. Cell stem cell *7*, 343-354.

Smith, M.A., Morton, C.L., Kolb, E.A., Gorlick, R., Keir, S.T., Carol, H., Lock, R., Kang, M.H., Reynolds, C.P., Maris, J.M.*, et al.* (2010b). Initial testing (stage 1) of mapatumumab (HGS-ETR1) by the pediatric preclinical testing program. Pediatric blood & cancer *54*, 307-310.

Smyth, G.K. (2004). Linear models and empirical bayes methods for assessing differential expression in microarray experiments. Statistical applications in genetics and molecular biology *3*, Article3.

Sole, C., Dolcet, X., Segura, M.F., Gutierrez, H., Diaz-Meco, M.T., Gozzelino, R., Sanchis, D., Bayascas, J.R., Gallego, C., Moscat, J.*, et al.* (2004). The death receptor antagonist FAIM promotes neurite outgrowth by a mechanism that depends on ERK and NF-kapp B signaling. The Journal of cell biology *167*, 479-492.

Somia, N.V., Schmitt, M.J., Vetter, D.E., Van Antwerp, D., Heinemann, S.F., and Verma, I.M. (1999). LFG: an anti-apoptotic gene that provides protection from Fas-mediated cell death. Proceedings of the National Academy of Sciences of the United States of America *96*, 12667-12672.

Sridhar, S., Al-Moallem, B., Kamal, H., Terrile, M., and Stallings, R.L. (2013). New insights into the genetics of neuroblastoma. Molecular diagnosis & therapy *17*, 63-69.

Stanke, M., Stubbusch, J., and Rohrer, H. (2004). Interaction of Mash1 and Phox2b in sympathetic neuron development. Molecular and cellular neurosciences *25*, 374-382.

Stanton, B.R., Perkins, A.S., Tessarollo, L., Sassoon, D.A., and Parada, L.F. (1992). Loss of N-myc function results in embryonic lethality and failure of the epithelial component of the embryo to develop. Genes & development *6*, 2235-2247.

Stassi, G., Garofalo, M., Zerilli, M., Ricci-Vitiani, L., Zanca, C., Todaro, M., Aragona, F., Limite, G., Petrella, G., and Condorelli, G. (2005). PED mediates AKT-dependent chemoresistance in human breast cancer cells. Cancer research *65*, 6668-6675.

Steffan, J.S., Agrawal, N., Pallos, J., Rockabrand, E., Trotman, L.C., Slepko, N., Illes, K., Lukacsovich, T., Zhu, Y.Z., Cattaneo, E.*, et al.* (2004). SUMO modification of Huntingtin and Huntington's disease pathology. Science *304*, 100-104.

Stegh, A.H., Barnhart, B.C., Volkland, J., Algeciras-Schimnich, A., Ke, N., Reed, J.C., and Peter, M.E. (2002). Inactivation of caspase-8 on mitochondria of Bcl-xL-expressing MCF7-Fas cells: role for the bifunctional apoptosis regulator protein. The Journal of biological chemistry *277*, 4351-4360.

Stoica, G.E., Kuo, A., Aigner, A., Sunitha, I., Souttou, B., Malerczyk, C., Caughey, D.J., Wen, D., Karavanov, A., Riegel, A.T.*, et al.* (2001). Identification of anaplastic lymphoma kinase as a receptor for the growth factor pleiotrophin. The Journal of biological chemistry *276*, 16772-16779.

Stoica, G.E., Kuo, A., Powers, C., Bowden, E.T., Sale, E.B., Riegel, A.T., and Wellstein, A. (2002). Midkine binds to anaplastic lymphoma kinase (ALK) and acts as a growth factor for different cell types. The Journal of biological chemistry *277*, 35990-35998.

Strobl-Mazzulla, P.H., and Bronner, M.E. (2012). Epithelial to mesenchymal transition: new and old insights from the classical neural crest model. Seminars in cancer biology *22*, 411-416.

Stupack, D.G., Teitz, T., Potter, M.D., Mikolon, D., Houghton, P.J., Kidd, V.J., Lahti, J.M., and Cheresh, D.A. (2006). Potentiation of neuroblastoma metastasis by loss of caspase-8. Nature *439*, 95-99.

Su, W.T., Alaminos, M., Mora, J., Cheung, N.K., La Quaglia, M.P., and Gerald, W.L. (2004). Positional gene expression analysis identifies 12q overexpression and amplification in a subset of neuroblastomas. Cancer genetics and cytogenetics *154*, 131-137.

Suenaga, Y., Islam, S.M., Alagu, J., Kaneko, Y., Kato, M., Tanaka, Y., Kawana, H., Hossain, S., Matsumoto, D., Yamamoto, M.*, et al.* (2014). NCYM, a Cis-antisense gene of MYCN, encodes a de novo evolved protein that inhibits GSK3beta resulting in the stabilization of MYCN in human neuroblastomas. PLoS genetics *10*, e1003996.

Sugino, Y., Misawa, A., Inoue, J., Kitagawa, M., Hosoi, H., Sugimoto, T., Imoto, I., and Inazawa, J. (2007). Epigenetic silencing of prostaglandin E receptor 2 (PTGER2) is associated with progression of neuroblastomas. Oncogene *26*, 7401-7413.

Szakacs, G., Paterson, J.K., Ludwig, J.A., Booth-Genthe, C., and Gottesman, M.M. (2006). Targeting multidrug resistance in cancer. Nature reviews Drug discovery *5*, 219-234.

Takada, H., Chen, N.J., Mirtsos, C., Suzuki, S., Suzuki, N., Wakeham, A., Mak, T.W., and Yeh, W.C. (2003). Role of SODD in regulation of tumor necrosis factor responses. Molecular and cellular biology *23*, 4026-4033.

Takahashi, R., Deveraux, Q., Tamm, I., Welsh, K., Assa-Munt, N., Salvesen, G.S., and Reed, J.C. (1998). A single BIR domain of XIAP sufficient for inhibiting caspases. The Journal of biological chemistry *273*, 7787-7790.

Takahashi, Y., Sipp, D., and Enomoto, H. (2013). Tissue interactions in neural crest cell development and disease. Science *341*, 860-863.

Taneyhill, L.A., Coles, E.G., and Bronner-Fraser, M. (2007). Snail2 directly represses cadherin6B during epithelial-to-mesenchymal transitions of the neural crest. Development *134*, 1481-1490.

Tanno, B., Sesti, F., Cesi, V., Bossi, G., Ferrari-Amorotti, G., Bussolari, R., Tirindelli, D., Calabretta, B., and Raschella, G. (2010). Expression of Slug is regulated by c-Myb and is required for invasion and bone marrow homing of cancer cells of different origin. The Journal of biological chemistry *285*, 29434-29445.

Tao, H.F., Liu, Y.S., Fang, J.L., Su, Y.Z., Chen, F.H., Zhou, L.Y., and Zhu, Y.S. (2014). Significance of SODD expression in childhood acute lymphoblastic leukemia and its influence on chemotherapy. Genetics and molecular research : GMR *13*, 2020-2031.

Tartaglia, L.A., Ayres, T.M., Wong, G.H., and Goeddel, D.V. (1993). A novel domain within the 55 kd TNF receptor signals cell death. Cell *74*, 845-853.

Tauber, S.C., Harms, K., Falkenburger, B., Weis, J., Sellhaus, B., Nau, R., Schulz, J.B., and Reich, A. (2014). Modulation of hippocampal neuroplasticity by Fas/CD95 regulatory protein 2 (Faim2) in the course of bacterial meningitis. Journal of neuropathology and experimental neurology *73*, 2-13.

Teitz, T., Inoue, M., Valentine, M.B., Zhu, K., Rehg, J.E., Zhao, W., Finkelstein, D., Wang, Y.D., Johnson, M.D., Calabrese, C.*, et al.* (2013). Th-MYCN mice with caspase-8 deficiency develop advanced neuroblastoma with bone marrow metastasis. Cancer research *73*, 4086-4097.

Teitz, T., Lahti, J.M., and Kidd, V.J. (2001). Aggressive childhood neuroblastomas do not express caspase-8: an important component of programmed cell death. Journal of molecular medicine *79*, 428-436.

Teitz, T., Wei, T., Valentine, M.B., Vanin, E.F., Grenet, J., Valentine, V.A., Behm, F.G., Look, A.T., Lahti, J.M., and Kidd, V.J. (2000). Caspase 8 is deleted or silenced preferentially in childhood neuroblastomas with amplification of MYCN. Nature medicine *6*, 529-535.

Theveneau, E., and Mayor, R. (2012). Neural crest delamination and migration: from epithelium-to-mesenchyme transition to collective cell migration. Developmental biology *366*, 34-54.

Thiele, C.J., Reynolds, C.P., and Israel, M.A. (1985). Decreased expression of N-myc precedes retinoic acid-induced morphological differentiation of human neuroblastoma. Nature *313*, 404-406.

Thome, M., Schneider, P., Hofmann, K., Fickenscher, H., Meinl, E., Neipel, F., Mattmann, C., Burns, K., Bodmer, J.L., Schroter, M.*, et al.* (1997). Viral FLICE-inhibitory proteins (FLIPs) prevent apoptosis induced by death receptors. Nature *386*, 517-521.

Thornberry, N.A., and Lazebnik, Y. (1998). Caspases: enemies within. Science *281*, 1312-1316.
Torres, V.A., Mielgo, A., Barbero, S., Hsiao, R., Wilkins, J.A., and Stupack, D.G. (2010). Rab5 mediates caspase-8-promoted cell motility and metastasis. Molecular biology of the cell *21*, 369-376.

Tsujimoto, Y., Gorham, J., Cossman, J., Jaffe, E., and Croce, C.M. (1985). The t(14;18) chromosome translocations involved in B-cell neoplasms result from mistakes in VDJ joining. Science *229*, 1390-1393.

Valentijn, L.J., Koster, J., Haneveld, F., Aissa, R.A., van Sluis, P., Broekmans, M.E., Molenaar, J.J., van Nes, J., and Versteeg, R. (2012). Functional MYCN signature predicts outcome of neuroblastoma irrespective of MYCN amplification. Proceedings of the National Academy of Sciences of the United States of America *109*, 19190-19195.

Valiente, M., Obenauf, A.C., Jin, X., Chen, Q., Zhang, X.H., Lee, D.J., Chaft, J.E., Kris, M.G., Huse, J.T., Brogi, E.*, et al.* (2014). Serpins promote cancer cell survival and vascular co-option in brain metastasis. Cell *156*, 1002-1016.

Valmiki, M.G., and Ramos, J.W. (2009). Death effector domain-containing proteins. Cellular and molecular life sciences : CMLS *66*, 814-830.

Valsesia-Wittmann, S., Magdeleine, M., Dupasquier, S., Garin, E., Jallas, A.C., Combaret, V., Krause, A., Leissner, P., and Puisieux, A. (2004). Oncogenic cooperation between H-Twist and N-Myc overrides failsafe programs in cancer cells. Cancer cell *6*, 625-630.

van Limpt, V., Chan, A., Schramm, A., Eggert, A., and Versteeg, R. (2005). Phox2B mutations and the Delta-Notch pathway in neuroblastoma. Cancer letters *228*, 59-63.

van Limpt, V., Schramm, A., van Lakeman, A., Sluis, P., Chan, A., van Noesel, M., Baas, F., Caron, H., Eggert, A., and Versteeg, R. (2004). The Phox2B homeobox gene is mutated in sporadic neuroblastomas. Oncogene *23*, 9280-9288.

Varani, J., Dame, M.K., Taylor, C.G., Sarma, V., Merino, R., Kunkel, R.G., Nunez, G., and Dixit, V.M. (1995). Age-dependent injury in human umbilical vein endothelial cells: relationship to apoptosis and correlation with a lack of A20 expression. Laboratory investigation; a journal of technical methods and pathology *73*, 851-858.

Varfolomeev, E., Maecker, H., Sharp, D., Lawrence, D., Renz, M., Vucic, D., and Ashkenazi, A. (2005). Molecular determinants of kinase pathway activation by Apo2 ligand/tumor necrosis factor-related apoptosis-inducing ligand. The Journal of biological chemistry *280*, 40599-40608.

Varlakhanova, N.V., Cotterman, R.F., deVries, W.N., Morgan, J., Donahue, L.R., Murray, S., Knowles, B.B., and Knoepfler, P.S. (2010). myc maintains embryonic stem cell pluripotency and self-renewal. Differentiation; research in biological diversity *80*, 9-19.

Vaux, D.L. (1993). Toward an understanding of the molecular mechanisms of physiological cell death. Proceedings of the National Academy of Sciences of the United States of America *90*, 786-789.

Vaux, D.L., Cory, S., and Adams, J.M. (1988). Bcl-2 gene promotes haemopoietic cell survival and cooperates with c-myc to immortalize pre-B cells. Nature *335*, 440-442.

Verbrugge, I., and Johnstone, R.W. (2012). Regulating the TRAIL of destruction: how A20 protects glioblastomas from TRAIL-mediated death. Cancer discovery *2*, 112-114.

Viana Lde, S., Affonso, R.J., Jr., Silva, S.R., Denadai, M.V., Matos, D., Salinas de Souza, C., and Waisberg, J. (2013). Relationship between the expression of the extracellular matrix genes SPARC, SPP1, FN1, ITGA5 and ITGAV and clinicopathological parameters of tumor progression and colorectal cancer dissemination. Oncology *84*, 81-91.

Vigliotta, G., Miele, C., Santopietro, S., Portella, G., Perfetti, A., Maitan, M.A., Cassese, A., Oriente, F., Trencia, A., Fiory, F*., et al.* (2004). Overexpression of the ped/pea-15 gene causes diabetes by impairing glucose-stimulated insulin secretion in addition to insulin action. Molecular and cellular biology *24*, 5005-5015.

Vitali, R., Mancini, C., Cesi, V., Tanno, B., Mancuso, M., Bossi, G., Zhang, Y., Martinez, R.V., Calabretta, B., Dominici, C*., et al.* (2008). Slug (SNAI2) down-regulation by RNA interference facilitates apoptosis and inhibits invasive growth in neuroblastoma preclinical models. Clinical cancer research : an official journal of the American Association for Cancer Research *14*, 4622-4630.

Wakamatsu, Y., Watanabe, Y., Nakamura, H., and Kondoh, H. (1997). Regulation of the neural crest cell fate by N-myc: promotion of ventral migration and neuronal differentiation. Development *124*, 1953-1962.

Waligorska-Stachura, J., Jankowska, A., Wasko, R., Liebert, W., Biczysko, M., Czarnywojtek, A., Baszko-Blaszyk, D., Shimek, V., and Ruchala, M. (2012). Survivin--prognostic tumor biomarker in human neoplasms--review. Ginekologia polska *83*, 537-540.

Walton, J.D., Kattan, D.R., Thomas, S.K., Spengler, B.A., Guo, H.F., Biedler, J.L., Cheung, N.K., and Ross, R.A. (2004). Characteristics of stem cells from human neuroblastoma cell lines and in tumors. Neoplasia *6*, 838-845.

Wang, M., Zhou, C., Cai, R., Li, Y., and Gong, L. (2013). Copy number gain of MYCN gene is a recurrent genetic aberration and favorable prognostic factor in Chinese pediatric neuroblastoma patients. Diagnostic pathology *8*, 5.

Wang, Q., Diskin, S., Rappaport, E., Attiyeh, E., Mosse, Y., Shue, D., Seiser, E., Jagannathan, J., Shusterman, S., Bansal, M.*, et al.* (2006). Integrative genomics identifies distinct molecular classes of neuroblastoma and shows that multiple genes are targeted by regional alterations in DNA copy number. Cancer research *66*, 6050-6062.

Wei, M.C., Zong, W.X., Cheng, E.H., Lindsten, T., Panoutsakopoulou, V., Ross, A.J., Roth, K.A., MacGregor, G.R., Thompson, C.B., and Korsmeyer, S.J. (2001). Proapoptotic BAX and BAK: a requisite gateway to mitochondrial dysfunction and death. Science *292*, 727-730.

Weiss, W.A., Aldape, K., Mohapatra, G., Feuerstein, B.G., and Bishop, J.M. (1997). Targeted expression of MYCN causes neuroblastoma in transgenic mice. The EMBO journal *16*, 2985-2995.

Welchman, R.L., Gordon, C., and Mayer, R.J. (2005). Ubiquitin and ubiquitin-like proteins as multifunctional signals. Nature reviews Molecular cell biology *6*, 599-609.

Westermark, U.K., Wilhelm, M., Frenzel, A., and Henriksson, M.A. (2011). The MYCN oncogene and differentiation in neuroblastoma. Seminars in cancer biology *21*, 256-266.

Wheelock, M.J., Shintani, Y., Maeda, M., Fukumoto, Y., and Johnson, K.R. (2008). Cadherin switching. Journal of cell science *121*, 727-735.

Wieckowski, E., Atarashi, Y., Stanson, J., Sato, T.A., and Whiteside, T.L. (2007). FAP-1-mediated activation of NF-kappaB induces resistance of head and neck cancer to Fas-induced apoptosis. Journal of cellular biochemistry *100*, 16-28.

Wilkinson, J.C., Cepero, E., Boise, L.H., and Duckett, C.S. (2004). Upstream regulatory role for XIAP in receptor-mediated apoptosis. Molecular and cellular biology *24*, 7003-7014.

Willis, D.E., van Niekerk, E.A., Sasaki, Y., Mesngon, M., Merianda, T.T., Williams, G.G., Kendall, M., Smith, D.S., Bassell, G.J., and Twiss, J.L. (2007a). Extracellular stimuli specifically regulate localized levels of individual neuronal mRNAs. The Journal of cell biology *178*, 965-980.

Willis, S.N., Fletcher, J.I., Kaufmann, T., van Delft, M.F., Chen, L., Czabotar, P.E., Ierino, H., Lee, E.F., Fairlie, W.D., Bouillet, P.*, et al.* (2007b). Apoptosis initiated when BH3 ligands engage multiple Bcl-2 homologs, not Bax or Bak. Science *315*, 856-859.

Wilson, N.S., Dixit, V., and Ashkenazi, A. (2009). Death receptor signal transducers: nodes of coordination in immune signaling networks. Nature immunology *10*, 348-355.

Wolmer-Solberg, N., Baryawno, N., Rahbar, A., Fuchs, D., Odeberg, J., Taher, C., Wilhelmi, V., Milosevic, J., Mohammad, A.A., Martinsson, T.*, et al.* (2013). Frequent detection of human cytomegalovirus in neuroblastoma: a novel therapeutic target? International journal of cancer Journal international du cancer *133*, 2351-2361.

Wright, J.H. (1910). Neurocytoma or Neuroblastoma, a Kind of Tumor Not Generally Recognized. The Journal of experimental medicine *12*, 556-561.

Xu, L., Wang, X., Wan, J., Li, T., Gong, X., Zhang, K., Yi, L., Xiang, Z., Xu, M., and Cui, H. (2012). Sonic Hedgehog pathway is essential for neuroblastoma cell proliferation and tumor growth. Molecular and cellular biochemistry *364*, 235-241.

Yamaguchi, N., Oyama, M., Kozuka-Hata, H., and Inoue, J. (2013). Involvement of A20 in the molecular switch that activates the non-canonical NF-small ka, CyrillicB pathway. Scientific reports *3*, 2568.

Yang, J., Mani, S.A., Donaher, J.L., Ramaswamy, S., Itzykson, R.A., Come, C., Savagner, P., Gitelman, I., Richardson, A., and Weinberg, R.A. (2004). Twist, a master regulator of morphogenesis, plays an essential role in tumor metastasis. Cell *117*, 927-939.

Yang, X., and Thiele, C.J. (2003). Targeting the tumor necrosis factor-related apoptosis-inducing ligand path in neuroblastoma. Cancer letters *197*, 137-143.

Yao, H., Song, E., Chen, J., and Hamar, P. (2004). Expression of FAP-1 by human colon adenocarcinoma: implication for resistance against Fas-mediated apoptosis in cancer. British journal of cancer *91*, 1718-1725.

Yeh, W.C., Itie, A., Elia, A.J., Ng, M., Shu, H.B., Wakeham, A., Mirtsos, C., Suzuki, N., Bonnard, M., Goeddel, D.V.*, et al.* (2000). Requirement for Casper (c-FLIP) in regulation of death receptor-induced apoptosis and embryonic development. Immunity *12*, 633-642.

Yu, A.L., Gilman, A.L., Ozkaynak, M.F., London, W.B., Kreissman, S.G., Chen, H.X., Smith, M., Anderson, B., Villablanca, J.G., Matthay, K.K.*, et al.* (2010). Anti-GD2 antibody with GM-CSF, interleukin-2, and isotretinoin for neuroblastoma. The New England journal of medicine *363*, 1324-1334.

Zhang, H., Xu, Q., Krajewski, S., Krajewska, M., Xie, Z., Fuess, S., Kitada, S., Pawlowski, K., Godzik, A., and Reed, J.C. (2000). BAR: An apoptosis regulator at the intersection of caspases and Bcl-2 family proteins. Proceedings of the National Academy of Sciences of the United States of America *97*, 2597-2602.

Zhong, X., Schneider, T.J., Cabral, D.S., Donohoe, T.J., and Rothstein, T.L. (2001). An alternatively spliced long form of Fas apoptosis inhibitory molecule (FAIM) with tissue-specific expression in the brain. Molecular immunology *38*, 65-72.

Zhou, X., Liao, J., Hu, L., Feng, L., and Omary, M.B. (1999). Characterization of the major physiologic phosphorylation site of human keratin 19 and its role in filament organization. The Journal of biological chemistry *274*, 12861-12866.

Zimmerman, K.A., Yancopoulos, G.D., Collum, R.G., Smith, R.K., Kohl, N.E., Denis, K.A., Nau, M.M., Witte, O.N., Toran-Allerand, D., Gee, C.E., *et al.* (1986). Differential expression of myc family genes during murine development. Nature *319*, 780-783.

Zimmermann, K.C., Bonzon, C., and Green, D.R. (2001). The machinery of programmed cell death. Pharmacology & therapeutics *92*, 57-70.

Zufferey, R., Nagy, D., Mandel, R.J., Naldini, L., and Trono, D. (1997). Multiply attenuated lentiviral vector achieves efficient gene delivery in vivo. Nature biotechnology *15*, 871-875.

ANNEX

Annex

Annex 1. Publications

F Marques-Fernandez, **L Planells-Ferrer**, R Gozzelino, KMO Galenkamp, S Reix, N Llecha-Cano, J Lopez-Soriano, VJ Yuste, RS Moubarak and JX Comella. *TNFa induces survival through the FLIP-L-dependent activation of the MAPK/ERK pathway.* Cell Death and Disease 4, e493 (2013).

Ester Rodríguez, Carolina Romero, Adolfo Río, Marta Miralles, Aida Raventós, **Laura Planells**, Joan F. Burgueño, Hirofumi Hamada, Jose Carlos Perales, Assumpció Bosch, Miguel Angel Gassull, Ester Fernández, and Miguel Chillon. *Short-Fiber Protein of Ad40 Confers Enteric Tropism and Protection Against Acidic Gastrointestinal Conditions.* Human Gene Therapy Methods 24:195-204 (2013).

Rana S. Moubarak, **Laura Planells-Ferrer**, Jorge Urresti, Stéphanie Reix, Miguel F. Segura, Paulina Carriba, Fernando Marqués-Fernàndez, Carme Sole, Nuria Llecha-Cano, Joaquin Lopez-Soriano, Daniel Sanchis, Victor J. Yuste, and Joan X. Comella. *FAIM-L Is an IAP-Binding Protein That Inhibits XIAP Ubiquitinylation and Protects from Fas-Induced Apoptosis*. The Journal of Neuroscience 33(49):19262-19275 (2013).

L Planells-Ferrer, J Urresti, A Soriano, S Reix, DM Murphy, JC Ferreres, F Borràs, S Gallego, RL Stallings, RS Moubarak, MF Segura and JX Comella. *MYCN repression of Lifeguard/FAIM2 enhances neuroblastoma aggressiveness*. Cell Death and Disease 5, e1401 (2014).

Urresti J, Arévalo JC, Sanz C, Ruiz-Meana M, Galenkamp K, **Planells-Ferrer L**, Malagón MM, Moubarak RS, García-Dorado D, Reix S, Barneda-Zahonero V, Comella JX. *LFG inhibits Fas ligand-mediated endoplasmic reticulum-calcium release and prevents type II apoptosis in a Bcl-xL-dependent manner*. Submitted to The Journal of Neuroscience, under revision.

Galenkamp, K, Carriba P, **Planells-Ferrer L**, Urresti J, Coccia E, López-Soriano J, Barneda-Zahonero B, Segura MF, Comella JX. *Characterization of the TNFα-induced Fas expression and activation in neuroblastoma cells: implications for its use in the treatment of neuroblastoma tumors.* In preparation.

Ramón Martínez-Marmol, Bruna Barneda-Zahonero, Rosa Andrés, **Laura Planells-Ferrer**, Rana Moubarak, Eduardo Soriano, and Joan Comella. *FAIM-L inhibition of XIAP degradation blocks Axon Degeneration and Long-Term Depression of Synaptic Transmission*. In preparation.